



Avian-Keratin Refinement and Application in Biomaterials

A thesis submitted in fulfilment of the requirements for the Degree of
Doctor of Philosophy

Firoozeh Pourjavaheri

M.Eng. in Chemical Engineering
B.App.Sc. in Food Science and Technology

School of Science
College of Science, Engineering and Health
RMIT University
Melbourne, Australia

August 2017



DECLARATION

I, Firoozeh Pourjavaheri, certify that except where due acknowledgement has been made, the work is that of the author alone; the work has not been submitted previously, in whole or in part, to qualify for any other academic award; the content of the thesis is the result of work which has been carried out since the official commencement date of the approved research program; any editorial work, paid or unpaid, carried out by a third party is acknowledged; and, ethics procedures and guidelines have been followed.

The work described in this research project was carried out in the School of Science, RMIT University since the official date of commencement of the program.

I acknowledge the support I have received for my research through the provision of an Australian Government Research Training Program Scholarship.

Signed:

Date: 08/08/2017

Firoozeh Pourjavaheri

*I dedicate this thesis to my best friend, my mother **Hela Sabetzadeh-Afshar** for giving me the gift of life, teaching me to live life and helping me to survive the challenges of life by holding my hand since day one. I promise to use your precious gift to the best of my ability!*





ACKNOWLEDGEMENTS

This PhD project has been a wonderful experience and of course a delightful memory to cherish for the rest of my life and I am truly grateful for the Research Training Program (RTP) scholarship administered by RMIT University that made this amazing journey possible. I have been blessed to be surrounded by incredible energy kindly given by many individuals who have made this research more joyful. Mentors and colleagues, friends and family, all of you deserve my utmost thanks and appreciation for the love, support and guidance that you have provided over the years.

I would like to express my gratitude foremost to my supervisors, Professor Dr Robert Shanks for his understanding, constant guidance, wealth of knowledge, outstanding supervision and building all your student's confidence; Associate Professor Dr Frank Sherkat for his mentoring, continual advice and feedback, care and support since the first day of my undergraduate studies to date; Associate Professor Dr Oliver Jones for his timely and consistent assistance, encouragement, motivation, inspiration and friendship; Associate Professor Dr Arun Gupta for identifying my potential to contribute to his area of research when we first met at the International Chemeca 2011 Conference in Sydney, Australia and for offering me the opportunity to join his exciting field of study.

My sincere appreciation to Mr Arash Sabetzadeh for his remarkable marketing advices; Professor Peter Smooker, Ms Ibukun Aibinu, Miss Wanlapa Chaibangyang, Mr Andrew Sujecki, Ms Ivana Skakic and Ben Vezina for their significant help with protein analysis; Mrs Prue Bramwell, Ms Anita Markovska and Ms Kristie Shannon Bigornia for their assistance with microbiological and antimicrobial studies; Dr Robert Brkljaca for his generous collaboration in NMR spectroscopy; the Australian Microscopy and Microanalysis Research Facility (RMMF) staff, especially Dr Matthew Field and Mr Philip Francis for their technical support in microscope analysis; Miss Tara Nazaryan and Mr Arash Sabetzadeh for their timely help on separating the feather components; Miss Mardi O'Donnell, Dr Swee Mak, Dr Lisa Dias, Mr Karl Lang, Ms Zahra Human, Ms Dianne Mileo, Mr Michael Mileo, Mr David Baldie, Mr Frank Antolasic, Ms Nadia Zakhartchouk, Ms Fiona De-Mendonca, Ms Ruth Cepriano-Hall for their constant support; and Baiada Poultry Pty Ltd for supplying the chicken feathers.

Sincere thanks are extended to the wonderful life-long friends who I am so grateful to have made over the last four years. To Dr Michael Czajka, Ms Christine Close, Dr Armin Mostafavi, Associate Professor Michelle Spencer, Ms Ladan Azizsoltani, Dr Saeideh Ostovar pour, Professor Ewan Blanch, Mr Nabeen Dulal, Mr Isaac Martinez, Dr Nedaossadat Mirzadeh, Associate Professor Nichola Porter, Associate Professor Ing Kong, Associate Professor Fugen Daver, Dr Amir Minagar, Ms Melissa Papalie, Dr Dipa Jadhav, Dr Kambiz Shamsi, Mrs Asal Najafi-Miri, Dr Ahmad Esmaelzadeh Kandjani, Dr Ylias Sabri, Mr Ricardo Bernardi Castilhos, Mr Thomas Agathocléous, Mr William Sullivan, Dr Oliver Buddrick, Mr Varun Prasath Babu Reddiar, Ms Patience Shoko Mponda, Dr Mahsa

Mohammad-TaHERi, and Dr Alexandru Zabara for their companionship, enthusiastic encouragements and moral support.

Finally yet most importantly, I am profoundly grateful to my loving family; my beloved father Mr Touraj Afshar, my loving mother Mrs Hela Sabetzadeh-Afshar, my smart sister Mrs Paria Allan-Blitz and her adorable husband Dr Lao-Tzu Allan-Blitz, particularly my kind-hearted brother Mr Arash Sabetzadeh and his beautiful partner Miss Tara Nazaryan, for their love and care, being such an important part of my life, especially their irreplaceable emotional support during the course of my doctoral research. Without you, this PhD would not have been worth the challenge ...



PUBLICATIONS

The following publications have resulted from the research performed in this study:

Journal Publications:

1. **Pourjavaheri, F.**, Jones, O.A.H., Mohaddes, F., Sherkat, F., Kong, I., Gupta, A., & Shanks, R.A. (2017) "Avian Keratin Fiber Based Bio-composites" *World Journal of Engineering* **14**(3) · Doi: 10.1108/WJE-08-2016-0061.
2. **Pourjavaheri, F.**, Mohaddes, F., Bramwell, P., Sherkat, F., & Shanks, R.A. (2015) "Purification of avian biological material to refined keratin fibres" *RSC Advances*: **5**(86), p. 69899-69906.
3. **Pourjavaheri, F.**, Mohaddes, F., Shanks, R. A., Czajka, M., & Gupta, A. (2014) "Effects of Different Purification Methods on Chicken Feather Keratin" *Advanced Materials Research*, 941-944, 1184-1187. doi: 10.4028.

Manuscripts under preparation:

4. **Pourjavaheri, F.**, Jones, O.A.H., Sherkat, F. & Shanks, R. A. "Characterisation of green keratin–fibre polyurethane–polyether bio-composites" *Green Chemistry*. To be submitted in 2017.
5. Pourjavaheri, F., Jones, O.A.H., Martinez Pardo, I., & Shanks, R. A. "Keratin–fibre polysiloxane–polyurethane bio-composites" *Green Chemistry*. To be submitted in 2017.
6. **Pourjavaheri, F.**, Jones, O.A.H., Sherkat, F., Gupta, A. & Shanks, R. A. "Keratin from chicken feather fibers" *Green Chemistry*. To be submitted in 2017.
7. **Pourjavaheri, F.**, Jones, O.A.H., Sherkat, F. & Shanks, R. A. "Applications of chicken feather keratin" *Green Chemistry*. To be submitted in 2017.

8. **Pourjavaheri, F.**, Jones, O.A.H., Sherkat, F. & Shanks, R. A. "Bio-composites of natural keratin fibres and polysiloxane polyether thermoplastic polyurethanes". To be submitted in 2017.
9. **Pourjavaheri, F.**, Jones, O.A.H., Sherkat, F. & Shanks, R. A. "Optimising extraction of keratin from chicken feather using sodium sulfide and L-cysteine". To be submitted in 2017.
10. **Pourjavaheri, F.**, Jones, O.A.H., Sherkat, F. & Shanks, R. A. "Antibacterial studies of chicken feather keratin and bio-composites". To be submitted in 2017.
11. **Pourjavaheri, F.**, Jones, O.A.H., Sherkat, F. & Shanks, R. A. A review paper on "the history of keratin extraction methods from waste chicken feathers". To be submitted in 2017.
12. **Pourjavaheri, F.**, Jones, O.A.H., Sherkat, F. & Shanks, R. A. A review paper on "when chicken feathers grabbed the scientist's attention and what has happened to date?". To be submitted in 2017.

Refereed Conference Publications:

13. **Pourjavaheri, F.**, Jones, O.A.H., Martinez Pardo, I., Sherkat, F., Gupta, A., & Shanks, R.A. (2017) "Keratin bio-composites with polysiloxane thermoplastic polyurethane", *Society of Plastic Engineers Annual Technical Conference (SPE-ANTEC)*, 8-10 May, Anaheim, California, USA.
14. **Pourjavaheri, F.**, Jones, O.A.H., Mohaddes, F., Sherkat, F., Kong, I., Gupta, A., & Shanks, R.A. (2016) "Analysis and Characterization of Novel Avian Keratin Fibre Based Bio-composites", *International Conference on Composites/Nano-Engineering (ICCE)*, 17-23 July, Hainan Island, China.
15. **Pourjavaheri, F.**, Jones, O.A.H., Mohaddes, F., Sherkat, F., Gupta, A., & Shanks, R.A. (2016) "Green Plastics: Utilizing Chicken Feather Keratin in Thermoplastic Polyurethane Composites to Enhance Thermo-Mechanical Properties", *Society of Plastic Engineers Annual Technical Conference (SPE-ANTEC)*, 23-25 May, Indianapolis, Indiana, USA.
16. **Pourjavaheri, F.**, Mohaddes, F., Shanks, R., Czajka, M. & Gupta, A. (2014) "Effects of Different Purification Methods on Chicken Feather Keratin", *The 5th International Conference on Manufacturing Science & Engineering (ICMSE)*, 19-20 April, Shanghai, China.
17. **Pourjavaheri, F.**, Shanks, R., Czajka, M., & Gupta, A. (2014) "Purification and characterisation of feathers prior to keratin extraction", *The 8th International Chemical Engineering Congress & Exhibition (IChEC)*, 24-27 February, Kish, Iran.

18. **Pourjavaheri, F.**, Shanks, R., Czajka, M., & Gupta, A. (2013) "Purification Methods for Chicken Feather Keratin", *International conference on Advanced Polymeric Materials (ICAPM)*, Kottayam, 11-13 October, Kerala, India.

Other Conference Publications:

19. **Pourjavaheri, F.**, Jones, O.A.H. & Shanks, R.A. (2017) "Chicken Feather Keratin Hair Conditioner", *Emerging Polymer Technologies Summit*, 22-24 November, Melbourne, Australia. (Oral Presentation)
20. **Pourjavaheri, F.**, Jones, O.A.H. & Shanks, R.A. (2017) "Biomaterial Applications of Avian-Keratin Refinement", *Emerging Polymer Technologies Summit*, 22-24 November, Melbourne, Australia. (Poster Presentation)
21. **Pourjavaheri, F.**, Jones, O.A.H., Sherkat, F. & Shanks, R.A. (2017) "Eco-friendly keratin extraction from waste chicken feathers", *Society for Environmental Toxicology and Chemistry (SETAC)*, 4-6 September, Gold Coast, Queensland, Australia. (Oral Presentation)
22. **Pourjavaheri, F.**, Jones, O.A.H., Sherkat, F. & Shanks, R.A. (2017) "Avian-Keratin Refinement", *Society for Environmental Toxicology and Chemistry (SETAC)*, 4-6 September, Gold Coast, Queensland, Australia. (Poster Presentation)
23. **Pourjavaheri, F.**, Jones, O.A.H., Smooker, P.M., Brkljača, R., Ostovar pour, S., Sherkat, F., Gupta, A., & Shanks, R.A. (2017) "Ecofriendly keratin extraction and characterisation from waste chicken feathers", *RACI National Centenary Conference*, 23-28 July, Melbourne, Australia. (Oral Presentation)
24. **Pourjavaheri, F.**, Jones, O.A.H., & Shanks, R.A. (2017) "Applications of chicken feather keratin", *ACS on Campus*, 21 July, Melbourne, Australia. (Poster Presentation)
25. **Pourjavaheri, F.**, Jones, O.A.H., Sherkat, F. & Shanks, R.A. (2017) "Applications of chicken feather keratin", *8th Annual ASMR VIC Student Research Symposium*, 1 June, Melbourne, Australia. (Abstract only)
26. **Pourjavaheri, F.**, Jones, O.A.H., Martinez Pardo, I., Sherkat, F., Gupta, A., & Shanks, R.A. (2017) "Design and characterisation of keratin composites", *Society of Plastic Engineers Annual Technical Conference (SPE-ANTEC)*, 8-10 May, Anaheim, California, USA. (Poster Presentation)
27. **Pourjavaheri, F.**, Jones, O.A.H., & Shanks, R.A. (2017) "Chicken feather keratin", *Beyond Research*, 21-23 February, Melbourne, Australia. (Poster Presentation)
28. **Pourjavaheri, F.**, Jones, O.A.H., & Shanks, R.A. (2016) "CF keratin in TPU-polyether", *Plastics & Waste Conference (SPE-ANTEC)*, 17 November, Melbourne, Australia. (Poster Presentation)

29. **Pourjavaheri, F.**, Jones, O.A.H., & Shanks, R.A. (2016) “Feather keratin fibres in composites”, *Asian Workshop on Polymer Processing (AWPP)*, 6-9 November, Melbourne, Australia. (Poster Presentation)
30. **Pourjavaheri, F.**, Jones, O.A.H., & Shanks, R.A. (2016) “Chicken feather keratin in bio-composites”, *All Hands Australia Conference*, 5 October, Melbourne, Australia. (Poster Presentation)
31. **Pourjavaheri, F.**, Jones, O.A.H., Mohaddes, F., A., & Shanks, R.A. (2016) "Chicken Feather Keratin and Thermoplastic Polyurethane Composites", *Society of Plastic Engineers Annual Technical Conference (SPE-ANTEC)*, 23-25 May, Indianapolis, Indiana, USA. (Poster Presentation)
32. **Pourjavaheri, F.**, Jones, O.A.H., Mohaddes, F., Sherkat, F., Kong, I., Gupta, A., & Shanks, R.A. (2016) “Development of Keratin Biofiber-TPU Green Plastics with Improved Thermo-Mechanical Properties”, *AGILENT Young Scientist Forum*, 4 March, Melbourne, Australia. (Oral Presentation)
33. **Pourjavaheri, F.**, Jones, O.A.H., & Shanks, R.A. (2016) “Green plastics: utilising chicken feather keratin as a sustainable resource to enhance the thermo-mechanical properties of polyurethane composites”, *Environmental Science Research Forum (EnSuRe)*, 18 February, Melbourne, Australia. (Oral Presentation)
34. Pourjavaheri, F., Shanks, R., **Close, C.** & Gupta, A. (2013) “Preliminary study on chicken feathers prior to Keratin Extraction”, *21st Annual RACI Environmental and Analytical Division R&D Topics Conference (RACI R&D)*, 12 December, Canberra, Australia. (Abstract published only) (Orally presented by Christine Close)
35. **Pourjavaheri, F.**, Shanks, R. & Gupta, A. (2013) “Derivation and Characterisation of Keratin Protein from Poultry Feathers”, *12th International Conference on Frontiers of Polymers and Advanced Materials (ICFPAM)*, 8-13 December, Auckland, New Zealand. (Abstract published only) (Poster Presentation)

Awards and Prizes:

1. Won the ACTS Conference 2017 Student Scholarship.
2. The scholarships to take part in the 2017 Journey environment entrepreneurship summer school in Europe, allocated by Climate KIC, EIT European Union and University of Melbourne to attend the Journey that took place from Budapest, Hungary (29 June) to Sofia, Bulgaria (23 July).
 - Meeting Hon. Lily D'Ambrosio MP on Wednesday 21st of June 2017, 3 pm, Minister for Energy, Environment and Climate Change, Minister for Suburban Development, at Parliament House.
 - Won the ‘award for Best Idea’ of the Climate KIC Journey 2017 competition, supported by EIT, a body of the European Union.

3. The Society of Plastics Engineers (SPE) Australia-New Zealand 2016 Section student award (\$3300) for the best conference paper titled: 'Green Plastics: Utilizing chicken feather Keratin in thermoplastic polyurethane composites to enhance thermo-mechanical properties', to go to the SPE conference in America, which was orally presented at ANTEC 2016 and published in the conference proceedings; and won a poster award of US \$100 voucher while there.
 - Complimentary registration to attend ANTEC 2017 held on 8-10 May, Anaheim, California, USA.
 - This article was selected for inclusion on the SPE blog:
<https://plasticsengineeringblog.com/2016/05/17/trolling-for-new-technology-antec-2016/>
 - This article appeared in the SPE magazine as an item of special interest in August 2016 (Vol 72, no. 7, page 41).
 - RMIT University is developing a story regarding this research for the media as well through Ms Gosia Kaszubska, who is a senior communications advisor and editor at RMIT News.
 - By presenting a poster titled 'Chicken feather keratin and thermoplastic polyurethane composites' I got positive and useful feedback from the viewers and the judges such as Dr Wedlake who is the President of Wedlake Industries, LLC., leading to an offer of collaboration involving his suggested polymer

4. Research Training Program (RTP) scholarship administered by RMIT University (2013 – 2016).



Summary

The aim of this research project was to curb the environmental impact of chicken feathers, a waste from the poultry industry, by value-adding and development of bio-composites with improved biodegradability and thermo-mechanical properties, and to extract keratin from the feathers for inclusion in biomaterials for potential consumer applications.

The first step in the application of chicken feathers involved thorough cleaning and disinfection since plucked chicken feathers impose severe microbiological hazards. Therefore, the design of a proper purification method in respect to the final application was necessary. Different surfactants including anionic, non-ionic, and cationic; bleach such as ozone and chlorine dioxide; ethanol extraction; and a combined method comprising surfactant–bleach–ethanol extraction were applied to chicken feathers and their bactericidal performance was investigated via a) Standard Plate Count, b) the enumeration of *Escherichia coli*, *Pseudomonas* species, coagulase positive *Staphylococcus*, aerobic and anaerobic spore-formers and c) *Salmonella* and *Campylobacter* detection tests. Among all practices, only the ethanol extraction and combined method eliminated *Salmonella* from the feathers. Although ethanol-extraction showed superior bactericidal decontamination compared with the combined method, the feathers purified with the latter method showed better morphological and mechanical properties. Scanning electron microscopy-energy dispersive spectroscopy

confirmed the presence of sodium lauryl sulphate remnants in the feathers after applying the combined method. Fourier-transform infrared spectroscopy was adopted for the qualitative characterisation of the feathers before and after purification. Chicken feather characterisation including α -helix conformation in the feather wool, and pleated sheet in barbs and rachis, are presented herein. The pH, visual observation, optical microscopy under visible and ultraviolet lights, scanning electron microscopy, micro X-ray diffraction, wide-angle X-ray scattering, infrared spectroscopy, vibrational spectroscopy and thermogravimetry were used to characterise the feathers before and after purification and residues after extraction.

The next consideration was to find a use for waste feathers. Two polyurethane based polymers were combined with chicken feather fibres, to form bio-composites. Thermoplastic polyether-polyurethane was used via solvent-casting-evaporation-compression moulding method at 10, 20, 30, 40, 50, 60 and 70 %·w/w of chicken feather fibres; and thermoplastic polysiloxane-polyurethane was used via solvent-casting-evaporation-compression moulding, and solvent-precipitation-evaporation-compression moulding methods to create new bio-composites incorporating 10 and 20 %·w/w of chicken feather fibres into the polyurethane. Compatibility of polyurethanes with the feather fibres and the thermo-mechanical properties of the resulting bio-composites were determined and using thermogravimetry, dynamic mechanical analysis and stress-strain measurements with hysteresis loops. The uniformity of the feather fibres dispersion in the polyurethane matrix was investigated via macro-photography. Scanning electron microscopy of fractured surfaces of the bio-composites was used to verify that the adhesion between fibre and polymer was effective. Molecular modelling visualisation predicted the existence of hydrogen bonding between fibres and polyurethane molecules and this result was supported by Fourier-transform infrared analysis of the composite. The addition of chicken feather fibres to the polyurethane matrixes was found to decrease the glass transition temperature, recovery strain

and thermal mass loss of the composites, but increase the elastic modulus (hardness), storage modulus and char level on thermal decomposition. The thermo-mechanical properties of these polymers were enhanced by addition of keratin feather fibres. The utilization of ecofriendly, bio-based composites has been reported in many areas including, but not limited to, the packaging, insulation, automotive, building and roofing industries, as well as for separation membranes for water treatment. The applications of the produced bio-composites are steps towards more environmentally-friendly and more cost effective products.

Keratin was then extracted from different segments of disposable chicken feathers including whole feathers, calamus and rachis (composed mainly of beta-pleated sheet structures), barbs and barbules (composed mainly of alpha-helix), using sodium sulfide or L-cysteine. The extraction process involved dissolving the chicken feathers by reducing its disulfide links, then separating the protein from the medium by centrifugation. Once the feathers were dissolved, the pH of solution was adjusted to the isoelectric point using hydrochloric acid, to precipitate the proteins, and the yield of extracted keratin with sodium sulfide ($88 \pm 3 \%$) was higher than with L-cysteine ($66 \pm 4 \%$). The precipitated keratin was washed three times with distilled water. The presence of protein obtained from different methods was confirmed using the biuret test, and the Bradford assay enabled the concentration of keratin to be determined. The precipitated keratin was characterised using gel electrophoresis, which confirmed soluble protein of molar mass 11 kg/mol and estimated its purity to be over 95 %. Liquid chromatography-mass spectrometry verified the molar mass of the extracted material matched that of chicken keratin. Vibrational and nuclear magnetic resonance spectroscopy confirmed the structure of keratin was retained following extraction. Thermogravimetry of original purified chicken feather and keratin extracted via sodium sulfide treatment showed virtually identical decomposition behaviour, proving the

purity of the keratin. In contrast, thermogravimetry of keratin extracted with L-cysteine indicated it may contain residual L-cysteine.

The structure of keratins extracted from different segments of waste chicken feathers via sodium sulfide and L-cysteine, have been subjected to further nuclear magnetic resonance spectroscopy and analysed for their antibacterial properties on *Staphylococcus aureus* and *Escherichia coli* as Gram-positive and Gram-negative species, respectively. The goal of this section was to produce an extract and to characterise several aspects of its behaviour that may have implications for its use as a biomaterial. Hence, the keratin extracted using sodium sulfide was incorporated into hair conditioner and cream, and used in hair and leather treatments to determine their interactions with animal tissues. These experiments confirmed and expanded earlier findings that keratin demonstrated excellent compatibility in biological systems, as the highest keratin concentration experimental cream and conditioner, had the best outcomes.

Finally, this study presents suggestions for future fundamental studies and proposals for the development of keratin-based materials for biomedical and consumer product applications.



Table of Contents

Declaration	II
Dedication	III
Acknowledgement	IV
Publications	VII
Summary	XII
Table of Contents	XVI
List of Figures	XXIX
List of Tables	XXXIX
Abbreviations, Acronyms and Nomenclature	XLII

Chapter 1 _____ **Introduction**

1.1	Overview	2
1.2	Rationale	3
1.3	Scope	4
1.4	Aim	5
1.5	Objectives	5
1.6	Research questions	6
1.7	Thesis structure	8
1.8	References	11

2.7	Chicken feather keratin	48
2.7.1	Extraction of keratin from chicken feather fibres	48
2.8	Antibacterial effects of chicken feather keratin	55
2.9	Applications of chicken feather keratin	56
2.10	References	58

Chapter 3 --- **Experimental**

3.1	Introduction	69
3.2	Materials	70
3.3	Characterisation equipment	74
3.3.1	Stereoscopic optical microscopy	74
3.3.2	Scanning electron microscopy-energy dispersive spectroscopy	75
3.3.3	X-ray diffraction analysis	77
3.3.3.1	X-ray scattering via Bruker D8 Discover micro-XRD diffractometer	78
3.3.3.2	Wide angle X-ray scattering via Bruker AXS D4 Endeavour .	79
3.3.4	Nuclear magnetic resonance spectroscopy	80
3.3.5	Fourier-transform infrared spectroscopy	82
3.3.6	Vibrational spectroscopic analysis	84
3.3.7	Thermal analysis	86
3.3.7.1	Differential scanning calorimeter	86

3.3.7.2	Thermogravimetric analyser	87
3.3.9	Heated hydraulic press	88
3.3.10	Mechanical properties	89
3.3.10.1	Dino-Lite digital microscope	89
3.3.10.2	Stress–strain tensile mechanical analysis	90
3.3.10.3	Hysteresis analysis	90
3.3.10.4	Dynamic mechanical analysis - Temperature scanning	91
3.3.10.5	Dynamic mechanical analysis - Isothermal scanning	93
3.3.11	Feather processing	93
3.3.12	pH measurements	94
3.3.13	Centrifuge	95
3.4	References	95

Chapter 4 ___ Purification of waste chicken feathers to refined keratin fibres

4.1	Introduction	98
4.2	Experimental	100
4.2.1	Materials	100
4.2.2	Purification methods	100
4.2.2.1	Purification by surfactants	101
4.2.2.2	Purification via Soxhlet extraction with ethanol	102
4.2.2.3	Purification by ozone	102
4.2.2.4	Purification by chlorine dioxide	103

4.2.2.5	Combined purification treatment	104
4.2.3	Microbiological tests on CFFs	104
4.2.3.1	Bacterial enumeration	106
4.2.3.2	Detection of <i>Salmonella</i> and <i>Campylobacter</i> species	107
4.3	Characterisation	107
4.3.1	Morphological analysis	107
4.3.2	Scanning electron microscopy-energy dispersive spectroscopy	107
4.3.3	Fourier-Transform Infrared spectroscopy	108
4.3.4	Mechanical properties of purified CFFs	108
4.4	Results and discussion	109
4.4.1	Standard aerobic plate count	109
4.4.2	Aerobic and anaerobic spore-formers, coagulase positive <i>Staphylococcus</i> , <i>Escherichia coli</i> , <i>Pseudomonas</i> , <i>Salmonella</i> and <i>Campylobacter</i> species	111
4.4.3	Morphological analysis	112
4.4.4	Scanning electron microscopy and energy dispersive spectroscopy	113
4.4.5	FTIR spectroscopy	115
4.4.6	Mechanical properties	116
4.5	Conclusions	118
4.6	References	119
4.7	Publications from this Chapter	121

Chapter 5 Characterisation of chicken feather fibres

5.1	Introduction	123
5.2	Experimental	123
5.2.1	Materials	123
5.2.2	Characterisation methods	123
5.2.2.1	Storage of feathers	124
5.2.2.2	Morphological analysis and stereoscopic microscopy	124
5.2.2.3	Scanning electron microscopy	124
5.2.2.4	Micro X-ray diffraction and wide angle X-ray scattering analysis	125
5.2.2.5	Fourier-Transform Infrared spectroscopy	125
5.2.2.6	Vibrational spectroscopic analysis	125
5.2.2.7	Thermal analysis	125
5.3	Results and discussion	125
5.3.1	Storage of feathers	125
5.3.2	Visual observation	127
5.3.3	Stereoscopic microscopy	128
5.3.4	Scanning Electron Microscopy	131
5.3.5	X-ray analysis	132
5.3.5.1	Micro X-ray diffraction	132
5.3.5.2	Wide angle X-ray scattering	136

5.3.6	Infrared Spectroscopy	137
5.3.7	Vibrational Spectroscopy	143
5.3.8	Thermal behaviour	144
5.4	Conclusions	145
5.5	References	146
5.6	Publications from this Chapter	148

Chapter 6 _____ Design and characterisation of sustainable bio-composites from chicken feather keratin and thermoplastic Polyether–Polyurethane

6.1	Introduction	150
6.2	Experimental	153
6.2.1	Materials	153
6.2.2	Composites fabrication	154
6.2.3	Molecular modelling visualisation of the interaction between keratin and TPU-polyether	155
6.2.3.1	Molecule construction	156
6.2.3.2	Amorphous cell	156
6.2.3.3	Molecular interaction	156
6.2.4	Characterisation of bio-composites	157

6.2.4.1	Morphological analysis and scanning electron microscopy	157
6.2.4.2	Thermal analysis	157
6.2.4.3	Thermo-mechanical analysis	158
6.2.4.4	Infrared spectroscopy	159
6.3	Results and discussion	159
6.3.1	Fibre dispersion and physical appearance	159
6.3.2	Molecular visualisation	161
6.3.3	Scanning electron microscopy	164
6.3.4	Thermal behaviour	165
6.3.4.1	Differential scanning calorimetry	165
6.3.4.2	Thermogravimetry	166
6.3.5	Mechanical properties	170
6.3.5.1	Stress–strain tensile mechanical analysis	170
6.3.5.2	Modulated force – thermomechanometry	173
6.3.6	Infrared spectroscopy	176
6.4	Conclusions	180
6.5	References	183
6.6	Publications from this Chapter	187

Chapter 7 _____ Design and characterisation of sustainable bio-composites

from chicken feather keratin and thermoplastic Polysiloxane-Polyurethane

7.1	Introduction	189
7.2	Experimental	191
7.2.1	Materials	191
7.2.2	Composites fabrication	191
7.2.3	Physical appearance	192
7.2.4	Molecular modelling visualisation	192
7.2.5	Thermal analysis	193
7.2.6	Thermo-mechanical analysis	193
7.3	Results and discussion	194
7.3.1	Fibre dispersion	194
7.3.2	Molecular visualisation	196
7.3.3	Thermal degradation and remaining char ratio	197
7.3.4	Stress–strain tensile mechanical analysis	200
7.3.5	Modulated force – thermomechanometry	202
7.4	Conclusions	202
7.5	References	203
7.6	Publications from this Chapter	205

Chapter 8 _____ Extraction of keratin from waist chicken feather fibres

8.1	Introduction	207
8.2	Experimental	209
8.2.1	Materials	209
8.2.2	Chicken feather preparation	209
8.2.3	Extraction of keratin	209
8.2.4	Yield calculation	211
8.2.5	Characterisation of keratin	211
8.2.5.1	Biuret test	211
8.2.5.2	Keratin concentration	212
8.2.5.3	Sodium dodecyl sulfate-polyacrylamide gel electrophoresis ..	212
8.2.5.4	Proteomic analysis	213
8.2.5.4.1	LC-MS/MS	213
8.2.5.4.2	MS data analysis	213
8.2.5.5	Fourier-transform infrared spectroscopy	214
8.2.5.6	Vibrational spectroscopic analysis	214
8.2.5.7	Nuclear magnetic resonance spectroscopy (solid-state)	214
8.2.5.8	Thermogravimetry	214
8.3	Results and discussion	215
8.3.1	Reduction of disulfide bonds	215
8.3.2	Yield analysis	217
8.3.3	Characterisation of the extracted chicken feather keratin	217

8.3.3.1	Biuret test	217
8.3.3.2	Keratin concentration	218
8.3.3.3	Keratin molar mass	219
8.3.3.4	LC-MS/MS	220
8.3.3.5	Infrared spectroscopy	220
8.3.3.6	Vibrational spectroscopic analysis	223
8.3.3.7	Solid-state NMR studies	225
8.3.3.8	Thermal behavior	228
8.4	Conclusions	231
8.5	References	232
8.6	Publications from this Chapter	235

Chapter 9 _____ Applications of keratin extracted from chicken feather fibres

9.1	Introduction	237
9.2	Experimental	240
9.2.1	Materials	240
9.2.2	Nuclear magnetic resonance spectroscopy (NMR) (liquid-state)	241
9.2.3	Antimicrobial assays on chicken feathers and chicken feather keratins .	242
9.2.3.1	Standardising of <i>Escherichia coli</i> and <i>Staphylococcus aureus</i> to 0.5 McFarland (ca. 1 x 10 ⁸ cfu/mL)	242
9.2.3.2	Disk diffusion plating method	242
9.2.3.3	Well diffusion plating method	243

9.2.3.4	Feather diffusion plating method	243
9.2.4	Keratin hair conditioning preparation	244
9.2.5	Keratin-enriched cream preparation	244
9.2.6	Characterisation of keratin-based materials	244
9.2.6.1	Morphological analysis via scanning electron microscopy	244
9.2.6.2	Mechanical properties	245
9.3	Results and discussion	245
9.3.1	Liquid-state NMR studies	245
9.3.2	Antibacterial analysis	248
9.3.3	Scanning electron microscopy	251
9.3.4	Mechanical properties	253
9.4	Conclusions	257
9.5	References	258
9.6	Publications from this Chapter	260

Chapter 10 _____ **Overall project analysis and evaluation**

10.1	Overall discussion	262
10.2	References	268

Chapter 11 _____ **Conclusions and Recommendations**

11.1	Conclusions	270
------	-------------------	-----

11.2	Applications	272
11.3	Future directions and novel applications of keratin	273
11.4	Recommendations	274
11.5	References	276

Appendix _____

Appendix 1	Journal Publications	A2
Appendix 2	Journal manuscripts to be Published	A6
Appendix 3	Conference Publications	A11
Appendix 4	Poster Publications	A18

	represents the main covalent interaction in α -keratin fibres and may exist as either an interchain linkage between two chains or as an intrachain linkage between two components of the same polypeptide chain	26
Figure 2.9	Chemical skeletal structures of amino acid found in chicken feather keratin	28
Figure 2.10	Schematic diagram of different components of keratin; (A) polypeptide single unit, (B) amino acid sequence, (C) α -helix, and (D) β -Sheets conformations of keratin protein	29
Figure 2.11	Turbulent flow chamber for feather separation a) an organ separator having an inner input tube concentric with an outer cylinder and b) the organ separator of (a) modified to utilise cascading flared circular sections concentric with the outer cylinder	33
Figure 2.12	Schematic drawing showing the basic steps of making fibres from feathers and some uses for the fibre and fibre pulp compositions	33
Figure 2.13	Schematic representative of a cone separator having a cylindrical base with a cone-shaped cover through which separated fibres may exit	34
Figure 2.14	Schematic drawing of a comb/brush separator (side and top views)	34
Figure 2.15	Sketch of Stripping Machine	35
Figure 2.16	Separation of quill segments from barb fibres, the quill floated and the barb fibre sunk in a plastic cylinder	36
Figure 2.17	Different types of composites: (a) reinforced by particles, (b) reinforced by chopped strands, (c) unidirectional composites, (d) laminates, (e) fabric reinforced plastics, (f) honeycomb composite structure (adopted from Kokcharov)	42
Figure 2.18	Diagrammatic representation of fibre reinforcement composites: (a) continuous fibre reinforcements, and (b) Discontinuous fibre reinforcements	43
Figure 2.19	Diagrammatic representation of fibre origins	44
Figure 2.20	Reduction of disulfide bonds by ammonium bisulfide	49
Figure 2.21	Basic chemical structure of an ionic liquid	49

Figure 2.22	Chemical structure of BMIM ⁺ Cl ⁻	50
Figure 2.23	Diagram of production of regenerated chicken feather fibres	52
Figure 2.24	Schematic representations for SDS-keratin complexes with a high amount of SDS added prior to dialysis	54
Figure 2.25	Bacterial cell wall representation, difference between (a) Gram-negative and (b) Gram-positive bacteria	56

Chapter 3 _____ **Experimental**

Figure 3.1	An optical microscope, Nikon Labophot, model 1.25, with Nikon phase contrast 2	75
Figure 3.2	FEI Quanta 200 scanning electron microscopy with an attached Oxford Instruments XMaxN20 spectrometer for EDS	76
Figure 3.3	Preparing an SEM sample: (a) the chicken feather used, (b) the calamus, rachis, and barbs of a chicken feather on a stub with double sided carbon tape (c) gold-coated sample	76
Figure 3.4	Gold and carbon vacuum sputter coater SPI Sputter Coater Z11430 .	77
Figure 3.5	The Bragg Law Principle	78
Figure 3.6	Bruker D8 Discover micro-XRD diffractometer (GADDS).....	78
Figure 3.7	Bruker AXS D4 Endeavour Wide-angle X-ray scattering (WAXS) ...	79
Figure 3.8	(a) A 500 MHz Agilent DD2 console; (b) NMR tubes contain keratin samples (c) in a tube holder	81
Figure 3.9	(a) PerkinElmer 400 FTIR, (b) feather on crystal with force gauge	83
Figure 3.10	(a) ethanol from the soxhlet flask containing feather residues, (b) portion of extraction poured in a watch glass for ethanol evaporation (c) the last drop transferred on the FTIR using a pipette, and (d) a drop of the extraction on the FTIR diamond	84

Figure 3.11	(a) PerkinElmer Raman Station 400F, (b) showing glass slide and camera (with protective hood raised), (c-e) Xplora Plus (Horiba LabRAM HR Evolution micro-Raman system)	85
Figure 3.12	(a) PerkinElmer Pyris 1 differential scanning calorimeter (DSC) and (b) Mettler Toledo MX5.....	86
Figure 3.13	Perkin Elmer TGA 7 thermogravimetric analyser	88
Figure 3.14	Heated hydraulic press or thermal press or compression moulding	89
Figure 3.15	A Dino-Lite AM4013T-M40 from AnMon Electronics Co.	90
Figure 3.16	A DMA Q800 system from TA Instruments	90
Figure 3.17	A PerkinElmer Pyris Diamond DMA 2003	91
Figure 3.18	DMA showing mounting of a TPU/CFFs bio-composite (centre), heater unit (right-hand side) and metal protective plate (bottom)	92
Figure 3.19	Measurement range graph showing Log (geometry factor) (m) versus Log (elasticity)/Pa of the sample (blue circle) which must remain between the red lines	93
Figure 3.20	IKA® A11 Crushing Analytical Mill, equipped with stainless steel cutting blades and inner tank, grinding CFFs to the size of 5 µm to 2 cm	94
Figure 3.21	Rocklabs Ringmill Grinder, equipped with a zirconia mill head, grinding CFFs to powder form from Rocklabs Ltd., Auckland, New Zealand ...	94
Figure 3.22	A Sorvall RC-5C from 1991 centrifuge	95

Chapter 4 _____ Purification of CFFs

Figure 4.1	Comparing the microbiological and mechanical properties of CFFs purified by surfactants, disinfectants, sanitisers and their combinations	100
Figure 4.2	Purification of chicken feather fibres by surfactants	101
Figure 4.3	Purification of chicken feather fibres with Soxhlet method	102

Figure 4.4	An Enaly Ozone Generator (left) and purification of chicken feather fibres by ozone (right).....	103
Figure 4.5	Purification of chicken feather fibres by Chlorine dioxide	103
Figure 4.6	Purification of chicken feather fibres via combined purification treatment	104
Figure 4.7	Microbial analyses on purified CFFs	105
Figure 4.8	Microbial count (cfu/g) of SPC, aerobic spore-formers and anaerobic spore-formers for (T0) untreated chicken feathers upon receipt, versus chicken feathers purified with (T1) SEEt treatment, (T2) O3 solution, (T3) ClO ₂ solution, (T4) PEG solution, (T5) SLS solution, (T6) CTAC solution and (T7) SLS-ClO ₂ -SEEt combination	109
Figure 4.9	The structure of a semiplume chicken feather (fibre or wool: barbs/barbules), (quill: calamus/rachis or shaft), (vane: rachis/barb/barbules) treated with T7; B) Images of the semiplume chicken feathers: (T0) untreated upon receipt, (T1) SEEt treatment, (T2) O3 solution, (T3) ClO ₂ solution, (T4) PEG solution, (T5) SLS solution, (T6) CTAC solution, and (T7) SLS-ClO ₂ -SEEt combination.....	113
Figure 4.10	(a): SEM, SEM-EDS, and elemental data derived from the CFFs treated via SEEt (T1) (b): SEM, SEM-EDS, and elemental data derived from the CFFs treated via SLS-ClO ₂ -SEEt (T7)	114
Figure 4.11	FTIR spectra of original CFFs (T0) and CFFs purified via SEEt (T1) and SLS-ClO ₂ -SEEt (T7)	116
Figure 4.12	Tensile stress-strain curve of single CFFs purified via SEEt (T1) and SLS-ClO ₂ -SEEt (T7)	117

Chapter 5 Characterisation of CFFs

Figure 5.1	pH measurement of CFs rinsed water using pH HACH [®] SensION5™ Portable pH Meter	127
Figure 5.2	a) Untreated contour chicken feather (T0) after oven drying versus semiplume chicken feathers purified with b) SEEt treatment (T1), c)	

	SLS solution (T5), d) PEG solution (T4), e) O ₃ solution (T2), f) ClO ₂ solution (T3), and g) untreated contour pigeon feather 127
Figure 5.3	Optical microscopic images of a chicken feather segments at (a) 60X, (b), (c) and (d) 100X magnification 128
Figure 5.4	The structures of a semiplume chicken feather under natural visible and ultraviolet light at 80X magnification, (a) calamus, (b) rachis, barb and barbules from the bottom of a chicken feather, (c) rachis, barb and barbules from the top of a chicken feather 129
Figure 5.5	The structures of a contour pigeon feather under natural visible and ultraviolet light at 80X magnification 130
Figure 5.6	Chicken segments under natural and ultraviolet light at 80X magnification a) untreated chicken feathers upon receipt (T0), chicken feathers purified with b) SLS solution (T5), c) PEG solution (T4), d) SEEt treatment (T1), e) O ₃ solution (T2) and f) ClO ₂ solution (T3) 131
Figure 5.7	The SEM images of the chicken feather fibres purified by SLS solution (T5) at a) 40X, b) 50X, c) 100X, d) 160X, e) 200X, f and g) 400X, h and i) 800X, j) 1500X, k and l) 3000X magnifications 133
Figure 5.8	The micro X-ray diffraction pattern of chicken feather barbs and barbules (α -keratin) with a 2θ at a) 30°, b) 50° and c) 70° 134
Figure 5.9	The micro X-ray diffraction pattern of chicken feather calamus and rachis (β -keratin) with a 2θ at a) 30°, b) 50° and c) 70° 135
Figure 5.10	Diffraction intensities of a) barbs/barbules and b) calamus/rachis of chicken feathers 136
Figure 5.11	FTIR analysis of different parts of a feather: a) calamus, b) middle of the rachis c) tip of the rachis and d) barb 138
Figure 5.12	FTIR spectra of a chicken feather segments a) (T0) untreated chicken feathers upon receipt, versus chicken feathers purified with b) (T1) SEEt treatment, c) (T5) SLS solution, d) (T4) PEG solution, e) (T2) O ₃ solution f) (T3) ClO ₂ solution, g) (T6) CTAC solution and h) (T7) SLS-ClO ₂ -SEEt combination 139
Figure 5.13	Comparison of FTIR spectra of an untreated chicken feather with its Soxhlet extraction residues 140

Figure 5.14	Comparison of FTIR spectra of a) α -keratin (barb middle) and b) β -keratin (calamus) of a chicken feather fibres: untreated chicken feathers upon receipt (T0), versus chicken feathers purified with SEEt treatment (T1), O ₃ solution (T2), ClO ₂ solution (T3), PEG solution (T4) and SLS solution (T5)	141
Figure 5.15	Comparison of FTIR spectra of chicken and pigeon feather fibres and sheep wool fibres, a) individually, and b) superimposed	142
Figure 5.16	Raman spectra of chicken feathers a) barb and b) rachis c) residue from (T1) SEEt treatment	143
Figure 5.17	Comparison of the thermogravimetry (TG) curves for untreated and treated chicken feathers along with their derivatives (DTG) curves; (T0) untreated chicken feathers upon receipt, (T1) SEEt treatment, (T2) O ₃ solution, (T3) ClO ₂ solution, (T4) PEG solution, (T5) SLS solution	145

Chapter 6 _____ **TPU-polyether–CFF Bio-composites**

Figure 6.1	Chicken feather keratin, TPU-polyether granules and schematic representation of the chemical structure of TPU-CFF bio-composite	152
Figure 6.2	Macro photographic images of the TPU-CFF reinforced bio-composites; a) TPU-polyether polymer, b) 10%·w/w CFF, c) 20 %·w/w CFF, d) 30 %·w/w CFF e) 40 %·w/w CFF, f) 50 %·w/w CFF g) 60 %·w/w CFF h) 70 %·w/w CFF	160
Figure 6.3	Possible links between the CFF and TPU(polyether)	161
Figure 6.4	One molecule of CFF keratin surrounded by one molecule of TPU-polyether a) Amorphous cell with periodic boundary conditions of the keratin surrounded by the TPU-polyether; b) Molecular modelling visualization of the intermolecular hydrogen bonds (purple dashed lines) between TPU-polyether and CFF keratin	162
Figure 6.5	The SEM micrographs showing cross-sections of a 20 %·w/w CFF reinforced bio-composite at 500X magnifications	164
Figure 6.6	The DSC of CFFs, TPU-polyether and TPU-CFF bio-composites at 10 and 20 %·w/w concentrations	166

Figure 6.7	Panel a) TGA thermograms (mass loss), and b) derivative mass of CFFs, TPU-polyether polymer and TPU-CFF bio-composites at 10 to 70 %·w/w CFF concentrations 167
Figure 6.8	Stress–strain tensile mechanical analysis of pure TPU-polyether and TPU-CFF bio-composites at 10 to 70 %·w/w concentrations, (a) Stress–strain hysteresis, (b) Elastic modulus (E) 172
Figure 6.9	Dynamic mechanical analysis curves of pure TPU-polyether and TPU-CFF bio-composites at 10 to 70 %·w/w concentrations, (a) Storage modulus (E'), (b) Loss modulus (E'') and c) Loss tangent ($\tan\delta$) 174
Figure 6.10	FTIR spectra of (a) TPU-polyether and TPU-CFF bio-composites before and after compression moulding or thermal pressing (b) Comparison of TPU-CFF 20 %·w/w spectra before and after compression moulding or thermal pressing 177
Figure 6.11	Comparison of the physical properties of the TPU-CFF bio-composites with related materials 179

Chapter 7 _____ Polysiloxane-TPU–CFF Bio-composites

Figure 7.1	Proposed links between the CFF and polysiloxane-TPU 190
Figure 7.2	Macro photographic images of a) pure TPU-polysiloxane and b) TPU-polysiloxane with 20 %·w/w CFF made via the casting technique; c) pure TPU-polysiloxane and d) 20 %·w/w CFF - TPU-polysiloxane made via the precipitation method 194
Figure 7.3	Schematic representation of the chemical structure of TPU-polysiloxane 195
Figure 7.4	Molecular modeling visualization of one molecule of CFF keratin surrounded by one molecule of TPU-polysiloxane. Key: O: red, Si: yellow, C: grey, H: pink, N: blue, purple dashed lines: hydrogen bonds 196
Figure 7.5	TGA thermograms of TPU-polysiloxane polymer and TPU-CFF bio-composites at 0 to 20 %·w/w CFF concentrations via casting and precipitation techniques a) mass loss, b) first derivative 198

Figure 7.6	Stress–strain hysteresis tensile mechanical analysis of pure TPU-polysiloxane and 20 %-w/w CFF bio-composites via casting and precipitation techniques	201
------------	--	-----

Chapter 8 _____ **Keratin extraction from CFFs**

Figure 8.1	The extraction process of keratin from waste chicken feathers using sodium sulfide and L-cysteine	210
------------	---	-----

Figure 8.2	Reducing disulfide bonds of chicken feather keratin via Solutions-A and -B	216
------------	--	-----

Figure 8.3	The peptide bond in the Biuret solution caused violet colour in different keratin solutions containing CFFs in Na ₂ S (a) whole, (b) β -sheet, (c) α -helix, and in L-cysteine (d) whole, (e) β -sheet, (f) α -helix	218
------------	---	-----

Figure 8.4	The SDS-PAGE patterns of (a) protein standard, and the various extracted CFK using Na ₂ S (b), α -helix (c) β -sheet, d) whole, and in L-cysteine (e) α -helix, (f) β -sheet, (g) whole. The red arrow indicates the main keratin bands at 11 kg/mol (11 kDa)	219
------------	--	-----

Figure 8.5	FTIR spectra of (a) purified CFFs, (b) keratin extracted from whole CFF via Na ₂ S aged after six months, (c) keratin extracted from whole CFF via Na ₂ S, (d) keratin extracted from β -sheet parts of CFF via Na ₂ S, (e) keratin extracted from α -helix parts of CFF via Na ₂ S, (f) Solution-A, (g) keratin extracted from whole CFF via L-cysteine aged after six months, (h) keratin extracted from whole CFF via L-cysteine, (i) keratin extracted from β -sheet parts of CFF via L-cysteine, (j) keratin extracted from α -helix parts of CFF via L-cysteine, (k) Solution-B, (l) L-cysteine powder, (m) urea powder	221
------------	---	-----

Figure 8.6	Raman spectra of (a) β -sheet parts of CFFs, (b) α -helix parts of CFFs, (c) keratin extracted from whole CFF via Na ₂ S aged after six months, (d) fresh keratin extracted from whole CFF via Na ₂ S, (e) keratin extracted from β -sheet parts of CFF via Na ₂ S, (f) keratin extracted from α -helix parts of CFF via Na ₂ S, (g) Solution-A, (h) keratin extracted from whole CFF via L-cysteine aged after six months, (i) keratin extracted from whole CFF via L-cysteine, (j) keratin extracted from β -sheet parts of CFF via L-cysteine, (k) keratin extracted from α -helix parts of CFF via L-cysteine, (l) Solution-B, (m) L-cysteine powder, (n) urea powder	224
------------	--	-----

Figure 8.7	¹ H SSNMR spectra of chicken feathers (a) barbs and barbules (composed mainly of α -helix), (b) calamus and rachis (composed mainly of β -sheet structures), (c) whole feather 227
Figure 8.8	¹ H SSNMR spectra of extracted chicken feathers (a) barbs and barbules (composed mainly of α -helix), (b) calamus and rachis (composed mainly of β -sheet structures), and (asterisk indicates residual cysteine) 228
Figure 8.9	(a) TGA, and (b) DTG thermograms (mass loss) of L-cysteine, urea and purified CFFs compared with keratin extracted from whole CFF, β -sheet and α -helix parts via Na ₂ S and L-cysteine 230

Chapter 9 Applications of CFFs

Figure 9.1	¹ H NMR spectra of (a) authentic human epidermis keratin, and keratin extracted with sodium sulfide from chicken feathers components: (b) barbs and barbules (composed mainly of α -helix) (c) calamus and rachis (composed mainly of β -sheet structures) 247
Figure 9.2	The gCOSY NMR spectra of (a) authentic human epidermis keratin, and extracted chicken feather keratins using sodium sulfide; (b) barbs and barbules (composed mainly of α -helix) (c) calamus and rachis (composed mainly of β -sheet structures) 247
Figure 9.3	Human hair at 800X to 1500X magnifications: (a) Untreated natural, (b) dyed relaxed; Treated with experimental keratin-free conditioner (c) natural and (d) dyed relaxed hair treated with experimental conditioner with 2.5 % keratin, (e) natural and (f) dyed relaxed hairs treated with experimental conditioner with 5.0 % keratin, (g) natural and (h) dyed relaxed hair treated with commercial keratin conditioner, (i) natural and (j) dyed relaxed hairs 252
Figure 9.4	Original bovine leather at (upper = 70-250X, lower = 1000X) magnifications: (a) Untreated, (b) Treated with experimental 0 % keratin cream, (c) Treated with experimental 2.5 % keratin cream, (d) Treated with experimental 5.0 % keratin cream 253
Figure 9.5	Tensile stress–strain curve of (a) human hair, and (b) bovine leather . 254

Chapter 5 _____ **Characterisation of CFFs**

Table 5.1	pH of the chicken feathers purified with different techniques	126
Table 5.2	Peak decomposition temperature of purified and untreated chicken feathers	144

Chapter 6 _____ **TPU-polyether–CFF Bio-composites**

Table 6.1	Compositions of developed TPU-CFF bio-composites and their respective densities	155
Table 6.2	Amino acid sequences with corresponding colour residue and secondary structure	163
Table 6.3	Thermal data of CFFs, TPU-polyether and TPU-CFF bio-composites at 10 to 70 %·w/w concentrations obtained by TGA	168
Table 6.4	Mechanical test properties of TPU-polyether and TPU-CFF bio-composites at various CFF concentrations	171
Table 6.5	Comparison of the physical properties of the TPU-CFF bio-composites with related materials	179

Chapter 7 _____ **Polysiloxane-TPU–CFF Bio-composites**

Table 7.1	Concentrations used in the preparation and characterisation of TPU-CFF bio-composites and their respective densities	192
Table 7.2	Thermal data of TPU-polysiloxane and TPU-CFF bio-composites at 20 %·w/w concentrations via casting and precipitation techniques obtained by TGA	199
Table 7.3	DMA data of TPU-polysiloxane and 20 %·w/w CFF composites via casting and precipitation techniques	200

Chapter 8 _____ **Keratin extraction from CFFs**

Table 8.1	The keratin yield analysis	217
Table 8.2	Estimated concentrations of extracted keratins (via BioPhotometer plus Eppendorf spectrophotometer and Bradford assay)	218
Table 8.3	Thermal data of L-cysteine, urea, purified CFFs and keratin extracted from whole CFF, β -sheet and α -helix parts via Na ₂ S and L-cysteine	231

Chapter 9 _____ **Applications of CFFs**

Table 9.1	Concentrations of extracted chicken feather keratins (CFKs) with sodium sulfide or L-cysteine from different segments of chicken feather fibres (CFFs) dissolved in <i>d</i> ₆ -DMSO and UTM-Solution	248
Table 9.2	Zone of inhibition diameter of keratin powders in <i>d</i> ₆ -DMSO or UTM-Solution, on selected strains, using disk diffusion method	249
Table 9.3	Zone of inhibition diameter of keratin powders on selected strains using well diffusion method	250
Table 9.4	Mechanical properties of keratin-treated and untreated human hair	256
Table 9.5	Mechanical properties of untreated and treated bovine leather	256



ABBREVIATIONS, ACRONYMS AND NOMENCLATURE

α	alpha	BMIM ⁺ Cl ⁻	1-butyl-3-methylimidazolium chloride
β	Beta	BPA	Baird-Parker Agar
θ	Theta - Angle of diffraction	BSA	Bismuth sulphite agar
$^{\circ}$	Degree	C	Celsius
μ	Micro (10^{-6})	C=C	Carbon-carbon double bond
μm	Micrometre	<i>ca.</i>	circa
\sim	Approximately	CF	Chicken feather
/	Per	CFs	Chicken feathers
%	Percent	CFF	Chicken feather fibre
Å	Angstrom (1 Å = 0.1 nm)	CFFs	Chicken feather fibres
2D	Two-dimensional	CFK	Chicken feather keratin
aka	Also known as	CFKs	Chicken feather keratins
API	Analytical profile index	CMC	Critical micelle concentration
AR	Analytical Reagents	cfu/g	Colony forming units per gram
ATR	Attenuated total reflectance	ClO ₂	Chlorine dioxide

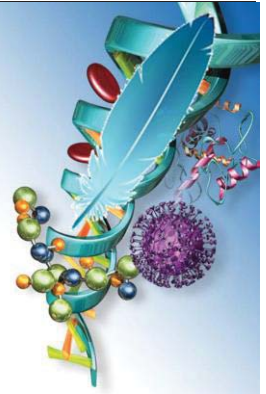
CO ₂	Carbon dioxide	etc.	Et cetera
cm	Centimetre	FBP	Fish bone peptides
cm ³	Centimetre cubed	FF	Feather fibre
COSY	Correlation spectroscopy	FF	Feather fibres
CPS	Coagulase positive <i>staphylococcus</i>	FTIR	Fourier-transform infrared
CPSA	Coagulase positive <i>Staphylococcus aureus</i>	g	Gram
¹³ C SSNMR	Carbon-13 solid-state nuclear magnetic resonance	G	Giga (10 ⁹)
CTAC	Cetyltrimethylammonium chloride	gCOSY	Gradient correlation spectroscopy
d	Day/s	GADDS	General area detector diffraction system
<i>d</i> ₆ -DMSO	Deuterated DMSO Dimethyl sulfoxide-d ₆	h	Hour
Da	Dalton	H ₂ O ₂	Hydrogen peroxide
DI	Deionised	HCl	Hydrochloric acid
DMA	Dynamic mechanical analysis	HSQC	Heteronuclear single quantum coherence or correlation
DSC	Differential scanning calorimetry	HSQCAD	Heteronuclear single quantum coherence (or correlation) adiabatic (refers to the shape of the pulse)
DTG	Derivative thermogravimetry	¹ H SSNMR	proton (hydrogen-1) solid-state nuclear magnetic resonance
<i>E</i>	Elastic modulus	HV	High vacuum
<i>E'</i>	Storage modulus	Hz	Hertz (unit of frequency) 1 cycle/second
<i>E''</i>	Loss modulus	i.e.	That is
<i>E. coli</i>	<i>Escherichia coli</i>	Laser	Light amplification by stimulated emission of radiation
e.g.	Example		

lm	Lumens	Mn	Molecular weight
IL	Ionic liquid	MT	Melting temperature
LR	Laboratory reagents	Mol	Mole
k	Kilo (10^3)	N	Newton (unit of force)
K	Kelvin (unit of temperature)	N/A	Not applicable
KF	Keratin fibre	NA	Nutrient Agar
KFs	Keratin fibres	NaClO ₂	Sodium chlorite
KOH	Potassium hydroxide	NaOH	Sodium hydroxide
L	Litre	Na ₂ S	Sodium sulfide
m	Metre	NMR	Nuclear magnetic resonance
M	Molarity	NOE	Nuclear Overhauser effect
M	Mega (10^6)	O ₃	Ozone
MDI	Methylene diphenyl diisocyanate	Pa	Pascal (unit of pressure)
mf-TM	Modulated force thermomechanometry	PAGE	Polyacrylamide gel electrophoresis
mg	Milligram	PC2	Physical containment level 2
Milli (10^{-3})	when used with other units e.g. mg, mL, mm, mN	PCA	Plate count agar
min	Minute	PEG	Poly(ethylene glycol)
Mixed-Solution	0.33 mol/L urea, 0.05 mol/L sodium dodecyl sulfate (SDS), 0.095 mol/L 2-mercaptoethanol and 0.016 mol/L tris adjusted the pH at 8.0 using HCl	pH	Potential of hydrogen
mL	Millilitre	PhD	Philosophy Doctor
mm	Millimetre	pI	Isoelectric-point
mN	Millinewton	PTFE	Polytetrafluoroethylene
		r _{cf}	Relative centrifugal force
		RH	Relative humidity
		rpm	Revolutions per minute

RT	Room temperature	T2	Purification via ozonation
s	Second	T3	Purification via ClO ₂
<i>S. aureus</i>	<i>Staphylococcus aureus</i>	T4	Purification via PEG
SDS-PAGE	Sodium dodecyl sulfate-polyacrylamide gel electrophoresis	T5	Purification via SLS
SEEt	Soxhlet extraction with ethanol	T6	Purification via CTAC
SD	Standard deviation	T7	Purification via SLS-ClO ₂ -SEEt
SDS	Sodium dodecyl sulphate	T _g	Temperature glass transition: change from hard (glassy) to soft (rubberlike)
SEM	Scanning electron microscope	tanδ	Damping or loss tangent
-SH	Thiol	TGA	Thermo gravimetry analysis
SLS	Sodium lauryl sulphate	THF	Tetrahydrofuran
Solution-A	0.5 mol/L sodium sulfide (Na ₂ S)	TPU	Thermoplastic polyurethane-polyether
Solution-B	8 mol/L urea (NH ₂ CONH ₂) and L-cysteine (0.165 mol/L), adjusted to pH 10.5 using NaOH (2 mol/L)	TSA	Tryptone soy agar
SPC	Standard plate count	TW80	Tween 80
Spp	Species	UTI	Urinary tract infection
SS	Solid-state	USDA	United States Department of Agricultural
SSNMR	Solid-state nuclear magnetic resonance	UV	Ultraviolet (10 – 380 nm)
S-S	Sulfur-sulfur or disulphide	UV-Vis	Ultraviolet-visible
t	Tons	v/v	Volume/volume
T0	Untreated chicken feathers	W	Watts
T1	Purification via SEEt	WAXD	Wide-angle X-ray diffraction
		WAXS	Wide-angle X-ray scattering (aka XRD)

WCA	Wilkins-chalgren anaerobic agar	XLD	Xylose lysine desoxycholate agar
w/v	Weight/volume	XRD	X-ray Diffraction (aka WAXS)
w/w	Weight/weight		

CHAPTER 1



INTRODUCTION

1.1 Overview

According to Rouse and Van Dyke [1], the word ‘keratin’ comes from the Greek word ‘kera’, meaning horn first appears in the literature *ca.* 1850 to describe the protein that made up hard tissues such as animal horns and hooves; it attracted scientists because it did not behave like other proteins. Normal methods for dissolving proteins were ineffective for solubilising keratin, although methods such as burning and grinding had been known for some time, many scientists and inventors were more interested in dissolving hair and horns in order to make better products [1]. The resolution to the insolubility problem came in 1905 with issuing a United States patent (Pat. DE184915) to John Hofmeier that described a process for extracting keratins from animal horns using lime [2]. Between 1905 and 1935, many methods were developed to extract keratin using oxidative and reductive chemicals [3-7]. These technologies were initially applied to animal horns and hooves, but were eventually used to extract keratin from wool and human hair. During the 1920s, keratin research changed its focus from products made from keratin to the structure and function of keratin proteins. Driven by the development of reliable methods to solubilise keratins, researchers were beginning to understand the many sub-classes of keratins (varies in the number and sequence of amino acid along with polarity, charge, size and further classified by their acidic or basic amino acid content), their different properties, and that each played a different role in the structure and function [1, 8-13]. In 1934, a key research paper was published that described different types of keratins, distinguished primarily by having different molecular weights [14]. In 1965, CSIRO’s (Commonwealth Scientific and Industrial Research Organisation) established scientist Crewther and his colleagues published the definitive text on the chemistry of keratins that contained references to more than 640 published studies on keratins [15].

Keratin is structural fibrous protein [16] and is the major components of hair, feathers, nails, wool, hooves and horns of mammals, reptiles, birds, and humans epithelial cells, which are highly resistant to degradation compare to other animal tissues except the bones, available in great quantity, and represents an important source of renewable and sustainable raw materials (biopolymer) for many applications [17-20]. Keratin has a high cysteine concentration compared with other proteins [21]. The sulphur atoms in cysteine residues tend to mutually cross-link and this makes the protein tough and strong with low density [22].

1.2 Rationale

Request for keratin-based products is continuously increasing in line with the increasing fowl meat production [23]. Feathers of these chickens are the most abundant and renewable keratinous biomass worldwide, which is a by-product from the poultry industry, and is only used to a small extent [24]. Thus far, chicken feather fibre (CFF) is used in energy recovery by incineration, composting or fertilizers, animal feedstock preparation as poor quality meal (lacking some essential amino acids and having poor digestibility by animals) that are subjected to expensive processes (such as autoclaving, drying and grinding) [1].

Currently, chicken feathers (CFs) are considered as waste product in the poultry industry because their uses are economically marginal and their disposal by burning or burying are causing environmental problems since burning feathers in installations is uneconomical and causes air pollution; whereas in a landfills feathers decompose slowly and would require a lot of land [16, 24, 25]. Even though the uncontrolled disposal of feather leads to pollution in our environment, the utilisation of this valuable biomass will be beneficial to the environment by reducing health hazards, and reducing solid wastes being sent to landfills. Therefore, from both an economic and environmental point of view, it is

quite desirable to develop an effective and profitable process to use this resource. The challenge is to turn this waste material into usable items and valuable products. Materials derived from CFs could be used advantageously for many applications that could potentially consume the majority of the feathers produced annually since feathers possess unique properties including low density, good acoustic and thermal insulating properties.

While some properties of the feather fiber fraction have previously been reported, this project comprehensively quantifies the basic properties of both processed feather components (barbs and rachis). Another intention of the project is to study the feasibility of incorporating chicken feather fibres (CFFs) in the formulation of polymer composites for industrial applications such as the plastic industry; the physical and mechanical properties of CF materials will be studied since in order to successfully develop applications for CFs in the realm of composite materials, this information must first be understood. This project will then concentrate on extracting the keratin protein from CFs since feathers as a bio-resource have a high protein content. The research is being undertaken to develop new keratin-based biomedical materials. The extracted keratin will be used to design and prepare formulations in polymers, waxes or oils for applications in cosmetic and/or health industries. The current project offers potential for novel products from CFs, and solving an environmentally sensitive problem of waste disposal.

1.3 Scope

The scope of this research is to study the purification of raw poultry feathers, extraction of keratin protein from them, design of biomedical keratin-based materials together with characterisation and comparison of the chemical, physical and morphological structure of keratin using FTIR spectroscopy, wide angle X-ray scattering, optical microscopy, macro

photography and scanning electron microscopy.

1.4 Aim

The aim of this research is to purify, characterise, compare and evaluate keratin derived from waste CFs as a material for inclusion in biomaterials with potential structural and biomedical application.

1.5 Objectives

The main objectives of this project are:

1. To purify CFs by ionic, non-ionic and cationic surfactant treatments, bleaching with ozone and/or chlorine dioxide, de-fatting with Soxhlet extraction using ethanol and combination of these techniques then characterise and compare the chemical, physical and morphological structure of CF keratin using FTIR spectroscopy, wide angle X-ray scattering, optical microscopy, macro photography and SEM.
2. To compare the chemical, physical and morphological structure of CF keratin (using FTIR spectroscopy, wide angle X-ray scattering, optical microscopy, macro photography and SEM) with keratin from other feather sources such as pigeon, or with other keratins such as sheep wool.
3. To separate the CFs into wool (alpha (α)-helix) and rachis (pleated sheet) components for separate evaluation and application.
4. To prepare bio-composites using CFFs in polymers, and evaluation of the thermal and mechanical properties of them.
5. To extract keratin from CFs using two different methods (i.e. sodium sulfide and L-cysteine), then optimise the keratin extraction method for a higher protein yield and

purification.

6. To evaluate the antibacterial effects of the chicken feather (CF) and extracted keratins for medical applications.
7. To prepare compositions using extracted chicken feather keratin (CFK) in hair conditioners and/or creams and evaluation of the thermal or mechanical properties of the biomaterial products.

1.6 Research questions

1. What is the most efficient purification method for CFs?
2. Does the preparation method affect the chemical, physical and morphological structures of CFs?
3. Can the CFFs or keratin separated from CFs be used to prepare compositions in polymers, waxes or oils for evaluation?
4. Does the purified CFF improve the thermo-mechanical properties of the bio-composites?
5. Which keratin extraction method will provide a higher yield and purification?
6. Does keratin extracted from CFs have any antimicrobial effect?
7. Which structural component will provide stable and uniform dispersions:
 - a) the barb (α -helix),
 - b) the rachis (pleated sheet) or
 - c) the whole CF?

Table 1.1 demonstrates the research objectives and questions with associated thesis chapters and publications in this project.

Table 1.1: Thesis chapters and publications addressing the project objectives and research questions

Chapter number	Publications	Objective number	Research question number
1	Not applicable	Not applicable	Not applicable
2	Drafts prepared (Review journal)	Not applicable	Not applicable
3	Not applicable	Not applicable	Not applicable
4	1. <i>RSC Advances</i> (2015) 2. <i>Advanced Materials Research</i> (2014)	1	1
5	3. <i>IChEC</i> 2014 4. <i>ICMSE</i> 2014 5. <i>ICAPM</i> 2013	1 2 3	2
6	1. Draft prepared (Journal) 2. <i>World Journal of Engineering</i> (2016) 3. <i>ICCE</i> (2016) 4. <i>SPE-ANTEC</i> (2016) 5. <i>SPE-ANTEC</i> (2016) – Poster	4	4
7	6. Draft prepared (Journal) 7. <i>SPE-ANTEC</i> (2017) 8. <i>SPE-ANTEC</i> (2017) – Poster		
8	1. Draft prepared (Journal) 2. Beyond Research – Poster 3. <i>SETAC</i> (2017) 4. <i>SETAC</i> (2017) – Poster 5. <i>FEMS-EUROMAT</i> (2017)	3 5	3 5
9	1. Draft prepared (Journal) 2. <i>ASMR</i> (2017) 3. <i>EPTS</i> (2017) 4. <i>EPTS</i> (2017) – Poster	4 6 7	3 4 6 7
10	Not applicable	Not applicable	Not applicable
11	Not applicable	Not applicable	Not applicable

1.7 Thesis structure

This first chapter presents an introduction to the project, which briefly explains the importance of the research carried out in this field.

The second chapter deals with the literature review and the background information to help understand the concept of feather keratin, purification of CFF, preparation of CFF composites, extraction of keratin and applications of CF keratin in biomedical materials. This chapter presents preliminary and analytical research undertaken by other researchers that underpins the methodology utilised in this thesis.

Chapter three presents the materials, methodologies (including standard test methods) and equipment required for the experimental studies described in this dissertation.

Chapter four investigates the safety of the CFFs by demonstrating the method to purify the CFFs and to decontaminate for safe handling of the feathers. The efficacy of different purification methods including anionic, non-ionic and cationic surfactants, bleaching with ozone and chlorine dioxide, Soxhlet extraction with ethanol and combination of sodium lauryl sulphate/chlorine dioxide/ethanol extraction was investigated prior to keratin extraction. The microbiological safety of purified feathers was studied via: A) Standard Plate Count, B) the enumeration of *E. coli*, *Pseudomonas* species, coagulase positive *S. aureus*, aerobic and anaerobic spore-formers and, C) The presence/absence of *Salmonella* and *Campylobacter*. The effects of purification treatments on the CFFs were studied using FTIR analysis, scanning electron microscopy and energy dispersive spectroscopy.

The different purified CFs were characterised and compared with other feathers such as pigeon feather and other keratin sources such as wool keratin, in the fifth chapter.

Chapter six and seven deals with the preparation of composites using thermoplastic polyurethane, TPU-polyether or polysiloxane-TPU, and CFFs in varying ratios. In research

works reported so far only the barbs and barbules are used but in our study the whole CFFs including the calamus, rachis, barbs and barbules are used as fiber reinforcement for a TPU-polyether matrix. The FTIR analysis, thermogravimetry and scanning electron microscopy have been used as characterisation techniques and the composites have been evaluated via dynamic mechanical analysis.

Chapter eight focuses on the extracting the keratin from purified CFFs using 0.5 M sodium sulphide solution as the reducing agent and 0.165 M L-cysteine for an enzymatic hydrolysis. The obtained keratin was then purified and measured and characterised with the biuret test, Bradford assay, FTIR spectroscopy and thermogravimetry. The size and the molecular mass of the extracted keratins were estimated using sodium dodecyl sulphate-polyacrylamide gel electrophoresis (SDS-PAGE) technique.

Chapter nine shows some detailed discussion of the types of hydrolysed keratins used commercially and the antimicrobial aspects of the extracted CFK. Designing of the hair keratin conditioner and keratin cream with the extracted keratin is explained in this chapter.

Chapter ten presents an overarching discussion of all findings, as described in chapters four to nine.

Chapter eleven includes a conclusive overview of the project along with recommendations for future studies.

The flow chart of this thesis structure is shown in Figure 1.1.

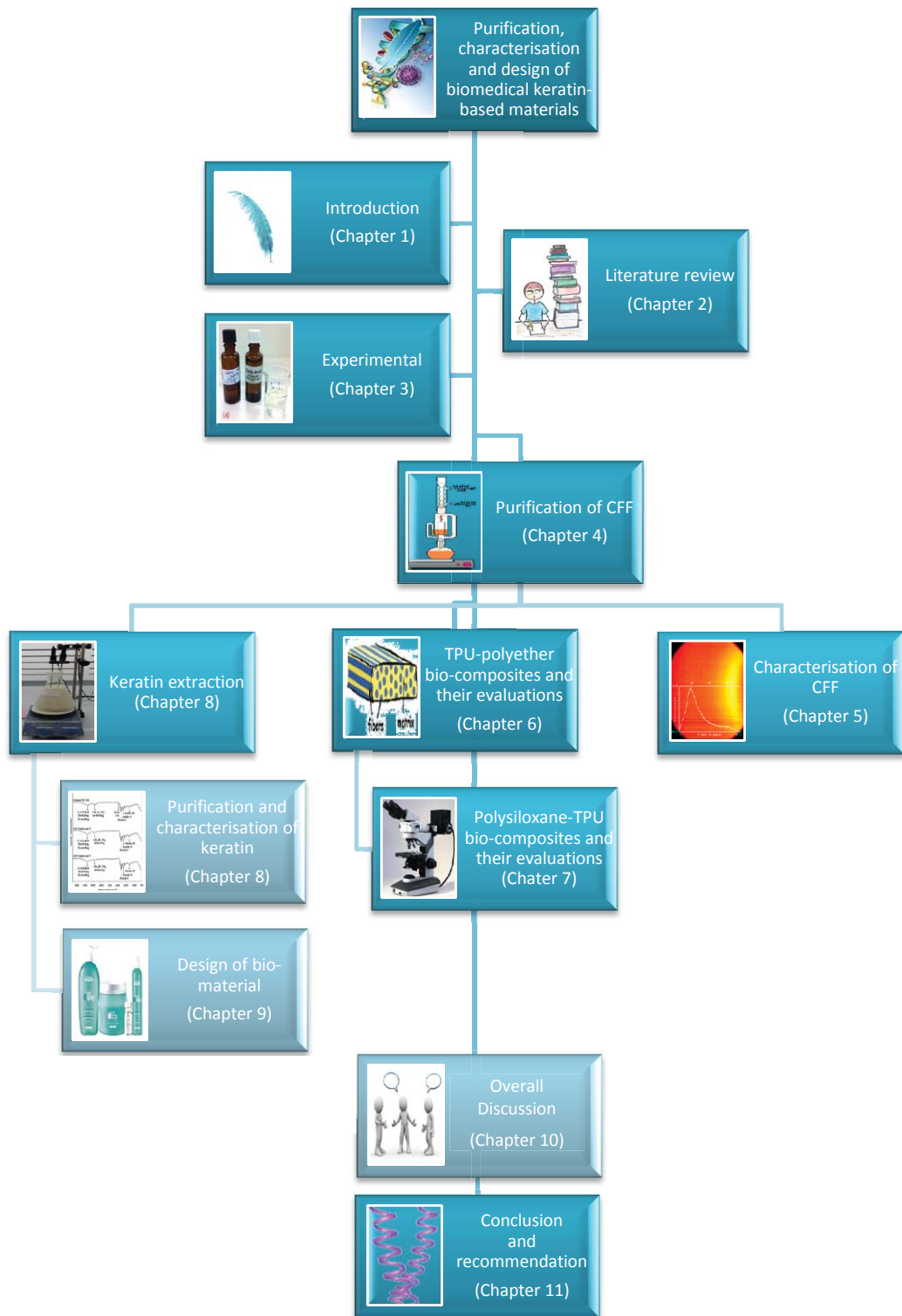


Figure 1.1: Flow chart of this thesis structure

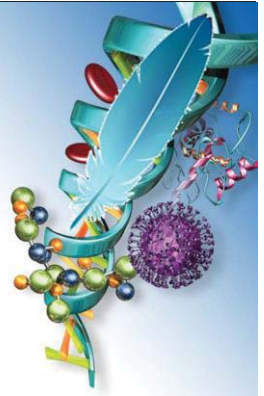
Norms and standards used in this project are according to SI unit and numbered referencing style has been chosen.

1.8 References

1. Rouse, J.G. and M.E. Van Dyke, *A review of keratin-based biomaterials for biomedical applications*. Materials, 2010. **3**(2): p. 999-1014.
2. Hofmeier, J., *Horn-lime plastic masses from keratin substances*. German Pat. DE184915, 1905. **18**.
3. Breinl, F. and O. Baudisch, *The oxidative breaking up of keratin through treatment with hydrogen peroxide*. Z Physiol Chem, 1907. **52**: p. 158-169.
4. Goddard, D.R. and L. Michaelis, *Derivatives of keratin*. Journal of Biological Chemistry, 1935. **112**(1): p. 361-371.
5. Lissizin, T., *Behavior of keratin sulfur and cystin sulfur, in the oxidation of these proteins by potassium permanganate*. Biochemistry Bulletin, 1915. **4**: p. 18-23.
6. Lissizin, T., *Über die durch Oxydation mit Permanganat erhaltenen Oxydationsprodukte des Keratins. II. Mitteilung*. Hoppe-Seyler' s Zeitschrift für physiologische Chemie, 1928. **173**(5-6): p. 309-311.
7. Neuberg, C., *Process of producing digestible substances from keratin*. 1909, Google Patents.
8. Buchanan, J.H., *A cystine-rich protein fraction from oxidized α -keratin*. Biochemical Journal, 1977. **167**(2): p. 489-491.
9. Crewther, W., R. Fraser, F. Lennox, and H. Lindley, *The chemistry of keratins*. Advances in protein chemistry, 1965. **20**: p. 191-346.
10. Kaku, M. and K. Kikkawa, *Field theory of relativistic strings. I. Trees*. Physical Review D, 1974. **10**(4): p. 1110.
11. Earland, C. and C. Knight, *Studies on the structure of keratin II. The amino acid content of fractions isolated from oxidized wool*. Biochimica et biophysica acta, 1956. **22**(3): p. 405-411.
12. Matsunaga, E., *Genetics of Wilms' tumor*. Human genetics, 1981. **57**(3): p. 231-246.
13. Orwin, D., *Cytological studies on keratin fibres*. Fibrous proteins, scientific, industrial, and medical aspects/edited by DAD Parry, LK Creamer, 1979.
14. Goddard, D.R. and L. Michaelis, *A study on keratin*. Journal of Biological Chemistry, 1934. **106**(2): p. 605-614.
15. Crewther, W.G., R.D.B. Fraser, F.G. Lennox, and H. Lindley, *The Chemistry of Keratins*, in *Advances in Protein Chemistry*, M.L.A.J.T.E. C.B. Anfinsen and M.R. Frederic, Editors. 1965, Academic Press. p. 191-346.
16. Fan, X., *Value-added products from chicken feather fiber and protein*. 2008: ProQuest.
17. Wang, K., R. Li, J. Ma, Y. Jian, and J. Che, *Extracting keratin from wool by using L-cysteine*. Green Chemistry, 2016. **18**(2): p. 476-481.
18. Alonso, L. and E. Fuchs, *The hair cycle*. Journal of Cell Science, 2006. **119**(3): p. 391-393.

19. Latha, P.P., R.K. Singh, A. Kukrety, R.C. Saxena, M. Bhatt, and S.L. Jain, *Poultry chicken feather derived biodegradable multifunctional additives for lubricating formulations*. ACS Sustainable Chemistry & Engineering, 2016. **4**(3): p. 999-1005.
20. Khosa, M. and A. Ullah, *A sustainable role of keratin biopolymer in green chemistry: a review*. J Food Processing & Beverages, 2013. **1**(1): p. 8.
21. Strasser, B., V. Mlitz, M. Hermann, E. Tschachler, and L. Eckhart, *Convergent evolution of cysteine-rich proteins in feathers and hair*. BMC evolutionary biology, 2015. **15**(1): p. 1.
22. Menefee, E., *Physical and chemical consequences of keratin crosslinking, with application to the determination of crosslink density*, in *Protein Crosslinking*. 1977, Springer. p. 307-327.
23. Winandy, J.E., J.H. Muehl, J.A. Micales, A. Raina, and W. Schmidt, *Potential of chicken feather fibre in wood MDF composites*. Proceedings of EcoComp, 2003. **20**: p. 1-6.
24. Whitfield, D., A.H. Fielding, and S. Whitehead, *Long-term increase in the fecundity of hen harriers in Wales is explained by reduced human interference and warmer weather*. Animal Conservation, 2008. **11**(2): p. 144-152.
25. Xu, S., T. Reuter, B.H. Gilroyed, L. Tymensen, Y. Hao, X. Hao, M. Belosevic, J.J. Leonard, and T.A. McAllister, *Microbial communities and greenhouse gas emissions associated with the biodegradation of specified risk material in compost*. Waste management, 2013. **33**(6): p. 1372-1380.

CHAPTER 2



LITERATURE REVIEW

2.1 Introduction

The global poultry industry includes chicken, turkey, duck, guinea fowl, goose, quail, pheasants and squabs, but chicken meat has dominated this industry for years, generating millions of tonnes of CFs annually worldwide, considering 5 % to 7 % of a chicken's body weight are feathers [1-6]. Victoria's chicken meat industry alone, produced 243,000 tonnes of chicken meat in 2013-14, accounting for around 22 % of Australia's 1,084,000 tonnes of chicken meat production [7]. Consumption of poultry in Australia, of which chicken meat is *ca.* 96 %, has increased from *ca.* 4.4 kg per person annually in 1960 to around 44.0 kg in 2012-13. This increase has been driven by a number of factors including chicken meat becoming more price competitive with improving community perceptions of chicken meat as a consistent, healthy, versatile and convenient food [8]. Consumer demand is expected to remain high as chicken meat prices will continue to be substantially lower than prices of most alternative meats, despite the effect of forecast higher feed grain prices [8].

Currently, CFs are a low-value by-product, being used in small amounts for animal feed and fertiliser since they have deficiencies of nutritionally essential amino acids such as methionine, lysine, histidine and tryptophan [6, 9-12]. When disposed of into landfill, the feathers often decompose slowly because of their structural composition and the amount generated on an annual basis requires large areas of land [5]. The disposal process for CFs such as burning or burying is expensive and uncontrolled disposal of feathers is environmentally unacceptable since it causes soil, water and air pollution, releases greenhouse gases [5, 13] and instigate various human ailments (bacterial contamination of animal feed and its relationship to human foodborne illness), chlorosis and fowl cholera [14-16].

Conversely, environmental concerns encourage studies to replace synthetic materials

with a variety of natural materials [5]. Presently, the keratin fibre (KF) from CFs is recognised as an almost infinite source of high-performance materials, but it needs further studies to demonstrate a basis for innovative technologies and useful raw materials [17, 18]. Moreover, economic interest in feather fibre usage has been gradually increasing [5]. Even though several alternatives have been invented for CF applications, the use of waste CFs still has not increased much due to its low demand. Therefore any investigations helping to increase the usage of waste CFs are beneficial [19]; hence it is presently the object of intensive investigations in many research centres on converting this waste material into usable items, so it is gradually gaining recognition to use CFFs in making commercial products. Many publications and patents proposing applications for this biopolymer have been issued as a result of these research works presented in this chapter. Because the aim of this project is to purify, characterise, compare and evaluate keratin derived from waste CFs as a material for inclusion in biomaterials with potential structural and biomedical application, discussion of the nature of CFs and their application is necessary. This chapter, therefore, examines feather types, categories and structure, purification, separation of fibres from quills and comminuted feathers and application of CFFs and CFK.

2.2 Feather types, categories and structure

2.2.1 Types and categories of feathers

The differences in keratin organisation results in *ca.* 30 macroscopically distinct poultry feather types [20, 21]. However, according to Bartels et al. [21] there are six commonly recognised categories of feathers based on their morphology: 1) Tail, 2) flight or contour, 3) semiplume, 4) filoplume, 5) bristle and 6) downy feathers (Figure 2.1). These different feather types come in many shapes and sizes. Tail feathers are balanced left and right of the

centre. Flight or contour or vaned feathers have a wider and narrower side and are found on a bird's back, tail and wings, give birds their colour and are primarily responsible for flight and provide defence against physical objects, sunlight, wind and rain. Semiplume feathers have characteristics of both contour and downy feathers and have long rachis and barbs similar to downy feathers. Filoplume feathers are smaller than semiplume ones, with only a few barbs at the tip of a fine shaft; they serve a sensory function in a chicken, registering vibrations and changes in pressure. Bristle feathers are found on the chicken's head, at the base of the beak, around the eyes and covering the nostrils; they are stiff and have short barbs near the tip and are protective in function. Downy feathers are soft and fluffy, located beneath the contour feathers, and are smaller than contour feathers; they lack barbules and the accompanying hooklets and provide most of the insulation to the birds [21]. Large contour feathers are approximately half feather fibre and half quill by mass [3, 22, 23].

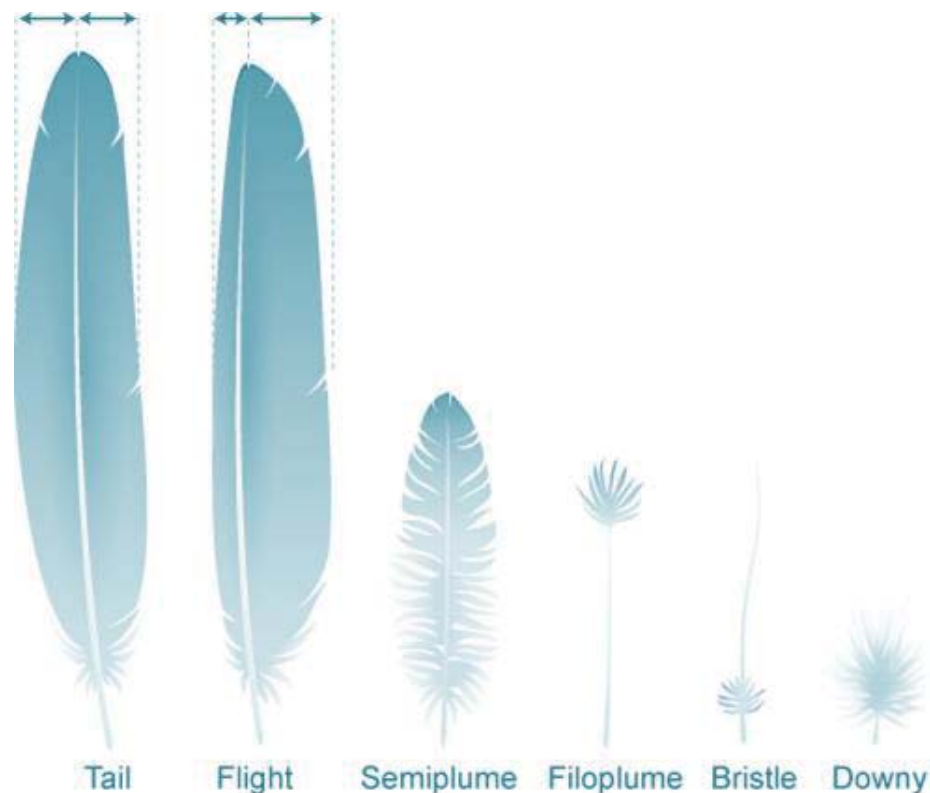


Figure 2.1: The five primary types of chicken feathers [21]

The CFs consist of 50 %·w/w fibre (barbs and barbules) and 50 %·w/w quill (calamus and rachis) [3, 22, 23]. Hong and Wool [24] assert that fibres and quills are characteristic of the two forms of microcrystalline keratin in feathers. The quill is the hard, central axis off which soft, interlocking fibres branch out; the fibres are hollow and the barbs of a feather can be used directly as fibres [24]. Smaller feathers have a greater proportion of fibre, which has a higher aspect ratio than the quill.

A plant might process chickens of different sizes on different days, and differently-sized chickens, presumably of different ages, could be expected to yield different proportions of feather types [23]. Smaller chickens have mostly downy feathers, while older and therefore larger chickens have relatively more contour feathers, hence, CF properties could vary by collection day. In order to maximise the yield of a desirable type of feathers, feather collection could be planned for days on which chickens of a particular feather type distribution are processed [23].

2.2.2 Physical structure of feathers

The different parts of a typical contour CF are shown in Figure 2.2. The naked portion of the shaft that is implanted in a bird's skin is the calamus [21]. The stiff, cylindrical, sharp-pointed 'midrib' of the contour feather is known as the rachis or shaft and is found above skin level. The slender, parallel side branches arising from two sides of the shaft are barbs, and all the barbs considered collectively as one flat thing are known as the vane (Figure 2.2) [25]. The portion bearing branches is the rachis, which is filled with a porous substance is termed the medulla (Figure 2.3) [26]. A barb bears minute hooked branches, which are barbules, and the barbules of adjacent barbs hook together to hold the barbs into a well-organised vane [25]. Barbules are closely spaced and interlock via hooklets (barbicels) [27]. The

portions of quill fraction is composed of more β -sheets than α -helices while the feather fibre has a higher percentage of α -helix [28].

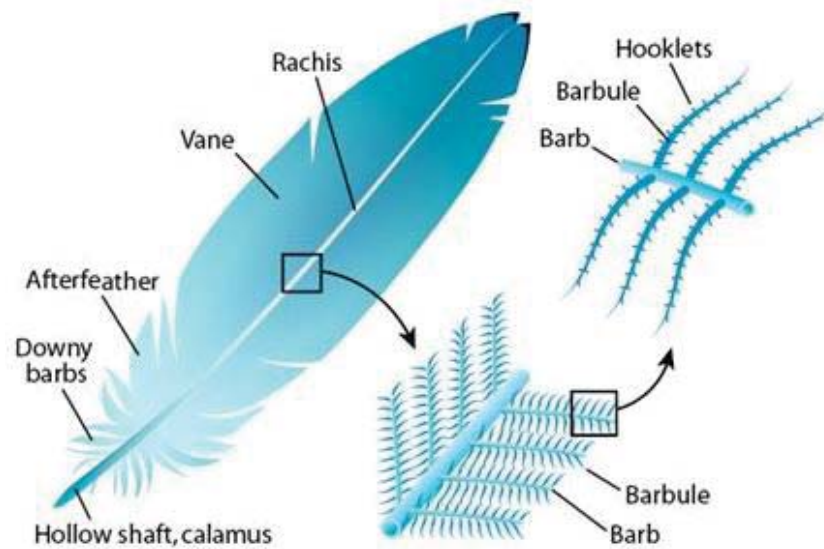


Figure 2.2: The structures of a chicken feather [29] (feather fibre or wool: barbs/barbules), (quill: calamus/rachis or shaft), (vane: rachis/barb/barbules)

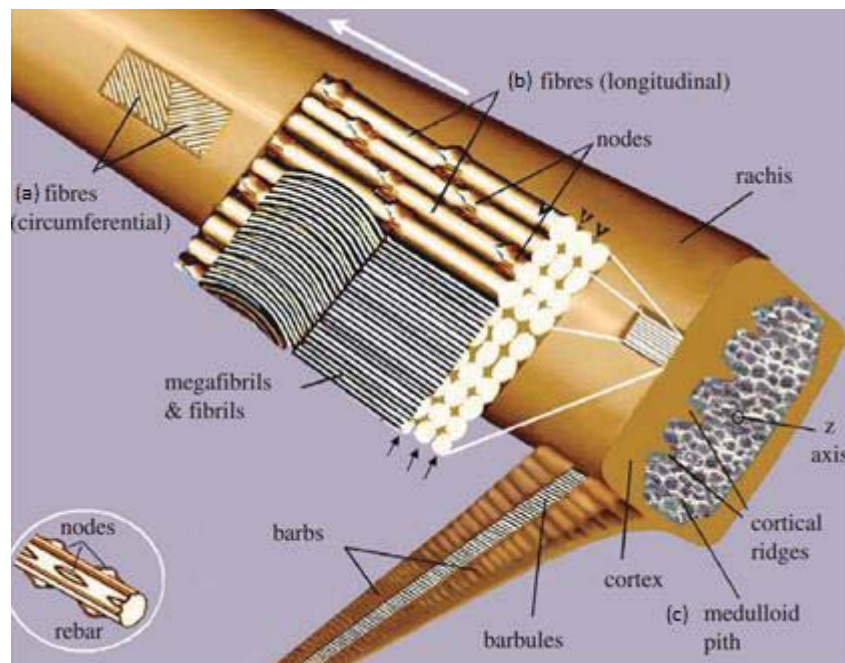


Figure 2.3: A schematic view of the major structural components of the feather rachis: (a) superficial layers of fibres, the ultimate size-class in the hierarchy of feather keratin filaments, (b) The majority of the fibres extending parallel to the rachidial axis and through the depth of the cortex, (c) It shows the medulloid pith comprising gas-filled polyhedral structures. Inset, part of a steel rebar with nodes [30]

Feathers have a hierarchical and branched structure (Figure 2.4a) and they can be divided into two parts: 1) calamus and rachis, 2) barbs and barbules [31]. The big part of a feather's physical structure is the barb, which has fibres that are up to 35 mm long and have a diameter of 40 μm to 400 μm [4, 5, 32], and can be used in composite materials. The barbules have lengths of less than 1 mm, diameters of 10 μm to 30 μm , and hooks known as barbicels (Figure 2.4b), which connect with barbules to adjacent barbs [4, 32]. The rachis length is typically between 40 mm to 120 mm and diameter can exceed 3 mm [4, 32]. A single KF has a maximum diameter of 50 μm [33].

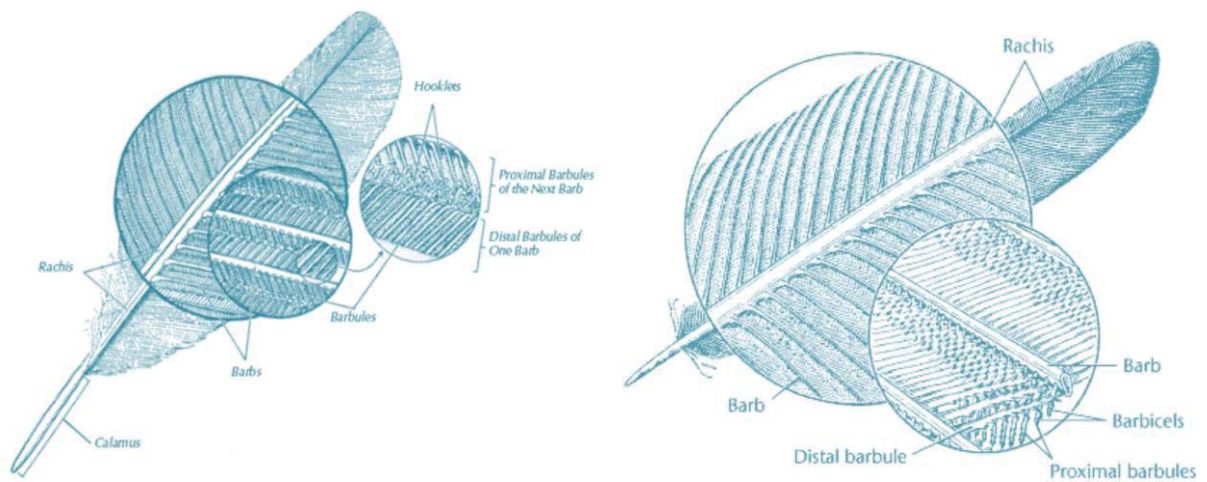


Figure 2.4 (a): Feather Structure [31], (b): A contour feather [21]

Quill fractions are composed of both inner and outer quill; the latter is more densely structured than inner quill and is porous as shown in Figure 2.5 [34]. A typical quill has dimensions in the order of centimetres (length) by millimetres (diameter) and the presence of quills among fibres result in a more granular, lightweight, and bulky material [35, 36]. Hong and Wool [24] suggested that the thermal energy required to perturb the fibre is higher than that required for the quill. Schmidt and Line [20] reported that the packing within outer quill keratin is less ordered and has less cross-linking than packing within the fibre and inner quill

keratin. Consequently, it is the outer quill component of a quill fraction which is weaker and would be weakened by mechanical stresses than the feather fibre and inner quill would be able to withstand [20, 24].

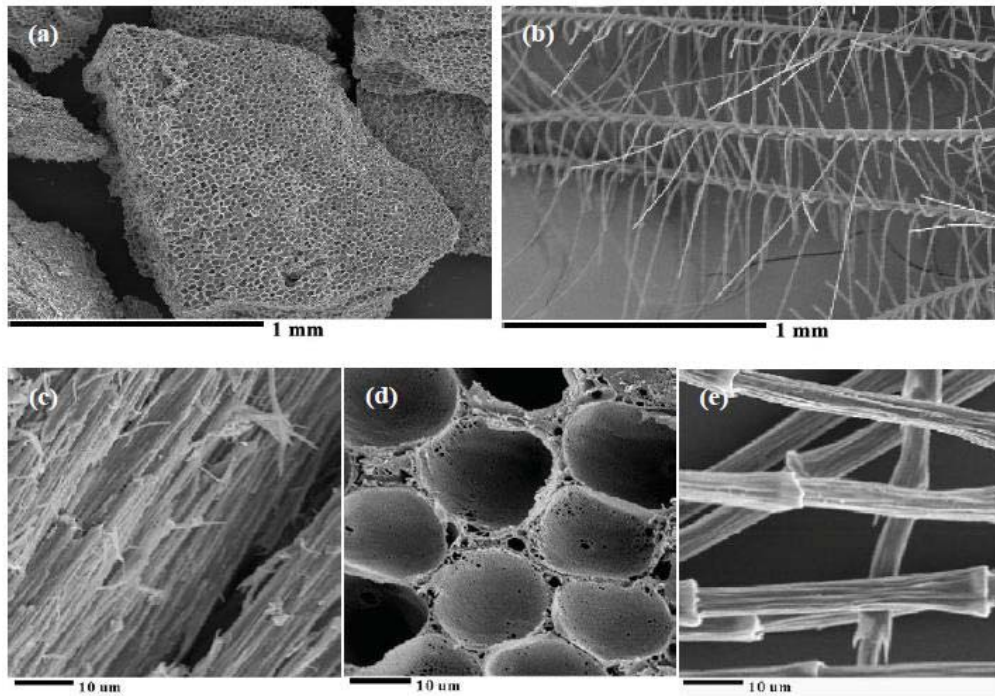


Figure 2.5: Scanning electron micrographs showing chicken feather (a) inner quill, (b) fibre, (c) outer quill, (d) inner quill, and (e) fibre [34]

2.2.3 Physical properties of feather fibres

2.2.3.1 Solubility of keratin

Keratin is insoluble in water, organic compounds weak acids and bases [37]. The CF calamus/rachis and barbs/barbules have *ca.* 7% moisture content [38]. Barone and Schmidt [39] reported that keratin of feather fibre has *ca.* 40 % hydrophilic and 60 % hydrophobic chemical groups as per its amino acid sequence structure. Feather keratin contains both hydrophilic and hydrophobic amino acids, with 39 of the 95 amino acids being hydrophilic [38]. Serine is the most abundant amino acid and the -OH group in each serine residue helps

CFs to absorb moisture, hence CFFs are hygroscopic [40]. The chemical structure of the CFs is further discussed in the next section.

2.2.3.2 Structure of keratin

According to Schmidt and Line [20], the keratin molecules can assemble into α -helix, β -sheet, or random coil macrostructure. Barone and Schmidt [39] reported that keratin feather fibre has *ca.* 41 % α -helix, 38 % beta (β)-sheet and 21 % random or disordered structures. The distribution of amino acids is highly non-uniform, with the basic and acidic residues and the cysteine residues concentrated in the N- and C-terminal regions, with the central portion, is rich in hydrophobic residues with a crystalline β -sheet conformation [2]. The α -helical structure contains intra-molecular hydrogen bonds between the amide and carbonyl groups in the protein backbone [39]. The β -sheet structure contains interchain hydrogen bonding between the amide and carbonyl groups in the protein backbone and the helices can pack together to form crystals [39]. Schmidt and Jayasundera [41] reported that the hydrogen bonding can be correlated with the bound water in the protein structure.

2.2.3.3 Size discretion of chicken feather fibres

The CFFs diameters are *ca.* 5 μm [42] and their length through different processing can vary from 3 mm to 13 mm, hence their aspect ratio (length/diameter or width) is in the range of 600 - 2600 [43, 44].

Since the CFF is hallowed, the fibre's volume includes both solid matter (the walls of fibre) and air (the hollow inside the fibre); its apparent density, is reported by Barone and Schmidt in 2005, as 0.89 g/cm^3 , which was measured by displacing a known volume of ethanol with an equivalent weight of feather [43]. This varied to what was been reported

in 1983 by Arai *et al.* [45] for the density of CFK as *ca.* 1.3 g/cm³.

2.2.3.4 Properties of keratin

The fibre and the quill have fundamentally different physical properties such as mechanical and/or thermal broken down first, and the quill melts at 15 °C lower than that of the fibre, which means the quill inherently takes more energy to break down the fibre than the quill under mechanical and/or thermal stress [20]. Some physical and mechanical properties of CFFs are shown in Table 2.1.

Table 2.1: Chicken feather fibre physical and mechanical properties

Properties	Feather segments	Value	Reference
Molecular weight	Not specified	10.5 kg/mol	[46-49]
		20 kg/mol	[50, 51]
		36 kg/mol	[50]
		60.5 kg/mol	[48]
Melting point	Barbs	240 °C	[20]
	Quills	230 °C	
Density	Not specified	0.89 g/cm ³	[43]
		1.3 g/cm ³	[45]
Diameter	Barbs	15 – 110 µm	[52]
	Barbules	4 – 10 µm	[52]
Length	Barbs	3 – 13 mm	[52]
	Barbules	0.060 – 1 mm	[52]
Aspect ratio	Barbs	212	[52]
	Barbules	61	[52]
Elongation	Not specified	7.7 %	[52]
Tensile strength	Not specified	41 – 130 MPa	[24]
	Not specified	190 – 203 MPa	[53]
	Not specified	113 MPa	[52]
Elasticity modulus	Not specified	0.045 GPa to 10 GPa	[54]
Young's modulus	Not specified	3 – 50 Gpa	[34]

In the hydrolysis of feathers for particles/fibres of the same surface area, the quills digest faster than the fibres hence nutrient value is more accessible in the quill than the fibre [20]. As over 90 % of the CFF is made up of the structural protein keratin, with extensive cross-linking and strong covalent bonding within its structure, the feather fibre shows durability and high resistance to degradation [5]. The experiments conducted by Rock et al. [55] showed that the CFF degrade rapidly in alkali environments, but significantly less in near-neutral and slightly acidic conditions.

The functions of a bird's feathers are highly related to their mechanical properties, which are related to the keratin structure that transports forces with negligible distortion [54, 56]. The elasticity moduli of CFK range from 0.045 GPa to 10 GPa [54], its Young's modulus was reported in the range of 3 GPa to 50 GPa [34] and the tensile strength of oven-dried CFFs is in the range of 41 MPa to 130 MPa [24].

2.2.4 Chemical structure of chicken feathers

2.2.4.1 Composition of keratin

The CFs consist of about 91 % keratin, 1 % lipids and 8 % water, therefore, they could potentially be used for protein fibre production [20, 57]. The chemical structures of the CF consist of β -keratin as its major structural instead of α -keratin [58]. The barbs and the barbules of the feathers have mostly the α -helical structure of the keratin [43]. Figure 2.6 shows the α -helical and β -pleated sheet secondary structures of keratin [59]. Infrared spectroscopy and X-ray crystallography reported by Schmidt and Jayasundera [41] rachis to have more β -sheet keratins aligned in arrayed layers, while the barbs, barbules and barbicels are in ordered α -helix conformation.

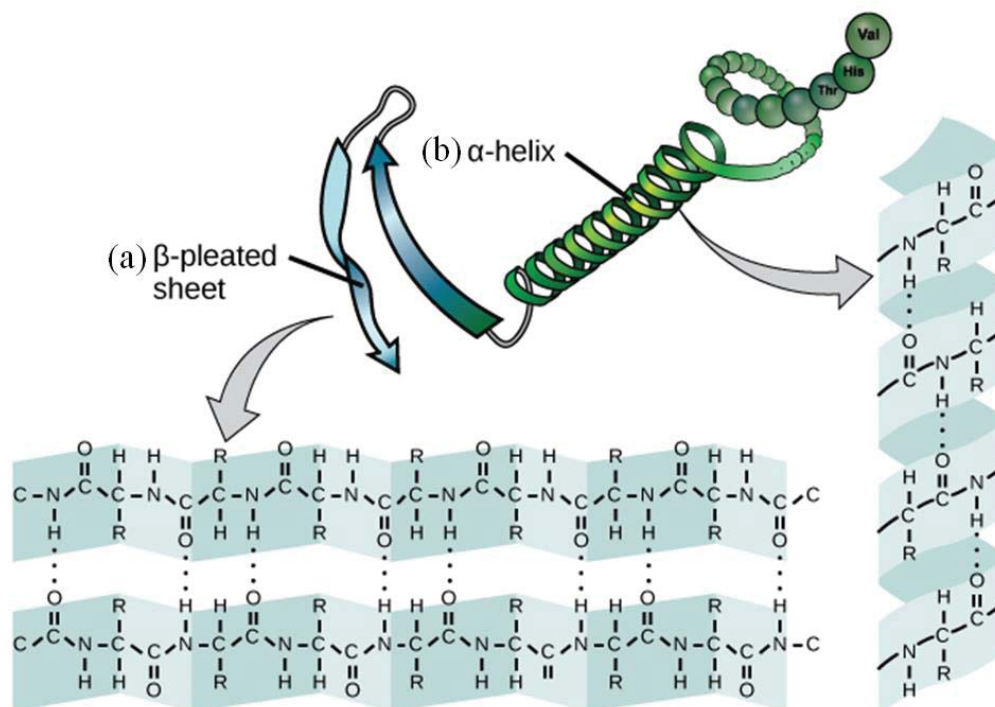


Figure 2.6: Chemical structure of keratin from chicken feather
(a) β -pleated sheet structure and (b) α -helix structure of keratin twists gradually [59]

The β -keratins in feathers, beaks, claws, scales and shells of reptiles are composed of protein strands hydrogen-bonded into β -pleated sheets, which are then further twisted and cross-linked by disulphide bridges into structures even tougher than the α -keratins of mammalian hair, horns and hoof [60]. The β -keratin contains ordered α -helix or β -sheet structures and some disordered structures [61]. The feather barb fraction has slightly more α -helix than the β -sheet structure, however, the quill has much more β -sheet than α -helix structure [20]. Approximately one-quarter of the keratin protein has a β -sheet conformation and is concentrated in the central portion of the molecule which is rich in hydrophobic residues [2]. The high content of hydrophobic residues indicates that the fibres are compatible with organic solvents [4].

Birds and reptiles have their own keratins, different from the keratins in mammals, which are composites made up of both fibrous and matrix components [62]. The fibrous

feather keratin can stretch *ca.* 6 % before breaking, unlike hair α -keratin that can stretch to twice its length [48]. The main secondary structure in bird and reptile keratin is the β -keratin, which does not lie flat but twists gradually (Figure 2.6) [48]. Each polypeptide chain in these β -keratins has a central helical section with less regular regions at each end [48]. These regions contribute to the matrix component and have some disulphide (cysteine) cross-links [48].

2.2.4.2 Chemical structure of keratin

Martinez-Hernandez et al. [63], characterised the microstructure of CFFs and claimed that the highly cross-linked structure gives the feather good mechanical properties. The high disulphide content of feathers contributes to the disagreeable odour that results when they are burned [60]. A disulphide bond is a covalent bond, usually derived by the coupling of two thiol groups, the linkage is called disulphide bridge or SS-bond and the overall connectivity is, therefore, R-S-S-R [60]. Disulphide bonds are usually formed by the oxidation of sulfhydryl (-SH) groups, especially in biological contexts [60] (Figure 2.7).

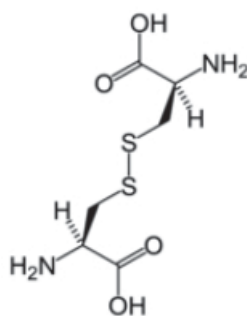


Figure 2.7: Disulfide bond between two Cysteine amino acids [60]

Hard β -sheet keratins have a much higher cysteine content than soft α -helix keratins and thus a much greater number of disulfide bonds which link adjacent keratin proteins (Figure 2.8) [64].

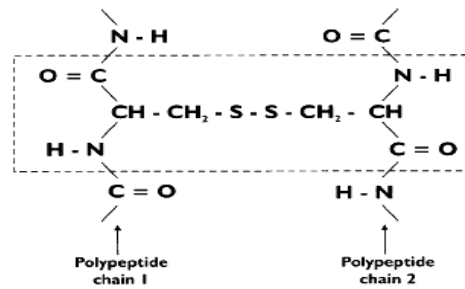


Figure 2.8: Diagrammatic representation of the diamino-acid cystine residue linking by covalent bonding two polypeptide chains 1 and 2. This bonding represents the main covalent interaction in α -keratin fibres and may exist as either an interchain linkage between two chains or as an intrachain linkage between two components of the same polypeptide chain [64]

2.2.4.3 Molecular mass of keratin

Proteins are polymers formed by various amino acids capable of promoting intra- and inter-molecular bonds, allowing the resultant materials to have a large variation in their functional properties [60]. The amino acids in a polymer are joined together by the peptide bonds between the carboxyl and amino groups of adjacent amino acid residues [60]. Keratin is a hierarchical structure, consisting of sub-nanometre-sized amino acids that polymerise in a known sequence into a large molecular mass protein molecule that is in the order of 101 nm to 102 nm in size [39]. Feather keratin molecular mass is reported between *ca.* 10 kg/mol to 36 kg/mol and a cysteine/cystine content in the amino acid sequence of 7 % allowing for -S-S- bonding or cross-linking in the keratin [49-51, 65, 66].

2.2.4.4 Amino acids of keratin

Arai et al. [67] have identified 95 amino acid sequence of keratin from duck and pigeon species. The most abundant amino acids found are serine, proline, glycine, valine, cysteine and leucine [67], but no methionine, histidine or lysine were found. The other amino acids, including aspartic acid, asparagine, glutamic acid, glutamine, threonine, and arginine, are found to be less than 6% abundance [67]. About half of these amino acids are hydrophilic

and half are hydrophobic [41]. The surface properties of the fibre primarily depend upon the degree to which the hydrophobic amino acids are internal or external to the surface of the fibre [41]. Homology in sequence among the avian species investigated is 85% [41]. Feather keratins are composed of about 20 types of proteins, which differ only by a few amino acids [68]. Table 2.2 shows the amino acids of CFK.

Table 2.2: Amino acid content in chicken feather keratin

No.	Amino acid	Content (%)				SD
		[2, 49]	[40, 41]	[69]	[37]	
1.	Serine	17.2	16.0	16	13.57	1.524
2.	Proline	11.1	12.0	12	1.01*	0.520
3.	Glycine	11.3	-	11	7.57	2.072
4.	Valine	7.4	9.00	9	7.24	0.972
5.	Cystine	6.7	7.00	7	2.11	2.399
6.	Glutamine	-	7.62	-	-	-
7.	Aspartic acid	-	5.00	-	-	-
8.	Arginine	4.5	4.30	5	6.57	1.028
9.	Asparagine	4.8	4.00	-	-	0.566
10.	Threonine	4.7	4.00	-	-	0.495
11.	Alanine	4.7	3.44	4	3.66	0.551
12.	Isoleucine	-	5.00	-	-	-
13.	Leucine	7.0	6.00	6	7.48	0.742
14.	Asparic Acid	-	2.10	5	4.76	1.610
15.	Tyrosine	1.0	1.00	1	1.85	0.425
16.	Methionine	0	1.02	-	0.025	0.582
17.	Phenylalanine	3.6	0.86	4	4.11	1.537
18.	Threonine	-	-	4	4.11	0.078
19.	Glutamic acid	7.4	Almost absent	7	9.18	1.161
20.	Isoleucine	4.6	-	5	4.93	0.214
21.	Histidine	0	Almost absent	-	0.016	0.011
22.	Lysine	0	Almost absent	-	0.57	0.403
23.	Tryptophan	0	Almost absent	-	-	-

* This number was excluded as an outlier
Adopted from [2, 37, 40, 41, 49, 69]

Harrop and Woods [70] reported a different amino acid percentage ration, which is shown in Figure 2.9, drawn by Tseng [71]. Only small differences occur in comparing the amino acid profile of feathers from ducks, pigeons and poultry [67]. According to Fraser [72], the amino acid sequence of a CF is similar to that of other feathers and has a great deal in common with reptilian keratins from claws.

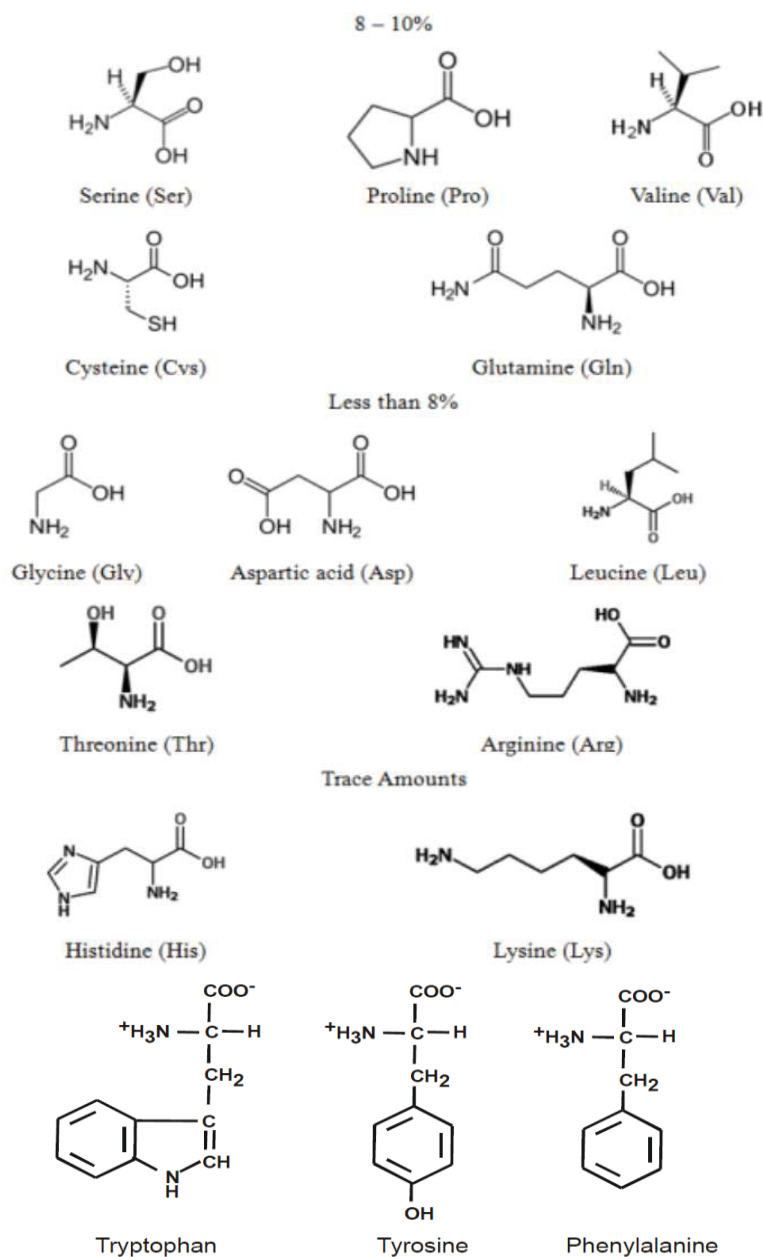


Figure 2.9: Chemical skeletal structures of amino acid found in chicken feather keratin [70, 71, 73]

The amino acid sequence of keratin in CFs is largely composed of serine, proline, glycine, cysteine and glutamine, whereas glutamic acid, histidine, lysine and tryptophan, are almost absent [40, 74, 75]. Keratin consists of both hydrophilic and hydrophobic amino acids, more respectively having 39 of its 95 amino acids hydrophilic [38].

The CFFs amino acid sequence are similar to the amino acid sequence of keratin in other birds and reptilian keratins from claws [40]. The α -keratins amino acid sequences are rich in cysteine but poor in hydroxyproline and proline whereas the β -keratins amino acid sequences are rich in uncharged glycine and alanine and poor in cysteine, proline and hydroxyproline [37]. Feather keratin has 7 % cysteine in disulphide bonds that can be hydrolyzed, reduced and oxidised [2, 37]. Different parts of the feathers have different cysteine levels, leading to harder or softer material [60]. The high content cysteine makes the keratin stable by forming a network structure through joining adjacent polypeptides by disulphide cross-links. The high strength of keratin is due to the two cysteine molecules bonded by disulphide bonds and hydrogen bonding of the helix in keratin results in increased its strength [76, 77]. Different components of keratin protein have been shown in Figure 2.10 [66].

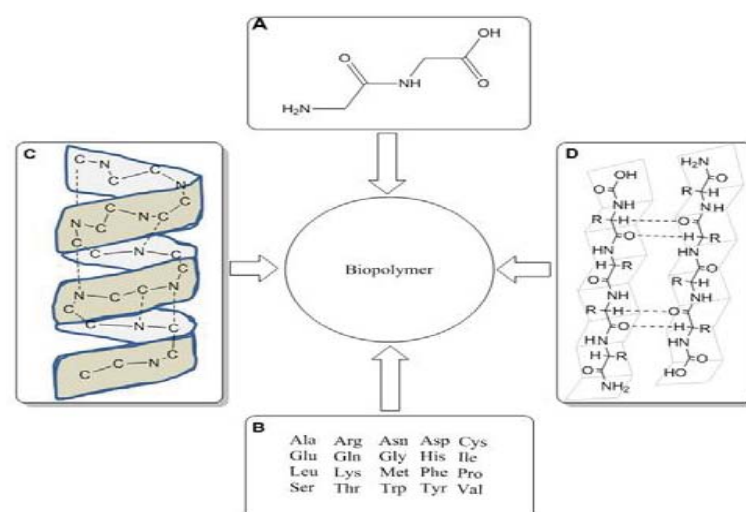


Figure 2.10: Schematic diagram of different components of keratin; (A) polypeptide single unit, (B) amino acid sequence, (C) α -helix, and (D) β -Sheets conformations of keratin protein [66]

2.3 Purification of chicken feathers

Chickens are warm-blooded animals, leading to a variety of microorganisms on or in the chicken, including mesophilic or psychrotrophic organisms that originate from the animal, its habitat, processing equipment and human handlers [71]. In chicken abattoirs, the feathers plucked from chickens often lie in heaps mixed with offal, dilute blood, grease and water; hence raw feathers appear straw-like, with a greasy texture and the barbs are stuck to the rachis, discoloured and have an obnoxious odour [9]. The freshly collected feathers could possibly be harbouring a variety of pathogenic microorganisms such as *Campylobacter*, *Enterobacter*, *Salmonella* and *Escherichia* that are known to cause gastroenteritis [71].

Free fatty acids from lipid decomposition cause pH changes and lead to microbial growth after slaughter; the secretion from the bird's skin glands has antimicrobial properties against *Bacillus licheniformis*, which can degrade keratin [78]. Impurities coat the entire feather, and particulates are trapped by layers of barbules and hooked barbicels [71]. Therefore, unprocessed feathers require pre-treatment, starting with decontamination to ensure process hygiene and cleaning to remove impurities that cause objectionable odour, discolouration and equipment fouling [71]. Processing of freshly collected feathers prevents their decay and they can then be stored safely at room temperature [9].

As described in patented literature [79], traditionally feathers are washed by organic solvents such as chlorinated hydrocarbons. The chemicals, C₂ hydrocarbon derivative mixtures, such as trichloroethylene, perchloroethylene, tetrachloroethylene, and tetrachloroethene are reused after distillation and solid removal. These chemicals are used for dry-cleaning but their discharge has detrimental effects on the environment [79]. Feathers are washed in polar organic solvents such as ethanol by the commercialised process filed by the

United States Department of Agriculture (1998), which required dual stage leaching, and solvent recovery requiring additional chemicals to break the ethanol-water azeotrope [35]. Another United States patent has recommended using an inorganic solvent such as hydrogen peroxide (H_2O_2), chlorine bleach (such as sodium hypochlorite) or detergents such as sodium dodecyl sulfate (SDS) [80]. The H_2O_2 is routinely used in waste water treatment, where proper use allows it to break down into innocuous water and oxygen [81].

According to the Encyclopaedia of Chemical Technology [82] a suitable solvent for feather leaching must meet the following criteria:

- compounds to be removed must be soluble in the solvent,
- the product must not contain solvent residues,
- the chemical should be recovered by distillation or evaporation without azeotrope formation and should have a small latent heat of vapourisation,
- interfacial tension, viscosity and wettability should allow the solvent to flow and penetrate pores and capillaries in the feather, and
- ideally, the solvent should be non-toxic, stable, non-reactive, non-flammable, harmless to the environment and be cheap.

Inorganic solvents like hydrogen peroxide, sodium hypochlorite and organic solvent detergents like sodium dodecyl sulfate (SDS), can be used for cleaning [80]. Schmidt [69] and Gassner [35] proposed that the feather should be washed with an organic solvent such as ethanol that has the following features:

- the solvent should be able to extract the target compounds in a short time,
- the solvent should be compatible with the sample and should not react with target compounds,

- the solvent should be chemically and thermally stable during operational conditions,
- low viscosity is necessary to increase the diffusion coefficient and to keep the extraction rate higher,
- low flammability,
- low toxicity,
- environmentally friendly.

2.4 Separation of fibres from quills and comminuted feather

Incorporating different parts of the feather fibres into a polymer matrix can result in different thermo-mechanical properties of the final product since different feather fractions contain different thermo-mechanical properties. Hence, it is important to control the usage of different feather segments into desirable ratio; so, the feather fibre barbs need to be stripped from the quill.

In poultry slaughter houses CFs are removed by mechanical pluckers fitted with rubber fingers, and de-feathering is completed by operators who manually finish plucking [71]. The feathers along with a mixture of diluted blood, grease, cleaning water and feathers are then pumped over a separation screen where the liquid waste products are separated into a container [71]. Gassner et al. [35] developed and patented a fibre and quill separation process that utilises turbulent air flow as shown in Figures 2.11, 2.13 and 2.14. In their method, the CFFs were cleaned with a polar organic solvent (ethanol) and dried (Figure 2.12) [35]. Then, fibres are removed from feather shafts using mechanical shredding shearing or a high-speed constant flow centrifugal grinder and light fibres are separated from the heavier quills through a turbulent airflow by apparent density difference [35]. The down industry separates

whole feathers into sizes to extract the finest feathers from other feather parts. The separation of the down feathers from the mixture is based on the principle that smaller, light weight features have a greater lift in an up flow of air than larger feathers [35].

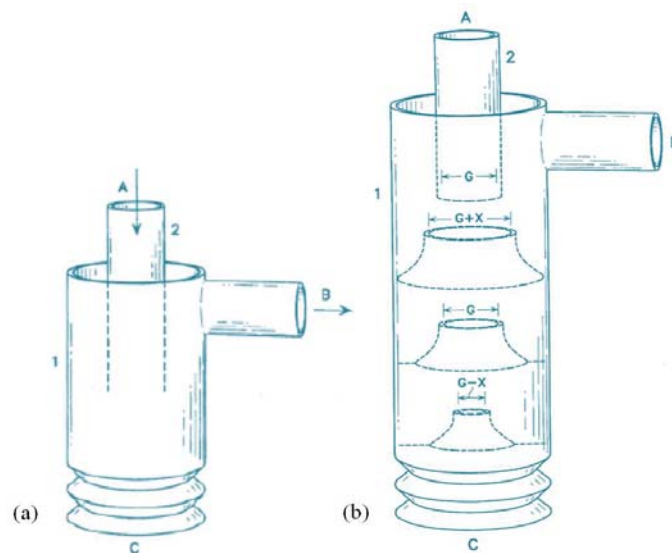


Figure 2.11: Turbulent flow chamber for feather separation

a) an organ separator having an inner input tube concentric with an outer cylinder and b) the organ separator of (a) modified to utilise cascading flared circular sections concentric with the outer cylinder [35]

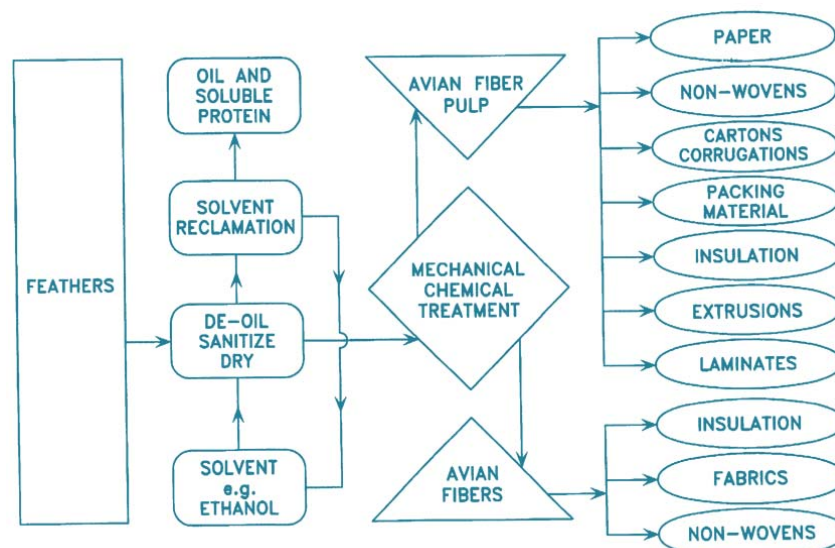


Figure 2.12: Schematic drawing showing the basic steps of making fibres from feathers and some uses for the fibre and fibre pulp compositions [35]

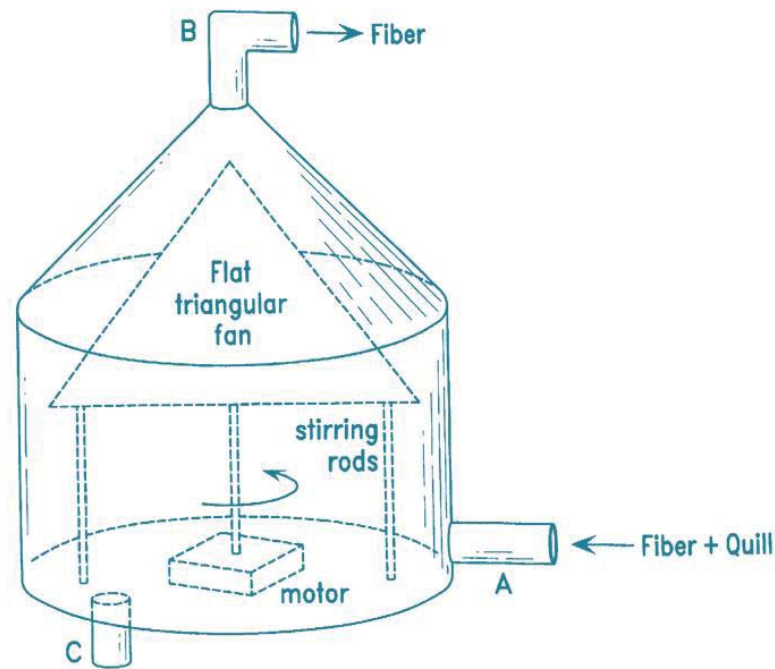


Figure 2.13: Schematic representative of a cone separator having a cylindrical base with a cone-shaped cover through which separated fibres may exit [35]

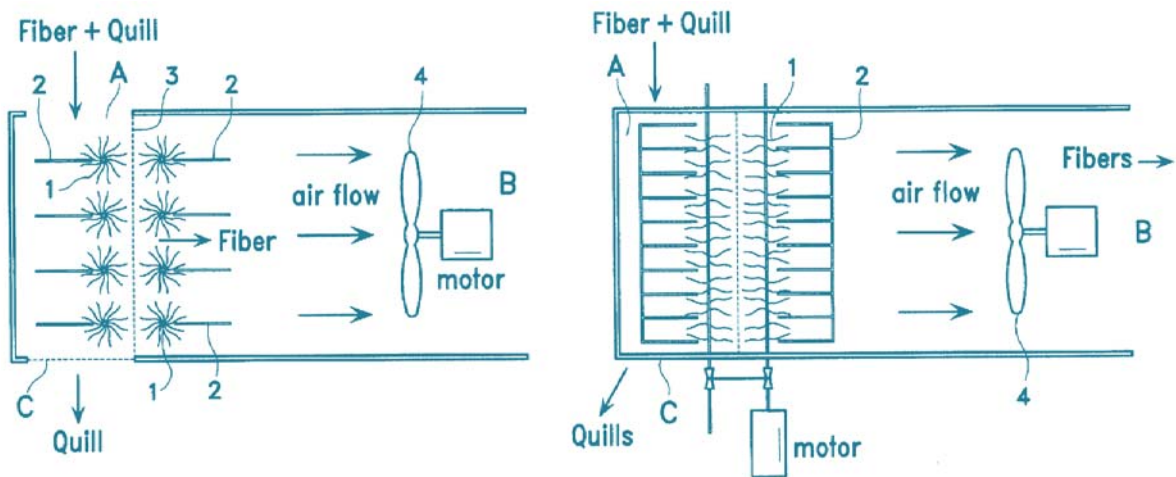


Figure 2.14: Schematic drawing of a comb/brush separator (side and top views) [35]

Fan [5] used a stripping machine built at Auburn University to strip feather fibre (barbs/barbules) from CF (calamus/rachis), using the main part of Fehrer DREF 2000 Friction Spinning Unit-friction unit with some modification (Figure 2-15).

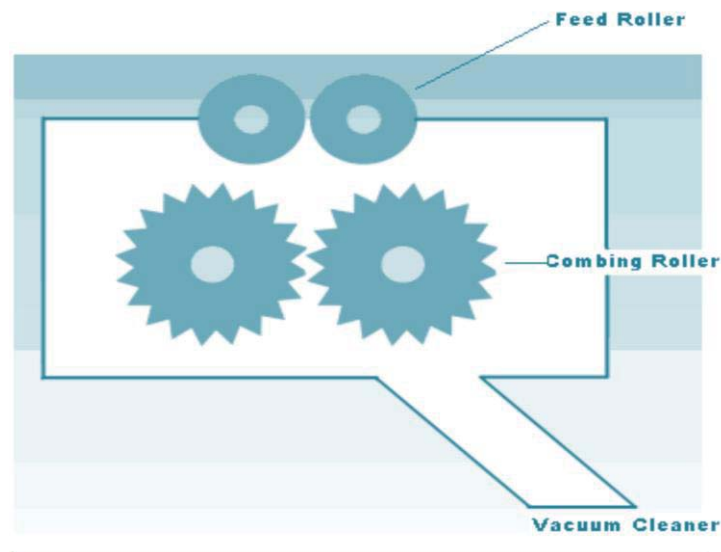


Figure 2.15: Sketch of Stripping Machine [5]

Feather comminution could broadly be divided into dry and wet processes. Gassner [35] described in his patent, dry comminution using a comb/brush separator in which fibres were combed by rotating brushes and air pulled through a screen. The screen aperture size prevented rachis from passing through but the complication was that dry barbs had a static charge and stuck to dry equipment surfaces. Griffith [80] overcame these problems in his patent using wet comminution by recommending the use of refiners, pulpers or disc mills; a high shear pulper used a coupled rotor and stator with a close tolerance to remove fibre from rachis. The refiners, or disc mill, ground, sheared, shredded, pulverised, rubbed and fluffed the feather into a suitable product.

Kock [34] separated the feather fiber barbs from the quill using their difference in specific gravity as a value >1.0 for the apparent specific gravity of barb fiber agrees with observations of the behaviour of the sample fractions in deionized water. In his study, CFs were added to a tapered measuring cylinder to which deionized water was added. The water was then decanted from the measuring cylinder. As water permeated the feather fibre barbs fraction, it sunk to the bottom. This is in contrast to the CF quill fraction, which due to the

fact that it is impenetrable to water, floated and subsequently stuck to the top half of the measuring cylinder because water could not infiltrate the porous inner quill, while it could infiltrate the hollow barb fibres. This tendency is depicted in Figure 2.16, showing a tapered plastic cylinder containing both fibre and quill particles, drained of deionized water [34].

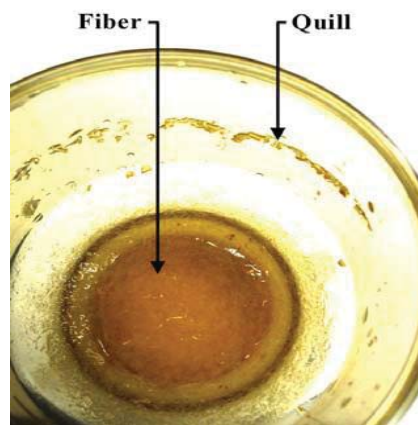


Figure 2.16: Separation of quill segments from barb fibres, the quill floated and the barb fibre sunk in a plastic cylinder [34]

2.5 Application of chicken feather fibres

The CFFs are cheap, biodegradable and a great source of small diameter, high surface area, tough and durable fibre making them attractive for use in different industries. Recent interest in alternative uses for CFFs has raised a number of potential applications such as polymers and composites [24, 83-87], adsorbents in bioremediation [88-95], enzymatic applications [96-102], crop fertilisers and plant antimicrobial control [103-105], animal products [97, 106-110], production of fibres [71], microchips [24], pharmaceuticals and sanitary products [111], as non-woven mats [95, 112], hydrogen storage [87], films and foils, bulletproof vests and flexible armors [113].

From the late 1970s, patent literature has suggested that poultry feathers should be dry-cleaned and used for quilts, pillow filling and jacket insulations [79]. Environmental concerns

have encouraged research in replacing synthetic materials with a variety of natural fibres such as CFFs, which recently attracted scientists' attention due to their advantages from an environmental standpoint [114]. Currently, the KF from CFs is recognised as an almost infinite source of high-performance materials, but further study is needed to demonstrate a basis for innovative technologies and useful raw materials [114]. The unique shape, a centre fibre with many branching fibres, makes CFFs ideal for processes such as injection moulding and dry or wet mat formation, which could be used to improve the properties of existing composite materials, to replace non-renewable constituents, or to develop entirely new bio-composite materials with novel applications [5]. There have been a few reports regarding useful products manufactured using CFFs. For example, Gassner and his colleagues [35] invented techniques to make paper and paper-like products, non-woven and woven fibres, insulation, vacuum, air and water filters, extrusions, and composite sheets and plates to use them as strong, less dense plastic composites, producing products such as car dashboards and boat exteriors. The CFFs can be used in lightweight, sound-deadening composite materials, perhaps with use in office cubicles, cars and sleeping compartments of tractor trailers [5]. The CFFs have been used in water filters that can filter particulates and some heavy metals, which might not only help solve the waste-feather problem, but it might produce better water filters than currently used, such as those made of activated carbon [115].

In addition, CFFs have adsorbent properties that can effectively remove heavy metals such as copper, lead, chromium, mercury, uranium, arsenic, compounds like phenols and some hazardous dyes from aqueous solutions [42]. Before the CFFs were placed in filters, they were 'activated' with ultrasound to produce additional microscopic pores in the fibre's structure [116]. The prototype of feather fibre water filters was produced by packing

the fibres into plastic columns [116]. Tests indicated that the feather filters took contaminants away from home drinking water or industrial waste [116]. In the laboratory experiments, it was found that CFFs filters removed nuclear by-products such as radioactive strontium and caesium by trapping these contaminants with the microstructure of feather fibres [115, 116].

A process of making air filters using CFFs has been patented in China [5]. The process includes mixing CFFs with plant fibre at a given ratio (49 % wood pulp and 51 % CFFs) [117] and making paper with multiple applications. Compared with existing paper-making processes it has the advantage of better air permeability, filterability, full re-utilisation of waste, less pollution to the environment, reduced consumption of wood pulp, reduced cost, and high application value [118].

In search of a new insulation material, Ye et al. [119] has prepared nonwoven insulation materials, instead of spreading on latex, after forming fibre sheets, synthetic fibres were blended with the CFFs and then the combination was moulded into 2-to-4-inch-thick sheets and upon heating, the synthetic material partially melted and held the CFFs in place [119]. It was found that feather insulation could prove useful in down quilts and even attics and walls [119].

Walter Schmidt (1998) invented a technique to mix CFFs with paper and strong, less dense plastic composites to produce products such as car dashboards and boat exteriors. A fibre that can be used in lightweight, sound-deadening composite materials may find use in office cubicles, cars and sleeping compartments of tractor trailers.

The unique shape of a centre fibre, with many branching fibres, makes CFFs ideal for processes such as injection moulding, dry or wet-lay mat formation. Materials derived from CFFs could be used to improve the properties of existing composite materials, to

replace non-renewable constituents, or to develop entirely new bio-composite materials with novel applications.

Adsorption is one of the most important methods for cleaning industrial effluents, and keratin protein can act as a fibrous, nano-filtering sponge [120]. The fibre fraction of CFs has a high surface area ($12 \text{ m}^2/\text{g}$) and partially hollow medulla structure due to a network of 0.05-0.10 μm nanopores [120]. Combined with the appropriate active functional groups, this CFFs has the unique and valuable capacity to bind and thereby remove heavy metals from wastewater [120]. Misra et al. [120] discovered that metal uptake is sensitive to pH, temperature, and the amount of KF used. The binding process is rapid and the metal cations most effectively removed by CFFs are chromium, copper, lead, mercury, nickel and zinc [120].

Another proposed application for CFs is in computer chips [121]. Wool and Hong [121] are prototyping a new generation of microchips that use CF materials to replace silicon due to their strength and porous structure that is filled with air, feathers are good conductors of electrons, which makes them suitable for this application. Circuit boards produced with feather material are approximately 50 % lighter and that electrical signals move twice as quickly through a CFF chip than a conventional silicon chip [122, 123].

A variety of studies have investigated the influence of CFF inclusion on composite properties. Winandy *et al.* [23] studied aspen fibre medium density fiberboard composite panels with CFF replacement in amounts ranging from 20 % to 95 % and 5 % phenol formaldehyde used as an adhesive. Compared with 0:95, CFF:aspen fiber, the 47.5 % CFF revealed 27 % loss in modulus of elasticity and 18 % loss in bending strength [23]. The 95 % CFF demonstrated 51 % loss in modulus of elasticity and 39 % loss in bending strength [23]. Addition of CFF showed a significant improvement in resistance to water absorption,

associated thickness swell, and mould growth, probably due to the hydrophobic elements in keratin's amino acid sequence [23].

Dweib *et al.* [124] fabricated composite sandwich beams made from all natural materials with the goal of developing 100 % natural monolithic structural members suitable for use in load-bearing roofs, floors, or walls of residential and commercial units. Bio-based thermoset resins made from plant oils such as soybean were used and the effects of different natural fibres, including flax, cellulose, recycled paper, and CFFs, were investigated [124].

In composites with thermoset polyesters, feathers were reported to increase the strength by 20 % and decrease the weight by 50 % [125].

Dweib *et al.* [84] used vacuum-assisted resin transfer moulding to infuse feather mats along with sheets of recycled paper with soybean oil-based resin that were combined with structural foam to construct sandwich beams. Those beams showed a global modulus of 950 MPa and a failure load of 24.2 kN during 4-point bend testing [84]. The flexural rigidity and strength of the feather/recycled paper beam were comparable to values for cedar wood.

Barone *et al.* [43] studied CFFs reinforced low-density polyethylene polymer matrix. Physical property testing and microscopy showed some interactions between the fibre and polymer without the need for coupling agents or chemical treatment of the fibres [43]. The CFFs were directly incorporated into the polymer using standard thermo-mechanical mixing techniques. The density of the composite upon introduction of 50 % w/w CFFs was reduced by 2 % [43].

Hamoush and El-Hawary [126] tried to improve concrete properties such as strength and durability by adding CFFs to the concrete mix. The feathers were washed, screened and dried, then added at in three levels of 1, 2 and 3 %. The study showed CFF reinforced concrete was lighter, stronger in flexure, and weaker in compressive and tensile strengths

and cheaper than plain concrete. Concrete containing 1 and 2 % CFFs had the higher flexural strength after 56 days; making it possible for these concrete mixtures to be used in situations where a high loading impact is required. The flexural strength decreased as the feather content was increased above 2 % [126]. It was found that the pore solution (cement in its liquid state) in cement-based materials was strongly alkaline (pH of 12.5-13.5) [127]. Alkaline environments accelerate CFFs decay and the alkaline testing conditions cause low compressive and tensile strength measurement value. Treating CFFs by impregnating them with a blocking agent followed by a water-repellent agent, reduced the alkalinity of the matrix and prevented both short- and long-term decay while increasing compressive and tensile strength. The compressive, tensile and flexural strengths of concrete containing treated CFFs were improved compared with concrete containing untreated CFFs [127].

2.6 Composites with CFFs

There are materials in nature with properties that yet have not been exploited to their full potential and therefore, there has been a surge in investigating the potential of using natural fibres such as CFFs for reinforcements in composite materials that have a huge potential for use in polymer composites. Scientists have looked for keratin source as alternatives to the standard synthetic reinforcements, not only for environmental reasons but due to its interesting intrinsic properties that made it worthy of studying [128]. Consisting of over 90 % keratin makes the CFFs tough reinforcements [4, 129, 130]. The short fibres of CFFs are mostly used as discontinuous fibre reinforcements and by processing and cleaning them, their surface is freed from lipids and fatty acid coatings. This enhances the bonding and stress

transferability between the matrix and fibre, hence increasing the quality of the composites manufactured [131].

2.6.1 Types of composites

Composite materials consist of two or more components, which are insoluble in each other and together they are stronger than individual component [132, 133]. The matrix grants toughness to the composite and keeps the reinforcement in desired location and orientation, whereas the reinforcing material is responsible for the strength and stiffness of the composite [134]. According to Kokcharov [135], composites types are: a) composites that reinforced by particles, b) composites that reinforced by chopped strands, c) unidirectional composites, d) laminates, e) fabric reinforced plastics, and f) honeycomb composite structure, as shown in Figure 2.17.

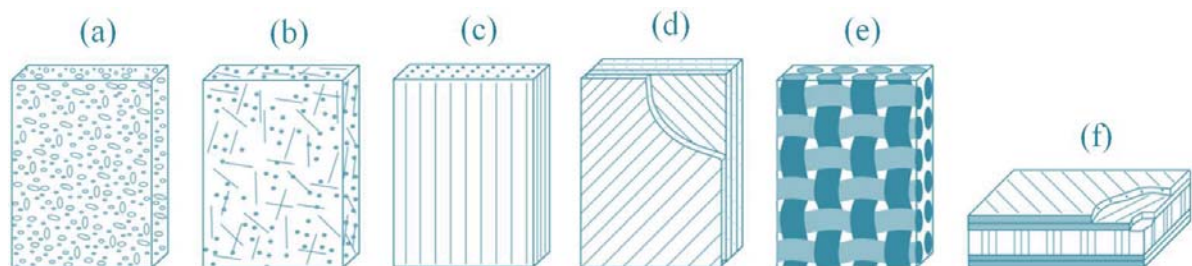


Figure 2.17: Different types of composites: (a) reinforced by particles, (b) reinforced by chopped strands, (c) unidirectional composites, (d) laminates, (e) fabric reinforced plastics, (f) honeycomb composite structure (adopted from Kokcharov [135])

Sudalaiyandi [9] reported that fibres are used as the reinforcement material on a plastic resin, in the type of fibre-reinforced composites and a fibre has a high length to diameter ratio, known as 'aspect ratio' [9]. Continuous and discontinuous fibre reinforcements are two major types of fibre reinforcement composites. In the continuous fibre reinforcement (Figure 2.18a) composite, fibres have high aspect ratios and generally have a preferred

orientation and any further increase in the length of the fibre will not change the properties of the composite. Continuous fibre composites are used where higher strength and stiffness are required but at a higher cost.

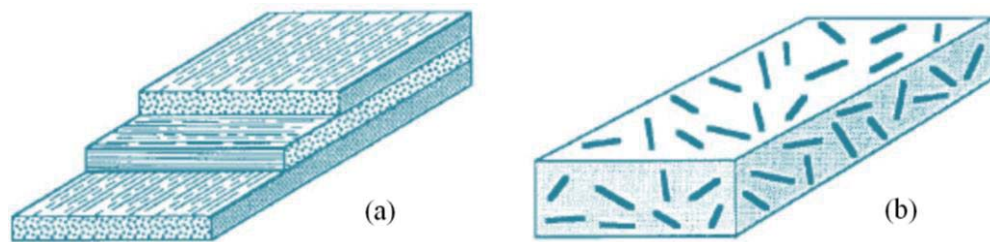


Figure 2.18: Diagrammatic representation of fibre reinforcement composites: (a) continuous fibre reinforcements, and (b) Discontinuous fibre reinforcements [9].

In discontinuous fibre reinforcements (Figure 2.18b) the fibres have low aspect ratios and normally have reduced orientation. The applications involving multi-directional applied stresses commonly use discontinuous fibres and are cheaper to manufacture [9].

Fiber-matrix bonding is an important factor which affects the strength of both continuous and discontinuous fibre-reinforced composites. Effective adhesion of the fibres to the matrix increases the strength of a composite material. However, the final properties of a composite material depend on factors such as mechanical properties of the fibre, type and orientation of fibres, volume fraction of fibres and processing techniques used [9].

2.6.2 Types of fibres

Polymers are often durable, environmentally resistant, tough and light and easily shaped by extrusion, injection moulding, vacuum forming and foaming, used in almost every field such as packaging, transport, construction and casings [41]. Tailoring mechanical polymer properties for specific purposes often requires fibre reinforcement and common synthetic fibres include carbon, aramid (aromatic polyamides) and glass fibres while natural fibres such as wood, hemp and sisal

have been shown to be effective as well [41]. Fibres are classified as natural or man-made fibres (Figure 2.19), which are synthesised from polymers. The raw materials used to manufacture the polymers are derived from petrochemical [9] or natural sources. For example, synthesised fibres can be prepared from non-petrochemical sources, such as cellulose (Lyocell, cellulose acetate and Modal are common examples of these ‘semi-synthetic’ fibres). Natural fibres have attracted scientists’ attention due to their environmental advantages [5].

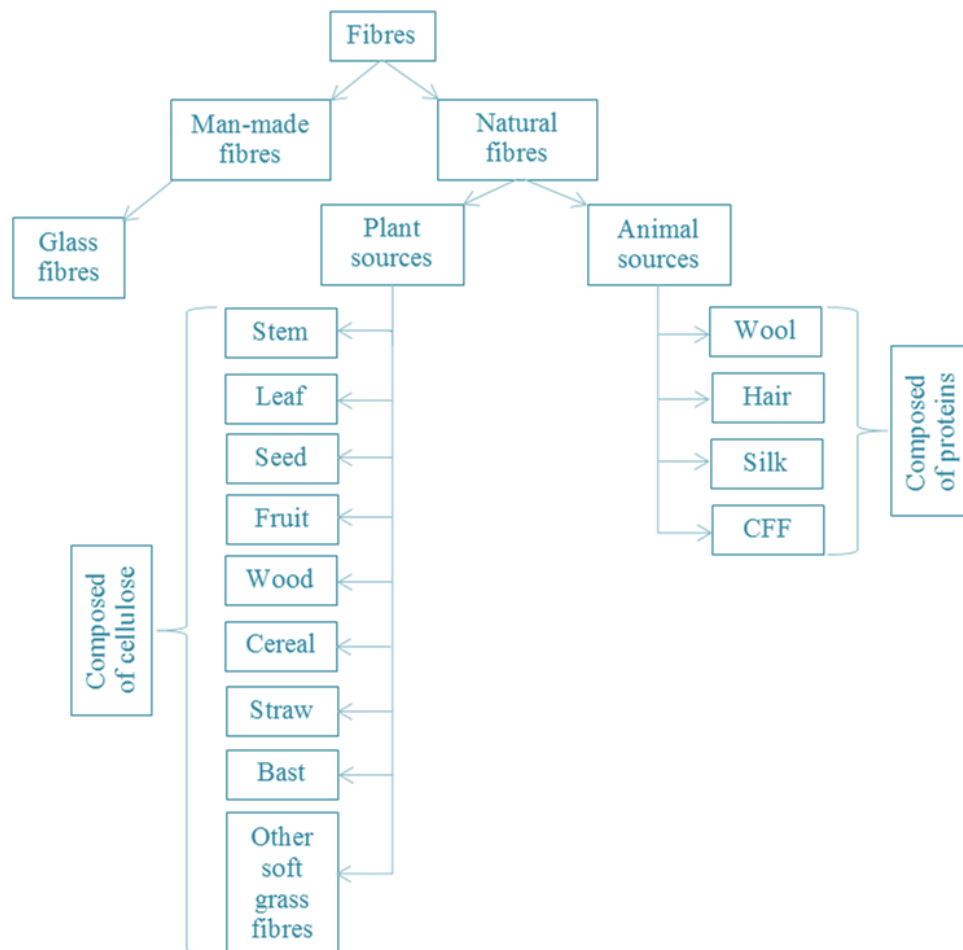


Figure 2.19: Diagrammatic representation of fibre origins

Some of the most widely used synthetic fibres are kevlar fibres, glass fibres, carbon fibres and aluminium fibres with the advantages of high tensile strength, stiffness, thermal stability and large-scale manufacturing [9]. On the other hand, natural fibres are obtained from plant and animal sources that are composed of cellulose and proteins respectively. Plant fibres include stem (ramie bamboo), leaf (Sisal and abaca), seed, fruit (cotton and coir fibres), wood, cereal, straw, bast (flax, hemp, jute and kenaf) and other soft grass fibres. Animal fibres include hair, wool (alpacas, llamas, vicunas, yaks, camels, cashmere goats and angora rabbits), silk (fibroin) and feather fibres (chicken, turkey, duck, guinea fowl, goose, quail, pheasants and squabs). Additional advantages of the use of natural fibres in composites are their renewability, biodegradability, non-toxicity, insulation properties and low machine wear [136].

The source of feather fibre is uniquely different to commercial fibres on the market since feather fibre is effectively a renewable source of fibre whereas synthetic fibres are renewable only to the extent that they are recycled [69]. Trees can be harvested every twenty years; wool, cotton, kenaf maybe twice a year; but poultry are raised for food continuously and concomitantly, thus a predictable supply of fibre always occurs. Acres of land on which plant fibre is raised are always in danger of routinely occurring natural disasters like frost, drought, pests, fire, floods and market forces. The longer the fibre takes to grow, the greater the risk of a significant loss of valuable assets. An alternative to the aforementioned fibres is CFFs, as they are widely available and have good mechanical properties [41]. The supply of fibre from feathers is potentially as dependable and as 'risk-free' as that for poultry meat [69]. After considerable research over years on the physical properties and chemical structure of CF protein, it is being recognised as a potential polymeric raw material for composites and

regenerated fibres. Most of the CF is a structural fibrous protein, keratin, which could easily be used for fibre production as an alternative for natural protein fibres [2].

When the fibre has similar properties to that of the polymer, composites can be made with them but instead of adding to the physical properties of the polymer, it just adds to the volume of polymer. Feather fibre then acts as a filler and/or extender of the polymer already in use. The value of an inert fibre in a polymer mixture which adds no new properties to the end-product is in the volume of polymer it has replaced within the original end-product [69]. The maximum value of feather fibre, however, is not in the polymer that it can replace, but in unique properties of the fibre which enables valuable new products to be created and for which existing fibres are inadequate; new markets, new products, new sales [69]. Feather fibre is a multipurpose, cost effective reinforcement for polymer composites [71]. Its incorporation in polymer, wood, concrete and cardboard makes the product lighter, insulated from heat loss with improved sound attenuation [71].

2.6.3 Bio-composites

Polymers reinforced with natural fibres, commonly named 'bio-composites', started to be industrially applied not only in the automotive and building sectors but in the broad area of consumer goods [136]. A recent work by La Mantia et al. [133] comprehensively reviewed the type of bio-composites with particular emphasis on strategies to overcome composite process-ability problems and improving composite performance.

The use of natural CFFs as potential reinforcement in composites offers an environmentally benign solution for feather disposal and provides profits for the poultry industry [137]. Compatibility with organic resins is essential for their applications in composite materials [137]. The CFFs offer advantages such as efficient thermal and

mechanical properties, effective insulation, fire resistance, low density, small diameter, high surface area, tough and durable, biodegradable, environmentally-friendly and relatively easy to obtain with low cost [43, 129, 138-140]. The unique shape of the feather with, a centre fibre and many branching fibres, makes feathers ideal for processes such as injection moulding, dry formation or wet laying [42]. The CFF diameter is *ca.* 5 μm to 50 μm and its length ranges from 1 mm to 35 mm [20, 43], which is an important consideration as it would affect the stress transferability between the matrix and the fibre [41]. The bonding between the polymer matrix and fibre is an important factor affecting the quality of composite manufactured [131]. In composites with thermoset polyesters, feathers are reported to increase the strength by 20 % and decrease the weight by 50 % [36].

In terms of fibre reinforcement, the use of down feather fibres with solid structures was found to give better results than flight feather fibres with hollow structures [41]. Kock [34] reported the fibre material was found to have a greater tensile strength than the quill material. The fibre was more durable and had a higher aspect ratio than the quill [141]. The presence of rachis in the CFs makes the composites more granular, bulkier and lighter in weight, therefore its exclusion results in smoother and denser products [35, 36]. However, in some studies, the rachis was preferable to be used as fillers, hence, for most of the fibre-reinforcement work, the fibre was cut from the rachis of the feathers.

According to Zini et al. [136], green composites are a specific class of bio-composites, where a bio-based polymer matrix is reinforced by natural fibres. Some authors label all the polymers reinforced with natural fibres as 'green composites' [133], irrespective of the nature of the polymeric matrix (both bio and petroleum-based).

2.7 Chicken feather keratin

The structure of keratin as the primary constituent of CFs, affects its chemical durability and resistance to degradation due to the extensive cross-linking and strong covalent bonding within keratin's structure and efforts to extract keratin proteins from feathers illustrate this point [34]. Extraction is a difficult task because it can only be achieved if the disulfide and hydrogen bonds are broken [34]. Schrooyen [142] found keratin to be insoluble in polar solvents, as well as in nonpolar solvents. The most common method of dissolving feather keratin is its solubilisation with concomitant peptide bond scission via acid or alkali hydrolysis, reduction of disulfide bonds with alkaline sodium sulfide solutions, or a combination of enzymatic and chemical treatment [143].

2.7.1 Extraction of keratin from chicken feather fibres

According to Goddard et al. [144], CFK can be converted to natural protein soluble in alkali or acid and digestible by trypsin and pepsin. As per Goddard et al. [145] oxidising agents such as bromine, permanganate and hydrogen peroxide act slowly in breaking the disulfide bonds thus slowing down the protein extraction process. In contrast, reducing agents act quickly and dissolve keratin only at pH 10 to 13 but the action is not due to alkali alone.

Strong fibres require high molecular weight polymers therefore, it is necessary to cleave the disulfide bonds without hydrolysing the peptide chain in KF production [146]. Both reducing agents and oxidising agents can be used to break the disulfide bonds, however in the study by Katoh et al. [146] ammonium bisulfide salt (pH 12), produced a reversible reduction of the molecules and produced keratin suitable for fibre production (Figure 2.20).

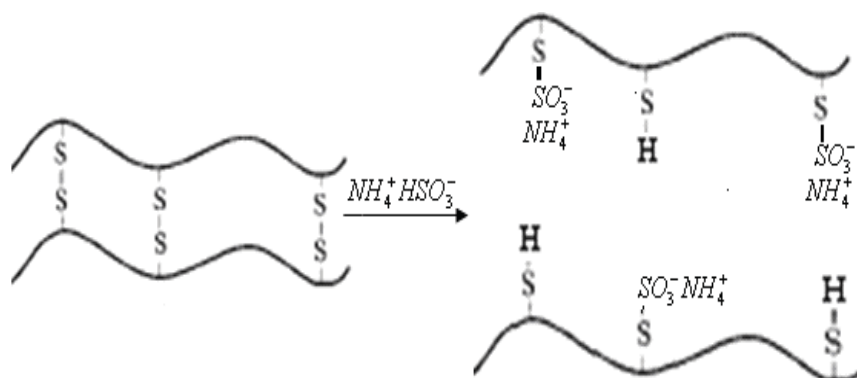


Figure 2.20: Reduction of disulfide bonds by ammonium bisulfite [5, 146]

An ionic liquid (IL) (is a salt with a melting temperature (MT) below 100 °C, typically consists of a heterocyclic nitrogen-containing organic cation and an inorganic anion) with the reducing agent was used as a solvent to dissolve the protein in a study done by Fan [5] (Figure 2.21).

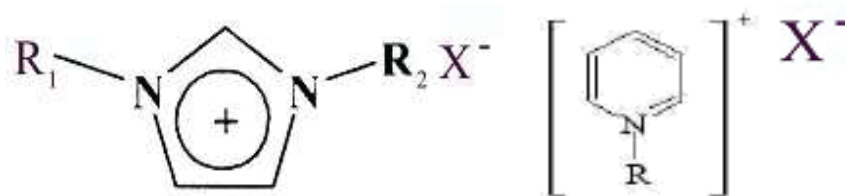


Figure 2.21: Basic chemical structure of an ionic liquid [5]

Although ionic liquids are considered to be as toxic as commonly used organic solvents [147], due to their recyclability, they are now seen as a valid option by many researchers [148]. Compared with the traditional solvents, IL has special molecular structure, which has many unique solubility characteristics such as electrically conductive, non-flammable, low vapour pressure, thermal stability, a wide liquid range and favourable solvating [149]. Ionic liquids have noticeable odours and solvating properties for different compounds, due to their impurities [149]. Hence, IL becomes a route to volatile organic solvent replacement and has

received a lot of attention due to acting as a green and designable solvent with the development of green chemistry and the requirement for environment protection [149]. It has been found that IL is used already in organic synthesis and catalysis [149, 150]. Even though, ionic liquids are promising green materials, the costs of using them are higher than inorganic reagents. Additionally, separation of keratin from hydrophilic ionic liquids after the reaction is an inconvenient and troublesome problem [151], which is the reason they were not used for investigation in this research project.

Schmidt and Line [20] reported that 1-butyl-3-methyl-imidazolium chloride (BMIM^+Cl^-), which is an ionic solution, is an excellent solvent to dissolve cellulose and is easy to prepare an up to 10 %·w/w solution by heating at 100 °C. The BMIM^+Cl^- has strong ability to disrupt hydrogen bonds under mild conditions and thus they can be used to dissolve biological macromolecules that are linked by intermolecular hydrogen bonds such as polysaccharides (cellulose) and protein [5, 20, 152]. Haibo Xie et al. [152] reported that BMIM^+Cl^- is an excellent solvent for wool keratin and obtained 11 %·w/w solution at 130 °C by adding and dissolving 1 %·w/w wool keratin step by step. Fan [5] investigated the dissolving of wool keratins with an aqueous solution of BMIM^+Cl^- (Figure 2.22).

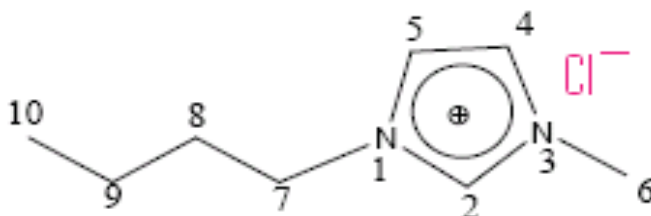


Figure 2.22: Chemical structure of BMIM^+Cl^- [5]

Fan [5] used BMIM^+Cl^- to dissolve CF directly with reducing agent bisulfite salt, and observed that BMIM^+Cl^- did not dissolve CF directly and only swelled it. Therefore, she obtained reduced keratin first and then dissolved it in BMIM^+Cl^- . The processing sketch is shown in Figure 2.23. Currently, there is an increasing interest in the development of materials that are environment-friendly, and obtained from renewable resources such as polysaccharides, lipid and proteins [60]. There is a demand for textile materials having specific properties such as the ability to absorb and retain humidity, hence the wool KF has been used as textile fibres or to produce strong fibres, but CF keratin has not found such use [5]. Due to the amount of CFs produced by the poultry industry worldwide, CF is the most abundant keratinous material in the world [5]. These hard keratins of CF which are recognised as solid wastes generated from poultry processing industry are insoluble and resistant to degradation by common proteolytic enzymes, such as trypsin, pepsin and papain because of their high degree of cross-linking by disulfide bonds, hydrogen bonding and hydrophobic interactions [60]. Methods for acid, alkaline hydrolysis, oxidation and reduction have been reported in the published literature [46]. This project is about extracting natural proteins from CFs by using reducing agents that will decrease the stability of keratin fibres (KFs) in the solid form found in feathers. These reagents broke down disulphide bonds, hydrogen bonds and salt linkages of the KFs in order to dissolve it into natural protein.

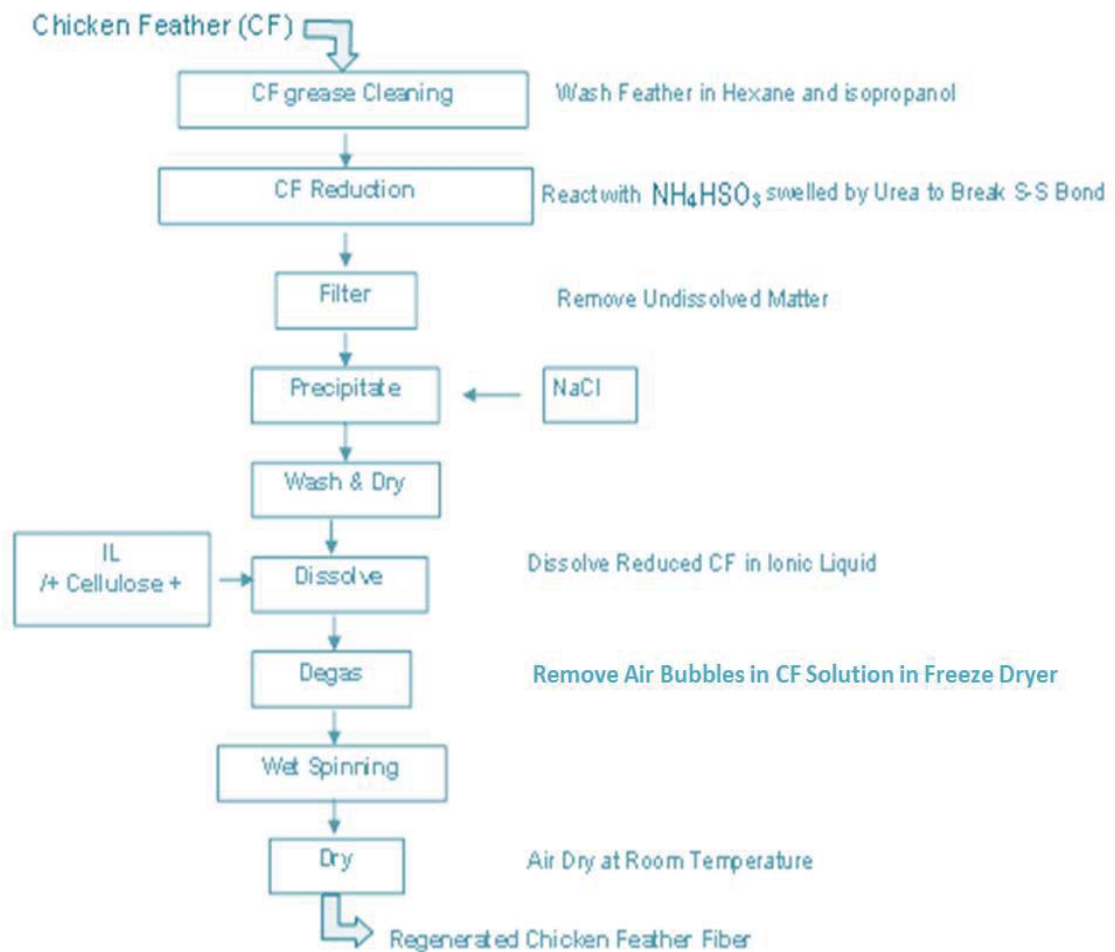


Figure 2.23: Diagram of production of regenerated chicken feather fibres [5]

Feather fibres are exceptionally strong and stiff [63]. Sulphur-sulphur cross-links between cysteine molecules as well as hydrogen bonds are responsible for the stiffness and strength of keratin [5]. Extraction of CF keratin can be achieved only if the disulfide and hydrogen bonds are broken [5]. During the 1940s and 1950s, a number of studies showed that the inter-molecular cross-links in keratin can be broken to obtain a spinnable fraction, which can be processed into polymeric materials, such as filament fibres [5]. Such new biopolymeric materials from CF keratin might find interesting applications as packaging material or matrix material in fibre-reinforced composites [3].

There is a close relation between the strength of fibre and length of the constituent chains [5]. To retain the mechanical properties, protein chains need to be kept during extraction of CF keratin, via -S-S- disulfide bonds to rupture only but not break the main polypeptide chain (peptide linkage) while dissolving CF keratin (Howitt, 1955). Currently, there are several methods to dissolve CF keratin [5]. Both reducing agents and oxidising agents can be used to break the disulfide bonds [5]. The cysteine residues are oxidised to produce both inter- and intramolecular disulfide bonds, which cause the mechanically strong three-dimensionally cross-linked network of KF with the limited conformational arrangement so feather fibre keratin has compact crystal structure [5].

The most common method is using reducing agents in alkaline solution [5]. Goddard et al. [144] worked on the extraction of the keratin of wool and CFs in alkaline thioglycolate, cyanide, and sulfide, and examined the properties of the precipitates obtained by acidification of the alkaline dispersions. They suggested that alkalinity was a prerequisite for the reduction. To explain the inability of reducing agents to disperse keratin in less alkaline solutions at pH 10, they hypothesised that, for the dispersion of keratin, both the disulfide groups and the salt linkages of the keratin molecule must be broken [5]. From their work, Goddard et al. [144] found that thioglycolic acid could reduce the disulfide groups of wool over a wide pH range, but no dispersion occurred if the reduction was carried out in neutral or acid solution.

Jones and Mecham [153] studied the dispersion of feather keratin in Na_2S solutions under various experimental conditions such as temperature, time, Na_2S concentration, and the ratio of keratin to Na_2S and recovered dispersed protein by acidification of the dispersion to pH 4.2. They discovered that when feathers were treated with 0.1 M Na_2S

(100 mL of solution per 7.5 g of keratin) for about 2 h at 30 °C, the maximum dispersion of feather keratin was obtained with minimal degradation. Additionally, they found that protein denaturants such as urea could help keratin disperse at neutral pH and alkali could act as a dispersing agent for the reduced keratin.

Schrooyen [154] studied stabilisation of solutions of feather keratins by sodium dodecyl sulfate (SDS) and effects of the addition of various quantities of SDS on the rate of aggregation of the polypeptide chains and the rate of oxidation of cysteine residues during dialysis. They extracted keratins from CFs with aqueous solutions of urea and 2-mercaptoethanol. Removal of 2-mercaptoethanol and urea by dialysis resulted in aggregation of the keratin polypeptide chains and oxidation of the cysteine residues to form a gel. SDS was added to the keratin solution prior to dialysis to prevent extensive aggregation of the keratin chains. It was found that higher SDS/keratin ratios (1 g to 2 g SDS/g keratin) seemed to prevent the oxidation reaction between different keratin chains, that result in more intramolecular disulfide bond formation (Figure 2.24).



Figure 2.24: Schematic representations for SDS-keratin complexes with a high amount of SDS added prior to dialysis [154]

2.8 Antibacterial effects of chicken feather keratin

Antibacterial activity can be defined as preventing the growth and propagation of bacteria [50]. Bacteria may be inhibited in a number of ways: a) by break down or prevention of peptidoglycan cell wall formation allowing excess water to enter the bacterial cell leading to cell apoptosis via osmotic pressure. This mode of action is quite common in polypeptide and penicillin antibiotics [50]. b) Bacterial protein interference, which stops the organism from producing essential proteins necessary for survival and targets the ribosome of the microbe that makes the essential protein [155] or targets nucleic acid breakdown via the enzyme that coils and uncoils deoxyribonucleic acid (DNA) during the synthesis process [50]. These mechanisms are more pronounced when using synthetically made antimicrobials [155, 156]. Both Wang *et al.* [157] and Tran *et al.* [158] used keratin in different ways but came to a similar conclusion that suggests keratin is an ideal antimicrobial for wound dressing as it exhibits bactericidal properties. Paul *et al.* [159] studied antimicrobial peptides and concluded that the keratin showed antibacterial effect.

Escherichia coli (*E. coli*) and *Staphylococcus aureus* (*S. aureus*) can be found in a mammalian body. *E. coli* resides in the intestines of the gut and *S. aureus* can be found carried on the skin [159]. Structurally *E. coli* (Gram-negative) and *S. aureus* (Gram-positive) can be distinguished by their Gram-morphology i.e. the structure of their cell wall [160]. Gram-morphology and the Gram-stain of the organism indicate more than just the outer cellular shape of the organism. For instance, Gram-negative organisms like *E. coli* which appear pink under the microscope, have a thin layer of disaccharides and amino acids, known as the peptidoglycan and it has lipopolysaccharide layer which is a combination of lipid molecules and polysaccharides [155]. This lipopolysaccharide level increases the chance of

Gram-negatives to become resistant to some antimicrobials. The lipid and polysaccharide coating prevents antimicrobial and chemical penetration. Unlike with Gram-positive organism, which lacks the lipid and polysaccharide coating, hence even with the thickness of its peptidoglycan antibacterial agents easily targets it [155]. The difference in Gram-negative and Gram-positive bacterial cell wall is shown in Figure 2.25.

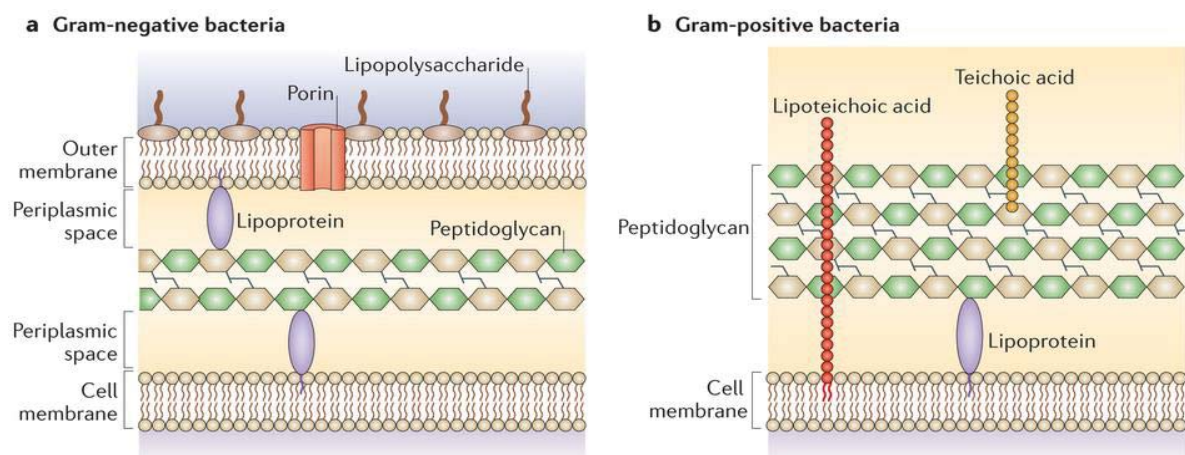


Figure 2.25: Bacterial cell wall representation, difference between (a) Gram-negative and (b) Gram-positive bacteria [161]

2.9 Applications of chicken feather keratin

Like many naturally-derived biomolecules, keratins have intrinsic biological activity and biocompatibility; extracted keratins are capable of forming self-assembled structures that regulate cellular recognition and behaviour, together with its antimicrobial properties [162]. This led to the development of keratin biomaterials with applications in wound healing and repairing products, drug delivery and pharmaceuticals, tissue engineering such as bone tissue regeneration, trauma and medical devices; as well as composites and textile applications to replace the two natural but more expensive protein fibres wool and silk [3, 163, 164]. The personal care product produced from the keratin protein include but are not limited to

conditioning shampoo, sulphite hair straightener, sanitary products, anti-aging cream (anti-wrinkle treatment cream), skin, hair and nails care products, facial cleanser, cosmetic product [37, 165, 166], etc. Wrzesniewska-Toski et al. [167] employed wet-spinning techniques to create novel fibrous keratin-based materials that have potential application as hygienic fabrics. Keratin extracted from CFs and bio-modified cellulose were combined and used to create fibres with better adsorption properties, higher hygroscopicity, and a smaller wetting angle than cellulose fibres. Although the introduction of keratin into cellulose fibres decreased the mechanical properties, a level was achieved that still enabled their application for manufacturing composite fibrous materials. In addition, the cellulose-keratin fibres had better biodegradation than pure cellulose fibres [167].

As can be seen, increasing the usage of waste CFs into usable, commercial products has been the object of intensive investigations in many research centres so it is gradually gaining recognition. However, clear purification treatment techniques and microbiological analysis for fresh raw CFFs from slaughterhouses are lacking in the literature. The incorporation of CFK into a linear thermoplastic polyether–polyurethane (Pellethane[®]) polymer matrix that consisted of poly(butane-1,4-diol), methylene diphenyl diisocyanate (MDI) with a butane-1,4-diol chain extender, has not been studied and characterised before. The enhancement of thermo-mechanical properties of bio-composites using keratin has not been thoroughly explored at all. Yield optimisation of keratin extraction methods using sodium sulfide together with using a more environmentally friendly enzyme such as L-cysteine has not been investigated. The present project on the CFFs and its extracted keratin could improve the development of keratin-based materials, and environmentally friendly technology for the treatment of keratin wastes and throws light on conversion of feather waste into value-added

products. The bioconversion of feathers will predictably benefit the poultry industry, the environment and human beings.

2.10 References

1. Williams, C., C. Richter, J. Mackenzie, and J.C. Shih, *Isolation, identification, and characterization of a feather-degrading bacterium*. Applied and Environmental Microbiology, 1990. **56**(6): p. 1509-1515.
2. Arai, K.M., R. Takahashi, Y. Yokote, and K. Akahane, *Amino-Acid Sequence of Feather Keratin from Fowl*. European Journal of Biochemistry, 1983. **132**(3): p. 501-507.
3. Reddy, N. and Y. Yang, *Structure and properties of chicken feather barbs as natural protein fibers*. Journal of Polymers and the Environment, 2007. **15**(2): p. 81-87.
4. Zhan, M. and R.P. Wool, *Mechanical properties of chicken feather fibers*. Polymer Composites, 2011. **32**(6): p. 937-944.
5. Fan, X., *Value-added products from chicken feather fiber and protein*. PhD Thesis. 2008, Auburn, Alabama: ProQuest, Auburn University.
6. Onifade, A., N. Al-Sane, A. Al-Musallam, and S. Al-Zarban, *A review: potentials for biotechnological applications of keratin-degrading microorganisms and their enzymes for nutritional improvement of feathers and other keratins as livestock feed resources*. Bioresource technology, 1998. **66**(1): p. 1-11.
7. Australian Bureau of Statistics (ABS). June 2014, Livestock Products, Australia, 7215.0.
8. Australian Bureau of Agricultural and Resource Economics and Sciences (ABARES) September 2014, Australian Commodity Statistics.
9. Sudalaiyandi, G., *Characterizing the cleaning process of chicken feathers*. Master of Engineering thesis, University of Waikato, Hamilton, New Zealand (2012).
10. BAKER, D.H., R.C. BLITENTHAL, K.P. BOEBEL, G.L. CZARNECKI, L. Southern, and G.M. WILLIS, *Protein-amino acid evaluation of steam-processed feather meal*. Poultry Science, 1981. **60**(8): p. 1865-1872.
11. Papadopoulos, M., A. El Boushy, and E. Ketelaars, *Effect of different processing conditions on amino acid digestibility of feather meal determined by chicken assay*. Poultry Science, 1985. **64**(9): p. 1729-1741.
12. Dalev, P., I. Ivanov, and A. Liubomirova, *Enzymic modification of feather keratin hydrolysates with lysine aimed at increasing the biological value*. Journal of the Science of Food and Agriculture, 1997. **73**(2): p. 242-244.
13. Xu, S., T. Reuter, B.H. Gilroyed, L. Tymensen, Y. Hao, X. Hao, M. Belosevic, J.J. Leonard, and T.A. McAllister, *Microbial communities and greenhouse gas emissions associated with the biodegradation of specified risk material in compost*. Waste management, 2013. **33**(6): p. 1372-1380.
14. Endo, R., K. Kamei, I. Iida, and Y. Kawahara, *Dimensional stability of waterlogged wood treated with hydrolyzed feather keratin*. Journal of Archaeological Science, 2008. **35**(5): p. 1240-1246.

15. Poole, A.J. and J.S. Church, *The effects of physical and chemical treatments on Na2S produced feather keratin films*. International journal of biological macromolecules, 2015. **73**: p. 99-108.
16. Kumawat, T.K., A. Sharma, and S. Bhadauria, *Chrysosporium queenslandicum: a potent keratinophilic fungus for keratinous waste degradation*. International Journal of Recycling of Organic Waste in Agriculture: p. 1-6.
17. Chinta, S., S. Landage, and K. Yadav, *Application of chicken feathers in technical textiles*. International Journal of Innovative Research in Science, Engineering and Technology, 2013. **2**(4): p. 1158-1165.
18. Montes-Zarazúa, E., A. Colín-Cruz, M.d.l.L. Pérez-Rea, M. de Icaza, C. Velasco-Santos, and A.L. Martínez-Hernández, *Effect of Keratin Structures from Chicken Feathers on Expansive Soil Remediation*. Advances in Materials Science and Engineering, 2015.
19. Rabiatal Adawiyah, Z., *Formulation of Wound Healing Hydrogel from Keratin Protein*. 2012.
20. Schmidt, W. and M. Line, *Physical and chemical structures of poultry feather fiber fractions in fiber process development*. Nonwovens. Conference, Atlanta, GA, USA, 1996: p. 135-140.
21. Bartels, T., *Variations in the morphology, distribution, and arrangement of feathers in domesticated birds*. Journal of Experimental Zoology Part B: Molecular and Developmental Evolution, 2003. **298**(1): p. 91-108.
22. Ullah, A. and J. Wu, *Feather Fiber-Based Thermoplastics: Effects of Different Plasticizers on Material Properties*. Macromolecular Materials and Engineering, 2013. **298**(2): p. 153-162.
23. Winandy, J.E., J.H. Muehl, J.A. Micales, A. Raina, and W. Schmidt, *Potential of chicken feather fiber in wood MDF composites*. Proceedings EcoComp 2003, 2003. **20**: p. 1-6.
24. Hong, C.K. and R.P. Wool, *Development of a bio-based composite material from soybean oil and keratin fibers*. Journal of Applied Polymer Science, 2005. **95**(6): p. 1524-1538.
25. Rogers, S.L., *The aboriginal bow and arrow of North America and Eastern Asia*. American Anthropologist, 1940. **42**(2): p. 255-269.
26. Subramani, T., S. Krishnan, S. K.Ganesan, and G. Nagarajan, *Investigation of Mechanical Properties in Polyester and Phenylester Composites Reinforced With Chicken Feather Fiber*. Int. Journal of Engineering Research and Applications 2014. **4**(12): p. 93-104.
27. Messinger, N.G., *Methods used for identification of feather remains from Wetherill Mesa*. Memoirs of the Society for American Archaeology, 1965: p. 206-215.
28. Wallenberger, F.T. and N. Weston, *Natural fibers, plastics and composites*. Materials Source Book, Editors: Wallenberger, Frederick T., Weston, Norman (Eds.) 2004.
29. Kazilek, C.J. *Feather Biology*. 2009 Accessed: December 11, 2016]; Available from: <https://askabiologist.asu.edu/explore/feather-biology>.
30. Lingham-Soliar, T., R.H. Bonser, and J. Wesley-Smith, *Selective biodegradation of keratin matrix in feather rachis reveals classic bioengineering*. Proceedings of the Royal Society of London B: Biological Sciences, 2009: p. DOI: 10.1098/rspb.2009.1980.

31. Bock, W.J., *Birds in Encyclopaedia of life support systems*, Eds: Contrafatto, G and Minelli, A. Oxford, UK: EOLSS. 2004.
32. Leeson, S. and T. Walsh, *Feathering in commercial poultry I. Feather growth and composition*. World's Poultry Science Journal, 2004. **60**(01): p. 42-51.
33. Misra, M., P. Kar, G. Priyadarshan, and C. Licata. *Keratin protein nano-fiber for removal of heavy metals and contaminants*. in *Materials Research Society (MRS) Proceedings*. 2001. Cambridge Univ Press.
34. Kock, J.W., *Physical and mechanical properties of chicken feather materials*. Master of Science thesis, Georgia Institute of Technology, Atlanta, Georgia, 2006.
35. Gassner, G., W. Schmidt, M.J. Line, C. Thomas, and R.M. Waters, *Fiber and fiber products produced from feathers*. 1998, U.S. Patent 5705030 A.
36. Lau, A.K.-T., F. Hussain, and K. Lafdi, *Nano-and biocomposites*. 2009, London: CRC Press.
37. Gupta, A., N.B. Kamarudin, C.Y.G. Kee, and R.B.M. Yunus, *Extraction of keratin protein from chicken feather*. Journal of Chemistry and Chemical Engineering, 2012. **6**(8): p. 732.
38. Alberts, B., D. Bray, J. Lewis, M. Raff, K. Roberts, J.D. Watson, and A. Grimstone, *Molecular Biology of the Cell (3rd edn)*. Trends in Biochemical Sciences, 1995. **20**(5): p. 210-210.
39. Barone, J.R. and W.F. Schmidt, *Effect of formic acid exposure on keratin fiber derived from poultry feather biomass*. Bioresource technology, 2006. **97**(2): p. 233-242.
40. Saravanan, K. and B. Dhurai, *Exploration on the Amino Acid Content and Morphological Structure in Chicken Feather Fiber*. Journal of Textile and Apparel, Technology and Management, 2012. **7**(3).
41. Schmidt, W.F. and S. Jayasundera, *Microcrystalline avian keratin protein fibers*, in *Natural Fibers, Plastics and Composites*. 2004, Springer. p. 51-66.
42. Kar, P. and M. Misra, *Use of keratin fiber for separation of heavy metals from water*. Journal of Chemical Technology and Biotechnology, 2004. **79**(11): p. 1313-1319.
43. Barone, J.R. and W.F. Schmidt, *Polyethylene reinforced with keratin fibers obtained from chicken feathers*. Composites Science and Technology, 2005. **65**(2): p. 173-181.
44. Jagadeeshgouda, K., P.R. Reddy, and K. Ishwaraprasad, *Experimental Study of Behaviour of Poultry Feather Fiber: A Reinforcing Material for Composites*. International Journal of Research in Engineering and Technology, 2014. **3**(2): p. 362-366.
45. Arai, K., N. Sasaki, S. Naito, and T. Takahashi, *Crosslinking structure of keratin. I. Determination of the number of crosslinks in hair and wool keratins from mechanical properties of the swollen fiber*. Journal of applied polymer science, 1989. **38**(6): p. 1159-1172.
46. Ma, B., X. Qiao, X. Hou, and Y. Yang, *Pure keratin membrane and fibers from chicken feather*. International Journal of Biological Macromolecules, 2016. **89**: p. 614-621.
47. Ullah, A., T. Vasanthan, D. Bressler, A.L. Elias, and J. Wu, *Bioplastics from feather quill*. Biomacromolecules, 2011. **12**(10): p. 3826-3832.
48. Fraser, R., T. MacRae, and G.E. Rogers, *Keratins: their composition, structure, and biosynthesis*. 1972: Charles C. Thomas.

49. Arai, K.M., R. Takahashi, Y. Yokote, and K. Akahane, *Amino-Acid Sequence of Feather Keratin from Fowl*. European Journal of Biochemistry, 1983. **132**(3): p. 501-507.
50. Yin, X.-C., F.-Y. Li, Y.-F. He, Y. Wang, and R.-M. Wang, *Study on effective extraction of chicken feather keratins and their films for controlling drug release*. Biomaterials Science, 2013. **1**(5): p. 528-536.
51. Ayutthaya, S.I.N., S. Tanpichai, and J. Wootthikanokkhan, *Keratin Extracted from Chicken Feather Waste: Extraction, Preparation, and Structural Characterization of the Keratin and Keratin/Biopolymer Films and Electrospuns*. Journal of Polymers and the Environment, 2015. **23**(4): p. 506-516.
52. Huda, S. and Y. Yang, *Feather fiber reinforced light-weight composites with good acoustic properties*. Journal of Polymers and the Environment, 2009. **17**(2): p. 131-142.
53. Sudalaiyandi, G., *Characterizing the cleaning process of chicken feathers*. 2012.
54. Bonser, R. and P. Purslow, *The Young's modulus of feather keratin*. The Journal of experimental biology, 1995. **198**(4): p. 1029-1033.
55. Kock, J., R. Barbieri, J. Justice, K. Kurtis, T. Gentry, and H. Nanko. *Characterization of chicken feather materials for use in biocomposites*. in *Proceedings of the American Society for Composites: Twentieth Technical Conference, Philadelphia, PA*. 2005.
56. McKittrick, J., P.-Y. Chen, S. Bodde, W. Yang, E. Novitskaya, and M. Meyers, *The structure, functions, and mechanical properties of keratin*. The Journal of The Minerals (JOM), 2012. **64**(4): p. 449-468.
57. Acda, M.N., *Waste chicken feather as reinforcement in cement-bonded composites*. Philippine Journal of Science, 2010. **139**(2): p. 161-166.
58. Sawyer, R.H., T. Glenn, J.O. French, B. Mays, R.B. Shames, G.L. Barnes, W. Rhodes, and Y. Ishikawa, *The Expression of Beta (β) Keratins in the Epidermal Appendages of Reptiles and Birds*. American Zoologist, 2000. **40**(4): p. 530-539.
59. OpenStaxCollege. *Proteins*. Accessed date: 09 January 2016]; Available from: <https://legacy.cnx.org/content/m44402/1.7/>.
60. Ramanan, P., *Production of natural protein using chicken feather*. 2010, Bachelor of Chemical Engineering thesis, Universiti Malaysia Pahang.
61. Petkova, A.T., W.-M. Yau, and R. Tycko, *Experimental constraints on quaternary structure in Alzheimer's β -amyloid fibrils*. Biochemistry, 2006. **45**(2): p. 498-512.
62. Alibardi, L., L. Dalla Valle, A. Nardi, and M. Toni, *Evolution of hard proteins in the sauropsid integument in relation to the cornification of skin derivatives in amniotes*. Journal of anatomy, 2009. **214**(4): p. 560-586.
63. Martinez-Hernandez, A.L., C. Velasco-Santos, M. De Icaza, and V.M. Castano, *Microstructural characterisation of keratin fibres from chicken feathers*. International journal of environment and pollution, 2005. **23**(2): p. 162-178.
64. Feughelman, M., *Natural protein fibers*. Journal of Applied Polymer Science, 2002. **83**(3): p. 489-507.
65. Harrap, B. and E. Woods, *Soluble derivatives of feather keratin. 2. Molecular weight and conformation*. Biochemical Journal, 1964. **92**(1): p. 19.
66. Khosa, M. and A. Ullah, *A sustainable role of keratin biopolymer in green chemistry: a review*. J. Food Process. Beverage, 2013. **1**: p. 1-8.
67. Arai, K.M., R. Takahashi, Y. Yokote, and K. Akahane, *The primary structure of feather keratins from duck (*Anas platyrhynchos*) and pigeon (*Columba livia*)*.

- Biochimica et Biophysica Acta (BBA)-Protein Structure and Molecular Enzymology, 1986. **873**(1): p. 6-12.
68. Woodin, A., *Molecular size, shape and aggregation of soluble feather keratin*. Biochemical Journal, 1954. **57**(1): p. 99.
69. Schmidt, W. *Innovative feather utilization strategies*. in *Proceedings of the 1998 National poultry waste management symposium*. 1998.
70. Harrap, B.t. and E. Woods, *Soluble derivatives of feather keratin. 1. Isolation, fractionation and amino acid composition*. Biochemical journal, 1964. **92**(1): p. 8.
71. Tseng, F.-C.J., *Biofibre production from chicken feather*. 2011.
72. Fraser, R. and D. Parry, *The molecular structure of reptilian keratin*. International Journal of Biological Macromolecules, 1996. **19**(3): p. 207-211.
73. Held, P., *Quantitation of peptides and amino acids with a Synergy™ HT using UV fluorescence*. B.-T. Instruments, Winooski, Vermont, 2003.
74. Schmidt, A., J. Kellermann, and F. Lottspeich, *A novel strategy for quantitative proteomics using isotope-coded protein labels*. Proteomics, 2005. **5**(1): p. 4-15.
75. McGovern, V., *Recycling poultry feathers: more bang for the cluck*. Environmental Health Perspectives, 2000. **108**(8): p. A366.
76. Gupta, A., P. Kumar, R. Bin Mohd Yunus, and N. Binti Kamarudin, *Extraction of keratin protein from chicken feather*. 2012.
77. Bitter, J., *A study of erosion phenomena part I*. wear, 1963. **6**(1): p. 5-21.
78. Rajchard, J., *Biologically active substances of bird skin: a review*. Vet Med, 2010. **55**(9): p. 413-421.
79. Kruchen, E., *Method of cleaning poultry feathers*. 1979, U.S. Patent 4,169,706.
80. Griffith, B., *Feather molding method and product*. 2002, U.S. Patent Application 10/133,200.
81. Jones, C.W., *Applications of hydrogen peroxide and derivatives*. Vol. 2. 1999: Royal Society of Chemistry.
82. Kirk, R.E. and D.F. Othmer, *Encyclopedia of Chemical Technology*. Vol. 2. 1953.
83. Huda, S. and Y. Yang, *Composites from ground chicken quill and polypropylene*. Composites science and technology, 2008. **68**(3): p. 790-798.
84. Dweib, M., B. Hu, A. O'donnell, H. Shenton, and R. Wool, *All natural composite sandwich beams for structural applications*. Composite structures, 2004. **63**(2): p. 147-157.
85. Zhan, M., R.P. Wool, and J.Q. Xiao, *Electrical properties of chicken feather fiber reinforced epoxy composites*. Composites Part A: Applied Science and Manufacturing, 2011. **42**(3): p. 229-233.
86. Brandelli, A., *Bacterial keratinases: useful enzymes for bioprocessing agroindustrial wastes and beyond*. Food and Bioprocess Technology, 2008. **1**(2): p. 105-116.
87. Mokrejs, P., P. Svoboda, J. Hrnčirik, D. Janacova, and V. Vasek, *Processing poultry feathers into keratin hydrolysate through alkaline-enzymatic hydrolysis*. Waste Management & Research, 2010.
88. Ahmaruzzaman, M., *Adsorption of phenolic compounds on low-cost adsorbents: a review*. Advances in colloid and interface science, 2008. **143**(1): p. 48-67.
89. Ishikawa, S.-i. and K. Suyama, *Recovery and refining of Au by gold-cyanide ion biosorption using animal fibrous proteins*, in *Biotechnology for Fuels and Chemicals*. 1998, Springer. p. 719-728.

90. Zheng, M., X.X. Li, S.F. Mao, M.Y. Huang, and Y.Y. Jiang, *Hydrogenation of anisol and benzaldehyde catalyzed by chicken feather–palladium complex*. *Polymers for Advanced Technologies*, 1997. **8**(11): p. 638-640.
91. Sun, P., Z.-T. Liu, and Z.-W. Liu, *Particles from bird feather: A novel application of an ionic liquid and waste resource*. *Journal of hazardous materials*, 2009. **170**(2): p. 786-790.
92. Teixeira, M.C. and V.S. Ciminelli, *Development of a biosorbent for arsenite: structural modeling based on X-ray spectroscopy*. *Environmental science & technology*, 2005. **39**(3): p. 895-900.
93. Teixeira, M.C., V.S. Ciminelli, M.S.S. Dantas, S.F. Diniz, and H.A. Duarte, *Raman spectroscopy and DFT calculations of As (III) complexation with a cysteine-rich biomaterial*. *Journal of colloid and interface science*, 2007. **315**(1): p. 128-134.
94. Senoz, E. and R.P. Wool, *Microporous carbon–nitrogen fibers from keratin fibers by pyrolysis*. *Journal of applied polymer science*, 2010. **118**(3): p. 1752-1765.
95. Senoz, E. and R.P. Wool, *Hydrogen storage on pyrolyzed chicken feather fibers*. *international journal of hydrogen energy*, 2011. **36**(12): p. 7122-7127.
96. Tiwary, E. and R. Gupta, *Extracellular expression of keratinase from Bacillus licheniformis ER-15 in Escherichia coli*. *Journal of agricultural and food chemistry*, 2010. **58**(14): p. 8380-8385.
97. Shrinivas, D. and G. Naik, *Characterization of alkaline thermostable keratinolytic protease from thermoalkalophilic Bacillus halodurans JB 99 exhibiting dehairing activity*. *International Biodeterioration & Biodegradation*, 2011. **65**(1): p. 29-35.
98. Fakhfakh-Zouari, N., N. Hmidet, A. Haddar, S. Kanoun, and M. Nasri, *A novel serine metallokeratinase from a newly isolated Bacillus pumilus A1 grown on chicken feather meal: biochemical and molecular characterization*. *Applied biochemistry and biotechnology*, 2010. **162**(2): p. 329-344.
99. Fakhfakh-Zouari, N., A. Haddar, N. Hmidet, F. Frikha, and M. Nasri, *Application of statistical experimental design for optimization of keratinases production by Bacillus pumilus A1 grown on chicken feather and some biochemical properties*. *Process Biochemistry*, 2010. **45**(5): p. 617-626.
100. Fakhfakh, N., S. Kanoun, L. Manni, and M. Nasri, *Production and biochemical and molecular characterization of a keratinolytic serine protease from chicken feather-degrading Bacillus licheniformis RPK*. *Canadian journal of microbiology*, 2009. **55**(4): p. 427-436.
101. Hmidet, N., N.E.H. Ali, N. Zouari-Fakhfakh, A. Haddar, M. Nasri, and A. Sellemi-Kamoun, *Chicken feathers: a complex substrate for the co-production of α -amylase and proteases by B. licheniformis NH1*. *Journal of industrial microbiology & biotechnology*, 2010. **37**(9): p. 983-990.
102. Haddar, A., A. Sellami-Kamoun, N. Fakhfakh-Zouari, N. Hmidet, and M. Nasri, *Characterization of detergent stable and feather degrading serine proteases from Bacillus mojavensis A21*. *Biochemical Engineering Journal*, 2010. **51**(1): p. 53-63.
103. Jeong, J.-H., K.-H. Park, D.-J. Oh, D.-Y. Hwang, H.-S. Kim, C.-Y. Lee, and H.-J. Son, *Keratinolytic enzyme-mediated biodegradation of recalcitrant feather by a newly isolated Xanthomonas sp. P5*. *Polymer Degradation and Stability*, 2010. **95**(10): p. 1969-1977.
104. Jeong, J.-H., O.-M. Lee, Y.-D. Jeon, J.-D. Kim, N.-R. Lee, C.-Y. Lee, and H.-J. Son, *Production of keratinolytic enzyme by a newly isolated feather-degrading*

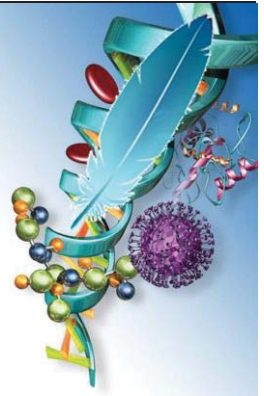
- Stenotrophomonas maltophilia* that produces plant growth-promoting activity. *Process biochemistry*, 2010. **45**(10): p. 1738-1745.
105. Jeong, J.-H., Y.-D. Jeon, O.-M. Lee, J.-D. Kim, N.-R. Lee, G.-T. Park, and H.-J. Son, *Characterization of a multifunctional feather-degrading Bacillus subtilis isolated from forest soil*. *Biodegradation*, 2010. **21**(6): p. 1029-1040.
106. Prakash, P., S.K. Jayalakshmi, and K. Sreeramulu, *Production of keratinase by free and immobilized cells of Bacillus halodurans strain PPKS-2: partial characterization and its application in feather degradation and dehairing of the goat skin*. *Applied biochemistry and biotechnology*, 2010. **160**(7): p. 1909-1920.
107. Jaouadi, B., S. Ellouz-Chaabouni, M.B. Ali, E.B. Messaoud, B. Naili, A. Dhouib, and S. Bejar, *Excellent laundry detergent compatibility and high dehairing ability of the Bacillus pumilus CBS alkaline proteinase (SAPB)*. *Biotechnology and Bioprocess Engineering*, 2009. **14**(4): p. 503-512.
108. Hongru, W. and W. Pengbo, *Modification of feather keratin and its retanning properties*. *Journal of the Society of Leather Technologists and Chemists*, 2006. **90**(6): p. 254-259.
109. Farag, A.M. and M.A. Hassan, *Purification, characterization and immobilization of a keratinase from Aspergillus oryzae*. *Enzyme and Microbial Technology*, 2004. **34**(2): p. 85-93.
110. Vermelho, A.B., A.M. Mazotto, A.C.N. de Melo, F.H.C. Vieira, T.R. Duarte, A. Macrae, M.M. Nishikawa, and E.P. da Silva Bon, *Identification of a Candida parapsilosis strain producing extracellular serine peptidase with keratinolytic activity*. *Mycopathologia*, 2010. **169**(1): p. 57-65.
111. Wallenberger, F.T. and N. Weston, *Natural fibers, plastics and composites*. 2003: Springer Science & Business Media.
112. Ye, W. and R. Broughton, *Chicken feather as a fiber source for nonwoven insulation*. *International Nonwovens Journal*, 1999. **8**(1): p. 53-59.
113. Dunbavand, I.E., *Flexible armor*. 1986, U.S. Patent 4,608,717.
114. Sangamithra Iyer, W.S. *Where Do All the Feathers Go?* 2006 [Accessed date: 09 January 2017]; Available from: <http://www.satyamag.com/feb06/schmidt.html>.
115. Schmidt, W.F. *Microcrystalline keratin: From feathers to composite products*. in *MRS proceedings*. 2001. Cambridge Univ Press.
116. Gorman, J. *Materials Take Wing - What to do with 4 billion pounds of feathers?* 2002 [Accessed date: 9 January 2017]; Available from: http://www.phschool.com/science/science_news/articles/materials_take_wing.html.
117. Durham, S. *Save a Tree, Use Some Feathers*. 2002 [cited 2016 Accessed date: 15 October 2016]; Available from: <http://www3.scienceblog.com/community/older/archives/H/usda597.html>.
118. Durham, S. *Save a Tree, Use Some Feathers*. 2002 [Accessed date: 9 January 2017]; Available from: <http://www3.scienceblog.com/community/older/archives/H/usda597.html>.
119. Ye, W., R. Broughton Jr, and J. Hess, *Chicken feather fiber: a new fiber for nonwoven insulation materials*. *INDA-TEC*, 1998. **98**: p. 7.01-7.16.
120. Misra, M., P. Kar, G. Priyadarshan, and C. Licata. *Keratin protein nano-fiber for removal of heavy metals and contaminants*. in *MRS Proceedings*. 2001. Cambridge Univ Press.

121. Wool, R. and C. Hong, *Low dielectric constant materials from plant oils and chicken feathers*. 2003, U.S. Patent Application 10/621,727.
122. Barnes, P., *Faster Chips with Chicken Feathers*. *Tech TV*. 2002.
123. Jacobson, L., *Can computers fly on the wings of a chicken*. *The Washington Post*, Retrieved April, 2002. **4**: p. 2004.
124. Dweib, M., T. Bullions, A. Loos, and R. Wool. *Recycled newspaper and chicken feathers as reinforcement fiber in bio-composite materials*. in *ANTEC... conference proceedings*. 2004. Society of Plastics Engineers.
125. Berenberg, B., *Natural fibers and resins turn composites green*. *Composites Technology*, 2001. **7**: p. 12-16.
126. Hamoush, S.A. and M.M. El-Hawary, *Feather fiber reinforced concrete*. *Concrete International*, 1994. **16**(6): p. 33-35.
127. Monteiro, P., *Concrete: Microstructure, Properties, and Materials*. 2006, New York: McGraw-Hill Publishing.
128. Pickering, K.L., M.A. Efendy, and T.M. Le, *A review of recent developments in natural fibre composites and their mechanical performance*. *Composites Part A: Applied Science and Manufacturing*, 2016. **83**: p. 98-112.
129. Dou, Y., X. Huang, B. Zhang, M. He, G. Yin, and Y. Cui, *Preparation and characterization of a dialdehyde starch crosslinked feather keratin film for food packaging application*. *RSC Advances*, 2015. **5**(34): p. 27168-27174.
130. Khosa, M.A., J. Wu, and A. Ullah, *Chemical modification, characterization, and application of chicken feathers as novel biosorbents*. *RSC Advances*, 2013. **3**(43): p. 20800-20810.
131. Li, M., *Temperature and moisture effects on composite materials for wind turbine blades*. 2000, Montana State University-Bozeman.
132. Behlau, L. and H.-J. Bullinger, *Technology guide: Principles-applications-trends*. 2009: Springer Science & Business Media.
133. La Mantia, F. and M. Morreale, *Green composites: A brief review*. *Composites Part A: Applied Science and Manufacturing*, 2011. **42**(6): p. 579-588.
134. Sabat, R.K., *Sliding Wear Behaviour of Bio-waste Reinforced Polymer Composite*. 2009, National Institute of Technology Rourkela.
135. Kokcharov, I. and A. Burov, *Structural Integrity Analysis*. Switzerland: Geneva, 2013.
136. Zini, E. and M. Scandola, *Green composites: an overview*. *Polymer composites*, 2011. **32**(12): p. 1905-1915.
137. Wool, R. and X.S. Sun, *Bio-based polymers and composites*. 2011, U.S.: Elsevier, Academic Press.
138. Flores-Hernández, C.G., A. Colín-Cruz, C. Velasco-Santos, V.M. Castaño, J.L. Rivera-Armenta, A. Almendarez-Camarillo, P.E. García-Casillas, and A.L. Martínez-Hernández, *All green composites from fully renewable biopolymers: Chitosan-starch reinforced with keratin from feathers*. *Polymers*, 2014. **6**(3): p. 686-705.
139. Martínez-Hernández, A.L., C. Velasco-Santos, M. de-Icaza, and V.M. Castaño, *Dynamical-mechanical and thermal analysis of polymeric composites reinforced with keratin biofibers from chicken feathers*. *Composites Part B: Engineering*, 2007. **38**(3): p. 405-410.
140. Bullions, T., D. Hoffman, R. Gillespie, J. Price-O'Brien, and A. Loos, *Contributions of feather fibers and various cellulose fibers to the mechanical properties of*

- polypropylene matrix composites*. Composites Science and Technology, 2006. **66**(1): p. 102-114.
141. Winandy, J.E., J.H. Muehl, J.A. Micales, A. Raina, and W. Schmidt, *Potential of chicken feather fibre in wood MDF composites*. Proceedings of EcoComp, 2003. **20**: p. 1-6.
 142. Schrooyen, P., *Feather keratins: modification and film formation*. 1999: Ph. D. Dissertation, University of Twente, Enschede, the Netherlands.
 143. Schrooyen, P., *Thermal and mechanical properties of films from partially carboxymethylated feather keratins*. Feather Keratins: Modification and Film Formation, 1999: p. 111-136.
 144. Goddard, D.R. and L. Michaelis, *A study on keratin*. Journal of Biological Chemistry, 1934. **106**(2): p. 605-614.
 145. Goddard, D.R. and L. Michaelis, *Derivatives of keratin*. Journal of Biological Chemistry, 1935. **112**(1): p. 361-371.
 146. Katoh, K., M. Shibayama, T. Tanabe, and K. Yamauchi, *Preparation and properties of keratin-poly (vinyl alcohol) blend fiber*. Journal of applied polymer science, 2004. **91**(2): p. 756-762.
 147. Pretti, C., C. Chiappe, D. Pieraccini, M. Gregori, F. Abramo, G. Monni, and L. Intorre, *Acute toxicity of ionic liquids to the zebrafish (Danio rerio)*. Green Chemistry, 2006. **8**(3): p. 238-240.
 148. Wu, B., W. Liu, Y. Zhang, and H. Wang, *Do we understand the recyclability of ionic liquids?* Chemistry-A European Journal, 2009. **15**(8): p. 1804-1810.
 149. Smith, P., A. Sethi, and T. Welton, *Synthesis and Catalysis in Room-Temperature Ionic Liquids*, in *Molten Salts: From Fundamentals to Applications*. 2002, Springer. p. 345-355.
 150. Sullivan, R. and K. Hertel, *The flow of air through porous media*. Journal of Applied Physics, 1940. **11**(12): p. 761-765.
 151. Wang, Y.-X. and X.-J. Cao, *Extracting keratin from chicken feathers by using a hydrophobic ionic liquid*. Process Biochemistry, 2012. **47**(5): p. 896-899.
 152. Xie, H., S. Li, and S. Zhang, *Ionic liquids as novel solvents for the dissolution and blending of wool keratin fibers*. Green Chemistry, 2005. **7**(8): p. 606-608.
 153. Jones, C.B. and D.K. Mecham, *The dispersion of keratins. I. Studies on the dispersion and degradation of certain keratins by sodium sulfide*. Arch. Biochem, 1943. **2**: p. 209.
 154. Schrooyen, P.M., P.J. Dijkstra, R.C. Oberthür, A. Bantjes, and J. Feijen, *Stabilization of solutions of feather keratins by sodium dodecyl sulfate*. Journal of colloid and interface science, 2001. **240**(1): p. 30-39.
 155. Tortora, G.J., B.R. Funke, C.L. Case, and T.R. Johnson, *Microbiology: an introduction*. Vol. 9. 2004: Benjamin Cummings San Francisco.
 156. Endres, J.R., A. Clewell, K.A. Jade, T. Farber, J. Hauswirth, and A.G. Schauss, *Safety assessment of a proprietary preparation of a novel Probiotic, Bacillus coagulans, as a food ingredient*. Food Chem Toxicol, 2009. **47**(6): p. 1231-8.
 157. Wang, Y., P. Li, P. Xiang, J. Lu, J. Yuan, and J. Shen, *Electrospun polyurethane/keratin/AgNP biocomposite mats for biocompatible and antibacterial wound dressings*. Journal of Materials Chemistry B, 2016. **4**(4): p. 635-648.

158. Tran, C.D., F. Prosenc, M. Franko, and G. Benzi, *Synthesis, structure and antimicrobial property of green composites from cellulose, wool, hair and chicken feather*. Carbohydrate Polymers, 2016. **151**: p. 1269-1276.
159. Paul, T., A. Mandal, S.M. Mandal, K. Ghosh, A.K. Mandal, S.K. Halder, A. Das, S.K. Maji, A. Kati, and P.K.D. Mohapatra, *Enzymatic hydrolyzed feather peptide, a welcoming drug for multiple-antibiotic-resistant Staphylococcus aureus: structural analysis and characterization*. Applied biochemistry and biotechnology, 2015. **175**(7): p. 3371-3386.
160. Silhavy, T.J., D. Kahne, and S. Walker, *The bacterial cell envelope*. Cold Spring Harbor perspectives in biology, 2010. **2**(5): p. a000414.
161. Brown, L., J.M. Wolf, R. Prados-Rosales, and A. Casadevall, *Through the wall: extracellular vesicles in Gram-positive bacteria, mycobacteria and fungi*. Nature Reviews Microbiology, 2015. **13**(10): p. 620-630.
162. Sundaram, M., R. Legadevi, N. Afrin Banu, V. Gayathri, and A. Palanisammy, *A study on antibacterial activity of keratin nanoparticles from chicken feathers waste against Staphylococcus aureus (Bovine mastitis bacteria) and its antioxidant activity*. European Journal of Biotechnology and Bioscience, 2015. **3**(6, 01-05): p. 1-5.
163. Rouse, J.G. and M.E. Van Dyke, *A review of keratin-based biomaterials for biomedical applications*. Materials, 2010. **3**(2): p. 999-1014.
164. Wang, J., S. Hao, T. Luo, Z. Cheng, W. Li, F. Gao, T. Guo, Y. Gong, and B. Wang, *Feather keratin hydrogel for wound repair: Preparation, healing effect and biocompatibility evaluation*. Colloids and Surfaces B: Biointerfaces, 2017. **149**: p. 341-350.
165. Goodwin, W., *Whole protein shampoo composition*. 1974, U.S. Patent 3,787,337.
166. Seger, G.E., K.A. Biedermann, K.A. Gbadamosi, S.R. Kelly, and P.T. Weisman, *Tissue products containing antiviral agents which are mild to the skin*. 2003, US Patents 6517849 B1.
167. Wrześniewska-Tosik, K., D. Wawro, M. Ratajska, and W. Stęplewski, *Novel biocomposites with feather keratin*. Fibres & Textiles in Eastern Europe, 2007(5-6 (64)): p. 157-162.

CHAPTER 3



EXPERIMENTAL

3.1 Introduction

This chapter provides details of materials and methods used in this research project. Several characterisation techniques were employed throughout this research in order to obtain information on morphology, microstructure, crystalline structure, thermal stability and mechanical properties of CFFs, bio-composites, CFK (chicken feather keratin) and bio-materials. Therefore, the techniques of optical microscopy, scanning electron microscopy (SEM), Fourier-transform infrared (FTIR) spectroscopy, vibrational spectroscopy (Raman), micro X-ray diffraction and wide-angle X-ray scattering (WAXS), thermogravimetry (TGA), tensile mechanical analysis (stress–strain analysis) and modulated force thermomechanometry (MF-TM or dynamic mechanical analysis (DMA)) have been used. These methodologies are summarised in Table 3.1.

Table 3.1: Characterisation methods and instruments used in this project

Experimental Phases	Description	Instruments and Methods	Chapters
Phase 1	Feather Purification and Characterisation	<ul style="list-style-type: none"> • Macro photography • Optical microscopy • SEM • Micro X-ray diffraction • WAXS • Raman • FTIR • pH • TGA • Dino-lite digital microscope • Tensile stress–strain analysis • DMA • ASTM D3822 [1] • Microbial study 	4, 5
Phase 2	Composites Preparation using Purified Keratin Fibres	<ul style="list-style-type: none"> • Thermal press • Macro photography • SEM • Tensile stress–strain analysis • DMA • TGA • FTIR • ASTM E 111-97 [2] 	6

Experimental Phases	Description	Instruments and Methods	Chapters
Phase 3	Keratin Denaturation, Extraction and Characterisation	<ul style="list-style-type: none"> pH Centrifuge UV-VIS SDS-PAGE LC-MS/MS FTIR Raman NMR XRD – WAXS Optical microscopy TGA Amino acid analysis 	7
Phase 4	Bio-material Preparation using Denatured Keratin and Characterisation	<ul style="list-style-type: none"> DMA SEM Antimicrobial study Australian Standard AS ISO 20776. 1:2017 ASTM D3822 [1] ASTM E 111-97 [2] 	8

3.2 Materials

The materials used in each chapter of this project are presented in Table 3.2. All the chemicals were used upon receipt without further purification.

Table 3.2: Materials used in this project

Category	Name	Conc./Density	Supplier/Brand	Chapter No.
Raw	Mixed chicken feathers (<i>ca.</i> 3 cm to 20 cm in length) of freshly slaughtered adult White Leghorn/Australorp (WL x AL) or broiler chickens	N/A*	Baiada Poultry Pty Ltd Melbourne, Australia	4, 5, 6, 7, 8, 9
	Sheep wool	N/A	Australian Wool Education Trust (AWET)	5
	Pigeon feather	N/A	Melbourne, Australia	
	Commercial conditioner, moisture + vitamin B ₅	Containing no keratin	OGX® beauty pure and simple, Florida, USA	9
	Commercial conditioner, ever straight Brazilian keratin therapy	Containing keratin		
Sterile 8 mm filter discs	N/A	Sigma-Aldrich,		

Category	Name	Conc./Density	Supplier/Brand	Chapter No.
Raw			Sydney, Australia	9
	Human epidermis keratin	≥ 90.0 %, CAS NO. 68238-35-7	Sigma-Aldrich, Sydney, Australia	
	Quantitative filter paper	125 mm circle	Advantec Toyo Roshi Kaisha, Ltd. Japan	
	Original bovine leather	Pre-treated for clothing purposes	Leather Cargo, Melbourne, Australia	
Chemicals	Dimethyl Sulfoxide-D6 (DMSO)	D, 99.9 % CD ₃ SOCD ₃ CAS NO. 67-68-5	Cambridge Isotope Laboratories, Inc. Massachusetts, USA	9
	Paraffin oil (white oil)	100 %, CAS No. 8042-47-5	Peter Aanensen Victoria, Australia	
	Cetyltrimethylammonium chloride (CTAC)	25 %·w/w aqueous solution	Aldrich Chemical Company, Milwaukee, USA	4
	Hydrochloric acid (HCl)	99 %	Sigma-Aldrich, Sydney, Australia	
	Poly(ethylene glycol) (PEG)	99 % with average molecular weight (Mn) of 400 g/mol		
	Sodium chlorite (NaClO ₂)	99 %		
	Sodium lauryl sulfate (SLS)	99.0 %		4
	Tetrahydrofuran (THF)	The median lethal dose (LD ₅₀) comparable to that of acetone	BDH Laboratory Supplies, Poole, England	6, 7
	Sorbitol 70 % solution	100 %·w/w CAS No. 50-70-4		9
	Sodium sulfide	AR hydrated, Na ₂ S·xH ₂ O, CAS No. 1313-82-2		8, 9
	Copper (II) sulfate	≥ 99.0 % LR, CuSO ₄ ·5H ₂ O, CAS No. 7758-99-8	Chem-Supply Pty Ltd Gillman, Adelaide, Australia	8
	Phosphoric acid	85 %·w/w, H ₃ PO ₄ , CAS. No. 7664-38-2 for phosphoric acid and 7732-18-5 for water)		
	Methanol	AR, CH ₃ OH, CAS No. 67-56-1		
	Glycerol	99.5 %, AR, C ₃ H ₈ O ₃		
	Peptone diluent solution	N/A	Sigma-Aldrich, Sydney, Australia	4
	Tween 80 (TW80)			
	Hydrochloric acid	32 %·w/w, AR, HCl, CAS No. 7647-01-0	Sigma-Aldrich, MO, USA	8
Bromophenol blue,	C ₁₉ H ₁₀ BR ₄ O ₅ S, CAS No. 115-39-9			

Category	Name	Conc./Density	Supplier/Brand	Chapter No.
Chemicals	Ammonium persulfate	≥ 98 %, H ₈ N ₂ O ₈ S ₂ , CAS No. 7727-54-0	Sigma-Aldrich, MO, USA	9
	2-mercaptoethanol	≥ 99.0 %, HSCH ₂ CH ₂ OH, CAS No. 60-24-2		
	Bovine serum albumin (BSA)	≥ 98 %, CAS No. 9048-46-8		
	Coomassie brilliant blue G-250	pure, C ₄₇ H ₄₈ N ₃ NaO ₇ S ₂ , CAS No. 6104-58-1		
	Benzyl alcohol	100 %·w/w CAS No. 100-51-6		9
	Stearic acid	100 %·w/w CAS No. 57-11-4		
	Sorbitan monooleate (span 80)	100 %·w/w CAS No. 1338-43-8		
	Sodium hydroxide	97 - 100.5 %, LR, NaOH, CAS No. 1310-73-2	Ajax Finchem Pty Ltd, Auckland, New Zealand	8
	Potassium hydroxide	85 - 100.5 %, LR, KOH, CAS No. 1310-58-3		
	Urea	99.0 %, LR, NH ₂ CONH ₂ , CAS No. 57-13-6		9
	Paraffin wax (polawax GP200)	100 %, CAS No. 8002-74-2		
	L-cysteine	99 %, BR, C ₃ H ₇ NO ₂ S	BDH Laboratory Supplies, Poole, England	8, 9
	Dodecyl sulfate sodium (SDS)	≥ 95.0 %, C ₁₂ H ₂₅ Na ₄ S, CAS No. 151-21-3	Merck-Millipore, Darmstadt, Germany	
	Tris	C ₄ H ₁₁ NO ₃ , CAS No. 77-86-1	Astral Scientific, NSW, Australia	
	Tris-HCl	C ₄ H ₁₁ NO ₃ HCl, CAS No. 1185-53-1		
	Temed	≥ 99.0 %, C ₆ H ₁₆ N ₂ , CAS No. 110-18-9	Invitrogen, Auckland, New Zealand	
	Bis-acrylamide mix	≥ 99.0 %, C ₇ H ₁₀ O ₂ N ₂ , CAS No. 110-26-9	Amresco, Solon, USA	
	Coomassie Brilliant Blue R-250 was used as the resolving gel in electrophoresis	C ₄₅ H ₄₄ N ₃ NaO ₇ S ₂ , CAS No. 6104-59-2	Bio-Rad Laboratories Pty Ltd, Sydney, Australia	
	Phosphate buffer saline (PBS) tablets	0.14 M NaCl, 0.0027 M KCl, 0.01 < Phosphate buffer pH 7.4	Astral Scientific Pty Ltd, Sydney, Australia	

Category	Name	Conc./Density	Supplier/Brand	Chapter No.
Chemicals	Dithiothreitol (DTT)	5 g ultra-pure, CAS No. 27565-41-9	Astral Scientific Pty Ltd, Sydney, Australia	8, 9
	Sorbitan monostearate (polysorbate 60) or Tween 60	100 %, CAS No. 9005-67-8	Acros Organics Geel, Belgium	9
Polymers	Linear thermoplastic polyether– polyurethane (Pellethane®) 2103- 85AE elastomer TPU-polyether	Consisted of poly(butane-1,4-diol), methylene diphenyl diisocyanate (MDI) with a butane-1,4-diol chain extender / density of 1.14 g·cm ⁻³	Lubrizol Corporation, Wickliffe, USA	6
	Linear thermoplastic Polysiloxane TPU (Elast-Eon™ 2A or E2A) , which is a polyurethane with a 40 % hard segment content and a 60% mixed polyether/siloxane soft segment	consisting of a periodic copolymer poly [Butane-1,4-diol-per- 1,1'-Methylenebis (4- isocyanatobenzene)- per- poly(dimethylsiloxane) -per-1,1'- Methylenebis(4- isocyanatobenzene)- per- Butane-1,4-diol]	AorTech International plc, Utah, USA	7
Microbiological	Biochemical detection strips API 20 E	N/A	Biomerieux, Baulkham Hills, NSW, Australia	4, 9
	Columbia blood agar base		Acumedia, a division of Neogen, USA	
	Baird-Parker Agar (BPA) CM0275		Oxoid, Altrincham, England	
	Bismuth Sulphite Agar (BSA) CM0201			
	Campylobacter Growth Supplement (FBP supplement) SR0232			
	Campylobacter Selective Agar (CM0689)			
	Laked Horse Blood SR0048			
	Mueller Hinton Agar (MHA) CM0337			
	Nutrient Agar (NA) CM0003			
	Nutrient Broth CM0001			
	Plate Count Agar (PCA) CM0325			
	Tryptone Soy Agar (TSA) CM0131			
	Urinary Tract Infection (UTI) Brilliance agar CM0949			
	Staphlytect Plus X240E			
Tryptone Soy Agar (TSA) CM0131				

Category	Name	Conc./Density	Supplier/Brand	Chapter No.
Microbiological	Urinary Tract Infection (UTI) Brilliance agar CM0949 Wilkins-Chalgren Anaerobic Agar (WCA) CM0619	N/A	Oxoid, Altrincham, England	4, 9
	Xylose Lysine Desoxycholate Agar (XLD) CM0469			
	Wilkins-Chalgren Anaerobic Agar (WCA) CM0619			
Microbiological	Gram-negative <i>Escherichia coli</i> (<i>E. coli</i> - ATCC 25922) Gram-positive <i>Staphylococcus aureus</i> (<i>S. aureus</i> - ATCC 25923) were standardised to ca. 5×10^5 cfu/mL.	rod-shaped with thin layer of peptidoglycan, and cocci shaped in clusters, with a thick layer of peptidoglycan cell wall reference	American Type Culture Collection (ATCC, Rockville, MD)	9
	Disks containing 10 µg gentamicin	N/A	Oxoid, SpA, Italy	

* N/A: Not applicable

The consumed water was distilled and all the chemicals utilised in the experiments were of analytical grade, used as received without further purification. The specific processing and compounding methods will be elaborated on in their respective chapters.

3.3 Characterisation equipment

3.3.1 Stereoscopic optical microscopy

The optical microscope uses visible light and a system of lenses to magnify images of small samples. The morphology (structure and form) of the CFFs was examined and analysed together with the fibre distribution in the TPU-CFFs matrix, under a Japanese optical microscope, Nikon Labophot, model 1.25, with Nikon phase contrast 2 (Figure 3.1). The images were recorded with a digital camera.



Figure 3.1: An optical microscope, Nikon Labophot, model 1.25, with Nikon phase contrast 2

3.3.2 Scanning electron microscopy-energy dispersive spectroscopy

Scanning electron microscopy (SEM) allows imaging of a sample by scanning it with a focused beam of electrons, which interact with atoms in the sample, producing various signals that contain information on the sample's surface topography and composition [3]. The electron beam is generally scanned in a raster scan pattern, and the beam's position is combined with the detected signal to produce an image. The most common SEM mode detects secondary electrons emitted by atoms excited by the electron beam. By scanning the sample and collecting the secondary electrons that are emitted using a special detector, an image displaying the structure of the surface is created [3]. Just as light is refracted and focused by an optical lens, the electron will have its path deviated by either a magnetic field or an electric field, due to its charge. With careful design of electric and magnetic fields within the instrument, an electron beam can be focussed like a light beam allowing objects to be detected at high magnifications [4]. Energy dispersive spectroscopy (EDS) allows the identification of particular elements and their relative proportions (e.g. Atomic %) of samples.

The SEM imaging was performed using an FEI Quanta 200 (FEI, Oregon, USA) (HV: 20 kV, WD: 10.0 - 10.2 mm, spot size of 3.5 - 5 nm in diameter at different magnifications up to 3000X) (tungsten filament) with an attached Oxford Instruments XMax^N20 spectrometer for EDS (Figure 3.2). The specimens were mounted onto aluminium stubs using carbon tape (Figure 3.3) and were coated either with Carbon or Gold *ca.* 20 nm thick, (depending on whether they were used for EDS or SEM imaging, respectively) using an SPI-Module Sputter Coater Z11430 (Structure & Probe Inc., West Chester, USA; Figure 3.4) to reduce charging artefacts.

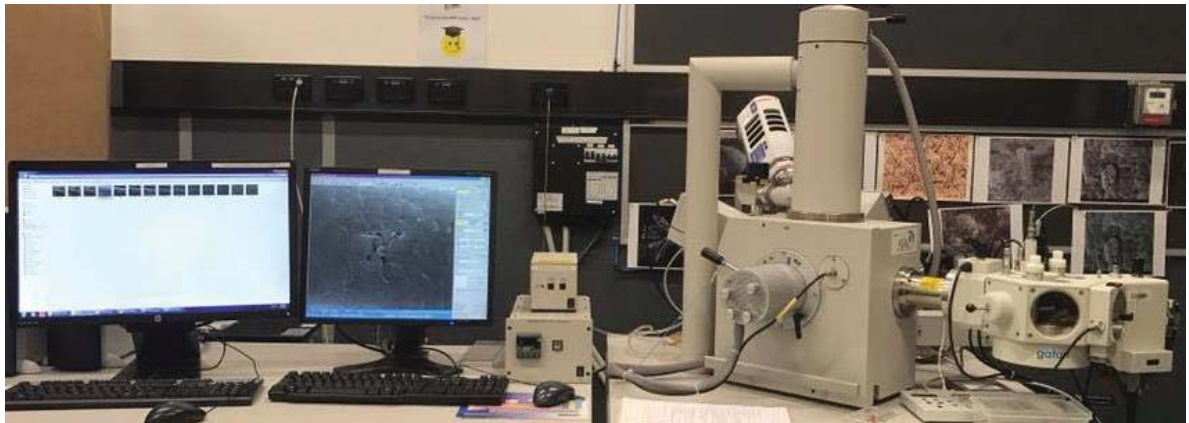


Figure 3.2: FEI Quanta 200 scanning electron microscopy with an attached Oxford Instruments XMax^N20 spectrometer for EDS

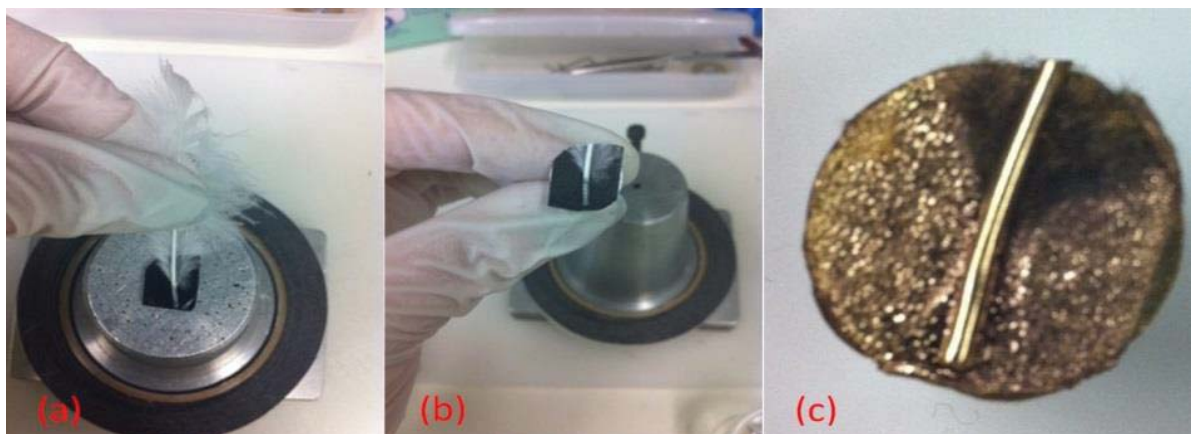


Figure 3.3: Preparing an SEM sample: (a) the chicken feather used, (b) the calamus, rachis, and barbs of a chicken feather on a stub with double sided carbon tape (c) gold-coated sample

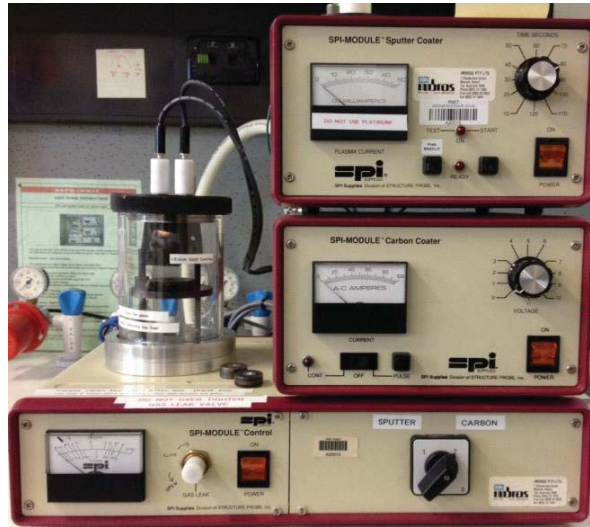


Figure 3.4: Gold and carbon vacuum sputter coater SPI Sputter Coater Z11430

3.3.3 X-ray diffraction analysis

Wide-angle X-ray diffraction (WAXD) or wide-angle X-ray scattering (WAXS) is an X-ray-diffraction technique that is commonly used to establish the crystallinity, crystal size and interlayer distances of crystalline structures. When X-rays are directed at solids they will scatter in predictable patterns based on the internal structure of the solid. A crystalline solid consists of regularly spaced atoms (electrons) that can be described by imaginary planes, with the distance between these planes being called the d-spacing [5]. The intensity of the d-space pattern is directly proportional to the number of electrons (atoms) that are found in the imaginary planes. Every crystalline solid will have a unique pattern of d-spacings (known as the powder pattern), which is a ‘finger print’ for that solid [5]. The fundamental relation governing the X-ray diffraction process is the Bragg Law [6] (Figure 3.5), which states:

$$n\lambda = 2d \sin\theta \quad \text{Equation 3.1}$$

Where d is the distance between the crystallographic planes, λ is the wavelength of the X-ray radiation used, n ($=1, 2, \dots$) is the order of reflection and θ is the angle of diffraction.

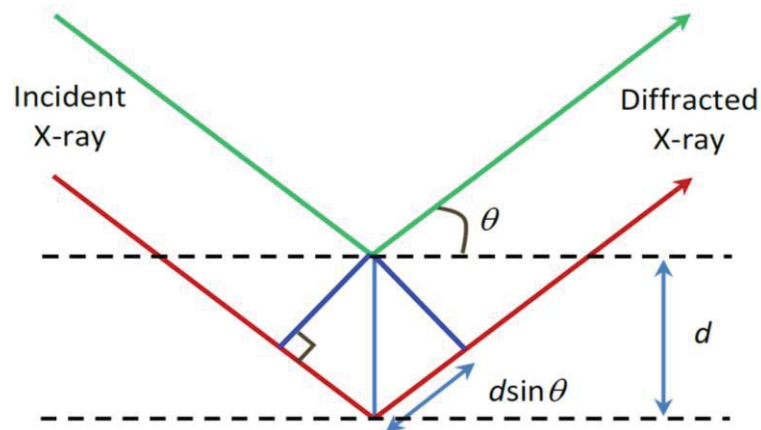


Figure 3.5: The Bragg Law Principle [7]

3.3.3.1 X-ray scattering via Bruker D8 Discover micro-XRD diffractometer

Diffraction patterns of the chicken feather rachis and barbs were obtained on the Bruker X-ray diffractometer in Chapter 5 (section 5.3.5). The feather calamus/rachis (β -sheet) and barb/barbules (α -helix) were targeted to obtain X-ray diffraction patterns from the diffractometer, with the diffractograms being analysed to calculate crystallinity percentage.

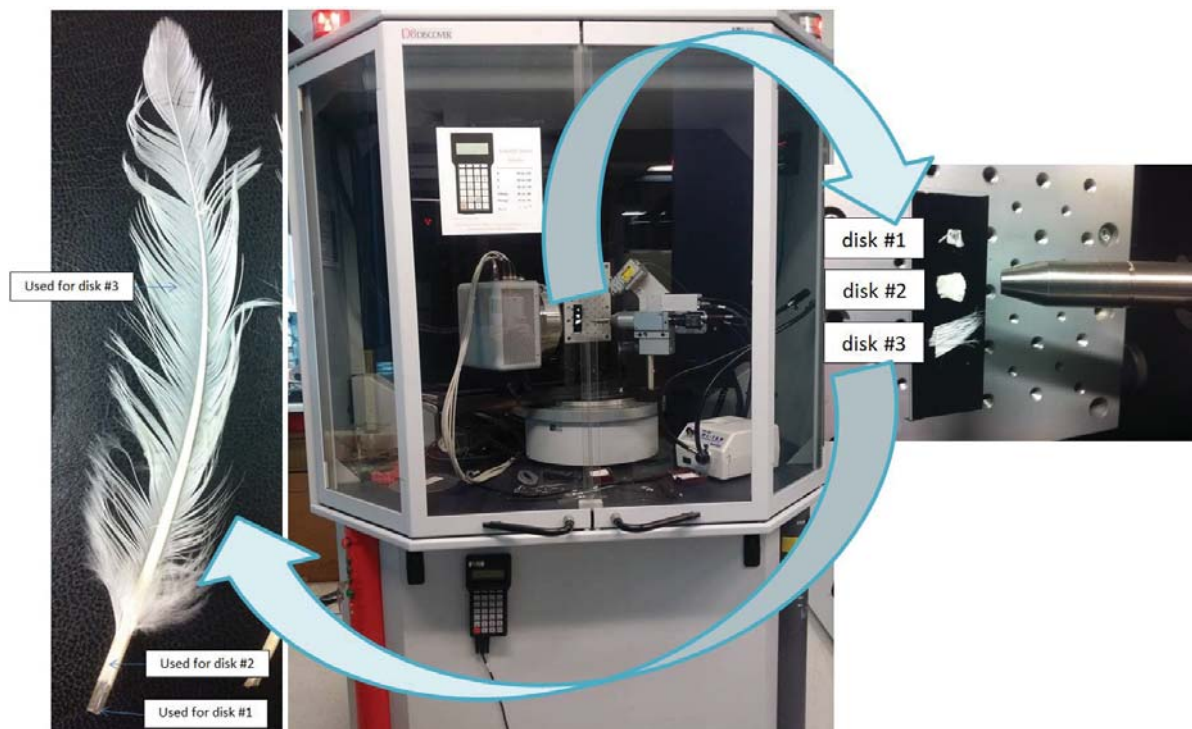


Figure 3.6: Bruker D8 Discover micro-XRD diffractometer (GADDS)

The specimens were dispersed onto a stub and sample holder with the X-ray beam perpendicular to them. The specimen was placed within the chamber of the analytical X-ray Bruker D8 Discover model diffractometer equipped with a General Area Detector Diffraction System (GADDS) (Bruker GADDS, Rheinfelden, Germany, Figure 3.6) micro X-ray diffractometer with Bragg–Brentano parafocusing geometry. A diffracted beam monochromator, a copper target X-ray tube set to 40 kV (generator intensity) and 40 mA (generator current) was used. The specimen was scanned from $2\theta = 12\text{--}87.7^\circ$, in 0.02° steps.

3.3.3.2 Wide-angle X-ray scattering via Bruker AXS D4 Endeavour

Wide-angle X-ray scattering (WAXS) analysis was carried out using a Bruker AXS D4 Endeavour system, Figure 3.7, employing copper (Cu) $K\alpha$ radiation ($\lambda = 0.154\text{ nm}$) operating at 40 kV and 40 mA and a Lynxeye linear strip detector. Samples were tested between 6 and $90^\circ 2\theta$ and the scattering patterns were collected. The crystallinity percentage was calculated as well as the crystallite size for the FR-treated samples using Bruker Diffrac, EVA 3.0 software.

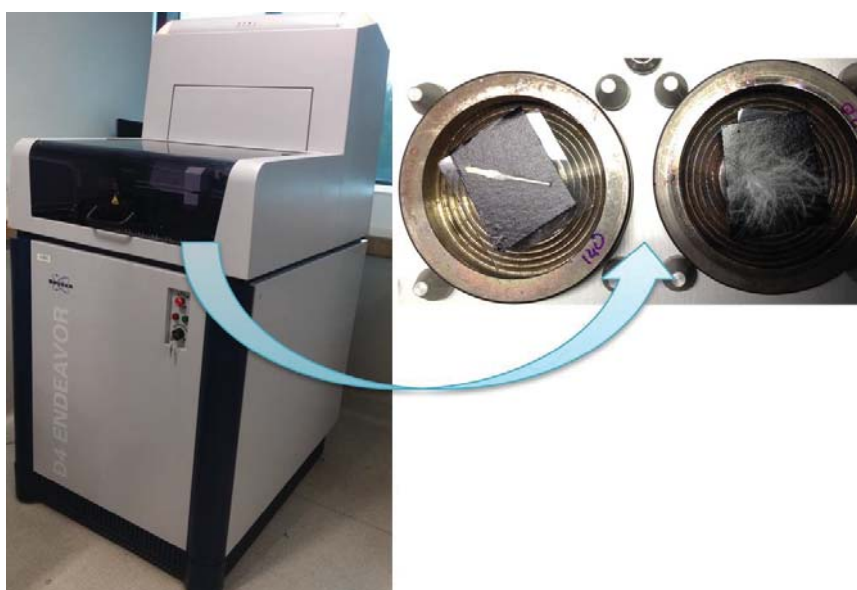


Figure 3.7: Bruker AXS D4 Endeavour Wide-angle X-ray scattering (WAXS)

3.3.4 Nuclear magnetic resonance spectroscopy

Nuclear magnetic resonance (NMR) spectroscopy exploits the nuclear magnetic resonance of certain atomic nuclei to confirm the identity of a substance by determining the physical and chemical properties of atoms or molecules such as the structure, dynamics, reaction state and chemical environment of molecules [8]. The intramolecular magnetic field around an atom in a molecule changes the resonance frequency, which provides details of the electronic structure of a molecule and its individual functional groups [9]. The NMR spectroscopy is applicable to any kind of specimen that contains nuclei possessing spin. Such specimens can range from small compounds analysed with 1-dimensional proton or carbon- ^{13}C NMR spectroscopy to large proteins or nucleic acids using 3 or 4-dimensional techniques [10]. Correlation spectroscopy (COSY) and heteronuclear single quantum coherence or correlation (HSQC) are two of several types of two-dimensional NMR (2D-NMR) experiments that provide more information concerning a molecule than one-dimensional NMR spectra. They are especially useful in determining the structure of a molecule, particularly for molecules that are too complicated to analyse using one-dimensional NMR techniques.

In correlation spectroscopy, the emission is centred on the peak of an individual nucleus. If its magnetic field is correlated with another nucleus by through-bond (COSY, HSQC, etc.) or through-space Nuclear Overhauser effect (NOE) coupling, a response can additionally be detected on the frequency of the correlated nucleus [11].

The vast majority of nuclei in a solution belong to the solvent. Most regular solvents are hydrocarbons containing NMR-reactive protons such as deuterium (hydrogen-2) and deuterated DMSO (d_6 -DMSO), which are used for hydrophilic analytes. A variety of physical circumstances do not allow molecules to be studied in solution to an atomic level by other

spectroscopic techniques. In solid-phase media, such as crystals, microcrystalline powders, gels and anisotropic solutions, it is the dipolar coupling and chemical shift anisotropy that becomes dominant in the behaviour of nuclear spin systems. In conventional solution-state NMR spectroscopy, these additional interactions would lead to a significant broadening of spectral lines. A variety of techniques offer high-resolution conditions that can, at least for ^{13}C spectra, be comparable to solution-state NMR spectra. Applications in which solid-state NMR effects occur often involve structural investigations of membrane proteins, protein fibrils or all kinds of polymer and chemical analysis in inorganic chemistry.

The CFK and a human epidermis keratin were dissolved in d_6 -DMSO and in an 8 M urea, 50 mM Tris, 0.1 M β -mercaptoethanol, and 0.1 % sodium azide (pH 8) solution at a concentration of 100 mg keratin / 700 μL solvent. NMR spectra were referenced to solvent signals using DMSO (δ_{H} 2.50) or using a D_2O capillary placed within the NMR tube (δ_{H} 4.64). The NMR spectra were acquired on a 500 MHz Agilent DD2 console (Santa Clara, CA, USA; Figure 3.8).

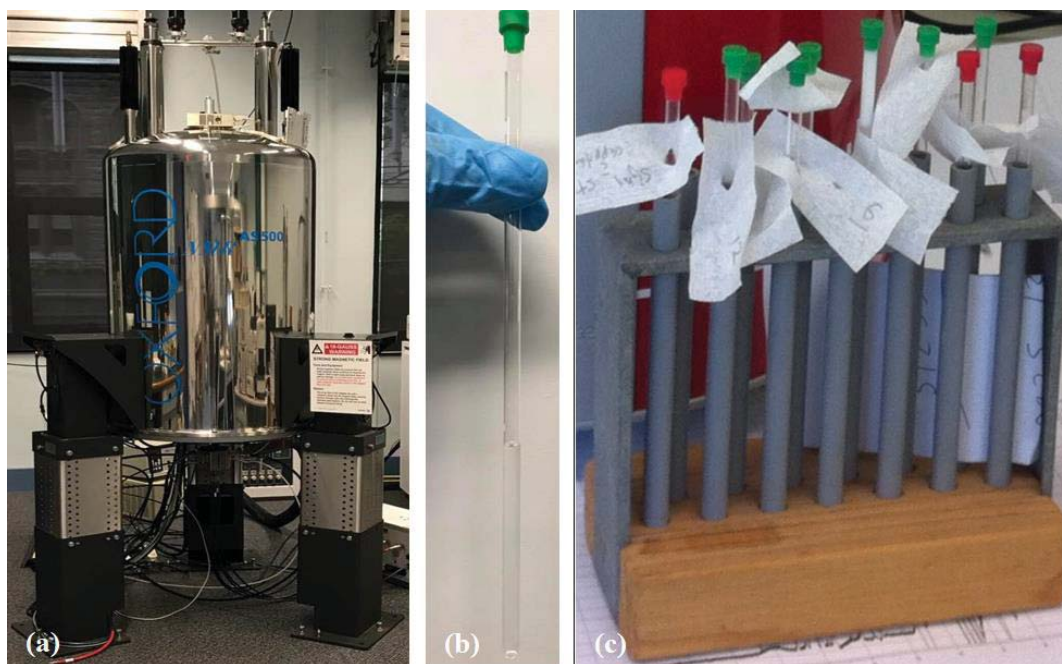


Figure 3.8: (a) A 500 MHz Agilent DD2 console; (b) NMR tubes contain keratin samples (c) in a tube holder

Acquired spectra for the feather keratin specimens dissolved in d_6 -DMSO included proton (256 scans) and gCOSY (gradient correlation spectroscopy) (16 scans, 512 increments) experiments. Proton spectra (256 scans) for the human epidermis keratin and two feather samples were dissolved in an 8 M urea, 50 mM Tris, 0.1 M β -mercaptoethanol and 0.1 % sodium azide (pH 8) solution and acquired using the PRESAT sequence (4-step purge) with suppression of both the water and urea signals. gCOSY (4 scans, 400 increments) and HSQCAD (adiabatic, refers to the shape of the pulse) (16 scans, 512 increments) NMR spectra were additionally acquired for these samples with suppression using the PRESAT sequence.

3.3.5 Fourier-transform infrared spectroscopy

Fourier transform infrared (FTIR) spectroscopy is a technique which is used to obtain an infrared spectrum of absorption of materials with the goal of any absorption spectroscopy (FTIR, ultraviolet-visible (UV-Vis) spectroscopy, etc.), to measure how well a sample absorbs light at each wavelength [12]. Infrared spectrophotometry provides information about the secondary structural features, such as α -helices and β -sheets, unlike X-ray crystallography and NMR spectroscopy which provide information about the tertiary structure. As infrared spectrophotometry makes it easy to measure samples in all forms (solid/liquid and crystalline/non-crystalline), it is used to complement the analytical methods in this project. The FTIR spectroscopy works by shining infrared radiation on a sample and seeing which wavelengths of radiation in the infrared region of the spectrum are absorbed by the sample. Each compound has a characteristic set of absorption bands in its infrared spectrum.

A PerkinElmer Spectrum 100/Universal diamond attenuated total reflectance (ATR), (Beaconsfield, Buckinghamshire, England) was used for all liquids or solids specimens (Figure 3.9(a)). The spectra were collected within the wavenumber range of $4000\text{--}650\text{ cm}^{-1}$ and recorded with 32 scans per spectrum and 4 cm^{-1} resolution. The crystal was cleaned with ethanol using a tissue and record a background scan recorded and subtracted from the sample signal. The sample was placed on the crystal (Figure 3.9(b)), if the sample was solid the force gauge was used to press down until it showed an optimal signal (while remaining at 90 % or less of maximum pressure). No pressure was required if the sample was liquid.

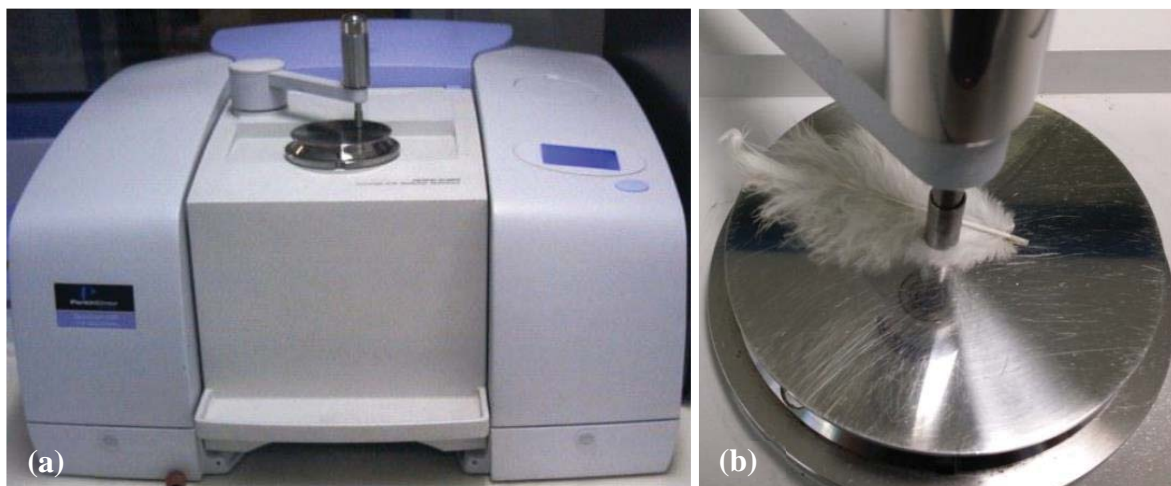


Figure 3.9: (a) PerkinElmer 400 FTIR, (b) feather on crystal with force gauge

A portion of the ethanol from the soxhlet flask containing feather residues was poured into a watch glass and evaporated till only a small amount remained. Then a drop was transferred onto the FTIR diamond crystal (internal reflectance element) for analysis to see what has been extracted (Figure 3.10).

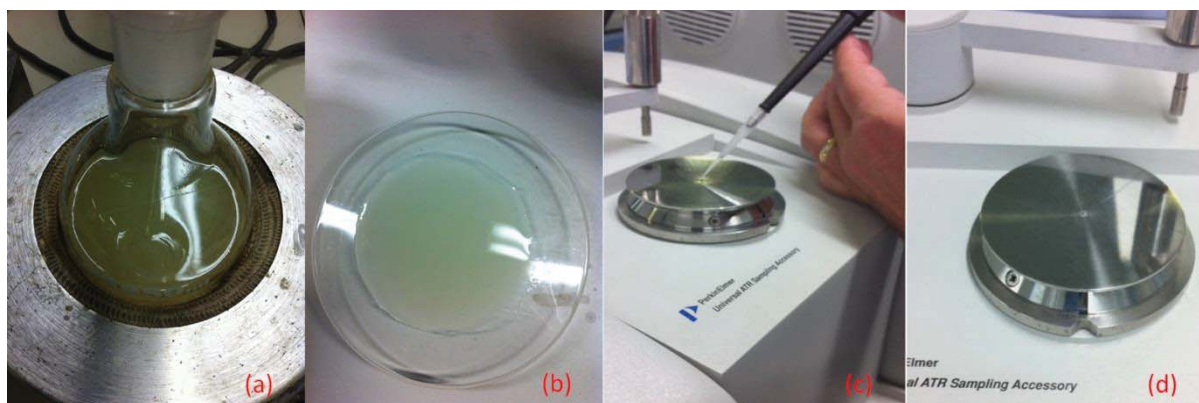


Figure 3.10: (a) ethanol from the soxhlet flask containing feather residues, (b) portion of extraction poured in a watch glass for ethanol evaporation (c) the last drop transferred on the FTIR using a pipette, and (d) a drop of the extraction on the FTIR diamond

3.3.6 Vibrational spectroscopic analysis

Raman spectroscopy is a spectroscopic technique used to observe vibrational, rotational and other low-frequency modes in a system and commonly used in chemistry to provide a fingerprint by which molecules can be identified in Raman spectroscopy relies on inelastic scattering, of monochromatic light, usually from a laser (light amplification by stimulated emission of radiation) in the visible ($\sim 457 - 660$ nm), near infrared ($\sim 785 - 1064$ nm), or near ultraviolet range ($\sim 244 - 364$ nm) [13]. The laser light interacts with molecular vibrations, phonons or other excitations in the system, resulting in the energy of the laser photons being shifted up or down, which gives information about the vibrational modes in the system [13].

In Raman spectroscopy a sample is illuminated with a laser beam and electromagnetic radiation from the illuminated spot is collected with a lens and sent through a monochromator. Elastic scattered radiation at the wavelength corresponding to the laser line (Rayleigh scattering) is filtered out by either a notch filter, edge pass filter, or a band pass filter, while the rest of the collected light is dispersed onto a detector [14].

Raman spectra were collected using a PerkinElmer Raman Station 400F

(Beaconsfield, Buckinghamshire, England; Figure 3.11(a-b)) to record spectra of the CFFs before and after purification treatments and residues after extraction in Chapter 5: 785 nm, max output of 250 mW and 100-micron laser spot size, in Chapter 5. Specimens were placed on a glass slide, centred using the video camera, and focusing was carried out to a spot of 1 μm diameter via the Raman option where the signal was strongest (100 \times microscope objective). A scan of 5 s was repeated 4 times (for optimal Raman spectra of feathers) and spectra were recorded by scanning the 200–3200 cm^{-1} region with a total acquisition time of 1000 s.

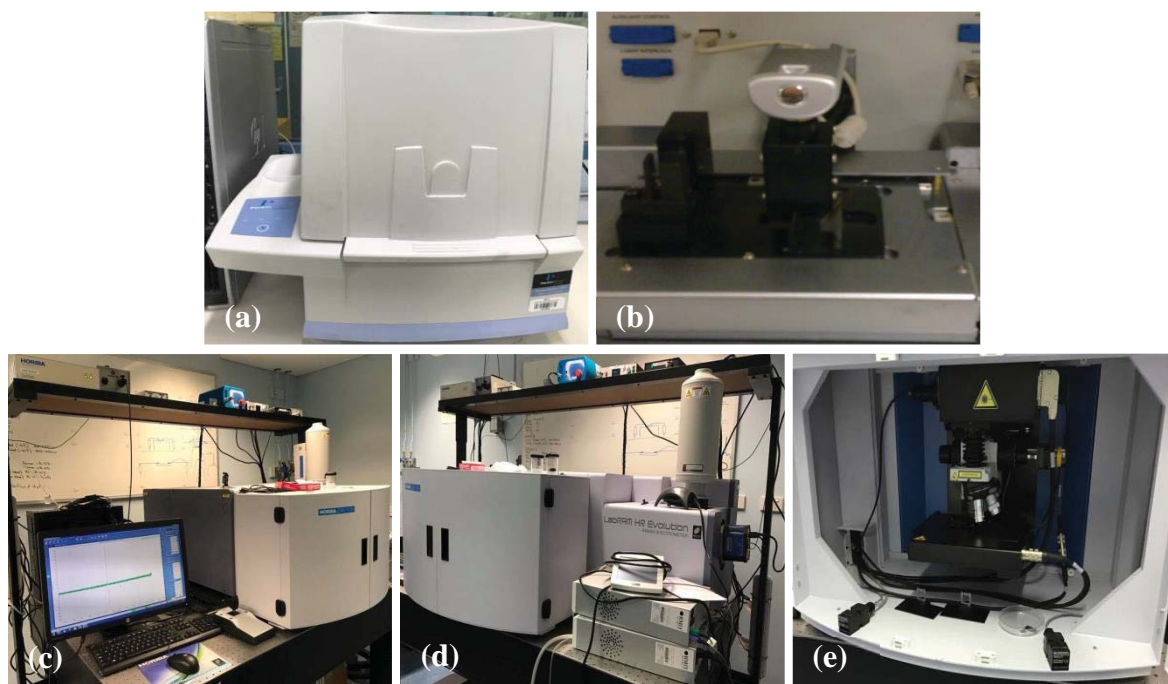


Figure 3.11: (a) PerkinElmer Raman Station 400F, (b) showing glass slide and camera (with protective hood raised), (c-e) Xplora Plus (Horiba LabRAM HR Evolution micro-Raman system)

Raman spectra were collected using a Raman Xplora Plus (Horiba LabRAM HR Evolution confocal micro-Raman system, Horiba Scientific, Lille, France; Figure 3.11(c-e)) equipped with a confocal microscope and motorised stage, to record spectra of the CFK in Chapter 7. Raman spectra were measured using excitation wavelengths 785 nm. Spectra were

collected through a 50x objective lens (Olympus, Melville, NY, USA) and numerical aperture of 0.75. The laser power on the sample was approximately 25–50 mW. Each spectrum was a co-addition of 10 scans with illumination time of 2 s across 200–1800 cm^{-1} (2.6–4.9 cm^{-1} resolution). Magnification, aperture and laser power were optimised between analyses to minimise spectral noise and to maximise spectral signal from samples with a range of energy tolerances.

3.3.7 Thermal analysis

3.3.7.1 Differential scanning calorimeter

According to Freire, 1995 [15], differential scanning calorimetry (DSC) is accepted as the technique to determine the energetics of protein folding/ unfolding transitions and the thermodynamic mechanisms underlying those reactions by measuring the apparent molar heat capacity of a macromolecule as a function of temperature, yields a complete thermodynamic characterisation of a transition.



Figure 3.12: (a) PerkinElmer Pyris 1 differential scanning calorimeter (DSC) and (b) Mettler Toledo MX5

A Pyris 1 differential scanning calorimeter (DSC), Figure 3.12(a), from PerkinElmer (Melbourne, Australia) was used in Chapter 6 to study the thermal properties of the TPU-polyether and TPU-fiber reinforced bio-composites between $-50\text{ }^{\circ}\text{C}$ and $140\text{ }^{\circ}\text{C}$. The tests were conducted in triplicate on sample sizes of *ca.* 3 mg (weighed using a Mettler Toledo MX5, Melbourne, Australia; Figure 3.12(b)) under nitrogen purge (20 mL/min) at identical heating and cooling rates of $5\text{ K}\cdot\text{min}^{-1}$. The accuracy of the peaks was found to be within 0.4 %.

3.3.7.2 Thermogravimetric analyser

Thermogravimetry analysis (TGA) is a method of thermal analysis in which changes in physical and chemical properties of materials are measured as a function of increasing temperature, with constant heating rate, or as a function of time, with constant temperature and/or constant mass loss and can provide information such as mass loss or gain due to decomposition [16].

A TGA 7 thermogravimetric analyser (Figure 3.13) (PerkinElmer, Glen Waverley, Victoria, Australia) was employed to evaluate thermal degradation, mass loss (and its derivative as a function of temperature), remaining char ratio, and the changes in degradation behaviour associated with CFFs, TPU-polyether and TPU-CFF bio-composites. The mass loss curve was recorded between $30\text{ }^{\circ}\text{C}$ and $750\text{ }^{\circ}\text{C}$ under nitrogen purge (20 mL/min) and between $750\text{ }^{\circ}\text{C}$ and $850\text{ }^{\circ}\text{C}$ under oxygen purge (20 mL/min) at a heating rate of $20\text{ K}\cdot\text{min}^{-1}$. In order to minimise the effect of thermal lag, a small sample mass of *ca.* 2 to 4 mg was used.



Figure 3.13: Perkin Elmer TGA 7 thermogravimetric analyser

3.3.9 Heated hydraulic press

In composite fabrication part of Chapter 6, the resulting sheets were pressed using a thermal press (or compression moulding or heated hydraulic press), with a maximum applied load of 15 tonne and temperature range of ambient to $300\text{ }^{\circ}\text{C} \pm 2\text{ }^{\circ}\text{C}$ (model number: L0003-1, IDM Instruments, Hallam, Victoria, Australia) as used to create flat TPU-CFF sheets of 0.7 mm to 0.9 mm in thickness (Figure: 3.14). The press was heated to $175\text{ }^{\circ}\text{C}$ (above the glass transition temperature (T_g) of the TPU-CFF composite). The composite was placed inside a square metal mould (1 mm thick) i.e. a metal sheet with the centre cut from it. A polytetrafluoroethylene (PTFE) sheet has placed either side. Metal plates were placed on the top and bottom. The assembly was placed between the two faces of the press and the jack was raised so that both metal plates contacted the hot press. The pressure was increased to 6 t and maintained for 5 min to create flat sheets of material. The composite was then removed from the press and cooled to ambient temperature before being removed from the plate assembly.

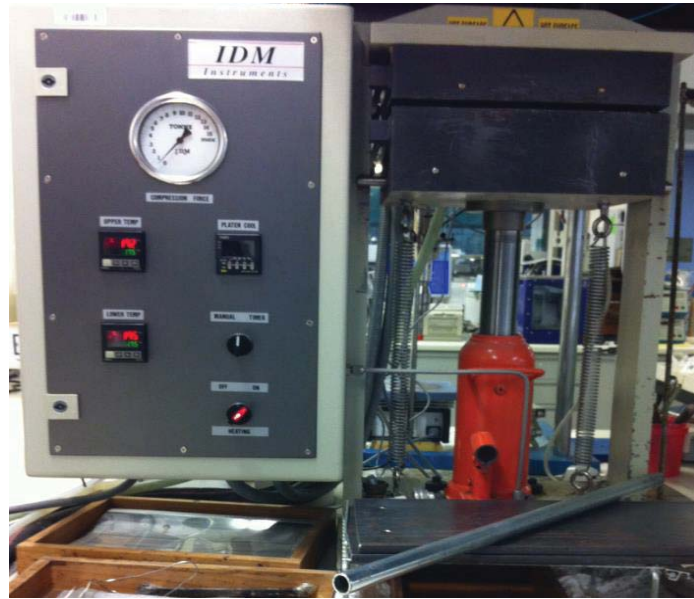


Figure 3.14: Heated hydraulic press or thermal press or compression moulding (IDM Instruments, model number: L0003-1) used for preparation of bio-composites

3.3.10 Mechanical properties

Dynamic mechanical analysis (DMA) is a technique used to study and characterise materials, useful for studying the viscoelastic behaviour of polymers, in which, a sinusoidal stress is applied and the strain in the material is measured, allowing one to determine the complex modulus, tensile, stress-strain and hysteresis analysis. The temperature of the sample or the frequency of the stress are often varied, leading to variations in the complex modulus; this approach can be used to locate the glass transition temperature (T_g) of the material, as well as to identify transitions corresponding to other molecular motions.

3.3.10.1 Dino-Lite digital microscope

A Dino-Lite digital microscope (Dino-Lite AM4013T-M40 from AnMon Electronics Co., (Figure 3.15) using DinoCapture 2.0 operating software) was used to measure the diameter of the CFFs barbs in Chapter 4 and 8.



Figure 3.15: A Dino-Lite AM4013T-M40 from AnMon Electronics Co.

3.3.10.2 Stress–strain tensile mechanical analysis

Tensile testing was performed using a DMA Q800 system from TA Instruments (Rydalmere, NSW, Australia; Figure 3.16) at 30 °C (using ramped force from 0.001 to 18 N at 1 N·min⁻¹), to measure stress-strain properties of the CFF barbs, in Chapter 4, TPU-polyether polymer and TPU-CFF bio-composites in Chapter 6 and human hair in Chapter 8.

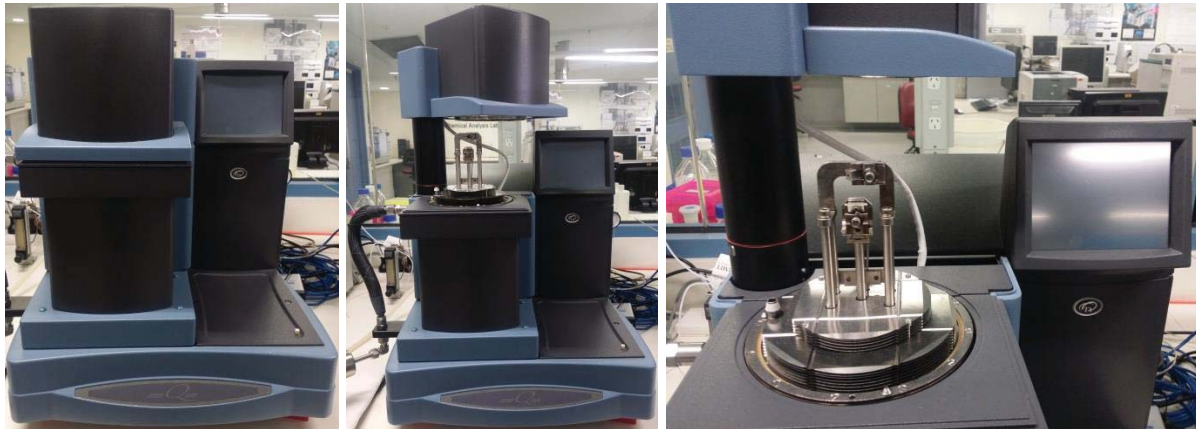


Figure 3.16: A DMA Q800 system from TA Instruments

3.3.10.3 Hysteresis analysis

In hysteresis analysis presented in Chapter 6, a DMA Q800 system from TA Instruments (Rydalmere, NSW, Australia; Figure 3.16) at 30 °C (using ramped force from 0.001 to 18 N at 1 N·min⁻¹) was used again. Each specimen was submitted to increasing amounts of stress and allowed to relax at zero loads for 5 min before starting each loop and each loop was

repeated three times. Reported data are means of at least three tests on different specimens. Measurements such as stress relaxation and cyclic hysteresis are essential in order to have a detailed understanding of the stability of interactions between the elastomer and filler with respect to time [17].

3.3.10.4 Dynamic mechanical analysis - Temperature scanning

The DMA was additionally carried out on a Pyris Diamond DMA 2003 from PerkinElmer (Figure 3.17) with TPU-polyether polymer and TPU-CFF bio-composites specimens displaying average dimensions of 25 mm x 7 mm x 1 mm (cut with an xacto knife), in Chapters 6 and 7. Test conditions included a specimen gauge length of 10 mm, operated in tension mode at 1 Hz frequency, and a temperature range of -90 °C to 120 °C. The liquid nitrogen dewar was filled to capacity prior to starting a scan.



Figure 3.17: A PerkinElmer Pyris Diamond DMA 2003

The cap on the dewar was raised on a metal rod and insulated with a glove to prevent the O-ring from freezing. A pliable O-ring allowed the top to be securely clamped and sealed. A firmly clamped top prevents excessive loss of nitrogen and allows more than one scan to be

carried out between refilling. The operating conditions used on the Pyris Diamond DMA are detailed below:

- Standard length (10 mm), width (usually between 4 - 7 mm) and the average thickness (*ca.* 0.45 mm) were input manually.
- Motor Control: Target position was adjusted to 10 mm (a standard distance)
- Response parameters of -90 °C to 120 °C
- Frequencies of 0.5, 1, 2, 5 and 10 Hz

The TPU/CFFs composite was mounted between two grips and secured in place with sufficient pressure (applied by tightening Allen bolts) to prevent slipping. A metal plate was placed in front of the specimen (to protect it from direct exposure to the N₂ stream). The heater compartment was raised (Figure 3.18).



Figure 3.18: DMA showing mounting of a TPU/CFFs bio-composite (centre), heater unit (right-hand side) and metal protective plate (bottom) [18]

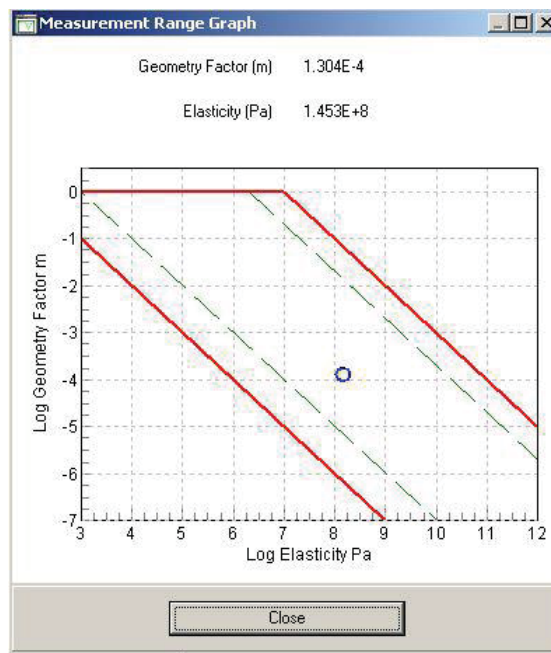


Figure 3.19: Measurement range graph showing Log (geometry factor) (m) versus Log (elasticity)/Pa of the sample (blue circle) which must remain between the red lines

3.3.10.5 Dynamic mechanical analysis - Isothermal scanning

Isothermal DMA (Figure 3.17) was used to determine viscoelastic properties associated with CFFs, in Chapter 4. Test conditions included specimen gauge length of 10 mm, deformation of 20 μm , the frequency of 0.5 Hz, and temperature at 18 $^{\circ}\text{C}$. The mf-TM was used In Chapters 6 and 7 to measure the viscoelastic properties with force and temperature.

3.3.11 Feather processing

The barbs were separated from the rest of the feather and were ground at 700 rpm for 5 min using an IKA[®] A11 Crushing Analytical Mill (IKA-Werke, Staufen, Germany; Figure 3.20), which was equipped with stainless steel cutting blades and inner tank. There was no active control on fibre length or distribution at, or after, grinding. The lengths of ground feathers were found to be 5 μm to 2 cm with aspect ratios (length/width) of 1:1 to 200:1. These ground CFFs were used in preparing the bio-composites, in Chapters 6 and 7.



Figure 3.20: IKA[®] A11 Crushing Analytical Mill, equipped with stainless steel cutting blades and inner tank, grinding CFFs to the size of 5 μm to 2 cm

The feather material, together with final keratin powders were ground up into a powder form using a Rocklabs Ringmill Grinder (equipped with a zirconia mill head; Figure 3.21) for up to 3 min, which was used in NMR studies in Chapter 8.



Figure 3.21: Rocklabs Ringmill Grinder, equipped with a zirconia mill head, grinding CFFs to powder form
Rocklabs Ltd., Auckland, New Zealand

3.3.12 pH measurements

The pH of CFFs specimens was determined in Chapters 4, 5 and 7, using Hanna Instruments, pH/mV Bench Meter, pH211 or HI2211pH HACH[®] SensION5[™] Portable pH Meter.

3.3.13 Centrifuge

A Sorvall RC-5C from 1991 centrifuge (Figure 3.23) was used in Chapter 7, keratin extraction, for separating the precipitated protein from the chemicals such as sodium sulfide reducing agent and L-cysteine, and in washing step. The Sorvall RC-5C super speed centrifuge offers advanced features that enhance centrifugation performance since it is engineered to operate on maximum rotor speed without the use of a vacuum system, the RC-5C can achieve 21,000 rpm with centrifugation forces of up to 51,427 x g. The total capacity of this high-performance centrifuge is 4 L.



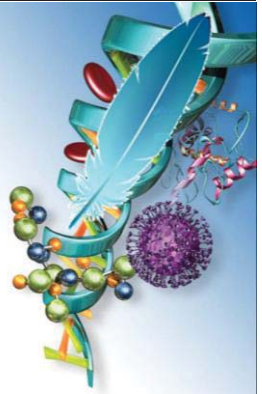
Figure 3.22: A Sorvall RC-5C from 1991 centrifuge

3.4 References

1. *ASTM D3822*. ASTM D3822, Standard Test Method for Tensile Properties of Single Textile Fibers.
2. *ASTM E 111 - 97*. Standard Test Method for Young's Modulus, Tangent Modulus, and Chord Modulus.
3. Oatley, C., W. Nixon, and R. Pease, *Scanning electron microscopy*. Advances in Electronics and Electron Physics, 1966. **21**: p. 181-247.

4. Clarke, A.R. and C.N. Eberhardt, *Microscopy techniques for materials science*. 2002: Woodhead Publishing.
5. Ghosal, A.K., *Crystallization of isotactic poly (propylenes) with enhanced melt strength*. PhD Thesis. 2008, Florida: ProQuest.
6. Cohen, M., *Precision lattice constants from X-Ray powder photographs*. Review of Scientific Instruments, 1935. **6**(3): p. 68-74.
7. Norlinda, D., *High Filler Content Polymer Composite Based on Biomimetics*, in *School of Science*. PhD Thesis, 2015, RMIT University.
8. Duus, J.Ø., C.H. Gotfredsen, and K. Bock, *Carbohydrate structural determination by NMR spectroscopy: Modern methods and limitations*. Chemical Reviews, 2000. **100**(12): p. 4589-4614.
9. Jackman, L.M. and S. Sternhell, *Application of Nuclear Magnetic Resonance Spectroscopy in Organic Chemistry: International Series in Organic Chemistry*. 2013: Elsevier.
10. Breitmaier, E. and W. Voelter, *Carbon-13 NMR spectroscopy*. 1987.
11. Martin, G.E. and A.S. Zektzer, *Two Dimensional NMR Methods for Establishing Molecular Connectivity*. 1988: VCH.
12. Griffiths, P.R. and J.A. De Haseth, *Fourier transform infrared spectrometry*. Vol. 171. 2007: John Wiley & Sons.
13. Bowley, H.J., D.L. Gerrard, J.D. Loudon, G. Turrell, D.J. Gardiner, and P.R. Graves, *Practical raman spectroscopy*. 2012, Berlin: Springer Science & Business Media.
14. Smith, E. and G. Dent, *Modern Raman spectroscopy: a practical approach*. 2013: John Wiley & Sons.
15. Freire, E., *Differential scanning calorimetry*. Protein Stability and Folding: Theory and Practice, 1995: p. 191-218.
16. Coats, A.W. and J.P. Redfern, *Thermogravimetric analysis. A review*. Analyst, 1963. **88**(1053): p. 906-924.
17. Ponnamma, D., K.K. Sadasivuni, M. Strankowski, P. Moldenaers, S. Thomas, and Y. Grohens, *Interrelated shape memory and Payne effect in polyurethane/graphene oxide nanocomposites*. RSC Advances, 2013. **3**(36): p. 16068-16079.
18. Czajka, M., *Thermoplastic Graphene Composites for Mechanical, Thermal Stability and Conductive Applications*. Ph.D. Thesis. 2016, Melbourne, Australia: RMIT University.

CHAPTER 4



PURIFICATION OF WASTE CHICKEN FEATHERS TO REFINED KERATIN FIBRES

4.1 Introduction

Due to contamination with intestinal contents, blood, fatty acids, offal fat, preen oil, debris, and its warmth freshly plucked feathers can be a suitable habitat for many microorganisms such as *Campylobacter*, *Salmonella* and *Escherichia* species (spp.), which are known to cause gastroenteritis [1]. The presence of pathogens in plucked feathers can impose potentially fatal biological hazards for humans; however, many microorganisms existing in feathers can be removed via either physical or chemical means [2, 3]. Efficient and non-degradative methods are required for purification and separation of chicken feather fibres (CFFs) keratin to render it safe, clarified and an accessible abundant resource for a variety of uses.

Disinfectants are non-sporicidal agents that destroy pathogenic microorganisms [4]. Rutala et al. [5] reported the disinfecting capacity of ethanol at various concentrations against a variety of microorganisms; *Pseudomonas aeruginosa* was killed in 10 s by ethanol at concentrations between 30 %·v/v and 100 %·v/v. *Escherichia coli* (*E. coli*) and *Salmonella typhosa* were killed in 10 s by any ethanol concentrations between 40 %·v/v and 100 %·v/v. *Staphylococcus aureus* (*S. aureus*) was slightly more resistant, requiring higher concentrations of ethanol, between 60 %·v/v and 95 %·v/v for the same period.

Sanitisers are defined as chemical agents capable of killing 99.999 % of specific bacterial populations within 30 s, yet they may or may not destroy pathogenic or harmful bacteria [5, 6]. Ozone (O₃) is a well-known sanitiser capable of killing various pathogens and bacterial spores [7, 8]. The bactericidal effect of O₃ is associated with its high oxidation potential and its ability to diffuse through biological cell membranes [7]. Naidu [9] reported that 0.35 mg/L of O₃ reduces *E. coli*, *Salmonella* Typhi and *S. aureus* by at least 5 log₁₀, and reduces the spores of *Bacillus* and *Clostridium* spp. by almost 3 log₁₀. Chlorine dioxide

(ClO₂) is an oxidising agent acting as an antimicrobial sterilising sanitiser, which is commonly used in hospitals for the removal of dirt, and disinfection [10, 11]. The oxidising effect of ClO₂ can be used for whitening of CFFs [7, 12]. According to Trakhtman and Manual [13, 14], ClO₂ is effective against *E. Coli* and *Bacillus anthracoides* at dosages in the range of 1 to 5 mg/L and against *Salmonella* Paratyphi B., *Pseudomonas aeruginosa* and *S. aureus* at concentrations lower than 1 mg/L.

Surfactants are a class of chemicals comprising both hydrophobic and hydrophilic groups in their chemical structure; thus being able to disperse fatty dirt particles that are normally insoluble in water [15]. Anionic surfactants are widely used for removing oily dirt and stains in the presence of soft water; however, the minerals available in hard water adversely affect their cleaning performance. Although the general decontamination ability associated with different type of surfactants is proven, the information regarding their antibacterial effect is limited [16].

The aim of this part of the project was to compare microbiological and mechanical properties of CFFs purified by surfactants, disinfectants, sanitisers and their combinations. The effectiveness of different purification methods on microbiological and mechanical properties of CFFs were evaluated, and the most suitable candidates for keratin extraction and development of bio-composite application are presented in Figure 4.1.

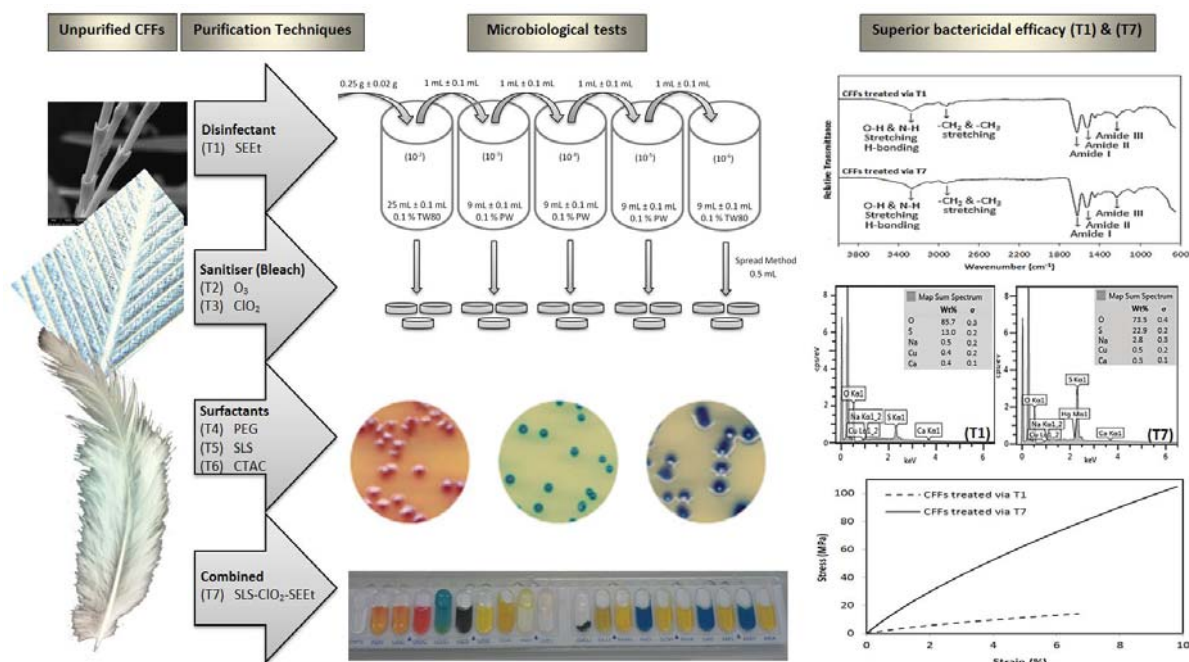


Figure 4.1: Comparing the microbiological and mechanical properties of CFFs purified by surfactants, disinfectants, sanitisers and their combinations

4.2 Experimental

4.2.1 Materials

All used materials are detailed in Chapter 3 (Table 3.2).

4.2.2 Purification methods

The untreated CFFs were purified via different methods: Soxhlet extraction with ethanol (SEEt) (T1), Ozonation (T2), purification by ClO₂ (T3), purification with a non-ionic surfactant (poly(ethylene glycol)) (T4), purification with an anionic surfactant (sodium lauryl sulphate) (T5), purification with a cationic surfactant (cetyltrimethylammonium chloride) (T6), and purification via a combination method (SLS-ClO₂-SEEt) (T7).

Except for the CFFs treated by T1 and T7, the feathers purified by other methods were rinsed in distilled water for 10 min until the pH of the rinsing water matched the pH of the

distilled water (sections 5.2.2.1 and 5.3.1). All treated CFFs were dried in an incubator at $34\text{ }^{\circ}\text{C} \pm 1\text{ }^{\circ}\text{C}$ (in order to not effecting the structure of feather protein) for 3 d and conditioned at $20\text{ }^{\circ}\text{C} \pm 2\text{ }^{\circ}\text{C}$ and $60\% \pm 2\% \text{ RH}$ for 72 h. Due to working with unknown type and count of bacteria present in the untreated CFFs, each purification method was timed for a total length of 5 h after each purification method. The microbiological tests were conducted in triplicate and the results were compared.

4.2.2.1 Purification by surfactants

The purification effect associated with three classes of surfactants (anionic sodium lauryl sulphate (SLS), non-ionic poly(ethylene glycol) (PEG), and cationic cetyltrimethylammonium chloride (CTAC)) was investigated on untreated CFFs.



Figure 4.2: Purification of chicken feather fibres by surfactants

Aqueous solutions of SLS, PEG, and CTAC were prepared (1.0 g/L) in separate containers and 10.0 g of untreated CFFs, was added to each vessel liquid to solid ration of 100:1 (Figure 4.2). The mixtures were agitated using magnetic stirrers (400 rpm) over hot plates at $20\text{ }^{\circ}\text{C}$. Then the temperature was gradually raised to $35\text{ }^{\circ}\text{C}$, and stirred continued for 5 h.

4.2.2.2 Purification via Soxhlet extraction with ethanol

Given the higher antimicrobial effect of alcohol at higher concentrations, continuous Soxhlet extraction with ethanol (SEEt) was carried out for 5 h on 10.0 g of untreated CFFs (Figure 4.3). The extraction time chosen was longer than suggested in the literature [5] due to the unknown type and load of bacteria in the untreated CFFs.

This treatment has advantages over other purification techniques since ethanol is not as hazardous as the other chemicals used, and less water was required to rinse alcohol off the CFFs than to remove detergent; moreover the ethanol can be distilled and reused.

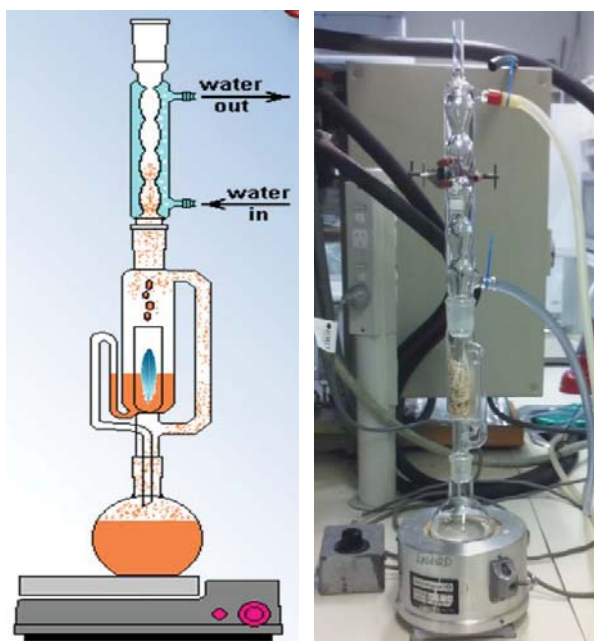


Figure 4.3: Purification of chicken feather fibres with Soxhlet method (left schema adopted from Wikipedia [17])

4.2.2.3 Purification by ozone

As shown in figure 4.4, ozonation of untreated CFFs was carried out using an ozone generator (Enaly Trade Co., Ltd Ozone Generator, Model OZX-300U, Canada) with ozone output of 200 mg/h. One gram of untreated CFFs was ozonated in an air-sealed flask

containing 100 mL of distilled water (liquid to solid ratio of 100:1) at 20 °C for 5 h. Upon contact with water, O₃ reacts to create an oxidising solution of hydrogen peroxide (H₂O₂), as shown in Equation 4.1 [18], which is expected to kill bacteria, fungus and spores [19].

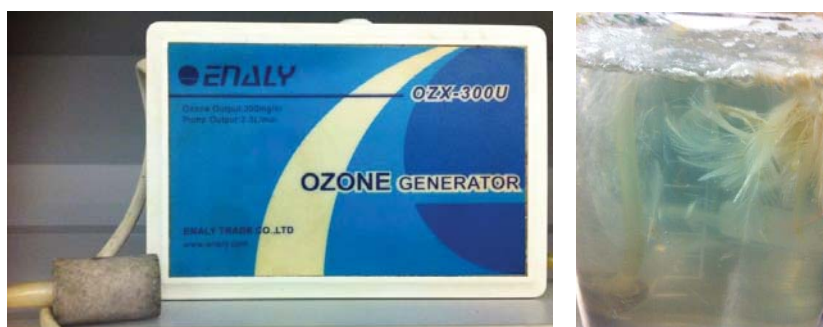
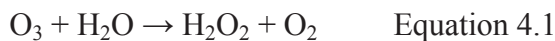


Figure 4.4: An Enaly Ozone Generator (left) and purification of chicken feather fibres by ozone (right)

4.2.2.4 Purification by chlorine dioxide

Chlorine dioxide can be produced from the reaction between sodium chlorite and hydrochloric acid, as shown in equation 4.2 [20]. In order to make 100 ppm ClO₂ aqueous solution, 1.85×10^{-3} mol of NaClO₂ and 1.48×10^{-3} mol of HCl were dissolved in distilled water to result in 1 L of purification solution, in which 10 g of untreated CFFs was stirred (liquid to solid ration of 100:1) at 400 rpm and 20 °C for 5 h (Figure 4.5).

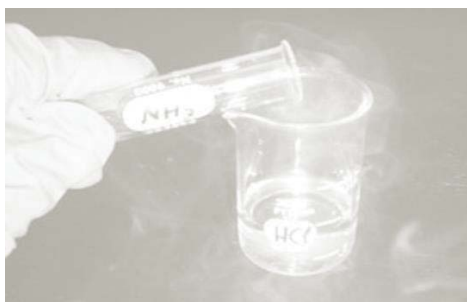


Figure 4.5: Purification of chicken feather fibres by Chlorine dioxide

4.2.2.5 Combined purification treatment

The effect of combining SLS, ClO₂, and SEEt methods was studied on the untreated CFFs (Figure 4.6). Untreated CFFs (10 g) was added to SLS (1 g/L) aqueous solution (liquid to solid ratio of 100:1); meanwhile, 1.85×10^{-3} mol of NaClO₂ and 1.48×10^{-3} mol of HCl were added to the same container in order to generate 100 mg/L ClO₂ in the system. CFFs were stirred at 400 rpm at 20 °C for 3 h, rinsed with distilled water, then Soxhlet extracted with ethanol for the remaining 2 h of the 5 h purification cycle as in previous treatments.

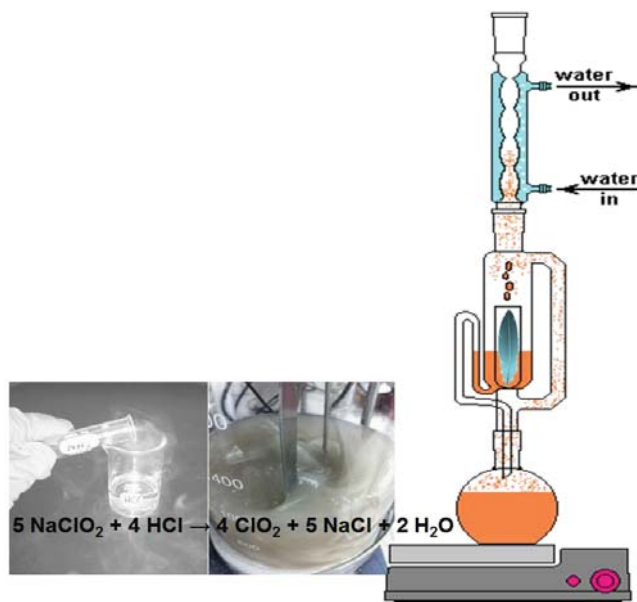


Figure 4.6: Purification of chicken feather fibres via combined purification treatment (right schema adopted from Wikipedia [17])

4.2.3 Microbiological tests on CFFs

The bactericidal efficacy of different purification treatments on CFFs was investigated via a standard plate count (SPC), followed by detection of hazardous bacteria such as *Escherichia coli*, *Pseudomonas* spp., coagulase positive *staphylococcus* (CPS), aerobic and anaerobic spore-formers, *Salmonella* spp. and *Campylobacter* spp., in a PC2 microbiology

laboratory. As shown in Figure 4.7, serial dilutions were performed according to Australian Standard AS 5013.11.1-2004 under a sterile Class II cabinet using aseptic technique.

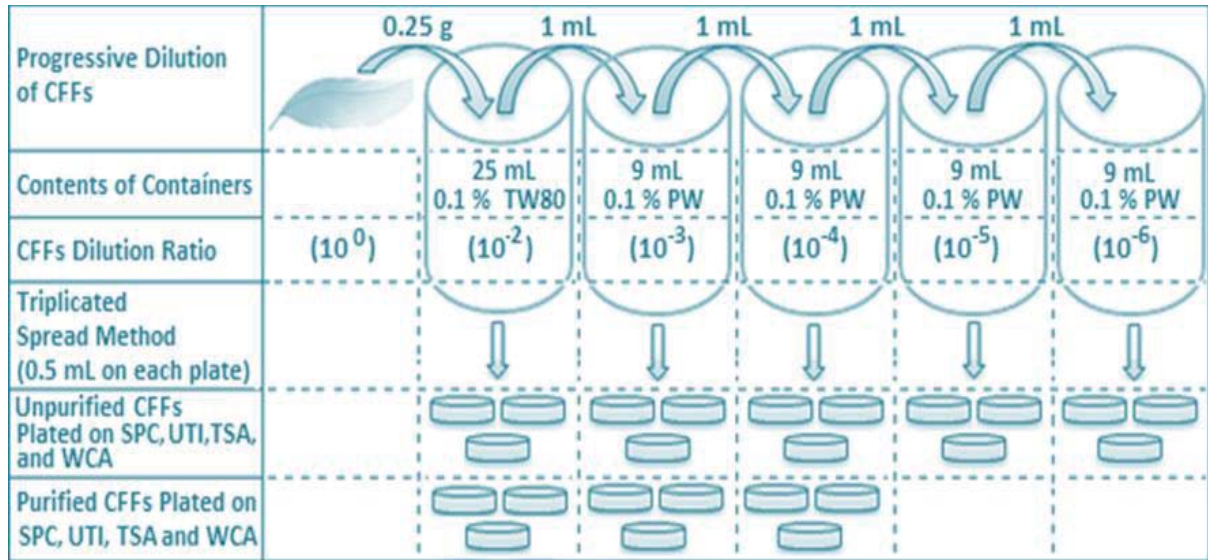


Figure 4.7: Microbial analyses on purified CFFs

Tween 80 (TW80) emulsifier was used for the initial dilution to separate the possible fat globules from CFFs as per the Oxoid Manual. To formulate the initial dilution, 10⁻², 0.25 g ± 0.02 g of CFFs was added to 25 mL of 0.1 % peptone water (PW) ± 0.1 mL of 0.1 % TW80 followed by serial dilutions with 9 mL ± 0.1 mL of 0.1 % PW. Prepared dilutions ranged from 10⁻² to 10⁻⁶ for unpurified and 10⁻² to 10⁻⁴ for purified CFFs. Using the spread plate method, 0.5 mL of each sample dilution was spread on selective media in triplicate. The specific growth condition for each microorganism is shown in Table 4.1. Plates chosen for enumeration were those having colony counts in the range of 10-150 colonies unless the initial dilution had less than 10 colonies in which case all typical colonies on that plate were counted. The corresponding microbial numbers are reported as colony forming units per gram (cfu/g) according to AS 5013.14.1-2006. From the cfu data obtained from time 0 and 24-48 h, log of reduction of bacteria defined as follows was calculated for each experiment:

$$\text{Log of reduction} = \log \frac{N_0}{N_t} \quad \text{Equation 4.3}$$

where N_0 is the number of bacteria at the beginning of the experiment and N_t is the number of bacteria after 24 or 48 h [21].

Table 4.1: Incubation conditions for the target microorganisms

Target Microorganism	Agar Type	Incubation Conditions	Used Method
General microbial count	SPC	37 °C ± 1 °C for 48 h to 72 h	AS 5013.14.3-2012
<i>E. coli</i>	UTI	37 °C ± 1 °C for 24 h	AS 5013.14.1-2010
<i>Pseudomonas</i> spp.	UTI	30 °C ± 1 °C for 24 h	AS 5013.11.1-2004
Coagulase positive staphylococcus	BPA	37 °C ± 1 °C for 48 h	AS 5013.12.1-2004
Aerobic spore-formers (<i>Bacillus</i> spp.)	TSA	37 °C ± 1 °C for 24 h to 48 h	AS 5013.2-2007
Anaerobic spore-formers (<i>Clostridium</i> spp.)	WCA	37 °C ± 1 °C for 24 h to 48 h	AS 5013.16-2004
<i>Salmonella</i> spp.	XLD, BSA, NA	37 °C ± 1 °C for 24 h	AS 5013.10-2009

4.2.3.1 Bacterial enumeration

Standard plate count (SPC) was performed according to AS 5013.14.3-2012. Enumeration of *S. aureus* individual colonies was performed as per AS 5013.12.1-2004 and was confirmed using Staphlytect Plus X240E (Oxoid). *Pseudomonas fluorescence*, *E. coli*, *S. aureus*, *Bacillus subtilis* and *Clostridium sporogenes* were used as positive controls and non-inoculated BPA, TSA and WCA plates were used as negative controls.

To determine the aerobic and anaerobic spore count of each of *Bacillus* and *Clostridium* spp. each dilution of the sample was heated in a water bath at 80 °C for 10 min before plating on TSA and WCA agars respectively to harvest the spores since spores need heat treatment before they can germinate. The aerobic growth on TSA plate was considered as *Bacillus* spp.

after confirmation as Gram-positive/catalase positive rods, and the anaerobic growth on WCA plates was considered as *Clostridium* spp. after confirmation as Gram-positive/oxidase negative rods [22].

4.2.3.2 Detection of *Salmonella* and *Campylobacter* species

Salmonella and *Campylobacter* spp. were detected according to AS 5013.10-2009 and AS 5013.6-2004, respectively. *Salmonella typhimurium* and *Campylobacter jejuni* were used as positive controls. After inoculation of the sample into standard pre-enrichment and selective enrichment broth, typical *Salmonella* colonies on XLD and BSA were inoculated onto NA plates, and the oxidase negative colonies were further tested using API 20 E for *Salmonella* spp. confirmation. In order to detect *Campylobacter*, samples were inoculated into Preston broth, in microaerophilic conditions for 24 h at 42 °C to select for *Campylobacter* spp., after which a loopful of this enrichment was plated on Campylobacter Selective Agar and incubated under the same conditions as mentioned earlier. Typical *Campylobacter* colonies were then confirmed by a Gram stain.

4.3 Characterisation

4.3.1 Morphological analysis

The overall impact of each purification method on the morphology of treated feathers was investigated using macro-digital photography as detailed in section 3.3.1.

4.3.2 Scanning electron microscopy-energy dispersive spectroscopy

The CFFs that showed superior bactericidal efficacy from purification methods were further analysed using SEM analysis. Elemental analysis of the treated CFFs was carried out

using energy dispersive spectroscopy (EDS) in the SEM. The SEM imaging was performed as detailed in section 3.3.2.

4.3.3 Fourier-transform infrared spectroscopy

Fourier-transform infrared (FTIR) spectroscopy was employed for the chemical characterisation of the superior bactericidal efficacy purified and untreated CFFs barbs, as detailed in section 3.3.5. Infrared spectroscopy can detect specific alterations in the chemical composition of peptides [23].

4.3.4 Mechanical properties of purified CFFs

Tensile and viscoelastic properties of the CFFs barbs purified with methods of superior bactericidal effect were evaluated via tensile mechanical analysis (stress–strain analysis) and mf-TM or DMA), respectively, as detailed in section 3.3.10.2. Sampling for a single fibre tensile testing was carried out according to ASTM D3822, using a paper template to mount the fibre and grip in the tensile clamps. Prior to testing, the diameter of the CFFs barbs (Figure 4.9 a) were measured by a Dino-Lite digital microscope, as detailed in section 3.3.10.4. The mf-TM was carried out to determine storage modulus (E') as an indication of elasticity, loss modulus (E''), representing the amount of energy absorbed, and loss tangent ($\tan\delta$), showing damping associated with CFFs.

4.4 Results and discussion

4.4.1 Standard aerobic plate count

The un-purified CFFs (T0) showed the highest count (1.2×10^7 cfu/g) of feathers whereas SEEt treatment (T1) showed the lowest count (3.5×10^2 cfu/g) among all purification treatments, with a mean reduction of *ca.* $5 \log_{10}$ (Figure 4.8).

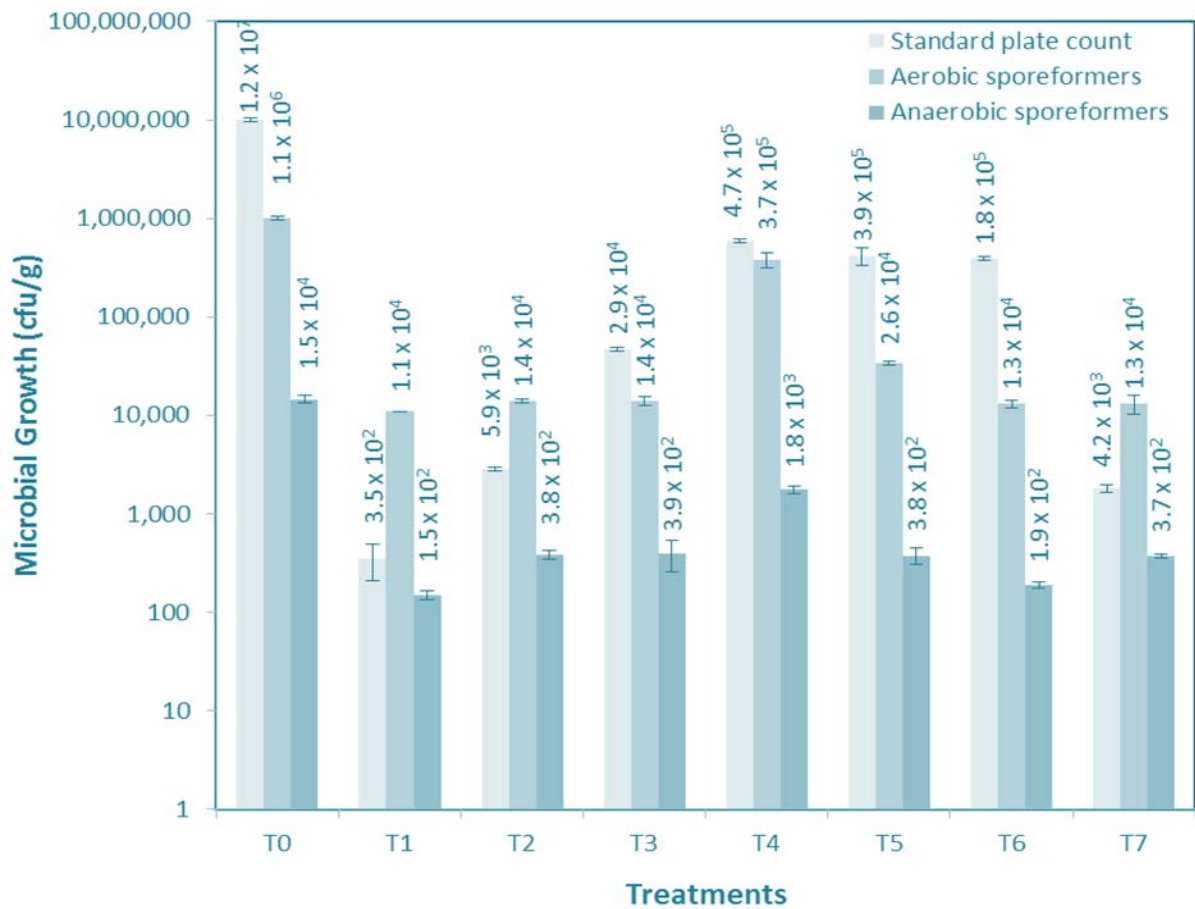


Figure 4.8: Microbial count (cfu/g) of SPC, aerobic spore-formers and anaerobic spore-formers for (T0) untreated chicken feathers upon receipt, versus chicken feathers purified with (T1) SEEt treatment, (T2) O₃ solution, (T3) ClO₂ solution, (T4) PEG solution, (T5) SLS solution, (T6) CTAC solution and (T7) SLS-ClO₂-SEEt combination

This is in agreement with literature as ethanol is capable of eliminating a broad spectrum of bacteria [5]. The SLS-ClO₂-SEEt combined method (T7) exhibited the second most favourable results with an average count of 4.2×10^3 cfu/g, which may be due to the

bactericidal effects of ethanol. Although the time required for ethanol to be effective against different bacteria was suggested to be 30 s [5], the large gap in bacteria count after 2 h (T7) and 5 h (T1) of ethanol Soxhilation suggested the continuation of Soxhilation for several hours. Prolonged treatment time can be due to dealing with unknown types and/or loads of bacteria on unpurified CFFs.

Surfactants are promising purifiers due to benefiting from their dual functionality namely surface activity and intrinsic disinfecting/bactericidal performance [16]. The surface activity of a surfactant is reliant on different factors such as pH, temperature, and concentration. Low values of surface tension and critical micelle concentration (CMC) translates as strong detergent properties associated with a surfactant [24]. The surface tension and CMC values of the surfactants used in descending order as follows:

PEG (74.5 mN/m and 0.78 mol/L) > SLS (47.5 mN/m and 0.44 mol/L) > CTAC (37.0 mN/m and 0.0015 mol/L) [24, 25].

As shown in Figure 4.8, the highest to lowest reduction in all counts including SPC, aerobic- and anaerobic sporeformers belonged to CTAC (T6), SLS (T5), and PGE (T4), respectively, which was the same trend observed for corresponding CMC and surface tension values. It can be concluded that detergents may more engage in the removal of bacteria mechanically than destroying them.

As shown in Figure 4.8, the counts resulted from O₃ (T2) (5.9×10^3 cfu/g) and ClO₂ (T3) (2.9×10^4 cfu/g) treatments were substantially lower than those obtained from detergents. The lower counts signify the superior bactericidal efficiency associated with the used bleaches compared with the selected surfactants. The SPC is an incapable method for

distinguishing pathogens from non-pathogens; therefore, further evaluation of the selected purification treatments requires targeting individual pathogens and indicator organisms.

4.4.2 Aerobic and anaerobic spore-formers, coagulase positive *Staphylococcus*, *Escherichia coli*, *Pseudomonas*, *Salmonella* and *Campylobacter* species

The viable count of aerobic and anaerobic spore-formers found in T0 to T7 treatments are shown in Figure 4.8. The T1 treatment was found to be the most effective in removing both aerobic (average of 1.1×10^4 cfu/g) and anaerobic spore-formers (average of 1.5×10^2 cfu/g). Even though ethanol is not effective in destroying spores [5], the viable spore count was lower than T0 (Figure 4.8) due to the washing step of the purification process. The T2 treatment was effective in reducing spore counts as ozone has been found to have sporicidal properties [7]. The T3 treatment was effective in reducing both aerobic and anaerobic spore. Surfactants are not known to have sporicidal properties, hence the most likely reason for reduced spores count in T4, T5 and T6 treatments is that spores were washed away in solution within the surfactant micelles.

The T4 treatment presented relatively higher count of spore-formers (Figure 4.8) than purification treatments, which is in agreement with a study reported by Vardaxis et al. [26] regarding PEG that has been shown to support the growth of spores.

E. coli was detected on T0 (4×10^2 cfu/g), whereas, it was not observed in none of the treatments, suggesting that all purification methods used were effective at eliminating *E. coli*. The absence of visible growth of presumptive *Pseudomonas* spp., coagulase-positive *S. aureus* (CPSA), and *Campylobacter* spp. on T0 ($< 1 \times 10^2$ cfu/g), does not necessarily imply that the purification treatments T1 to T7 were effective in eliminating the above species in the purified feathers. The *S. aureus* was possibly unable to compete with the other

microflora on the CFFs, due to a combination of inadequate time and temperature to allow it to flourish. The positive control (*Pseudomonas fluorescens* 283/2) was confirmed by Gram morphology, and the isolates appeared Gram-negative and at the same time, oxidase negative. Colonies that appeared similar to the *E. coli* positive control on the interpretation guide were considered as *E. coli*. All positive controls were effective in growing CPSA and *Campylobacter*.

Salmonella was detected in T0, T2, T3, T4, T5 and T6 but not in T1 and T7, as ethanol is known to destroy *Salmonella* [5]. Surfactants are known to be less efficient against Gram-negatives [27], therefore *Salmonella* spp. were detected. Detection of *Salmonella* in T2 and T3 was unexpected since O₃ and ClO₂ are known to destroy *Salmonella* [28]. Furthermore, the treatment period of over 5 h was assumed to be sufficient. It could be argued that the concentrations may not have been adequate for a 10 g sample loading, even though the concentrations used were higher than those suggested in the literature [9, 14]. The T7 result demonstrated that 2 h ethanol treatment is not reducing the microbial loads as effectively as 5 h treatment, however, it was sufficient for disinfecting pathogens such as *Salmonella* when combined with surfactant and bleach.

The ineffective treatments in eliminating the *Salmonella* should not be employed as they do not eliminate human pathogens carried by chicken feather. The microbiological findings in T0 and T7 will be utilised in this project and in industries to limit the exposure risk of human pathogens.

4.4.3 Morphological analysis

The impact of each purification method on the morphology of CFFs was investigated via visual observation (Figure 4.9 b). Except for T1 treatment, which exhibited a significant

shrinkage and crumpling of the treated CFFs, the main components of the feather were distinguishable in other purified CFFs. Comparing the CFFs from all treatments, those treated in T1 exhibited over-erection along the feather structure as well as lacking in the woolly part of the CFFs shown in Figure 4.9(b). These effects can be attributed to the over-drying nature of ethanol on CFFs and the fact that ethanol removed the fat on the feather surfaces and break most of the hydrogen bonds in the keratin, which can be used as a pre-treatment step for extraction of keratin and has influence on its yield depending on time and temperature [29].

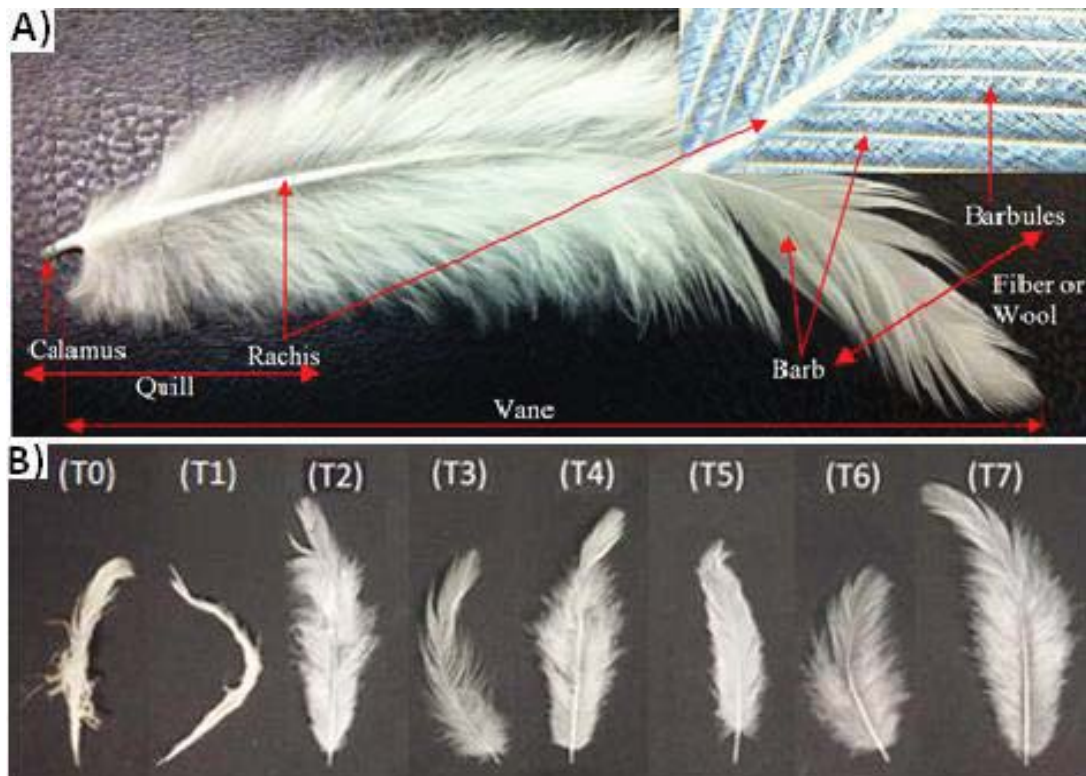


Figure 4.9: A) The structure of a semiplume chicken feather (fibre or wool: barbs/barbules), (quill: calamus/rachis or shaft), (vane: rachis/barb/barbules) treated with T7; B) Images of the semiplume chicken feathers: (T0) untreated upon receipt, (T1) SEEt treatment, (T2) O₃ solution, (T3) ClO₂ solution, (T4) PEG solution, (T5) SLS solution, (T6) CTAC solution, and (T7) SLS-ClO₂-SEEt combination

4.4.4 Scanning electron microscopy and energy dispersive spectroscopy

Figure 4.10 shows the SEM electron images, SEM-EDS maps, and elemental analysis associated with the total map spectrum obtained from CFF treated via T1 and T7 treatments.

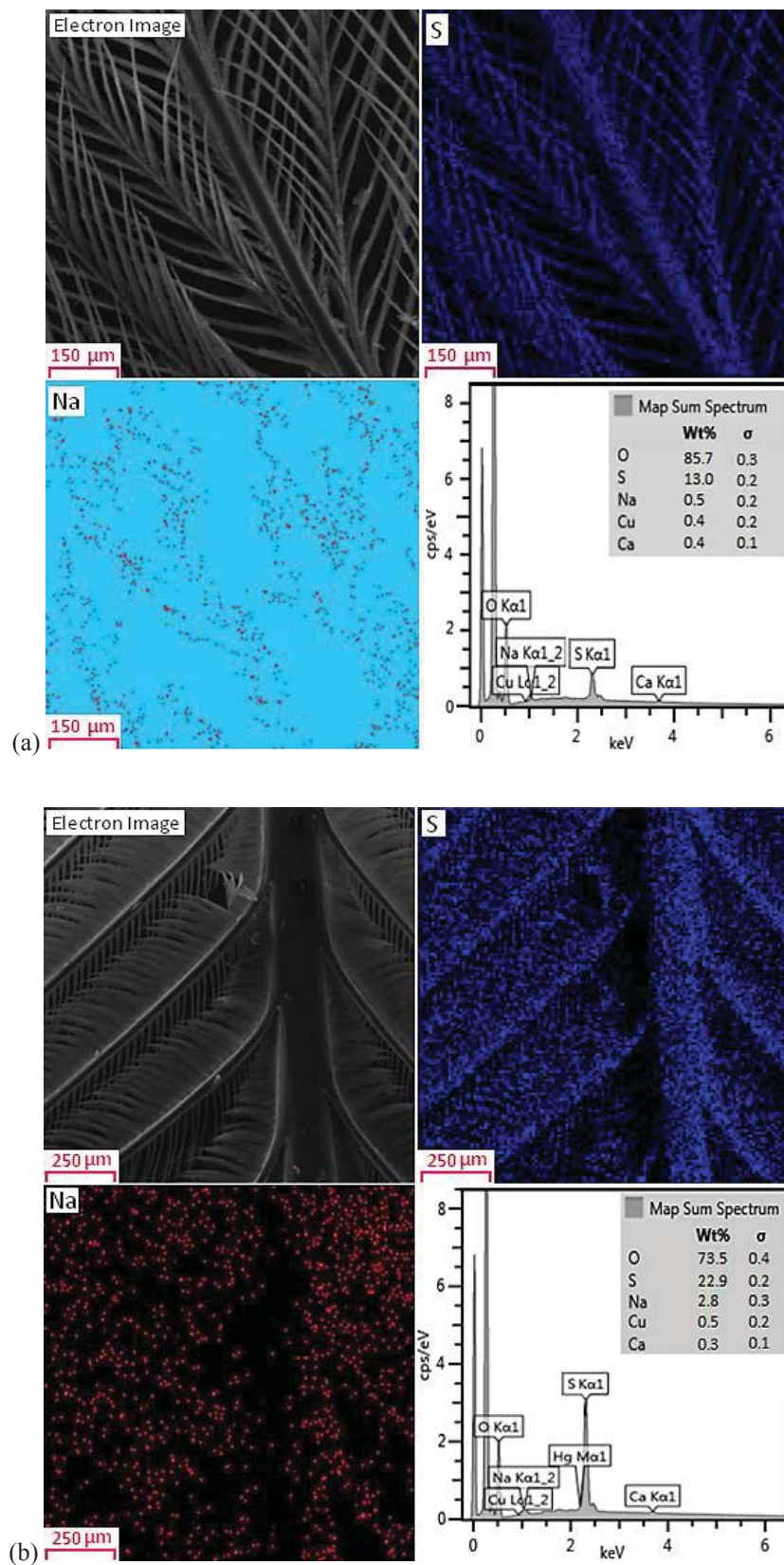


Figure 4.10 Figure 4.10: SEM, SEM-EDS, and elemental data derived from the CFFs treated via (a) SEEt (T1) and (b) SLS-CIO₂-SEEt (T7)

None of the CFFs purified via T1 and T7 showed any signs of detectable fibre damages. Eliminating N and C from elemental analysis, other major elements in T1 (Figure 4.10 a) and T7 (Figure 4.10 b) samples were found to be O, S, Na, Cu, and Ca. The relative weight proportions associated with S (22.9 %·w/w) and Na (2.8 %·w/w) in the CFFs treated by T7 were 9.9 %·w/w and 2.3 %·w/w higher than those of the CFFs treated by T1, respectively. This confirms the partial deposition of SLS on the purified CFFs, which from a safety point of view, can cause mild to moderate skin irritation on human skin upon contact [15].

4.4.5 FTIR spectroscopy

In order to examine the effectiveness of purification processes on CFFs, FTIR spectra of the untreated feather (T0) and CFFs purified via T1 and T7 treatments were obtained. The broad absorption band region from 3500 cm^{-1} to 3200 cm^{-1} is attributed to the stretching vibration of N–H and O–H bonds. Bands that fall in the 3000 cm^{-1} to 2800 cm^{-1} range are related to C–H stretching modes. The amide I band is attributed to C=O stretching vibration, which occurs in the range of 1700 cm^{-1} to 1600 cm^{-1} [23]. N–H bending stretching vibration associated with amide II occurs between 1580 cm^{-1} and 1480 cm^{-1} [30]. The amide III band occurs in the range of 1300 cm^{-1} to 1220 cm^{-1} , which can be due to the phase combination of C–N stretching and N–H in-plane bending [31, 32]. N–H out-of-plane bending associated with the amide group occurs in a range between 750 cm^{-1} and 600 cm^{-1} .

In the FTIR spectrum of un-purified CFFs the stretching vibration at around 1710 cm^{-1} can be associated with carbonyl groups (C=O) of a fatty acid ester namely adipic acid ester usually found on animal skins [33]. As the amide peaks cover the range between 1700 cm^{-1} and 1220 cm^{-1} [23, 34], the C–O stretching vibration associated with the ester-linkage occurring at 1267 cm^{-1} [33] was undetectable. Elimination of the stretching vibration at 1710

cm^{-1} associated with C=O of ester in T1 and T7 spectra confirms the capability of both purification methods in removing fatty materials from the untreated CFFs (Figure 4.11).

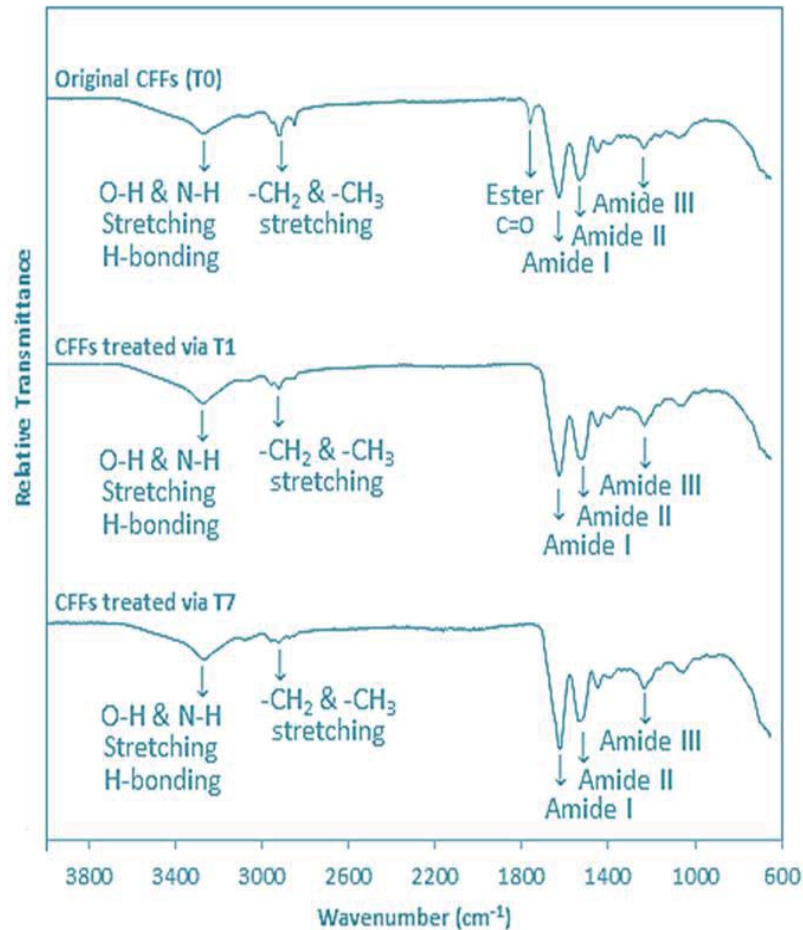


Figure 4.11: FTIR spectra of original CFFs (T0) and CFFs purified via SEEt (T1) and SLS-CIO₂-SEEt (T7)

4.4.6 Mechanical properties

Many bacteria including aerobic, anaerobic and enteric bacteria could adversely affect the mechanical properties of the untreated CFFs [35], therefore the mechanical properties of the CFFs were evaluated after implementing T1 and T7 treatments. The stress-strain properties of purified CFFs barbs were evaluated (Figure 4.12). The maximal strength values resulted from CFFs purified by T7 and T1 were found to be 104.9 MPa and 14.1 MPa, at corresponding strain values of 9.3 % and 6.5 %, respectively. The elastic modulus (E), which

is the initial slope of the stress–strain curve, was higher for T7 (2.0 GPa) than T1 (0.3 GPa). As the area below the stress-strain curve associated with T7 was considerably larger than that of T1, it was concluded that the CFFs barbs treated via T7 were significantly tougher than those treated via T1, which confirm the visual difference observed in feather structure in Figure 4.9(b). It is possible that both the time and concentration of T1 treatment has caused the CFF to either deteriorate or change structure. This potential alteration to the tensile strength must be taken into consideration if the final application requires advanced mechanical properties. The changes seen in the mechanical strength after the application of the T1 treatment maybe either due to the CFFs becoming dehydrated post T1 exposure or the T1 treatment may have caused some of the CFF keratin to denature. Table 4.2 shows the average measures of E' , E'' , $\tan\delta$, standard deviation (SD), and standards error values associated with 20 similar CFFs barbs purified via T7 and T1 determined within 90 % of confidence.

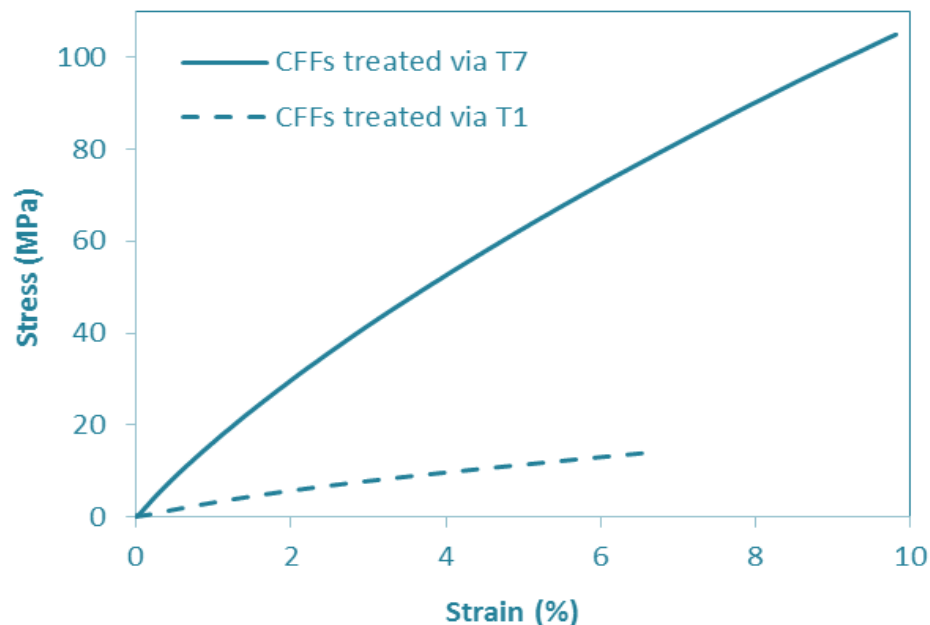


Figure 4.12: Tensile stress-strain curve of single CFFs purified via SEEt (T1) and SLS-ClO₂-SEEt (T7)

Table 4.2: Diameter, storage modulus (E'), loss modulus (E'') and $\tan\delta$ values with standard deviation (SD) values and standard error of CFFs barb purified via SEEt (T1) and SLS-ClO₂-SEEt (T7)

Purification treatments	T1	T7
Average Temperature (°C)	18.4	18.5
Average barb diameter (mm)*	0.168	0.119
SD	0.010	0.022
Standard Error (%)	3.04	9.31
Average E' (MPa)	1687	1243
SD	32	22
Standard Error (%)	1.107	1.038
Average E'' (MPa)	451	554
SD	6	5
Standard Error (%)	0.705	0.514
Average $\tan\delta$	0.268	0.446
SD	0.002	0.004
Standard Error (%)	0.5	0.5

*The mean diameter value of five-point measurements of 20 CFFs barb

Each DMA test performed at a constant temperature at 18.0 ± 0.1 °C, T7 demonstrated lower E' but higher values of E'' and $\tan\delta$ than T1. The stress–strain test showed T7 to have greater modulus and strength than T1, in contrast to the DMA test was where T1 had somewhat higher elastic modulus is interpreted as due to the higher rate of strain in the DMA test at 0.5 Hz. The T7 had a slightly greater loss modulus showing greater energy dissipation or viscoelasticity than T1 consistent with the increased ultimate strain in the stress–strain result. The barbs from CFF are potentially applicable as reinforcement in natural fibre composites (bio-composites) in lieu of cellulose fibres.

4.5 Conclusions

The CFs treated with ethanol-extraction purification (T1) were confirmed to have fatty esters and *Salmonella* removed while they exhibited minimal bacterial counts (3.5×10^2 cfu/g) compared with other practised methods. Combined surfactant-oxidant-ethanol purification method (T7) was found to be the second most efficient technique in reducing bacterial counts (4.2×10^3 cfu/g) and eliminating *Salmonella*.

The elimination of fatty esters from the CFFs purified via T1 and T7 was confirmed by FTIR. The T7 treated feathers resulted in superior morphological and mechanical properties compared with the T1 treated feathers. Optical evaluation of the treated CFFs suggested the similar morphology for the CFFs purified via ozonation and chlorine to the CFFs purified by anionic, non-ionic and cationic surfactants.

SEM-EDS results confirmed the presence of SLS residues in CFFs treated via T7; therefore, T1 was chosen as the safest single purification treatment among other practices. However, as far as benefiting from superior mechanical properties in bio-composites- or similar technologies is concerned, the T7 treatment, was found more promising due to offering fibres of superior tensile strength (104.9 MPa) than T1 (14.1 MPa).

4.6 References

1. Mills, J., ed. *Meat industry Microbiological Manual*. 2011, Agresearch: Hamilton, New Zealand.
2. Sudalaiyandi, G., *Characterizing the cleaning process of chicken feathers*. Master of Engineering thesis, University of Waikato, Hamilton, New Zealand (2012).
3. Rai, S.K., R. Konwarh, and A.K. Mukherjee, *Purification, characterization and biotechnological application of an alkaline β -keratinase produced by Bacillus subtilis RM-01 in solid-state fermentation using chicken-feather as substrate*. *Biochemical Engineering Journal*, 2009. **45**(3): p. 218-225.
4. FDA, *Guidance for Industry and FDA Reviewers: Content and Format of Premarket Notification - Submissions for Liquid Chemical Sterilants/High Level Disinfectants*. 2000.
5. Rutala, W.A., D.J. Weber, and C.f.D. Control, *Guideline for disinfection and sterilization in healthcare facilities, 2008*. 2008, Centers for Disease Control (US).
6. Joklik, W., *Ch. 10. Sterilization and disinfection*. *Zinsser Microbiology*, 1992: p. 188-200.
7. Singh, N., R. Singh, A. Bhunia, and R. Stroshine, *Efficacy of Chlorine Dioxide, Ozone, and Thyme Essential Oil or a Sequential Washing in Killing *Escherichia coli* O157: H7 on Lettuce and Baby Carrots*. *LWT-Food Science and Technology*, 2002. **35**(8): p. 720-729.
8. Foegeding, P., *Ozone inactivation of *Bacillus* and *Clostridium* spore populations and the importance of the spore coat to resistance*. *Food Microbiology*, 1985. **2**(2): p. 123-134.
9. Naidu, A., *Natural food antimicrobial systems*. 2000, London: CRC press.

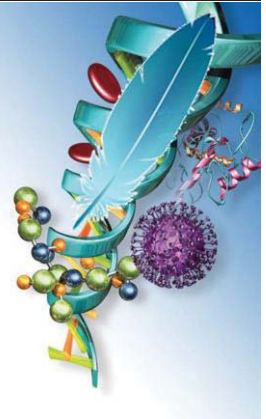
10. Shemesh, M., R. Kolter, and R. Losick, *The biocide chlorine dioxide stimulates biofilm formation in Bacillus subtilis by activation of the histidine kinase KinC*. Journal of bacteriology, 2010. **192**(24): p. 6352-6356.
11. Aieta, E.M. and J.D. Berg, *A review of chlorine dioxide in drinking water treatment*. Journal (American Water Works Association), 1986: p. 62-72.
12. Augurt, T.A. and J. van Asten, *Sterilization techniques*. Kirk-Othmer Encyclopedia of Chemical Technology, 2000.
13. Trakhtman, N. *Chlorine dioxide in water disinfection*. in *Chemical Abstracts*. 1949.
14. Manual, E.G., *Alternative disinfectants and oxidants*. Disinfectant Use in Water Treatment, Washington, DC, 1999.
15. Effendy, I. and H.I. Maibach, *Surfactants and experimental irritant contact dermatitis*. Contact dermatitis, 1995. **33**(4): p. 217-225.
16. Davis, J.G., *Methods for the evaluation of antibacterial activity of surface active compounds: technical aspects of the problem*. Journal of Applied Bacteriology, 1960. **23**: p. 318-344.
17. WikipediaContributors. *Soxhlet extractor*. 27/09/2016]; Available from: https://en.wikipedia.org/w/index.php?title=Soxhlet_extractor&oldid=737652608.
18. Meunier, B. and A. Sorokin, *Oxidation of pollutants catalyzed by metallophthalocyanines*. Accounts of chemical research, 1997. **30**(11): p. 470-476.
19. Newman, S.E. *Disinfecting irrigation water for disease management*. in *20th Annual Conference on Pest Management on Ornamentals*. 2004.
20. Mattei, D., S. Cataudella, L. Mancini, L. Tancioni, and L. Migliore, *Tiber River Quality in the stretch of a sewage treatment plant: Effects of river water or disinfectants to Daphnia and structure of benthic macroinvertebrates community*. Water, air, and soil pollution, 2006. **177**(1-4): p. 441-455.
21. Tran, C.D., F. Prosenc, M. Franko, and G. Benzi, *Synthesis, structure and antimicrobial property of green composites from cellulose, wool, hair and chicken feather*. Carbohydrate Polymers, 2016. **151**: p. 1269-1276.
22. Durmic, Z., D. Pethick, J. Pluske, and D. Hampson, *Changes in bacterial populations in the colon of pigs fed different sources of dietary fibre, and the development of swine dysentery after experimental infection*. Journal of applied microbiology, 1998. **85**(3): p. 574-582.
23. Mohanty, A.K., M. Misra, and L.T. Drzal, *Natural Fibers, Biopolymers, and Biocomposites*. 2005: CRC Press.
24. MANDAVI, R., S.K. SAR¹, and N. RATHORE, *Critical micelle concentration of surfactant, mixed-surfactant and polymer by different method at room temperature and its importance*. Oriental Journal of Chemistry, 2008. **24**(2): p. 559-564.
25. Xu, Q., L. Wang, and F. Xing, *Synthesis and properties of dissymmetric gemini surfactants*. Journal of surfactants and detergents, 2011. **14**(1): p. 85-90.
26. Vardaxis, N., M. Hoogeveen, M. Boon, and C. Hair, *Sporicidal activity of chemical and physical tissue fixation methods*. Journal of clinical pathology, 1997. **50**(5): p. 429-433.
27. Pérez, L., M.T. Garcia, I. Ribosa, M.P. Vinardell, A. Manresa, and M.R. Infante, *Biological properties of arginine-based gemini cationic surfactants*. Environmental toxicology and chemistry, 2002. **21**(6): p. 1279-1285.
28. Muthukumarpan, K., F. Halaweish, and A.S. Naidu, *Ozone*. In: *Natural Food Antimicrobial Systems*. 2000.
29. Yin, X.-C., F.-Y. Li, Y.-F. He, Y. Wang, and R.-M. Wang, *Study on effective*

- extraction of chicken feather keratins and their films for controlling drug release.* Biomaterials Science, 2013. **1**(5): p. 528-536.
30. Eslahi, N., F. Dadashian, and N.H. Nejad, *An investigation on keratin extraction from wool and feather waste by enzymatic hydrolysis.* Preparative Biochemistry and Biotechnology, 2013. **43**(7): p. 624-648.
 31. Vasconcelos, A., G. Freddi, and A. Cavaco-Paulo, *Biodegradable materials based on silk fibroin and keratin.* Biomacromolecules, 2008. **9**(4): p. 1299-1305.
 32. Wojciechowska, E., A. Włochowicz, and A. Weselucha-Birczyńska, *Application of Fourier-transform infrared and Raman spectroscopy to study degradation of the wool fiber keratin.* Journal of Molecular Structure, 1999. **511**: p. 307-318.
 33. Al-Itry, R., K. Lamnawar, and A. Maazouz, *Improvement of thermal stability, rheological and mechanical properties of PLA, PBAT and their blends by reactive extrusion with functionalized epoxy.* Polymer Degradation and Stability, 2012. **97**: p. 1898-1914.
 34. Aluigi, A., M. Zoccola, C. Vineis, C. Tonin, F. Ferrero, and M. Canetti, *Study on the structure and properties of wool keratin regenerated from formic acid.* International journal of biological macromolecules, 2007. **41**(3): p. 266-273.
 35. Fan, X., *Value-added products from chicken feather fiber and protein.* PhD Thesis. 2008, Auburn, Alabama: ProQuest, Auburn University.

4.7 Publication from this Chapter

- Pourjavaheri, F., Mohaddes, F., Bramwell, P., Sherkat, F., & Shanks, R.A. (2015) "Purification of avian biological material to refined keratin fibres" *RSC Advances*: **5**(86), p. 69899-69906.

CHAPTER 5



CHARACTERISATION OF CHICKEN FEATHER FIBRES

5.1 Introduction

Extensive research has been focused on the extraction, purification and characterisation of keratin [1, 2]. Advances in the extraction, purification and characterisation of keratins [3, 4] have resulted in the exponential availability of keratin materials and their derivatives. Due to the relatively high costs of traditional sources of keratin such as wool and silk, alternative materials such as CFs have been suggested. Poultry slaughterhouses worldwide produce huge quantities of feather annually, and their uncontrolled disposal of which leads to pollution in our environment [5]. From an economic and environmental view, it is desirable to develop an effective, profitable process to use waste CFs, therefore, studies have been conducted on value-adding to this sustainable source of fibres [6, 7]. The CF is proven to be a suitable, biodegradable, renewable and potentially valuable biopolymer [8]. Following from the CFF purification reported in Chapter 4, this chapter will concentrate on further characterising the purified CFF. The basic properties for the whole processed feathers and the separated barbs and rachis are determined to evaluate their suitability for various applications. The keratin in CFs will be compared with keratin sourced from pigeon feathers and sheep wool.

5.2 Experimental

5.2.1 Materials

All materials used are detailed in Chapter 3 (Table 3.2).

5.2.2 Characterisation methods

The CFs were purified as detailed in Chapter 4. Some of the purification treatments were further characterised as discussed in 5.3.2.1 to 5.3.2.8, which were:

(T1) purified by SEEt

(T2) purified by O₃

(T3) purified by ClO₂

(T4) purified by PEG surfactant

(T5) purified by SLS surfactant

then compared with (T0) untreated CF after oven drying. Some of the CFs characterisations have been compared with other keratin sources such as pigeon feather and sheep wool for either morphological analysis, optical microscopy under natural visible and UV light or infrared spectroscopy.

5.2.2.1 Storage of feathers

All the purified dry feathers were stored in sealed plastic bags, at controlled temperature (20 ± 2 °C) and relative humidity (RH 60 ± 2 %), after transferred in an oven at 34 °C ± 1 °C for 3 d to dry. The pH of CFFs specimens were determined as described in section 3.3.12.

5.2.2.2 Morphological analysis and stereoscopic microscopy

The semiplume purified CFs were imaged as detailed in Chapter 4, using an optical microscope under visible and UV light, as detailed in Chapter 3 (section 3.3.1), together with the untreated contour chicken and pigeon feathers.

5.2.2.3 Scanning electron microscopy

The SEM imaging was performed on CFFs that were cut into smaller pieces of about 1 cm and were attached to the stubs with double-sided carbon adhesive, as detailed in Chapter 3 (section 3.3.2).

5.2.2.4 Micro X-ray diffraction and wide-angle X-ray scattering analysis

Diffraction patterns of the CF rachis and barbs were obtained as detailed in Chapter 3 (sections 3.3.3).

5.2.2.5 Fourier-transform infrared spectroscopy

Infrared spectroscopy can detect specific alterations in the chemical composition of peptides [9], therefore, FTIR spectroscopy was employed to characterise the feathers before and after purification and residues after extraction, as detailed in Chapter 3 (section 3.3.5). Smoothing, baseline correction and normalisation to absorbance of 1 was used for all FTIR spectra.

5.2.2.6 Vibrational spectroscopic analysis

A Perkin Elmer Raman Station 400F was used to record spectra of the CFF before and after purification treatments and residues after extraction, as detailed in Chapter 3 (section 3.3.6).

5.2.2.7 Thermal analysis

In order to assess thermal stability of the untreated and purified CFF, thermogravimetry (TGA) was performed as detailed in Chapter 3 (section 3.3.7). Sample mass was chosen to be *ca.* 2 mg in this section to minimise the effect of thermal lag.

5.3 Results and discussion

5.3.1 Storage of feathers

Feathers are affected by the environment in which they remain; therefore providing

feathers with a neutral pH and stable environment will prolong their shelf-life [10].

According to Manual [10], standards for preserving feather properties are:

- Minimal handling and dust protection,
- Temperature *ca.* 15 °C to 22 °C,
- Humidity: 45 % to 55 %,
- pH of feather: 6.5 to 7.5,
- Visible light: 50 lm or less (the intensity of light in a dim room),
- Ultraviolet light: 75 μ W/lm or less.

Prior to drying, the feathers were rinsed with distilled water until the pH of the solution was stabilised. The pH of dry purified CFF is compared as shown in Table 5.1, after re-wetting them with distilled water to read their pH. The T2 demonstrated the lowest pH of *ca.* 3.9 versus T1 that demonstrated the highest pH of *ca.* 5.8. Therefore to store the feathers for long period it was required to adjust the final rinsing pH to *ca.* 7.

Table 5.1: pH of the chicken feathers purified with different techniques

Specimens	pH	Temperature (°C)
SEEt treatment (T1)	5.76	20.9
SLS solution (T5)	5.50	21.1
Untreated feather (T0)	5.36	20.8
Milli-Q pure water	5.26	21.9
Distilled water	4.73	21.5
ClO ₂ solution (T3)	4.72	21.3
PEG solution (T4)	4.41	21.0
O ₃ solution (T2)	3.93	20.8



Figure 5.1: pH measurement of CFs rinsed water using pH HACH® SensION5™ Portable pH Meter

5.3.2 Visual observation

The untreated CFs were clumped, lank, stringy and covered in debris due to residual lipids. Dried CFs ranged from pale yellow for untreated feathers to off white for treated feathers. The bulk of the treated CFs showed relatively clean rachis, which became fluffy with tufts of white down fibre starting to unfurl and having a soft texture. Each purification treatment made the feathers whiter and the substructures outspread. Macro photographic images of the treated semiplume CFs and untreated chicken and pigeon contour feathers are illustrated in Figure 5.2. Treatment T5 gave the best outcome since the anionic surfactant, was effective in removing oily dirt and stains. The T4 was the next most effective method without potential adsorption of what onto ionic groups of the protein backbone.

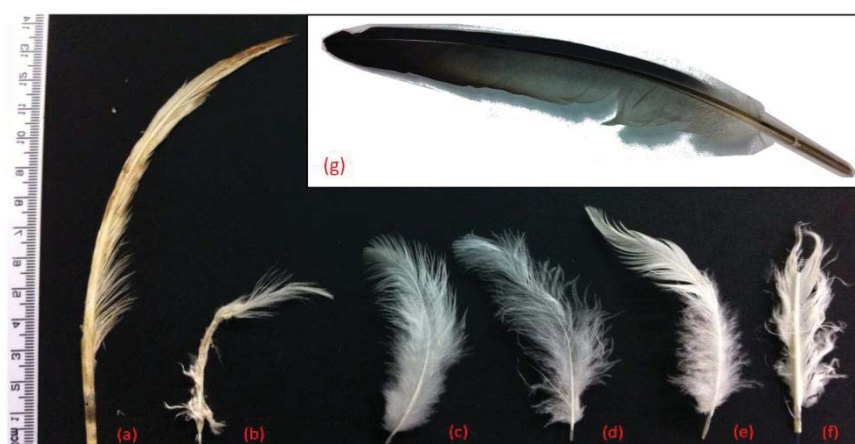


Figure 5.2: a) Untreated contour chicken feather (T0) after oven drying versus semiplume chicken feathers purified with b) SEEt treatment (T1), c) SLS solution (T5), d) PEG solution (T4), e) O₃ solution (T2), f) ClO₂ solution (T3), and g) untreated contour pigeon feather

Untreated CFs appeared straw-like with barbs and barbules coated with lipids, and the barbs were attached to the rachis in a greasy tangle (Figure 5.2(a)), had a yellow-brown colour with a distinct putrid smell. After all treatments except T1, which extracted the fatty waxy substances from CFs, the nodular structures were intact, and feathers had their barbs unfurled. The outer edges of the barbs in bleach solutions, T2 and T3 (Figures 5.2(e) and 5.2(f)) folded inwards, both whitened feathers, leaving them with similar texture to the surfactant treatments, i.e. T4 and T5 (Figures 5.2(d) and 5.2(c) respectively).

5.3.3 Stereoscopic microscopy

Figure 5.3 shows the optical microscopic images of a CF segments at different magnifications. The calamus, rachis, barb, barbules and hooklets are identified in the micrographs.

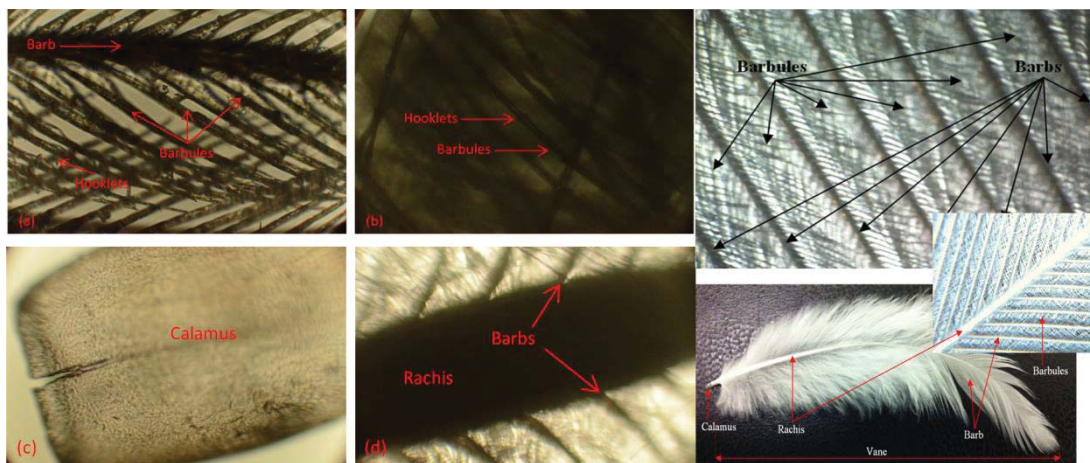


Figure 5.3: Optical microscopic images of a chicken feather segments at (a) 60X, (b), (c) and (d) 100X magnification

The structure and different parts of a chicken and pigeon feather as seen are shown in Figures 5.4 and 5.5, respectively under visible and UV light, which showed up differences in processing technique. The amino acid sequence of keratin in CFs is largely composed of cystine, glycine, proline and serine, alanine and valine, whereas methionine, histidine, lysine

and tryptophan are almost absent (Table 2.2). Tryptophan, tyrosine, phenylalanine and histidine fluoresce because they all contain aromatic ring structures (Figure 2.9) that absorb UV light for excitation [11]. Tryptophan in particular fluoresces more than tyrosine, phenylalanine or histidine [12] under UV, however as tryptophan and histidine are almost absent, hence, tyrosine and phenylalanine are responsible for the fluorescence. This may provide a useful way to determine the amount of protein degradation when using different purification techniques and for decontamination purposes prior to keratin isolation, as described in Chapter 4.

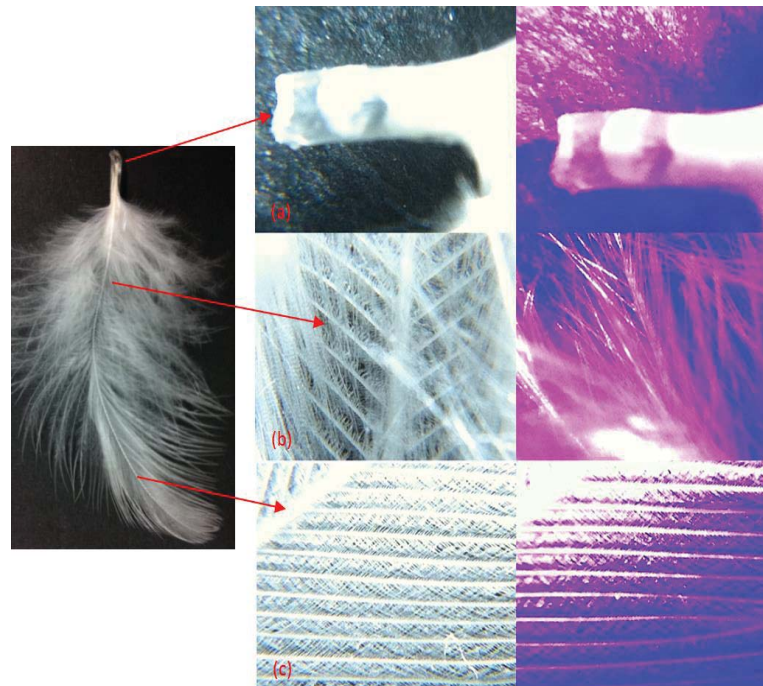


Figure 5.4: The structures of a semiplume chicken feather under natural visible and ultraviolet light at 80X magnification, (a) calamus, (b) rachis, barb and barbules from the bottom of a chicken feather, (c) rachis, barb and barbules from the top of a chicken feather

The treated CFF showed bundles of fine fibre, however were found to scatter light at 80X magnification as shown in Figure 5.4. Comparing the texture of the feather components, the T0 calamus and rachis, had a hard texture as they have a β -sheet structure, they were flexible compared with the other specimens. The feathers treated with T4 and T5 surfactants

and T3 had the same appearance and texture as the T0. However, T1 and T2 showed softened texture in the calamus and rachis, making the feathers more brittle compared with the other treatments.

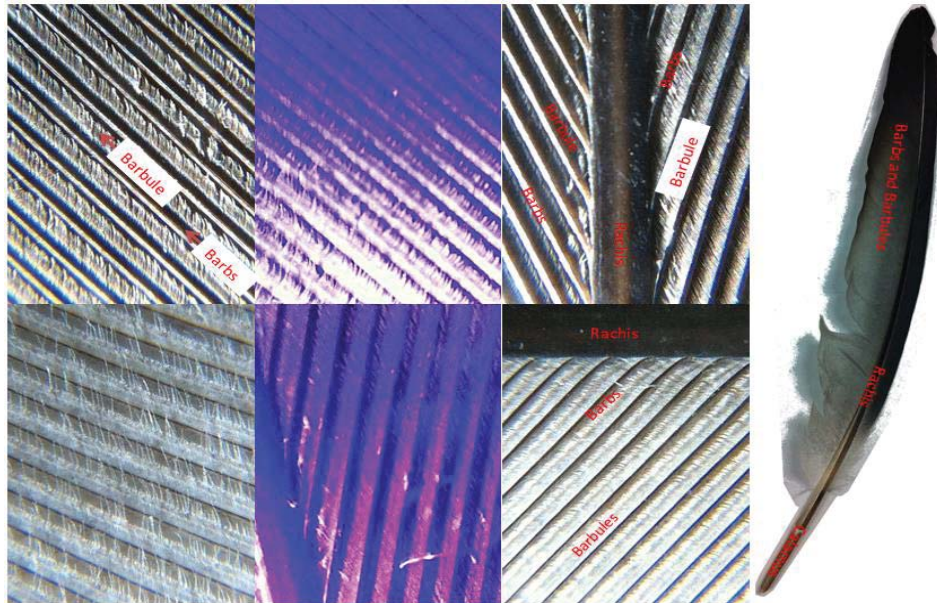


Figure 5.5: The structures of a contour pigeon feather under natural visible and ultraviolet light at 80X magnification

Figure 5.6 compares these different purification treatments on CFs under visible and UV light; The T0 shows an untreated CF as received. These purification treatments had produced different changes on tyrosine, phenylalanine and histidine contained in the CFs as demonstrated in Figure 5.6. This may be due to the interactions with aromatic groups and peptide bonds contained in CFs causing fluorescence emission at various wavelengths [2]. The T1 (Figure 5.6 panels T1) showed the second lowest fluorescence that was more of pink wavelengths. This is different to the unwashed feathers that show more purple wavelengths. The amount of fluorescence was low in T0 and high in the feathers treated with T2 and T3 (Figure 5.6, panels (T2) and (T3)). Further studies are required to determine if there is a relation between the amount of fluorescence and the feather qualities after each treatment.

Fluorescence with black and white backgrounds is shown in rows 2 and 3 respectively. The surfactant T4 and T5 washes show the pink and purple wavelengths depend on the black or white background (Figure 5.6, panels (T4) and (T5)).



Figure 5.6: Chicken segments under natural and ultraviolet light at 80X magnification
 a) untreated chicken feathers upon receipt (T0), chicken feathers purified with b) SLS solution (T5),
 c) PEG solution (T4), d) SEEt treatment (T1), e) O₃ solution (T2) and f) ClO₂ solution (T3)

5.3.4 Scanning electron microscopy

The morphologies of the CFFs were observed as Figure 5.7 depicts the SEM micrographs and surface morphology of the components of CFFs purified with SLS solution (T5 treatment), at different magnifications from 40X to 3000X. The bundled feathers are shown in Figures 5.7 (a) and (b). The feather microstructure was not damaged after purification and barbicels of 20 μm diameter were found intact. Figures 5.7 (b) to (g) contains a highly

concentrated area of barb and barbule fibres with nodular substructures. Figure 5.7 (c) shows the same area, where the nodes were barbules and barbicels. Figure 5.7 (f) shows the particles located between the layer of barbicels and barbules, with few particulate impurities, copious debris trapped in barbules and hooked barbicels linking to adjacent substructure and a smooth surface in the background. Figures 5.7 (g) to (l) shows a bundle of barbs, the barbules show serrated barbicels. The surface striations of the barbule showed in Figures 5.7 (k) and (l). The calamus, rachis, barb, barbules and hooklets are identified in the Figure 5.7 SEM histological morphology.

5.3.5 X-ray analysis

5.3.5.1 Micro X-ray diffraction

The X-ray diffraction analysis is widely used for the structural analysis of proteins and in addition to disulphide bonds, crystallinity is an important contributor to high strength and stiffness of feather keratins [13]. A decrease of crystallinity and decomposition of the β -sheet structures would contribute to the improved keratin extraction [13]. The superior T7 treated feathers was taken to examine the crystal structure by wide-angle X-ray diffraction. The X-ray diffraction pattern of CFFs barbs/barbules and calamus/rachis are represented in Figures 5.8 and 5.9 respectively. As shown in these figures, the XRD pattern of amino functionalised CFFs barbs/barbules remained almost similar to the calamus/rachis, which suggested a lower loading of complex units on the CFF support [14]. Since no significant changes such as increase of the crystallinity of calamus/rachis over barbs/barbules of feather keratins were found, therefore WAXD was used next for characterisation of T7 treated feather.

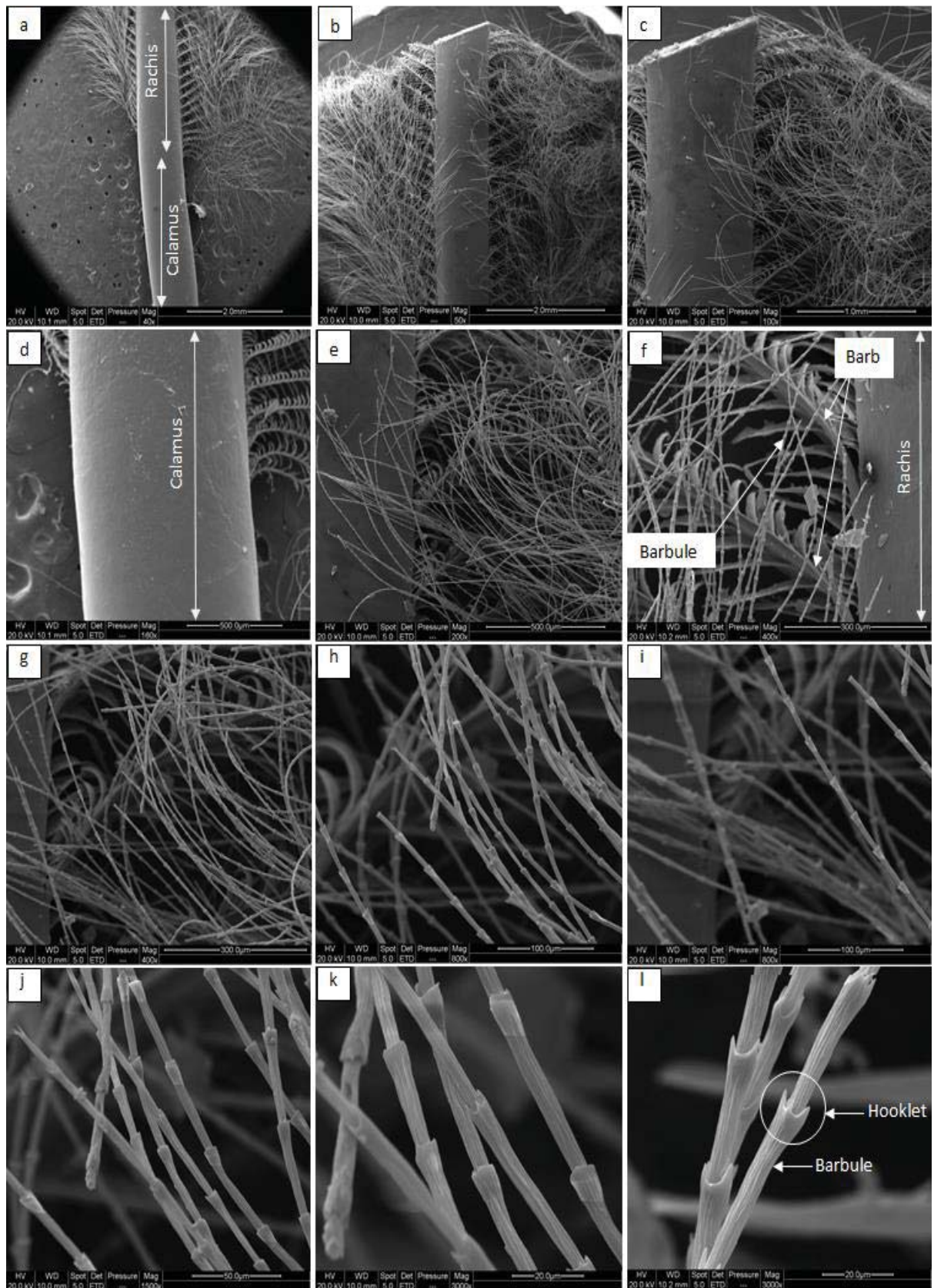


Figure 5.7: The SEM images of the chicken feather fibres purified by SLS solution (T5) at a) 40X, b) 50X, c) 100X, d) 160X, e) 200X, f and g) 400X, h and i) 800X, j) 1500X, k and l) 3000X magnifications

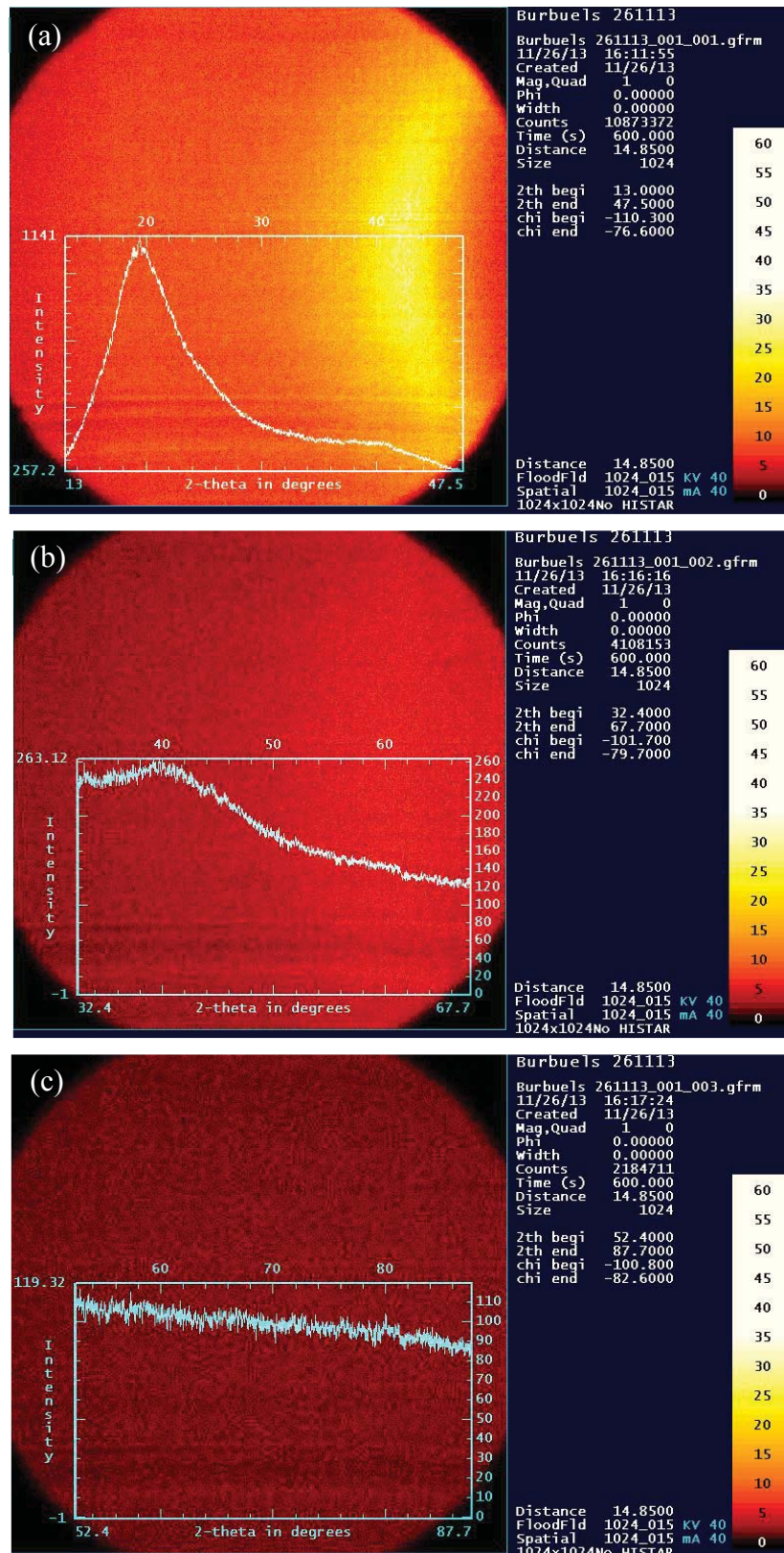


Figure 5.8: The micro X-ray diffraction pattern of chicken feather barb and barbules (α -keratin) with a 2θ at a) 30° , b) 50° and c) 70°

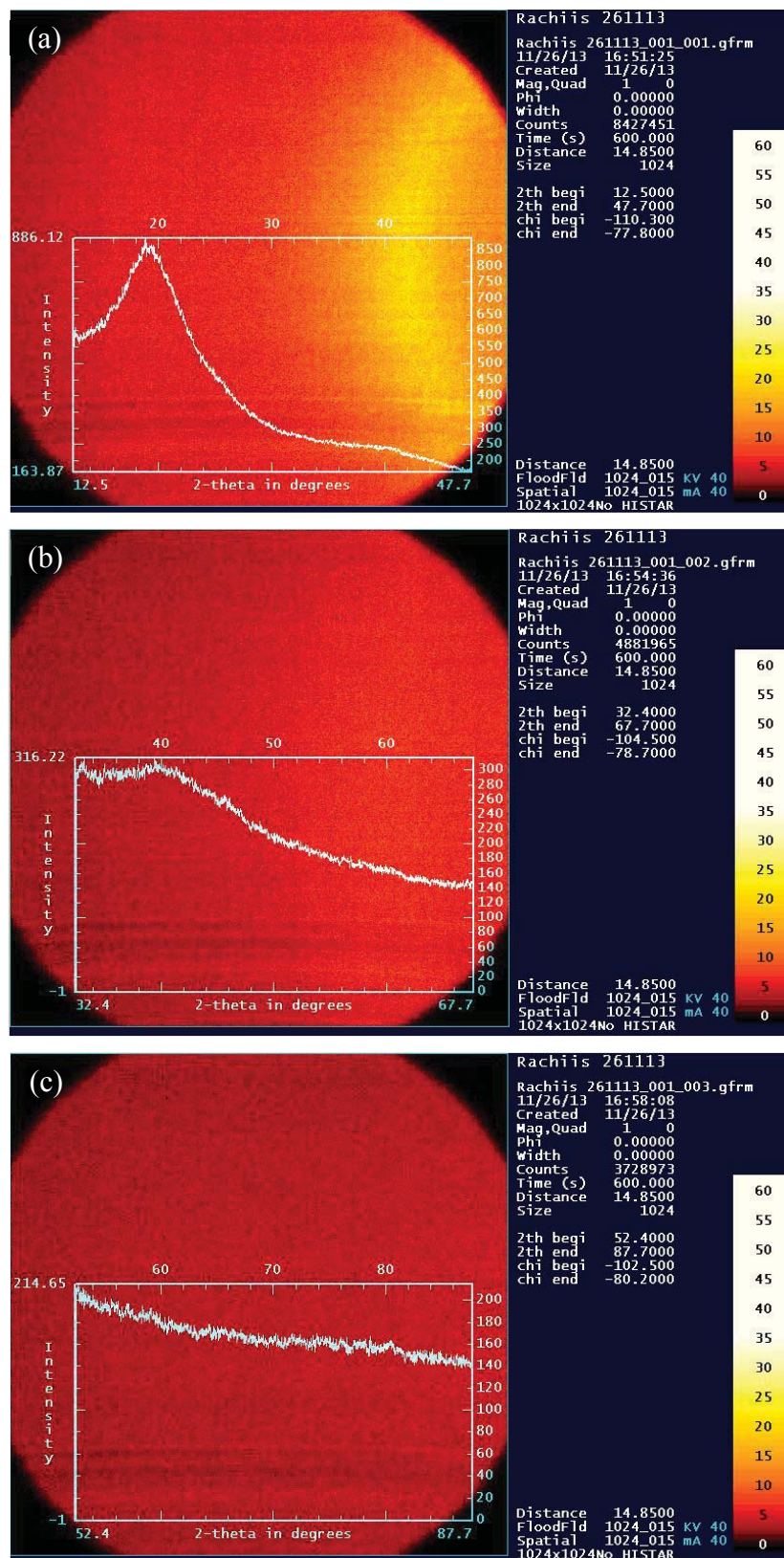


Figure 5.9: The micro X-ray diffraction pattern of chicken feather calamus and rachis (β -keratin) with a 2θ at a) 30° , b) 50° and c) 70°

5.3.5.2 Wide-angle X-ray scattering

The crystal structures of CFs purified with superior T7 treatment as analysed by WAXS is shown in Figure 5.10. The feather displayed a typical diffraction pattern of β -keratins (feather keratins) with a prominent 2θ peak at 8.2° corresponding to the α -helix configuration of the feather keratin, and a more intense band at 20.5° indexed as its beta strand secondary structure [13-15]. Different position and shape of the major peak in calamus/rachis X-ray pattern compared with barbs/barbules reconfirmed the difference in the crystalline structure of CF segments. As expected the crystalite size of calamus/rachis (1.75 nm – 96.5 %) was larger than those of barbs/barbules (1.47 nm – 82.9 %). These results agree with literature [13-15]. Further research using stronger radiation sources such as synchrotron sources could provide a better understanding of the structure of protein crystals in various parts of the feathers. Nakamura [16], reported the feather KF is semi-crystalline and constitutes a crystalline fibre phase and an inter-linked amorphous protein matrix phase. The crystalline phase consists of α -helical keratin braided into microfibrils where the protein matrix is fixed by intermolecular interactions, especially the many hydrogen bonds [16].

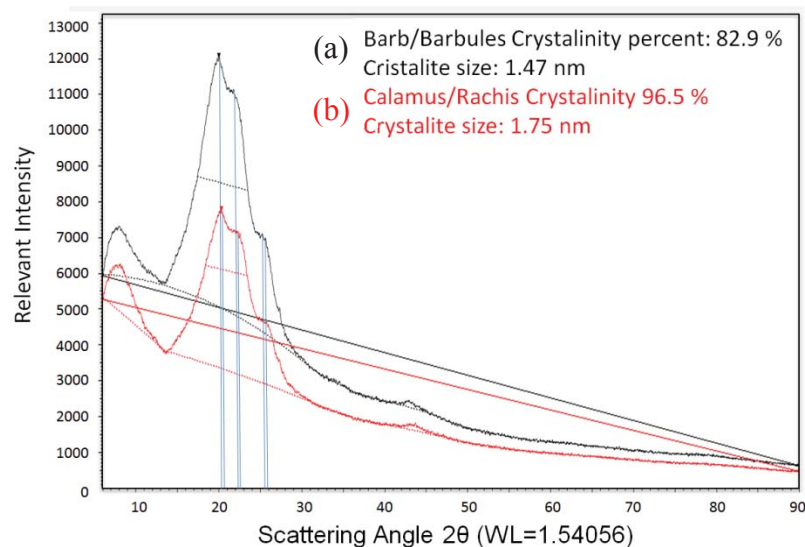


Figure 5.10: Diffraction intensities of a) barbs/barbules and b) calamus/rachis of chicken feathers

5.3.6 Infrared spectroscopy

Infrared spectroscopy investigation was used as an effective chemical bond identification technique to assess structural changes in proteins, resulting from purification of the feathers. FTIR spectroscopy provides information on the secondary structure content of the protein, unlike X-ray crystallography that provides information about its tertiary structure. The FTIR spectra are sensitive to α -helix and β -sheet content in different parts of the feathers including calamus, rachis in the middle and tip and barbs (Figures 5.11 and 5.12) were analysed. The content of β -sheet in CF was the same as α -helix, this may be because the CFF used were composed of equal proportion of quill and feather fibres (FFs) [17-20].

Characteristic bands were found in the infrared spectra of proteins and polypeptides that included amide I and II. The absorption associated with the amide I band led to stretching vibrations of the C=O bond of the amide (C=O stretch (primary amines) from 1630 cm^{-1} to 1695 cm^{-1}), and absorption associated with the amide II band led primarily to bending vibrations of the N-H bond. As both the C=O and the N-H bonds were involved in hydrogen bonding between the different elements of secondary structure, the locations of both the amide I and amide II bands were sensitive to the secondary structure content of keratin. Studies with proteins of known structure have been used to systematically correlate the shape of the amide I band to secondary structure content [21]. The N-H stretches of amines were in the region 3300 cm^{-1} to 3000 cm^{-1} , which were weaker and sharper than those of the alcohol O-H stretches that appeared in the same region. In the region of the primary amines (R-NH_2), there were two bands, the asymmetrical and symmetrical N-H stretch. Secondary amines ($\text{R}_2\text{-NH}$) showed only a single weak band in the 3300 cm^{-1} to 3000 cm^{-1} regions, since they had only one N-H bond. Tertiary amines ($\text{R}_3\text{-N}$) did not show any band in this region since they did not have an N-H bond. However, a shoulder band usually appears on

the lower wavenumber side in primary and secondary liquid amines arising from the overtone of the N–H bending band, which can confuse interpretation.

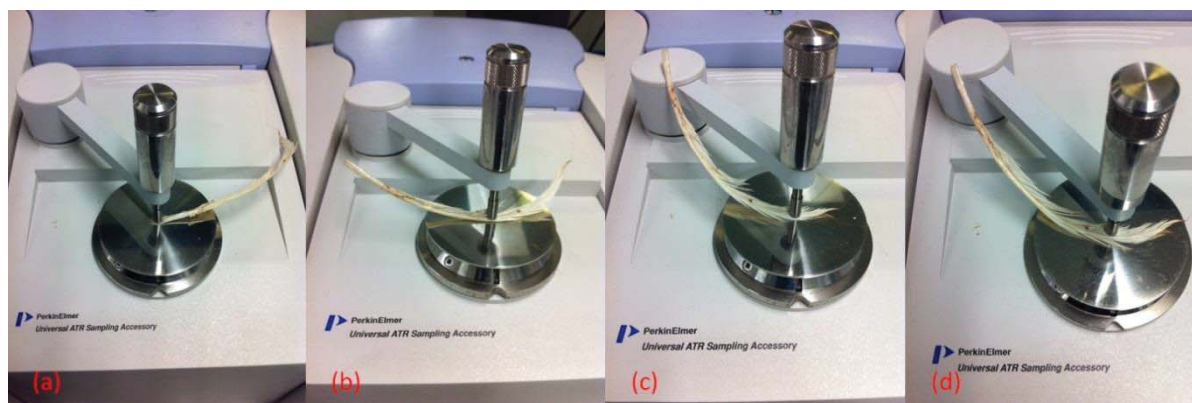


Figure 5.11: FTIR analysis of different parts of a feather:
a) calamus, b) middle of the rachis c) tip of the rachis and d) barb

The N–H bending vibration of primary amines was observed in the region 1650 cm^{-1} to 1580 cm^{-1} . Usually, secondary amines do not show a band in this region and tertiary amines never show a band in this region. This band could be sharp and close enough to the carbonyl region to interpret it as a carbonyl band.

In aromatic amines, the band was usually strong and in the region 1335 cm^{-1} to 1250 cm^{-1} . The C–N stretching vibration of aliphatic amines was observed as medium to weak bands in the region 1250 cm^{-1} to 1020 cm^{-1} . Another strong, broad band attributed to amines was detected in the region 910 cm^{-1} to 665 cm^{-1} , which was due to N–H wag and is observed only for primary and secondary amines. The vibrations in the peptide bonds originate bands known as amide I, II, and III. Overall, the obtained results confirm that there are no significant changes in the chemical structure of different segments of FFs after each purification treatment as discussed in chapter 4.

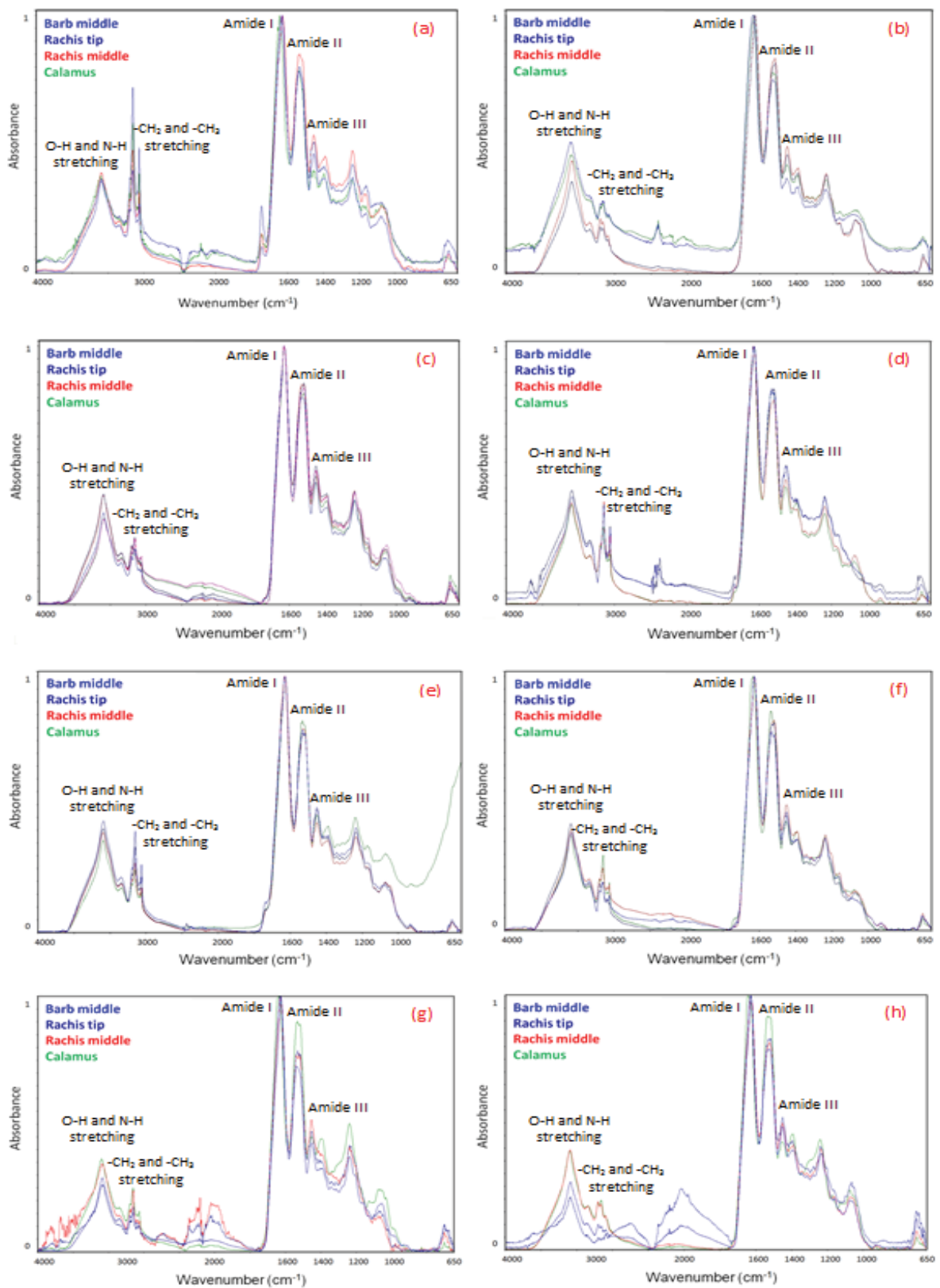


Figure 5.12: FTIR spectra of a chicken feather segments a) (T0) untreated chicken feathers upon receipt, versus chicken feathers purified with b) (T1) SEEt treatment, c) (T5) SLS solution, d) (T4) PEG solution, e) (T2) O₃ solution f) (T3) ClO₂ solution, g) (T6) CTAC solution and h) (T7) SLS-ClO₂-SEEt combination

Comparison of FTIR spectra of an untreated CF and residues from Soxhlet extraction is shown in Figure 5.13. Eslahi et al. [21] reported that the spectra of CFs show characteristic absorption bands assigned mainly to the peptide bonds ($-(C=O)NH$). The broad absorption band region from 3500 cm^{-1} to 3200 cm^{-1} is attributed to the stretching vibration of O–H and N–H bonds. The vibrations in the peptide bonds originate bands known as amide I, II and III. This analysis confirmed the presence of carboxyl acid and amino groups. Overall, the results obtained confirmed that there were no significant changes in the chemical structure of fibres after each treatment. However, the residue from ethanol extraction was characteristic of ester C=O stretching and long chain hydrocarbon (2918 cm^{-1} and 2851 cm^{-1}), typical of a fat.

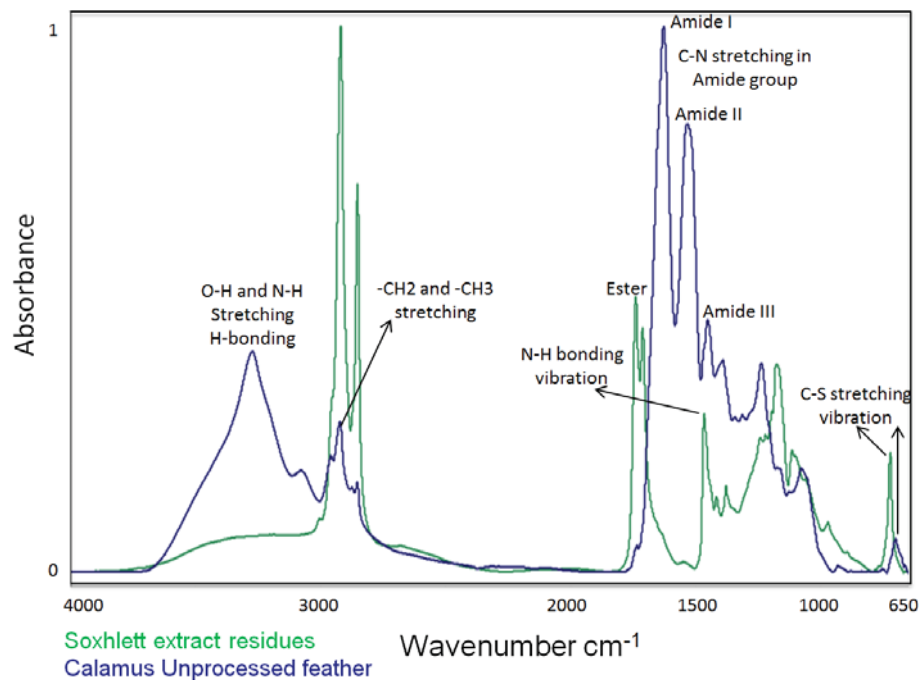


Figure 5.13: Comparison of FTIR spectra of an untreated chicken feather with its Soxhlet extraction residues

To confirm the chemical structure of CFFs, FTIR measurement was used and α -keratin (Figures 5.14(a)), from the middle part of a barb segment, and the β -keratin (Figures 5.14(b)), from the calamus segment, of treatments T0 to T5 are compared, demonstrating their characteristic peaks were similar. The FTIR spectra confirmed the treatment techniques had

minimal effect on the chemical structure of keratin. Whether it was α -keratin or β -keratin, they all showed characteristic transmission bands ascribed predominantly to the peptide bonds ($-\text{CONH}$), labelled as amide I, amide II and amide III [22-24]. The transmission band at 3281 cm^{-1} was attributed to the stretching vibrations of O–H and N–H (amides), the band at 2923 cm^{-1} was attributed to the symmetrical CH_3 stretching vibration [24], while the strong transmission band at 1630 cm^{-1} was related to the C=O stretching (amide I). The amide II with the band at 1521 cm^{-1} was derived from N–H bending and C–H stretching. A weak band at 1233 cm^{-1} was assigned to the amide III, which was due to the combination of C–N stretching and N–H in-plane bending as well as some contribution from C–C stretching and C–O bending vibration [25, 26]. The amide I–III bands give critical information on the protein conformation and backbone structure. According to the literature data, the peaks at 3293 cm^{-1} (amides) indicates α -helix structure, in the range of 1539 cm^{-1} to 1515 cm^{-1} (amide II) was related to the β -sheet structure, the split peaks at 1666 cm^{-1} and 1655 cm^{-1} (amide I) are the combination of α -helix and β -sheets [16, 24, 27]. Overall, no significant changes in the chemical structure of CFFs between the α - and β -keratin were observed with the FTIR analysis.

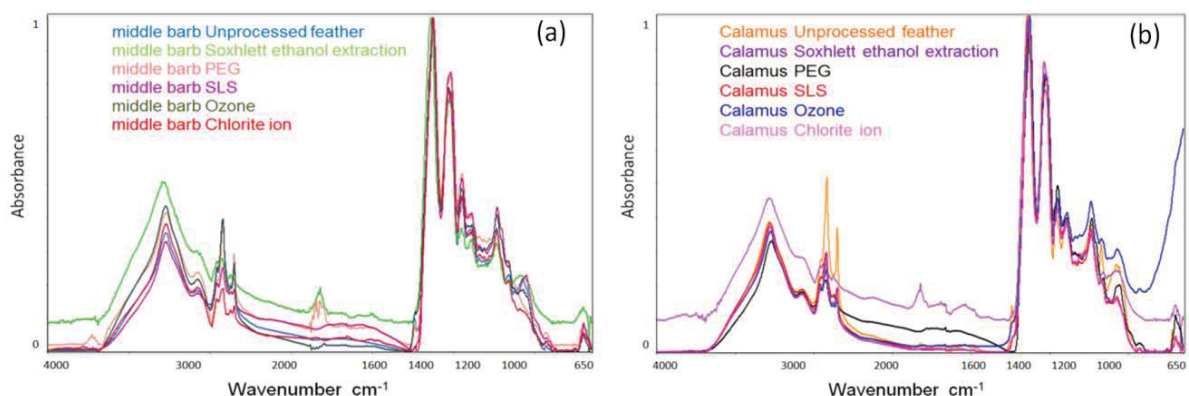


Figure 5.14: Comparison of FTIR spectra of a) α -keratin (barb middle) and b) β -keratin (calamus) of a chicken feather fibres: untreated chicken feathers upon receipt (T0), versus chicken feathers purified with SEEt treatment (T1), O_3 solution (T2), ClO_2 solution (T3), PEG solution (T4) and SLS solution (T5)

Figure 5.15 (a) shows the FTIR spectra of chicken and pigeon FFs, plus sheep wool fibres. As shown in figure 5.15 (b), the spectra of chicken and pigeon FFs are almost identical which suggest that most other types of feathers will be similar and the conclusions arrived at with these specimens should be applicable to other feather types.

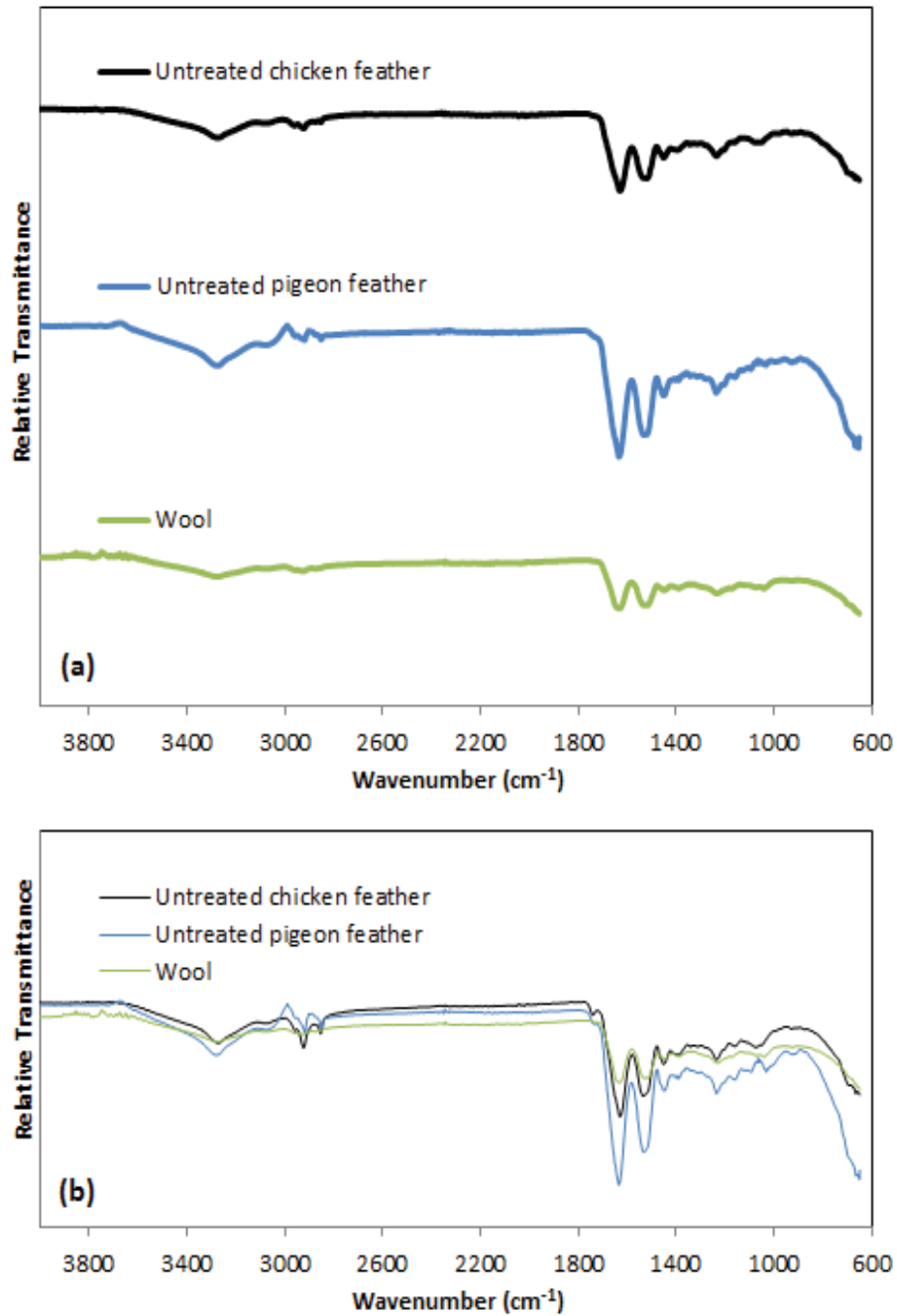


Figure 5.15: Comparison of FTIR spectra of chicken and pigeon feather fibres and sheep wool fibres, a) individually, and b) superimposed

5.3.7 Vibrational spectroscopy

Chemical fingerprinting of nanostructured carbon-containing materials is carried out by Raman spectroscopy [28, 29]. Raman spectroscopy was performed on CFs before and after five purification treatments (T0 to T5). Residues from T1 were additionally characterised similarly. Raman spectra of a single barb and rachis from CFs are shown in Figure 5.16.

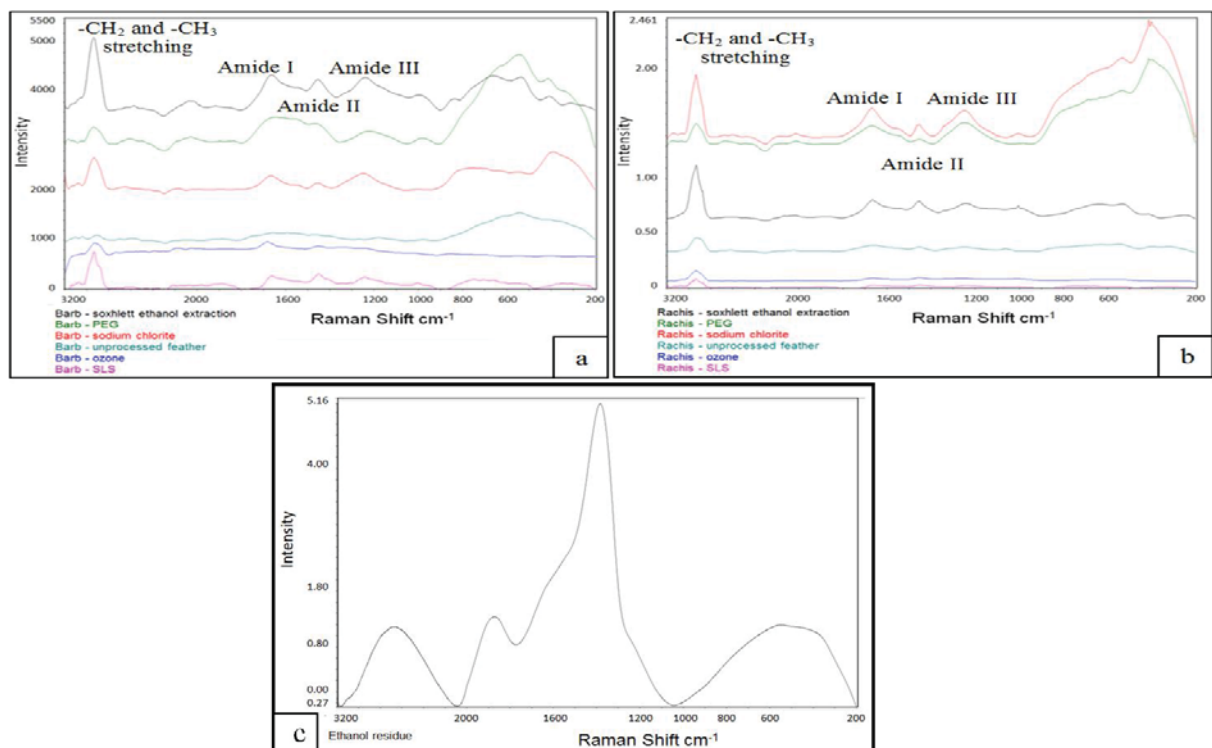


Figure 5.16: Raman spectra of chicken feathers a) barb and b) rachis c) residue from (T1) SEEt treatment

Bands associated with phenylalanine, the S-S band at 400 cm^{-1} and amide III bands appearing between 1200 cm^{-1} and 1400 cm^{-1} are present in the CFs spectra. A sharp Raman peak was identified at 1667 cm^{-1} , which was clearly detectable from the broad background Raman scattering covering the range between 1690 cm^{-1} and 1640 cm^{-1} . This 1667 cm^{-1} Raman band is associated with amide I vibration of the antiparallel-chain pleated sheet, in which all the peptide groups vibrate in-phase ($\nu(\text{O}, \text{O})$, in the following section). However,

the residue from T1 was characterised as a long hydrocarbon chain ester or typical fat (Figure 5.16).

5.3.8 Thermal behaviour

Thermal properties of untreated and treated CFs were investigated by TGA (Figure 5.17). The TGA curves of the CFs as a function of temperature show rapid decomposition in the temperature range between 225 °C and 500 °C. The resulting curves showed similar patterns but a close examination of the derivative diagrams showed that the peak decomposition temperature varied significantly: i.e. T5, T4, and T1 all showed higher decomposition temperatures (373 °C, 365 °C, and 364 °C) whereas T2 and T3 revealed lower decomposition temperatures of 349 °C and 345 °C respectively (Table 5.2). The decomposition temperature was only 363 °C for untreated feathers. According to Khosa et al [30], the increase in thermal stability (i.e. T1, T4 and T5) indicates esterification of the protein. At the completion of the pyrolysis, a total weight loss of ~80 % was observed for all feathers. The absorbed water evaporated below 100 °C for CFs with a more dramatic difference in the case of T2. The T2 and T3 (oxidants) resulted in a low thermal stability.

Table 5.2: Peak decomposition temperature of purified and untreated chicken feathers

Chicken feathers	Peak (°C)
SLS solution (T5)	373
PEG solution (T4)	365
SEEt treatment (T1)	364
Untreated (T0)	363
O ₃ solution (T2)	349
ClO ₂ solution (T3)	345

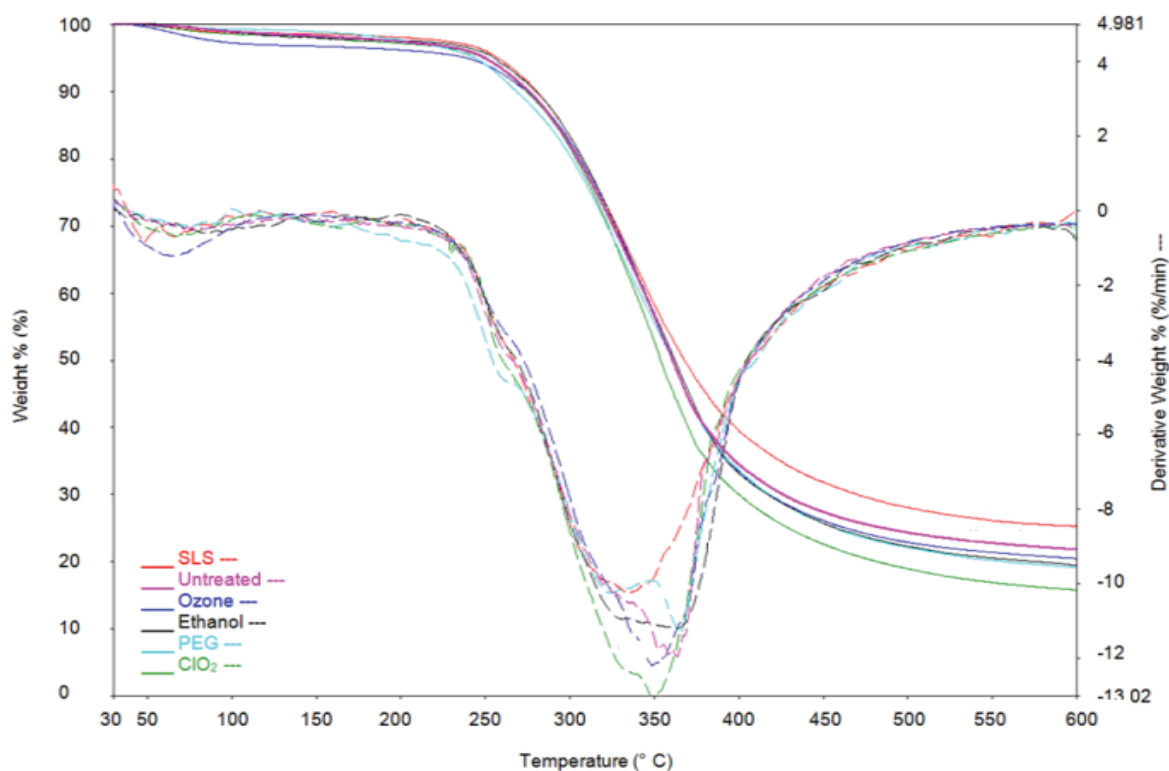


Figure 5.17: Comparison of the thermogravimetry (TG) curves for untreated and treated chicken feathers along with their derivatives (DTG) curves; (T0) untreated chicken feathers upon receipt, (T1) SEEt treatment, (T2) O₃ solution, (T3) ClO₂ solution, (T4) PEG solution, (T5) SLS solution

5.4 Conclusions

Analysis was performed on the untreated and treated CFs. Different feather segments treated with different purification techniques were further characterised. It was observed that T4 and T5 treatments cleaned the feathers without changing their structure. The T1 removed fatty and waxy substances leaving the KF to shrivel along the rachis. The T2 and T3 both bleached the feathers, leaving them with similar texture to those treated with the surfactants.

There was no fibre damage observed in any SEM images. No significant changes in the X-ray diffraction pattern of CFFs were observed, however, the WAXD analysis showed the crystalite size of calamus/rachis (96.5 %) was larger than the crystalite size of barbs/barbules (82.9 %).

Infrared spectra and Raman spectroscopy of the feathers were both unchanged consistent with the small amount of ethanol extract of fatty-waxy material. However, the residue from T1 was characteristic of C=O ester and C-H stretching, typical of a fat.

The TGA results showed rapid decomposition occurring between 225 °C and 500 °C for all feather specimens. A close examination of the derivatives showed that the peak temperature of T2 and T3 resulted in lower temperatures of decomposition whereas T1, T4 and T5 resulted in higher decomposition temperatures in comparison with the T0.

5.5 References

1. Khosa, M. and A. Ullah, *A sustainable role of keratin biopolymer in green chemistry: a review*. J. Food Process. Beverage, 2013. **1**: p. 1-8.
2. Yin, X.-C., F.-Y. Li, Y.-F. He, Y. Wang, and R.-M. Wang, *Study on effective extraction of chicken feather keratins and their films for controlling drug release*. Biomaterials Science, 2013. **1**(5): p. 528-536.
3. Rouse, J.G. and M.E. Van Dyke, *A review of keratin-based biomaterials for biomedical applications*. Materials, 2010. **3**(2): p. 999-1014.
4. Ehrlich, H., *Biological materials of marine origin*. Vol. 4. 2010, Germany: Springer.
5. Forgács, G., *Biogas production from citrus wastes and chicken feather: pretreatment and co-digestion*. PhD Thesis. 2012, Sweden: Chalmers University of Technology.
6. Wang, Y.-X. and X.-J. Cao, *Extracting keratin from chicken feathers by using a hydrophobic ionic liquid*. Process Biochemistry, 2012. **47**(5): p. 896-899.
7. Fan, X., *Value-added products from chicken feather fiber and protein*. PhD Thesis. 2008, Auburn, Alabama: ProQuest, Auburn University.
8. Wool, R. and X.S. Sun, *Bio-based polymers and composites*. 2011, U.S.: Elsevier, Academic Press.
9. Mohanty, A.K., M. Misra, and L.T. Drzal, *Natural Fibers, Biopolymers, and Biocomposites*. 2005: CRC Press.
10. Manual, E.G., *Alternative disinfectants and oxidants*. Disinfectant Use in Water Treatment, Washington, DC, 1999.
11. Held, P., *Quantitation of peptides and amino acids with a Synergy™ HT using UV fluorescence*. B.-T. Instruments, Winooski, VT, 2003.
12. Iwunze, M.O., *The characterization of the fluorescence of l-histidine in simulated body fluid*. Journal of Photochemistry and Photobiology A: Chemistry, 2007. **186**(2): p. 283-289.
13. Zhao, W., R. Yang, Y. Zhang, and L. Wu, *Sustainable and practical utilization of feather keratin by an innovative physicochemical pretreatment: high density steam flash-explosion*. Green Chemistry, 2012. **14**(12): p. 3352-3360.


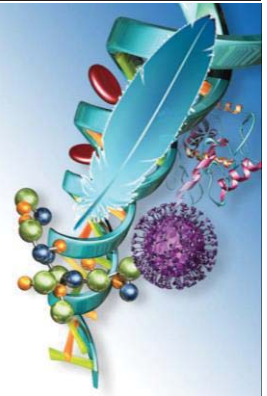
14. Chauhan, D.K., P.L. Patnam, S.K. Ganguly, and S.L. Jain, *A two in one approach: renewable support and enhanced catalysis for sweetening using chicken feather bound cobalt (ii) phthalocyanine under alkali free environment*. RSC Advances, 2016. **6**(57): p. 51983-51988.
15. Aguayo-Villarreal, I.A., A. Bonilla-Petriciolet, V. Hernández-Montoya, M.A. Montes-Morán, and H.E. Reynel-Avila, *Batch and column studies of Zn²⁺ removal from aqueous solution using chicken feathers as sorbents*. Chemical Engineering Journal, 2011. **167**(1): p. 67-76.
16. Martinez-Hernandez, A.L., C. Velasco-Santos, M. De Icaza, and V.M. Castano, *Microstructural characterisation of keratin fibres from chicken feathers*. International journal of environment and pollution, 2005. **23**(2): p. 162-178.
17. Schmidt, W., *Microcrystalline keratin: from feathers to composite products*. MRS Symp. Proceed., Boston, MA, 702: 25, DOI: 10.1557/PROC-702-U1.5.1, 2002. **29**.
18. Reddy, N. and Y. Yang, *Structure and properties of chicken feather barbs as natural protein fibers*. Journal of Polymers and the Environment, 2007. **15**(2): p. 81-87.
19. Winandy, J.E., J.H. Muehl, J.A. Micales, A. Raina, and W. Schmidt, *Potential of chicken feather fiber in wood MDF composites*. Proceedings EcoComp 2003, 2003. **20**: p. 1-6.
20. Ullah, A. and J. Wu, *Feather Fiber-Based Thermoplastics: Effects of Different Plasticizers on Material Properties*. Macromolecular Materials and Engineering, 2013. **298**(2): p. 153-162.
21. Eslahi, N., F. Dadashian, and N.H. Nejad, *An investigation on keratin extraction from wool and feather waste by enzymatic hydrolysis*. Preparative Biochemistry and Biotechnology, 2013. **43**(7): p. 624-648.
22. Yen, K.-C., C.-Y. Chen, J.-Y. Huang, W.-T. Kuo, and F.-H. Lin, *Fabrication of keratin/fibroin membranes by electrospinning for vascular tissue engineering*. Journal of Materials Chemistry B, 2016. **4**(2): p. 237-244.
23. Idris, A., R. Vijayaraghavan, U.A. Rana, A. Patti, and D. MacFarlane, *Dissolution and regeneration of wool keratin in ionic liquids*. Green Chemistry, 2014. **16**(5): p. 2857-2864.
24. Ma, B., X. Qiao, X. Hou, and Y. Yang, *Pure keratin membrane and fibers from chicken feather*. International Journal of Biological Macromolecules, 2016. **89**: p. 614-621.
25. Idris, A., R. Vijayaraghavan, U.A. Rana, D. Fredericks, A. Patti, and D. MacFarlane, *Dissolution of feather keratin in ionic liquids*. Green chemistry, 2013. **15**(2): p. 525-534.
26. Zhang, J., Y. Li, J. Li, Z. Zhao, X. Liu, Z. Li, Y. Han, J. Hu, and A. Chen, *Isolation and characterization of biofunctional keratin particles extracted from wool wastes*. Powder technology, 2013. **246**: p. 356-362.
27. Senoz, E. and R.P. Wool, *Microporous carbon-nitrogen fibers from keratin fibers by pyrolysis*. Journal of applied polymer science, 2010. **118**(3): p. 1752-1765.
28. Thomsen, C. and S. Reich, *Raman scattering in carbon nanotubes*, in *Light Scattering in Solid IX*. 2007, Springer. p. 115-234.
29. Sato-Berrú, R. and J. Saniger, *Application of principal component analysis to discriminate the Raman spectra of functionalized multiwalled carbon nanotubes*. Journal of Raman Spectroscopy, 2006. **37**(11): p. 1302-1306.

30. Khosa, M.A., J. Wu, and A. Ullah, *Chemical modification, characterization, and application of chicken feathers as novel biosorbents*. RSC Advances, 2013. **3**(43): p. 20800-20810.

5.6 Publication from this Chapter

- Pourjavaheri, F., Mohaddes, F., Shanks, R. A., Czajka, M., & Gupta, A. (2014) "Effects of Different Purification Methods on Chicken Feather Keratin" *Advanced Materials Research*, 941-944, 1184-1187. doi: 10.4028.
- Pourjavaheri, F., Jones, O.A.H., Mohaddes, F., Sherkat, F., Kong, I., Gupta, A., & Shanks, R.A. (2017) "Avian Keratin Fiber Based Bio-composites" *World Journal of Engineering* **14**(3) · Doi: 10.1108/WJE-08-2016-0061.
- Pourjavaheri, F., Shanks, R., Czajka, M., & Gupta, A. (2013) "Purification Methods for Chicken Feather Keratin", *International conference on Advanced Polymeric Materials (ICAPM), Kottayam, 11-13 October, Kerala, India*.
- Pourjavaheri, F., Shanks, R., Czajka, M., & Gupta, A. (2014) "Purification and characterisation of feathers prior to keratin extraction", *The 8th International Chemical Engineering Congress & Exhibition (IChEC)*, 24-27 February, Kish, Iran.
- Pourjavaheri, F., Mohaddes, F., Shanks, R., Czajka, M. & Gupta, A. (2014) "Effects of Different Purification Methods on Chicken Feather Keratin", *The 5th International Conference on Manufacturing Science & Engineering (ICMSE)*, 19-20 April, Shanghai, China.
- Pourjavaheri, F., Shanks, R., Close, C. & Gupta, A. (2013) "Preliminary study on chicken feathers prior to Keratin Extraction", *21st Annual RACI Environmental and Analytical Division R&D Topics Conference (RACI R&D)*, 12 December, Canberra, Australia. (Abstract published only)

CHAPTER 6



DESIGN AND CHARACTERISATION
OF SUSTAINABLE BIO-COMPOSITES
FROM CHICKEN FEATHER KERATIN
AND THERMOPLASTIC
POLYETHER–POLYURETHANE

6.1 Introduction

Polymers reinforced with natural fibres, commonly named 'bio-composites', started to be industrially applied not only in the automotive and building sectors but in the broad area of consumer goods. Green composites are a specific class of bio-composites where a bio-based polymer matrix such as a biodegradable polyurethane is reinforced by natural fibres such as keratin feather fibres; both matrix and reinforcement derive from renewable resources [1-3]. Bio-based polymers have been defined to include synthetic or machine-processed organic macromolecules derived from biological resources for plastic and fibre applications [1, 4].

The term bio-polymer polyurethane, or thermoplastic polyether–polyurethane (TPU-polyether) covers a large class of polymers with diverse physical and chemical properties, expected to be suitable for many biomedical or industrial applications [2]. While ether-based polyurethane is an excellent choice for applications involving water [5], the use of TPU-polyether in many other areas is often not practical due to its poor heat resistance and mechanical properties [6, 7]. Development of TPU-polyether with enhanced thermo-mechanical properties can be accomplished via the incorporation of reinforcing materials (the main aim of this study) and would be beneficial to a range of plastic–using industries. Biological material, in the form of feathers, has the potential to fulfil this reinforcing fibre role and has the added benefit of utilising a resource that would otherwise go to landfill or be incinerated. A bio-based TPU polymer (PearlthaneTM ECO) exists and is made up of block copolymers consisting of a sequence of polyol soft segments and hard polyurethane segments.

Keratin in the form of ground CFFs is an interesting candidate for the development of new plastic bio-composites. This has recently become an attractive

area of research due to the unique properties of feathers such as low density ($0.89 \text{ g}\cdot\text{cm}^{-3}$), low toxicity and abrasiveness (and associated machine wear), as well as high: thermal insulation, flame resistance, sustainability, biodegradability and biocompatibility and sheer physical abundance (and thus low cost) [1, 8-10]. There has however, been limited development and characterisation of TPU-polyether bio-composites made with these materials [9].

Feathers have a remarkably complex structure and it is known that incorporating different parts of the feather (e.g. calamus, rachis, barbs and barbules) into a polymer matrix can result in different thermo-mechanical properties of the final composite [11]. However, segregation of each feather segment is time-consuming and expensive. Hence, a mixture consisting of fibres from whole feathers is generally more easily prepared and incorporated into a polymer matrix. Different polymer-feather ratios can be used if needed.

Figure 6.1 shows a CF and the TPU-polyether granules with a schematic representation of their chemical structures together with a TPU-CFF bio-composite. Due to the miscibility and flexibility of TPU-polyether, arising from its intrinsic thermoplastic nature, it is generally assumed that incorporation of CFFs into a TPU-polyether matrix at a suitable level could result in a thermo-mechanically modified substrate [5].

Although the primary structures (chemical composition and sequence) of proteins are relevant for structural and molecular interactions, the secondary (regular local sub-structures on a polypeptide backbone, dependent on hydrogen bonding - primarily α -helices and β -pleated sheets) and tertiary (overall three-dimensional shape of an entire protein molecule) structures are more important for function [12]. Indeed, while the basic structural elements found in natural systems are sometimes relatively weak they can surpass the mechanical

properties of synthetic materials because of their secondary and tertiary structure. For example, keratin's strength comes from its structure rather than its composition [12].

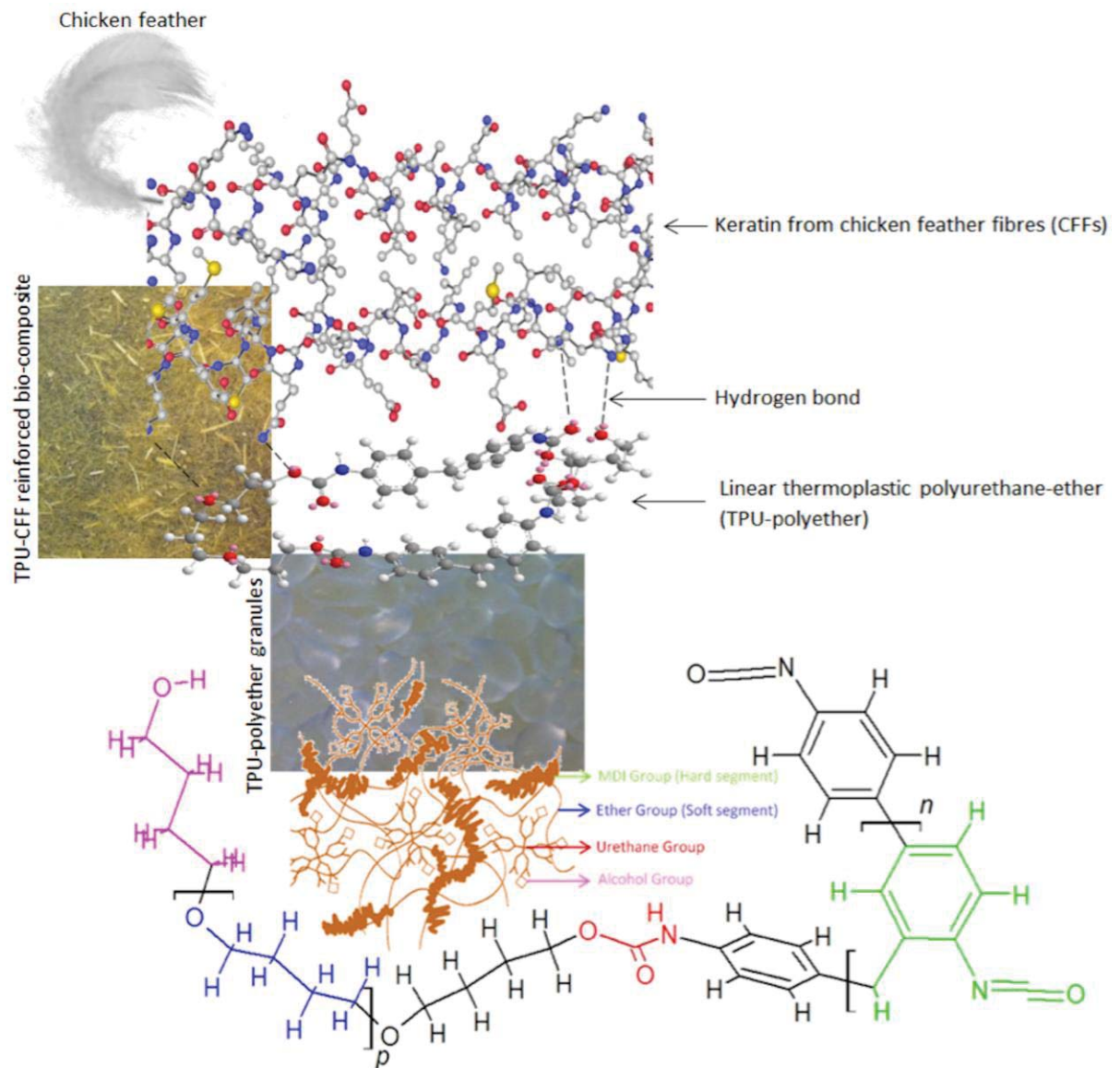


Figure 6.1: Chicken feather keratin, TPU-polyether granules and schematic representation of the chemical structure of TPU-CFF bio-composite (adapted from ref [13])

The properties and performance of thermoplastic polyurethane are determined by several factors such as chemical structures and micro-phase morphologies [14], the latter include the extent of competitive hydrogen bonding between the hard-hard and the hard-soft segments [15]. Therefore, knowing if there is any hydrogen bonding between the keratin and the TPU-

polyether is important.

Common methods to study and predict protein structure are X-ray crystallography, NMR spectroscopy and computational modelling. Computational modelling is convenient as virtually no equipment is required and there are open source on-line servers available to facilitate such experiments [16]. The Iterative Threading ASSEmbly Refinement (I-TASSER) server is one of the most widely used because it gives five different predicted structures and a comprehensive set of scores or parameters that are useful to evaluate its reliability. These parameters include characterisation-score (C-Score), an estimation of prediction accuracy, and template-modelling-score (TM-score) with which the root-mean-square deviation (RMSD) of atomic position values measure the structural similarity between the model and structures in database libraries [17].

The utilisation of eco-friendly, "green", bio-based composites has been reported in many areas including, but not limited to, the packaging, insulation, automotive, building and roofing industries, as well as for separation membranes for water treatment [6, 8, 18, 19]. The application of the produced bio-composites are steps towards more environmentally-friendly, greener and more cost effective products. The outcomes from this research can be used as a model system and/or the basis for research on similar composites based on alternative polymers and biological materials.

6.2 Experimental

6.2.1 Materials

The CFFs (3 - 20 cm long) of freshly slaughtered adult White Leghorn/Australorp (WL x AL) chickens [20] were obtained from Baiada Poultry Pty Ltd (Melbourne, Australia) as the natural fibre reinforcement. The CFFs were ground at 700 rpm for 5 min using an IKA A11

Crushing Analytical Mill (Werke Staufen, Germany) equipped with stainless steel cutting blades and inner tank. There was no active control on fibre length or distribution at, or after, grinding. The lengths of ground feathers were found to be 5 μm to 2 cm with aspect ratios (length/width) of 1:1 to 200:1. Prior to grinding, all CFFs were purified according to the ‘combined purification method’ detailed Chapter 4. Cleaning of CFFs is an important step to ensure the surface is free from blood and/or pathogenic organisms as well as lipids and fatty acids that might otherwise interfere with the bonding and stress transferability between the matrix and the fibre. Failure to implement an effective purification method prior to composite fabrication could adversely affect the structure of the final composites and hence their properties and prospective applications [21]. All the other materials used are detailed in section Table 3.2.

6.2.2 Composites fabrication

Solvent dispersion was performed by dissolving various amounts of TPU-polyether (matrix) in 100 mL of THF (solvent) and adding ground CFFs (reinforcement) to the polymer slurry or dispersion. The amounts of matrix, solvent and CFFs used in each experiment are listed in Table 6.1. All composites were prepared in triplicate by solvent–casting–evaporation under normal laboratory conditions ($20\text{ }^{\circ}\text{C} \pm 2\text{ }^{\circ}\text{C}$ and $60\% \pm 2\%$ relative humidity). Briefly, the polymer slurry was stirred for 24 h at 400 rpm using a magnetic stirrer, cast into a glass petri dish and the solvent allowed to evaporate overnight. The air-dried dishes were then placed in an oven at $70\text{ }^{\circ}\text{C}$ (above the boiling temperature of THF) for 24 h and a vacuum of 25 mm·Hg was applied for a further 24 h. The films were allowed to cool to room temperature gradually and were then removed from the petri dishes.

Table 6.1: Compositions of developed TPU-CFF bio-composites and their respective densities

Composites material ratios	Weight Fraction (%·w/w)		Volume Fraction (%·v/v)		Density (g cm ⁻³)
	Filler CFF	Matrix TPU	Filler CFF	Matrix TPU	
CFF:TPU 0	0	100	0	100	1.14
CFF:TPU 10	10	90	12	88	1.12
CFF:TPU 20	20	80	24	76	1.11
CFF:TPU 30	30	70	35	65	0.99
CFF:TPU 40	40	60	46	54	0.96
CFF:TPU 50	50	50	56	44	0.94
CFF:TPU 60	60	40	66	34	0.93
CFF:TPU 70	70	30	75	25	0.81

The resulting sheets were first cut into quarters, then stacked and placed inside a square metal mould (70 mm x 70 mm x 1 mm), sandwiched between two polytetrafluoroethylene (PTFE) sheets for compression moulding/thermal pressing. Metal plates were placed on above and below the laminate. The composite sheet was heated to 175 °C [22], to enable the composite to flow without degradation, and pressed for 5 min, at 1 t, using an IDM 15 t thermal press as detailed in section 3.3.9. The pressure was increased to 6 t and maintained for 5 min to create flat sheets of material. The composite was then removed from the press and cooled to ambient temperature before being removed from the plate assembly. All composites were left at ambient conditions for one week prior to testing.

6.2.3 Molecular modelling visualisation of the interaction between keratin and TPU-polyether

The aim of using computational modelling in this research was to assess how the secondary and tertiary structure of CFK, interacted with TPU-polyether [16]. The alterations in thermo-mechanical properties associated with such a modified system were evaluated both before and after incorporation of CFFs.

6.2.3.1 Molecule construction

The linear amino acid sequence of CFK [23] was used to construct a molecule using the server for protein structure prediction (I-TASSER) [17, 24]. Out of five possible models only the first model was used since it had superior scores (C-score = -3.51, TM-score = 0.33 \pm 0.11 and RMSD = 11.8 \pm 4.5) and was thus the most likely to be correct. The TPU-polyether polymeric chains were built as a block copolymer of MDI and butane-1,4-diol in a proportion of *ca.* 30 % and 70 % respectively with a molecular weight of approximately 24,768 g/mol. A video of this interaction can be seen in the supplementary on line material.

6.2.3.2 Amorphous cell

The keratin - TPU-polyether - unit cell was created with an amorphous configuration and periodic boundary conditions with Material Studio (Dassault Systèmes, Biovia Corp., San Diego, USA) using one chain of the TPU-polyether and one molecule of keratin. The unit cell had a cubic lattice of 3.87 nm x 3.87 nm x 3.87 nm with a density of 1.00 g/cm³ at 25 °C. This cell represented a TPU-CFF bio-composite with 28.8 % w/w CFF.

6.2.3.3 Molecular interaction

The amorphous cell was visualised and analysed using BIOVIA Discovery Studio Visualiser V16 software (Dassault Systèmes) and all non-intramolecular hydrogen bonds were shown using the standard setup, a distance parameter of 0.340 nm and an angle criterion between 90° and 180°.

6.2.4 Characterisation of bio-composites

6.2.4.1 Morphological analysis and scanning electron microscopy

The overall impact of each reinforcement-matrix ratio on the morphology of fabricated bio-composites was investigated using macro-digital photography. Composites were first fractured after cooling in liquid nitrogen. The fractured specimens were mounted onto aluminium stubs using carbon tape and were coated with a thin layer of gold (*ca.* 20 nm thick) using an SPI Sputter Coater Z11430 as detailed in section 3.3.2. The morphology of the fracture surfaces was then observed by SEM using an FEI Quanta 200 with a 20 kV acceleration voltage (section 3.3.2).

6.2.4.2 Thermal analysis

A Pyris 1 differential scanning calorimeter (section 3.3.7.1) was used to study the thermal properties of the TPU-polyether and TPU-fibre reinforced bio-composites at 10 and 20 % w/w concentrations, between -50 °C and 140 °C. The tests were conducted in triplicate on sample sizes of *ca.* 3 mg (weighed using a Mettler Toledo MX5, section 3.3.7.1) under nitrogen purge (20 mL/min) at identical heating and cooling rates of 5 K·min⁻¹. The accuracy of the peaks was found to be within 0.4 %.

A TGA 7 Thermogravimetric Analyser (section 3.3.7.2) was employed to evaluate thermal degradation, mass loss (and its derivative as a function of temperature), remaining char ratio, and the changes in degradation behaviour associated with CFFs, TPU-polyether and TPU-CFF bio-composites. The mass loss curve was recorded between 30 °C and 750 °C under nitrogen purge (20 mL/min) and between 750 °C and 850 °C under oxygen purge (20 mL/min) at a heating rate of 20 K·min⁻¹. In order to minimise the effect of thermal lag, a small sample mass of *ca.* 4 mg was used in this experiment.

6.2.4.3 Thermo-mechanical analysis

Stress-strain tensile mechanical analysis was performed using a DMA Q800 system from TA Instruments (section 3.3.10.2) with test specimens displaying average dimensions of 25 mm x 7 mm x 1 mm (cut with an xacto knife), at 30 °C (using ramped force from 0.001 to 18 N at 1 N·min⁻¹) to assess the stress-strain behaviour of the TPU-polyether polymer and TPU-CFF bio-composites. In hysteresis analysis (section 3.3.10.3), each specimen was submitted to increasing amounts of stress and allowed to relax at zero load for 5 min before starting each loop and each loop was repeated three times. Reported data are means of at least three tests on different specimens. Measurements such as stress relaxation and cyclic hysteresis are essential in order to have a detailed understanding of the stability of interactions between the elastomer and filler with respect to time [25].

Dynamic mechanical analysis (DMA) was carried out on a Pyris Diamond DMA 2003 (section 3.3.10.4) with test specimens displaying average dimensions of 25 mm x 7 mm x 1 mm (cut with an xacto knife). Test conditions included a specimen gauge length of 10 mm, operated in tension mode at 1 Hz frequency, and a temperature range of -90 °C to 120 °C. Modulated force thermomechanometry (mf-TM) was used to measure the viscoelastic properties with frequency and temperature. Time-temperature superposition was used to determine the extremes of the response time of the composites. The storage modulus (E' – elasticity), loss modulus (E'' – the amount of energy absorbed), loss tangent ($\tan\delta$ - damping related with CFFs) and associated glass transition temperature (T_g – where the films soften), were measured as a function of temperature at a heating rate of 2 K·min⁻¹.

6.2.4.4 Infrared spectroscopy

As detailed in section 3.3.5, FTIR spectroscopy was employed to investigate the possible damage during thermal pressing. For this purpose, the infrared spectra of the composites before and after thermal pressing were collected. The FTIR analysis was later used to verify the interactions between TPU-polyether and CFFs in the bio-composites.

6.3 Results and discussion

6.3.1 Fibre dispersion and physical appearance

The macro-photographic images of the TPU-polyether and TPU-CFF reinforced bio-composites are shown in Figure 6.2. The high transparency of TPU-polyether allows for the ready observation of the spatial distribution of CFFs in the bio-composites. Compression moulding organises and orients the CFFs in the plain of the composite so it is more uniform. The CFFs were equally distributed throughout the entire polymer matrix, and had a uniform colour throughout, without clumping or agglomeration, in all bio-composites but especially in 10 and 20 %·w/w CFF. This implies effective fibre-polymer interactions and compatibility of the TPU-polyether matrix with the CFFs. Both the size and hydrophobic behaviour associated with CFFs played important roles in creating this even dispersion during solvent casting and thermal pressing [8, 26]. In contrast, the 40 %·w/w and above CFF fractions, appeared to be overloaded, exhibiting a saturated appearance. Fibre cumuli were more evident as the reinforcement volume fraction increased (mainly as the fibres were not completely covered by the matrix) to the point that the 70 %·w/w CFF composite had a cardboard like texture (Figure 6.2).

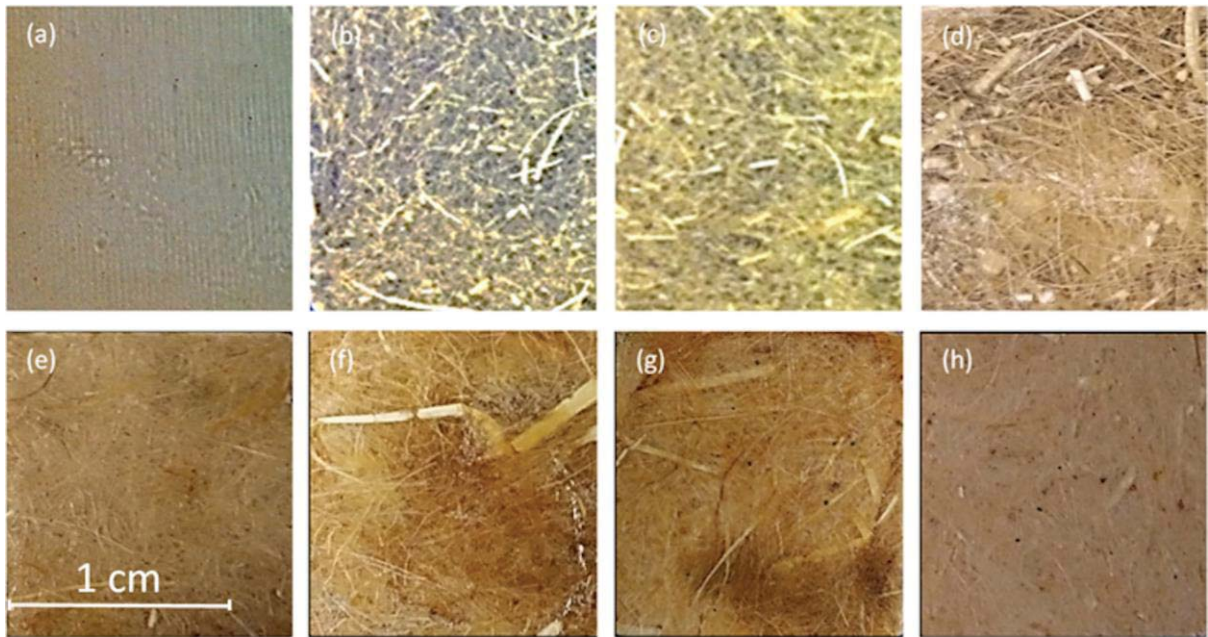
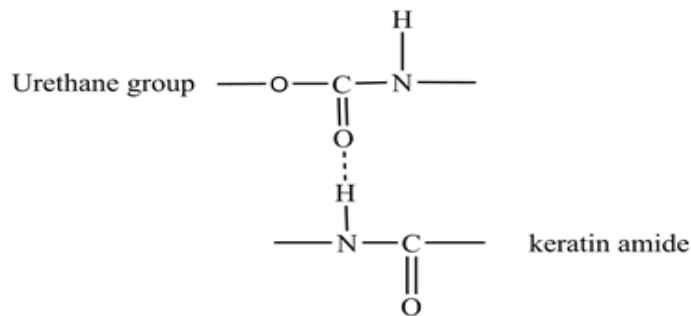


Figure 6.2: Macro photographic images of the TPU-CFF reinforced bio-composites; a) TPU-polyether polymer, b) 10%·w/w CFF, c) 20 %·w/w CFF, d) 30 %·w/w CFF e) 40 %·w/w CFF, f) 50 %·w/w CFF g) 60 %·w/w CFF h) 70 %·w/w CFF;

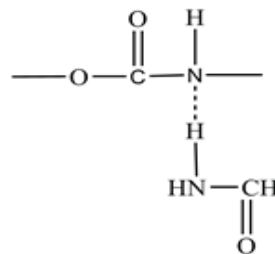
Note: The dark background was chosen to show the transparency of the bio-composites

No compatibiliser or coupling agent was required to improve the stability of the bio-composites since the TPU-polyether has a chemical structure compatible with CFF keratin [27, 28]. They both contain NH–C=O moieties and the urethane groups of the polymer are compatible with amide groups of the feathers via hydrogen bonding (as shown in the computational modelling). Linkages between urethane and amide groups are well known in organic chemistry and have been illustrated in bio-polymers in the literature previously [29]. Segments of the molecules in Figure 6.3 show the compatibility of the TPU-polyether and CFF keratin. Hydrophilic groups on the keratin backbone (e.g. serine, threonine, aspartate) of CFF fibres offer chemically distinct sites for covalently bonding the polymer to the fibre either directly or through a similar type of chemical “bridge” [30]. Covalent bonds are much stronger than induction or van der Waals interactions so a covalently bonded interface is advantageous for strong composites [30].

(1)



(2)



(3)

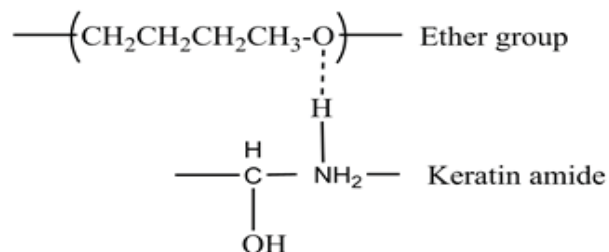


Figure 6.3: Proposed links between the CFF and TPU(polyether)

6.3.2 Molecular visualisation

The generated amorphous cell for the keratin protein surrounded by the TPU-polyether is shown in Figure 6.4(a). The colours of the keratin represent different amino acid residues in the primary structure. The full sequence, along with associated secondary structure(s) can be seen in detail in Table 6.2.

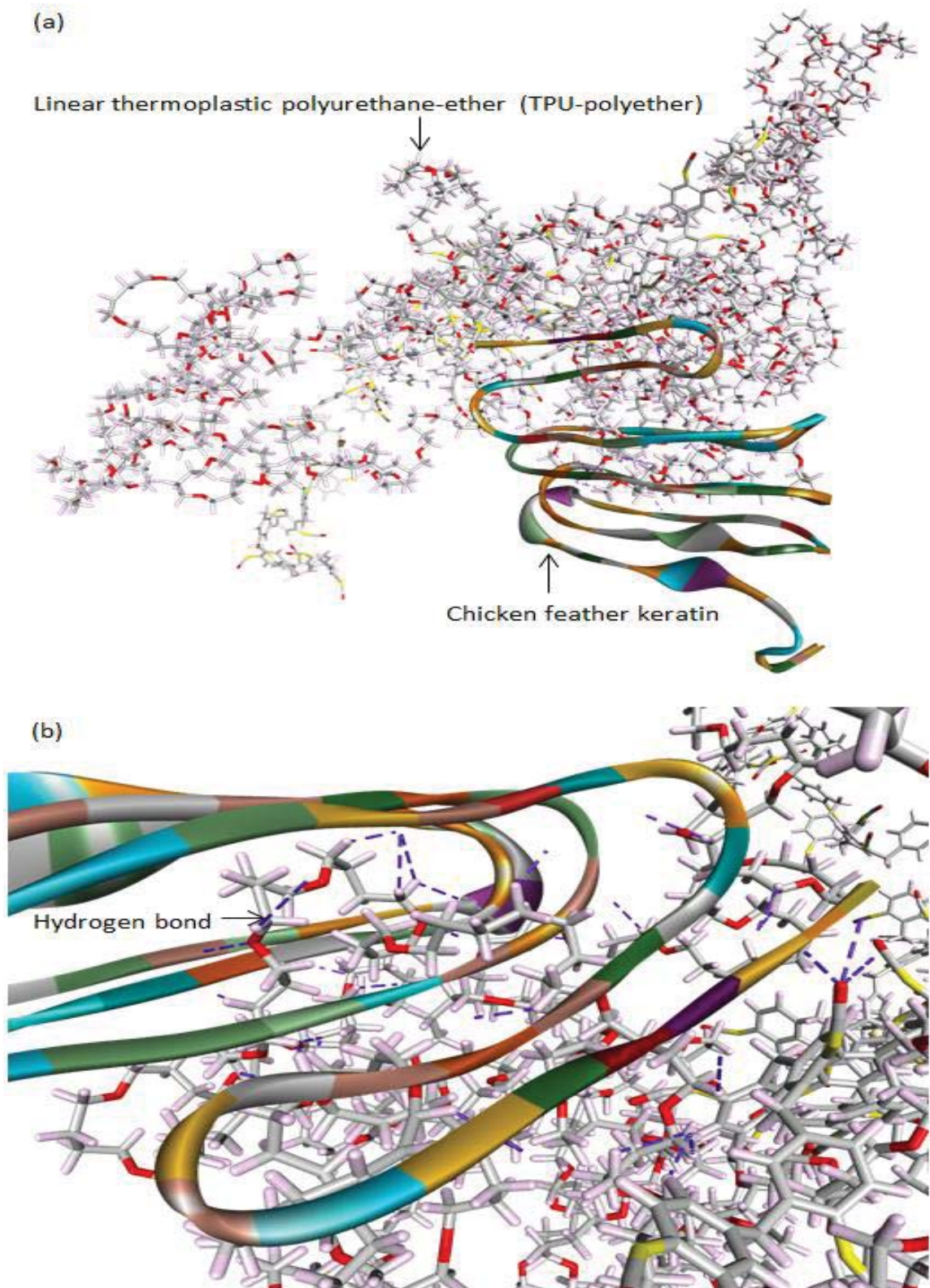


Figure 6.4: One molecule of CFF keratin surrounded by one molecule of TPU-polyether
a) Amorphous cell with periodic boundary conditions of the keratin surrounded by the TPU-polyether;
b) Molecular modelling visualization of the intermolecular hydrogen bonds (purple dashed lines) between TPU-polyether and CFF keratin

Table 6.2: Amino acid sequences with corresponding colour residue and secondary structure

ID	IUPAC amino acid code	Protein Data Bank Abbreviation	Residue	Color	Secondary Structure	ID	IUPAC amino acid code	Protein Data Bank Abbreviation	Residue	Color	Secondary Structure
1	M	Met	Methionine	Yellow-Green	Coil	50	S	Ser	Serine	Orange	Coil
2	S	Ser	Serine	Orange	Coil	51	F	Phe	Phenylalanine	Purple	Coil
3	C	Cys	Cysteine	Yellow	Coil	52	P	Pro	Proline	Brown	Coil
4	Y	Tyr	Tyrosine	Purple	Coil	53	Q	Gln	Glutamine	Light Blue	Coil
5	D	Asp	Aspartic Acid	Dark Red	Coil	54	N	Asn	Asparagine	Dark Red	Coil
6	L	Leu	Leucine	Green	Coil	55	T	Thr	Threonine	Orange	Coil
7	C	Cys	Cysteine	Yellow	Coil	56	A	Ala	Alanine	Grey	Coil
8	R	Arg	Arginine	Light Blue	Coil	57	V	Val	Valine	Green	Coil
9	P	Pro	Proline	Brown	Coil	58	G	Gly	Glycine	White	Coil
10	C	Cys	Cysteine	Yellow	Coil	59	S	Ser	Serine	Orange	Coil
11	G	Gly	Glycine	White	Coil	60	S	Ser	Serine	Orange	Coil
12	P	Pro	Proline	Brown	Coil	61	T	Thr	Threonine	Orange	Coil
13	T	Thr	Threonine	Orange	Coil	62	S	Ser	Serine	Orange	Coil
14	P	Pro	Proline	Brown	Coil	63	A	Ala	Alanine	Grey	Coil
15	L	Leu	Leucine	Green	Coil	64	A	Ala	Alanine	Grey	Sheet
16	A	Ala	Alanine	Grey	Coil	65	V	Val	Valine	Green	Sheet
17	N	Asn	Asparagine	Dark Red	Coil	66	G	Gly	Glycine	White	Coil
18	S	Ser	Serine	Orange	Coil	67	S	Ser	Serine	Orange	Coil
19	C	Cys	Cysteine	Yellow	Coil	68	I	Ile	Isoleucine	Green	Turn
20	N	Asn	Asparagine	Dark Red	Coil	69	L	Leu	Leucine	Green	Turn
21	E	Glu	Glutamic Acid	Red	Coil	70	S	Ser	Serine	Orange	Coil
22	P	Pro	Proline	Brown	Coil	71	Q	Gln	Glutamine	Light Blue	Coil
23	C	Cys	Cysteine	Yellow	Coil	72	E	Glu	Glutamic Acid	Red	Coil
24	V	Val	Valine	Green	Coil	73	G	Gly	Glycine	White	Coil
25	R	Arg	Arginine	Light Blue	Coil	74	V	Val	Valine	Green	Coil
26	Q	Gln	Glutamine	Light Blue	Coil	75	P	Pro	Proline	Brown	Coil
27	C	Cys	Cysteine	Yellow	Coil	76	I	Ile	Isoleucine	Green	Coil
28	Q	Gln	Glutamine	Light Blue	Turn	77	S	Ser	Serine	Orange	Coil
29	D	Asp	Aspartic Acid	Dark Red	Turn	78	C	Cys	Cysteine	Yellow	Coil
30	S	Ser	Serine	Orange	Coil	79	G	Gly	Glycine	White	Coil
31	R	Arg	Arginine	Light Blue	Coil	80	G	Gly	Glycine	White	Helix
32	V	Val	Valine	Green	Coil	81	F	Phe	Phenylalanine	Purple	Helix
33	V	Val	Valine	Green	Coil	82	G	Gly	Glycine	White	Helix
34	I	Ile	Isoleucine	Green	Coil	83	I	Ile	Isoleucine	Green	Turn
35	Q	Gln	Glutamine	Light Blue	Coil	84	S	Ser	Serine	Orange	Coil
36	P	Pro	Proline	Brown	Coil	85	G	Gly	Glycine	White	Coil
37	S	Ser	Serine	Orange	Coil	86	L	Leu	Leucine	Green	Coil
38	P	Pro	Proline	Brown	Coil	87	G	Gly	Glycine	White	Coil
39	V	Val	Valine	Green	Coil	88	S	Ser	Serine	Orange	Sheet
40	V	Val	Valine	Green	Coil	89	R	Arg	Arginine	Light Blue	Sheet
41	V	Val	Valine	Green	Coil	90	F	Phe	Phenylalanine	Purple	Coil
42	T	Thr	Threonine	Orange	Coil	91	S	Ser	Serine	Orange	Coil
43	L	Leu	Leucine	Green	Coil	92	G	Gly	Glycine	White	Coil
44	P	Pro	Proline	Brown	Coil	93	R	Arg	Arginine	Light Blue	Turn
45	G	Gly	Glycine	White	Coil	94	R	Arg	Arginine	Light Blue	Turn
46	P	Pro	Proline	Brown	Coil	95	C	Cys	Cysteine	Yellow	Coil
47	I	Ile	Isoleucine	Green	Coil	96	L	Leu	Leucine	Green	Coil
48	L	Leu	Leucine	Green	Coil	97	P	Pro	Proline	Brown	Coil
49	S	Ser	Serine	Orange	Coil	98	C	Cys	Cysteine	Yellow	Coil

The interactions between keratin and polyurethane are shown in Figure 6.4(b). The various intermolecular hydrogen bond interactions between the keratin and the TPU-polyether indicate that not only physical, but additional chemical interactions exist between

the feather keratin and the polymer. It appears that more intermolecular interactions between the keratin and the TPU-polyether could potentially exist but these are limited due to the large number of existing intramolecular interactions within the keratin molecule that create its complex structure. The molecular modelling found that most of the hydrogen bonds in the keratin are intramolecular. Since most of the secondary structure is helical, it can form a tertiary structure with hydrogen bonding both inside and outside without steric hindrance. The size of the keratin molecule was estimated to be *ca.* 3.3 nm.

6.3.3 Scanning electron microscopy

The SEM image of a selected fracture cross-section of a 20 %·w/w CFF bio-composite is shown in Figure 6.5.

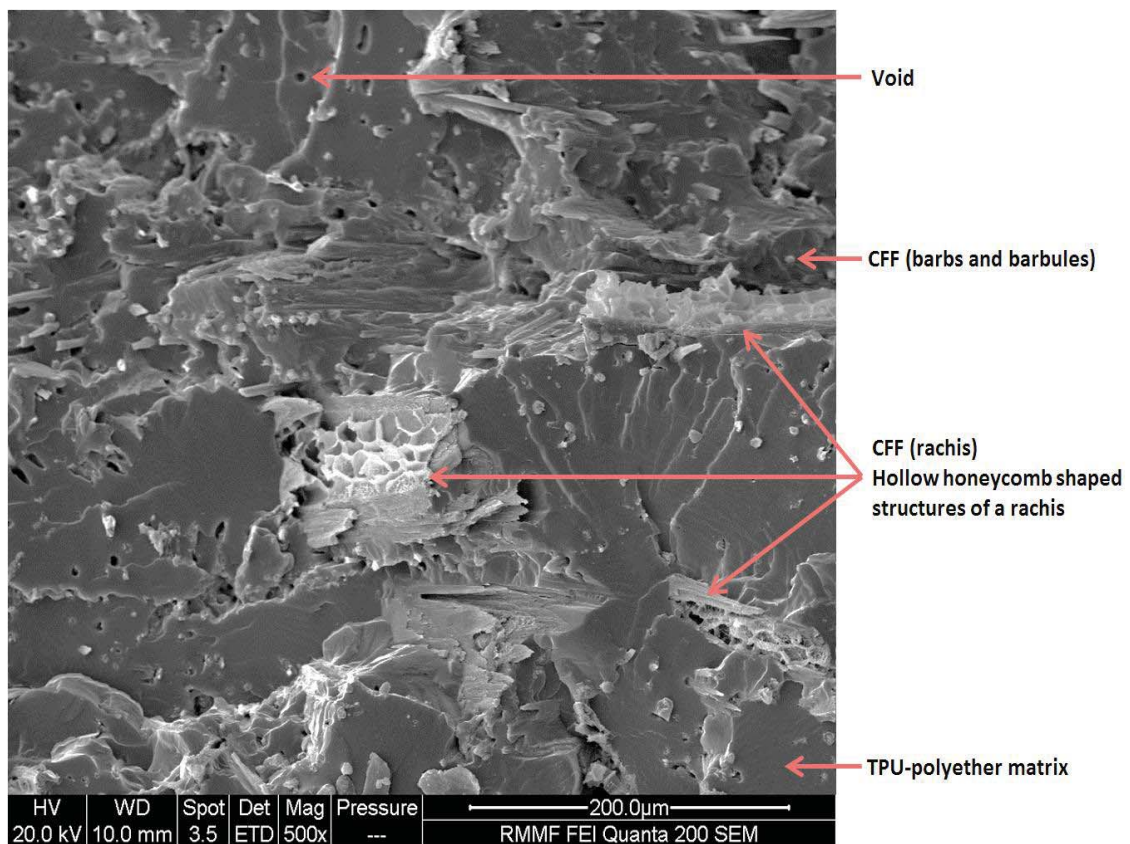


Figure 6.5: The SEM micrographs showing cross-sections of a 20 %·w/w CFF reinforced bio-composite at 500X magnifications

This demonstrates the morphology of the fracture surface of the CFFs and their interaction with the TPU-polyether polymer. It can again be observed that the CFFs were uniformly dispersed throughout the matrix. No continuous fractures or cracks were observed across the TPU-polyether polymer and TPU-CFF bio-composites, even at the interface of the matrix and the fibre. A small number of voids were seen on the fracture surface (Figure 6.5), where the CFFs were trapped but not held by the polymer matrix.

The SEM micrographs revealed that many fibres were fractured at the surface of the TPU matrix when the composite was freeze-fractured, instead of being pulled from the matrix. In addition, the bio-composites were cut, scraped and contorted under non-ambient conditions (since it is not possible to fracture them under ambient conditions as they would stretch), and checked for fibre 'pull-out' (which was not observed). Similar results were obtained for all the cryogenically fractured composites. This demonstrated that CFF had effective adhesion to the TPU-polyether matrix [8]. Effective adhesion means there will be stress transfer from matrix to fibre and the fibres will resist force until they break rather than be pulled out of the matrix. The fibres act as bridges within the polymer and prolong the fracture process of the TPU-CFF reinforced bio-composites [31]. Thus the failure rate of the composite can be mitigated by the bridging effect of CFFs inside [31]. Such bridging effects can prevent crack propagation and enable effective stress transfer between the matrix and the fibres, leading to better overall mechanical and tensile properties of the composite [31].

6.3.4 Thermal behaviour

6.3.4.1 Differential scanning calorimetry

The phase behaviour of both the TPU-polyether and TPU-CFF bio-composites only at 10 and 20 %·w/w concentrations was studied by DSC and the results are shown in Figure 6.6.

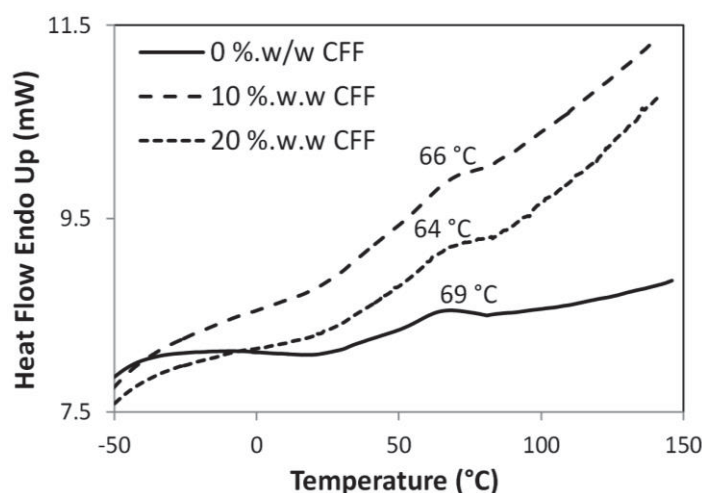


Figure 6.6: The DSC of CFFs, TPU-polyether and TPU-CFF bio-composites at 10 and 20 % w/w concentrations

The pure TPU-polyether was found to have thermal behaviour similar to the TPU-CFF bio-composites and showed only a small peak at 69 °C, which can be due to the disordering of crystallites with relatively short-range order [32]. The presence of the fibres affected the state of crystallinity in the matrix by showing the peaks moved towards lower temperatures (i.e. about 66 °C and 64 °C for 10 and 20 % w/w CFF, respectively). These peaks were almost insignificant since polyurethane is mostly amorphous and the peaks could be due to a small amount of crystallinity in the polyether groups. This could be due to the various reactions that keratin undergoes upon heating as a response to the thermal behaviour of the amino acids of which it is composed [8]. The peaks are unlikely to be caused by residual THF because all composites were heated to 70 °C, which is above the THF boiling temperature (between 65 °C and 67 °C), and held under vacuum for 24 h. These peaks could be due to the possible additives or impurities in the TPU-polyether matrix.

6.3.4.2 Thermogravimetry

The thermogravimetry of the pure CFFs, TPU-polyether and TPU-CFF bio-composites are presented in Figure 6.7 and Table 6.3.

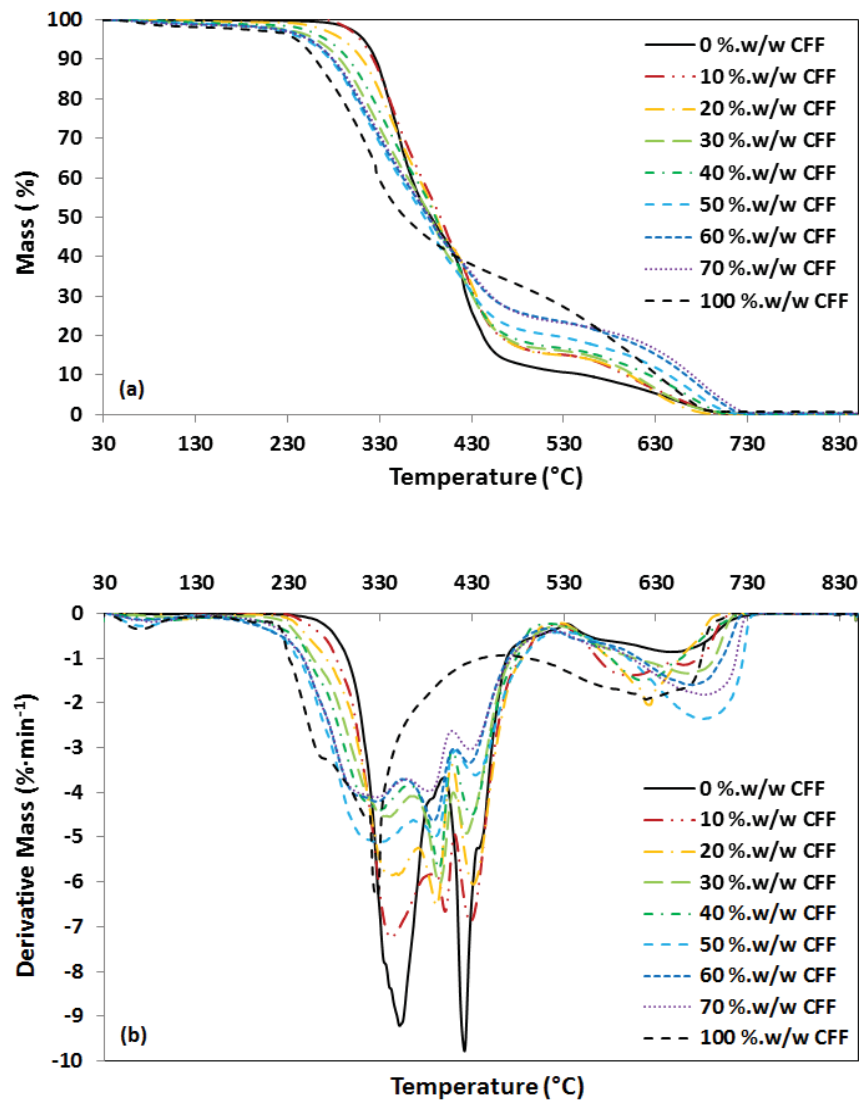


Figure 6.7: Panel a) TGA thermograms (mass loss), and b) derivative mass of CFFs, TPU-polyether polymer and TPU-CFF bio-composites at 10 to 70 %·w/w CFF concentrations

The thermal behaviour observed for these composites can be described in three main steps (Figure 6.7a). The first is a minor mass loss of approximately 4 % over the range of ~30 °C to ~230 °C. This loss is likely due to the loss of water bound up in the matrix released after denaturation of the helix structure of the keratin, as well as losses from thermal pyrolysis of the protein chain linkages and peptide bridges [33, 34]. This behaviour was explained by the presence of a high oxygen content and the dehydration reaction [6]. Herrera *et al.* [35], reported that carbon was observed during this phase of degradation, demonstrating

the scission of urethane bonds. Premature degradation in bio-composites was influenced by the presence of urea, which indicates that keratin was bonded to polyurethane segments and promoted the early degradation seen at this stage [35]. Although the TPU-CFF bio-composites started their mass loss at lower temperatures than the TPU-polyether polymer, they needed higher temperatures to fully decompose.

Table 6.3: Thermal data of CFFs, TPU-polyether and TPU-CFF bio-composites at 10 to 70 %·w/w concentrations obtained by TGA

TPU-CFF Composites	Temp. at 5 % Mass Loss (°C)	Mass Loss (%) at 300 °C	Mass Loss (%) at 600 °C	Char Levels (%) at 500 °C
TPU-polyether	313	2.6	92.6	11.9
CFF 10 %·w/w	309	3.0	90.3	15.9
CFF 20 %·w/w	290	7.0	89.8	15.8
CFF 30 %·w/w	272	11.3	89.2	16.9
CFF 40 %·w/w	260	14.5	87.6	17.8
CFF 50 %·w/w	254	17.7	85.0	20.7
CFF 60 %·w/w	249	18.4	81.4	24.9
CFF 70 %·w/w	254	18.7	80.4	24.5
Pure CFFs	240	25.0	84.1	30.9

The second mass loss step was much larger, around 90 %, and occurs from ~230 °C to ~500 °C. It is likely related to decomposition of the hard segments of the TPU-polyether (Figure 6.1) [13]. In the TPU-CFF bio-composites, this large mass loss was likely to be the result of several complex processes that include dehydration of the protein structures together with depolymerisation and decomposition of urethane and polyether and of amino acid derived structures [8, 36-38]. This stage is associated with the destruction of disulfide bonds and the elimination of H₂S originating from the amino acid cysteine, which is a major keratin component [33, 34]. Moreover, this step involves vaporisation of several components of the polyurethane [13, 39], resulting in the formation of isocyanate, alcohols, primary or secondary amines, olefins, and more carbon dioxide than the previous stage [13, 35, 40]. The

initial degradation of this stage was additionally affected by the presence of keratin [6]. The 10 to 40 %·w/w CFF bio-composites showed a slight synergistic effect at ~350 °C to ~400 °C.

The third mass loss step occurred from *ca.* 500 °C to 850 °C with the greatest mass loss corresponding to decomposition of the soft segments of the- TPU-polyether (Figure 6.1) [13] and complete degradation of the polymer [8, 36-38]. In this stage, isocyanates are dimerized to carbodiimides, which react with alcohol groups to form stable substituted ureas [13, 41]. All the reinforced bio-composites benefited from the presence of keratin bio-fibres here, since, at 600 °C, the highest mass loss was for the TPU-polyether polymer matrix (92.6 % at 600 °C). Among all materials, the pure CFFs had the highest mass loss (25.0 % at 300 °C) up to ~400 °C and the highest char level between ~400 °C to 560 °C (30.9 % at 500 °C). At temperatures >~560 °C however, the bio-composites showed better fire resistance by demonstrating more char than the TPU-polyether and pure CFFs. The TPU-polyether had the highest mass loss at 600 °C (92.6 %), even though it started to degrade at a higher temperature than the other composites and had the lowest mass loss at 300 °C (2.6 %).

Addition of CFFs to the matrix increased the remaining char level of the bio-composites (compared with TPU-polyether) only at temperatures above 400 °C. This effect is related to the inherent variations of natural materials and follows the progression of fibre fractions shown [8]. Both reinforced bio-composites showed better stability than those shown by the TPU-polyether matrix between 430 °C and 630 °C; likely due to the miscibility between CF keratin fibres and polymer matrix [9].

In the derivative mass curves, TPU-polyether exhibited two shows two mass loss regions at 350 °C and 420 °C, and a shoulder about 655 °C, potentially urethane and polyether portions of TPU. The sharper peak at 420 °C demonstrates less material, i.e. less polyether

contained, compared with urethane that has wider peak. Pure CFFs showed one peak at 324 °C, which is a broader mass loss temperature range due to the complex chemistries of the amino acids constituents; and a shoulder about 630 °C as shown in Figure 6.7(b). Similar trends were observed for bio-composites, which showed three peaks, one for keratin, one for urethane and one for polyether. The thermal stability of TPU-polyether was dependent on several factors, including hard segment volume, chain extender amount/type, and the diisocyanate group [13], [42]. The addition of fillers could further influence the thermal properties of the composites by restricting molecular vibrations and rotations that occur when thermally excited [43], increasing thermal stability. The enhanced thermal behaviour correlates with results obtained by Saucedo *et al.* [6], who prepared polyurethane membranes with CFK. Moreover, the TGA results validated the different thermal behaviour due to the grafting of two polymers, the synthetic polyurethane and keratin [6].

6.3.5 Mechanical properties

6.3.5.1 Stress–strain tensile mechanical analysis

Tensile mechanical analysis was used to characterise and compare the mechanical performance of the TPU-polyether and TPU-CFF bio-composites as summarised in Table 6.4. The slopes of the stress-strain curves represented the stiffness of the composites; therefore the addition of CFFs to TPU-polyether increased the stiffness of the polymer as shown in Figure 6.8(a). The maximal strength values at 18 N resulted from TPU-polyether (2.1 MPa at 11.6 % strain) and 20 %·w/w (2.0 MPa at 1.3 % strain); and the minimum (1.6 MPa at 0.5 % strain) resulted from 70 %·w/w bio-composite. The addition of CFFs to the polymer not only made the TPU-polyether stiffer but reduced the deformation of the bio-composites as well.

Table 6.4: Mechanical test properties of TPU-polyether and TPU-CFF bio-composites at various CFF concentrations

Composites	Strain at maximum force (%)	Minimum strain (%)	Recovery strain (%)	Relative recovery strain (%)	Storage Modulus (E') (GPa) at -90 °C	Storage Modulus (E') (GPa) at 25 °C	Loss modulus (E'') Peak T_g (°C)	Loss Tangent (Tan δ) Peak T_g (°C)
TPU-polyether	11.6	2.9	8.7	75	5.4	0.1	-52	-38
CFF 10 %·w/w	1.5	0.2	1.3	86	10.2	1.0	-55	-45
CFF 20 %·w/w	1.3	0.3	0.9	69	11.9	1.6	-54	-47
CFF 30 %·w/w	1.8	1.4	0.4	22	3.5	1.1	-53	-40
CFF 40 %·w/w	2.5	1.9	0.5	20	3.4	0.8	-58	-47
CFF 50 %·w/w	2.5	1.0	1.4	56	2.8	0.6	-55	-43
CFF 60 %·w/w	1.2	0.6	0.5	42	2.7	0.2	-56	-45
CFF 70 %·w/w	0.6	0.2	0.3	50	0.7	0.1	-61	-50

As per the ASTM E 111-97 standard [44], the elastic modulus (E) taken from the initial slope of the stress–strain curve (0.25 % strain), showed a minimum with pure CFF (0.2 MPa) and TPU-polyether (0.3 MPa); and a maximum at 20 %·w/w CFF bio-composite (2.0 MPa) (Figure 6.8b). The flexibility of the bio-fibres allowed for transfer of stress [9], with a decrease at higher volume fractions being due to inefficient wetting of CFF by TPU-polyether.

The hysteresis loops, which represent the reversible performance of the materials, were formed as stress was progressively increased and then decreased, showed the elastic-plastic behaviour of the TPU-polyether and TPU-CFF bio-composites [45]. The maximal strain value for the TPU-polyether was 11.6 % (at 2 MPa stress).

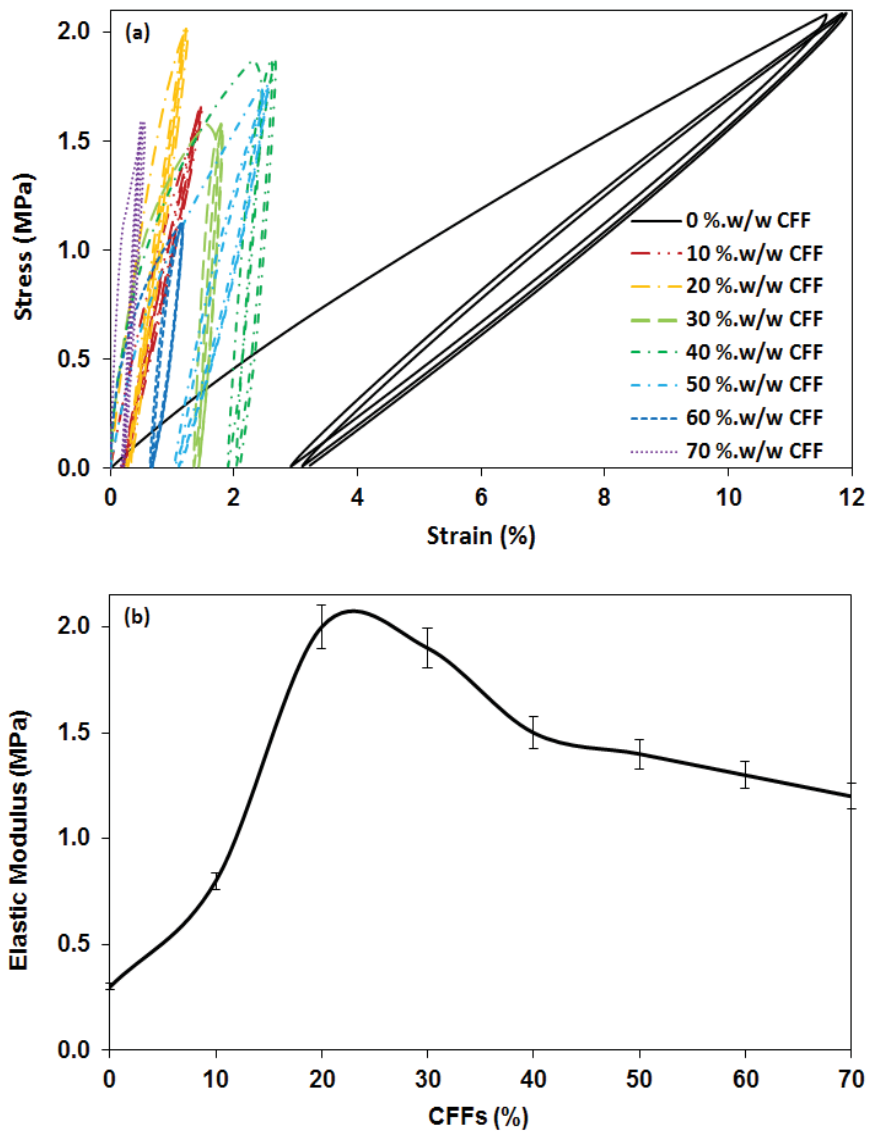


Figure 6.8: Stress-strain tensile mechanical analysis of pure TPU-polyether and TPU-CFF bio-composites at 10 to 70 %·w/w concentrations, (a) Stress-strain hysteresis, (b) Elastic modulus (E)

The incorporation of CFF diminished composite elongation, with strain values decreased to 1.3 % at 20 %·w/w CFF but then increased to 2.5 % at 40 and 50 %·w/w CFF, following by a decrease to 0.6 % at 70 %·w/w CFF (Table 6.4). The change in the strain on recovery (max strain – final strain) was compared between the hysteresis loops [46]. There was a decrease in the recovery strain, or deformation, as the CFFs were added up to 30 %·w/w CFF (0.4 %), then increased to 1.4 % for 50 %·w/w CFF and reduced again with the optimum decrease being at 70 %·w/w CFF (0.3 %). This value showed that the 70 %·w/w CFF bio-

composite was more consistent and uniform with the least amount of deformation on recovery after stress than other bio-composites. Conversely, pure TPU-polyether had the highest deformation rate of all (8.7 %) since CFFs are not as elastic as the TPU-polyether. The 10 %·w/w CFF showed the greatest relative recovery strain (86 %) but all the other bio-composites showed a decrease compared with TPU-polyether. The greatest decreases were at 30 %·w/w CFF (22 %) and 40 %·w/w CFF (20 %). Overall, there was only a slight difference between the second and third stress hysteresis loops for all composites. Slight deformation upon straining showed equal properties upon dynamic cycling.

6.3.5.2 Modulated force – thermomechanometry

The viscoelastic behaviour of the TPU-CFF reinforced bio-composites was studied using DMA, obtaining a storage modulus (E') - which represents solid-like, elastically - stored energy, loss modulus (E'') related to the liquid-like viscous flow, characteristic and loss tangent ($\tan\delta$) that denotes damping (Figure 6.9a-c). The results confirmed that maximum E' was at 20 %·w/w CFFs (Table 6.4) due to adhesion of CFFs by TPU-polyether matrix. The E' difference was greatest at -90 °C with the value increasing at both the 10 and 20 %·w/w CFF levels. The E' value of the reinforced composites decreased constantly until it plateaued, possibly due to the presence of the keratin that promoted intermolecular interactions that strongly reinforced the matrix and hence yielded good thermo-mechanical characteristics [8]. The E' of the TPU-CFF bio-composites was most relevant at ambient temperature (*ca.* 25 °C). At this temperature, the E' of TPU-polyether was 0.1 GPa, optimum for 20 %·w/w CFF (1.6 GPa) and decreased as fibre fractions increased. There was no change in the E' value from 0 °C to 120 °C for the TPU-polyether, but a slight decrease was observed for TPU-CFF bio-composites shown in Figure 6.9(a).

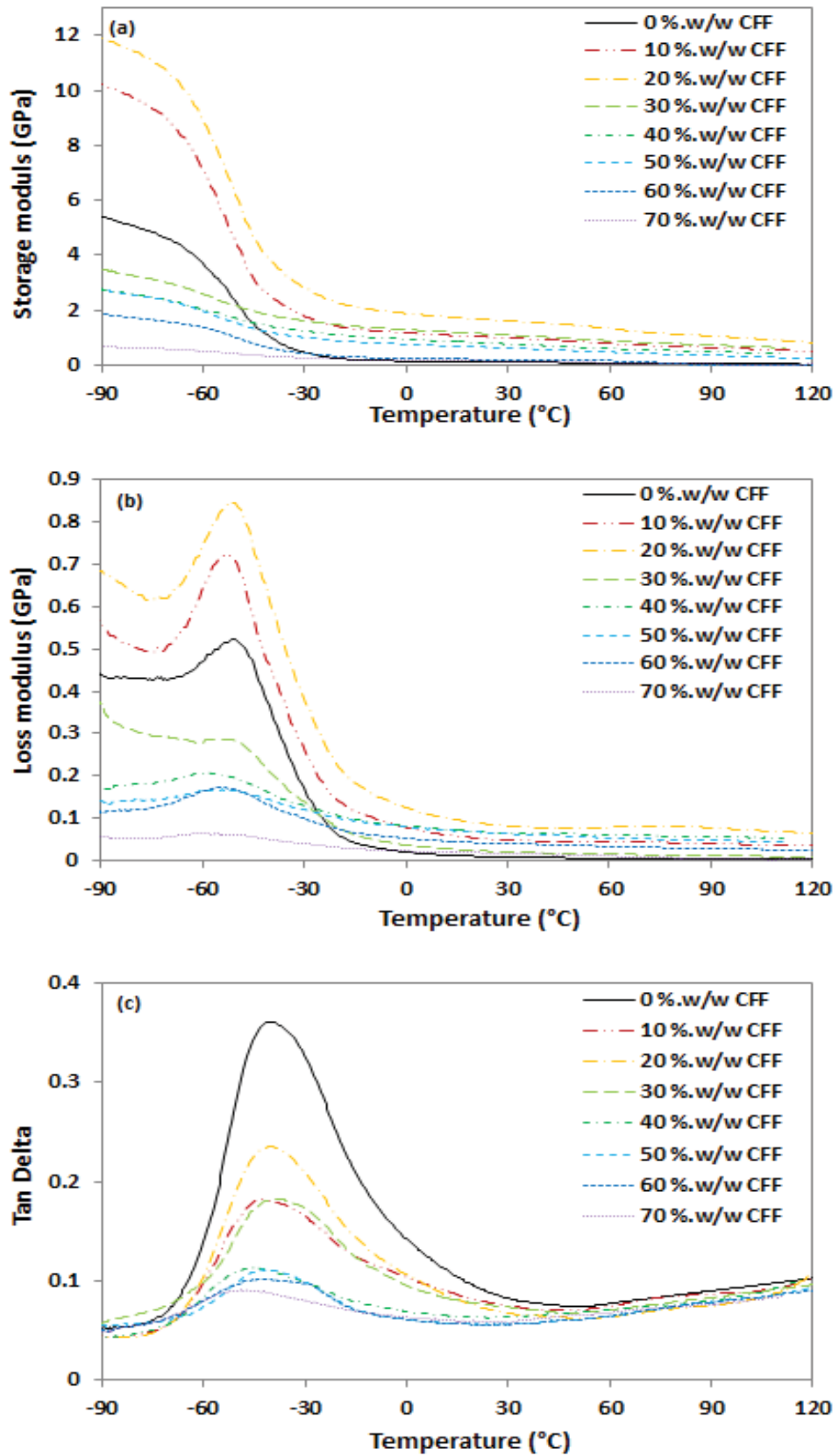


Figure 6.9: Dynamic mechanical analysis curves of pure TPU-polyether and TPU-CFF bio-composites at 10 to 70 % w/w concentrations, a) Storage modulus (E'), b) Loss modulus (E'') and c) Loss tangent ($\tan\delta$)

Incorporation of a higher CFF volume fraction yielded wider E'' curves that shifted the T_g towards lower temperatures. This is attributable to the keratin functional groups increasing free volume and hence molecular motions of the TPU chains, causing the composite to gain mobility [13, 47] since polymers above the T_g are rubbery and below the T_g polymers are brittle. These restrictions are usually facilitated by hydrogen bonding between the linear and dendritic keratin polymers [13]. Within the TPU-CFF bio-composites hydrogen bonds can occur through the unreacted OH groups on the keratin bio-fibres and the C=O groups on the polyether (soft segment) component of the linear TPU (Figure 6.1), decreasing the T_g properties [13]. The other possibility is that a reduction in T_g was due to poor bonding between the filler and polymer, which creates inefficient stress transfer, which means the molecules move easier and therefore the T_g can decrease. The T_g decrease is unlikely to be caused by residual THF because all composites were heated under vacuum for 24 h. From Figure 6.9(b) it may be assumed that the T_g of CFFs was lower than that of the TPU-polyether (-52 °C). The structure of CFFs is most likely to reduce restrictions on the mobility of the polymer chains and decrease T_g of bio-composites [13]. All blends displayed a single loss peak, corresponding to the T_g of linear TPU-polyether. This confirms that CFF was compatible with TPU soft, polyether segments. In addition, the single maximum strongly suggests that functionalised CFFs are primarily distributed throughout the soft TPU segment [13].

Damping ($\tan\delta$) represents the ratio between the loss modulus and storage modulus (E''/E') and depends on the fibre and matrix adhesion. Hence a weak fibre-matrix bonding will result in high $\tan\delta$ values [48, 49] and a strong fibre-matrix bonding will result in low $\tan\delta$ values. The TPU-polyether matrix had a T_g value of around -38 °C which is in agreement with the T_g obtained from the manufacturer. In contrast, for the TPU-CFF bio-

composites the values are in the region of $-45\text{ }^{\circ}\text{C}$ for 10 % and $-47\text{ }^{\circ}\text{C}$ for 20 % reinforcement. Even though some studies suggest using the maximum value of E'' as the transition temperature [50], most studies [51-55], assign this transition to the $\tan\delta$ peak, however the transition temperature obtained from E'' is more theoretically correct since it is a physical value while the $\tan\delta$ is a ratio (E''/E'). In both cases, the presence of CFF reinforcement decreased the T_g value (Figures 6.9b and c), which is in agreement with the literature [8]. The $\tan\delta$ at $25\text{ }^{\circ}\text{C}$ was decreased with increasing CFF concentrations, the same as $\tan\delta$ maximum in the range of $-38\text{ }^{\circ}\text{C}$ to $-50\text{ }^{\circ}\text{C}$. Therefore CFF reduced the damping or energy absorbing ability of TPU-polyether.

6.3.6 Infrared spectroscopy

Typical infrared spectra of pure CFFs, TPU-polyether and TPU-CFF bio-composites are shown in Figure 6.10(a). The characteristic IR absorption bands of polyether–polyurethane are marked. The spectra for both pure CFFs and TPU-polyether show no detectable changes in the pure CFF and TPU-polyether before and after compression moulding (the TPU-polyether spectrum shows that it was slightly crystalline) and this confirmed that composite structures, including keratin-based materials, were not decomposed during the thermal press processing at $175\text{ }^{\circ}\text{C}$. The only changes observed were for 20 % w/w CFF bio-composite after compression moulding (Figure 6.10b). However, a subtraction of the post-moulding spectra from the pre-moulding one revealed that whilst, not unexpectedly, some bands do not balance out exactly the significant bands were at 2960 , 1260 , doublet 1100 - 1000 , and 800 cm^{-1} . This is an excellent match to reference spectra of silicone oil/grease/rubber.

The spectral features from the urethane groups dominate the spectra of the TPU-polyether. These results support the molecular modelling outcomes, which suggested a

chemical interaction between the feather keratin and the TPU-polyether via hydrogen bonds, which are not seen in FTIR spectra. In the spectrum for pure CFFs, it can be observed that after the thermal pressing, the NH band around 3362 cm^{-1} shifted slightly to a higher wave number, 3380 cm^{-1} , which indicates a reduction in hydrogen bonding.

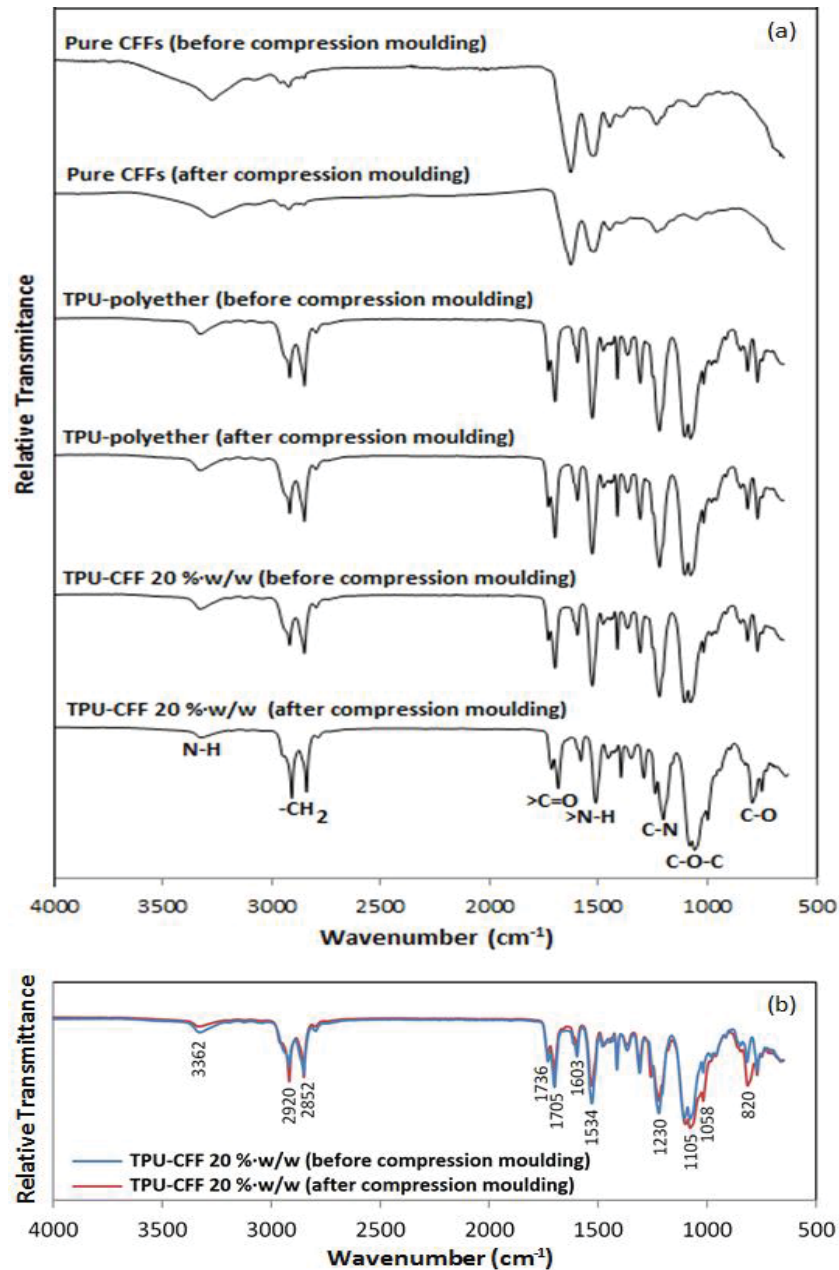


Figure 6.10: FTIR spectra of (a) TPU-polyether and TPU-CFF bio-composites before and after compression moulding or thermal pressing (b) Comparison of TPU-CFF 20 %-w/w spectra before and after compression moulding or thermal pressing

The FTIR spectra of pure CFFs have been described in detail by in Chapters 4 and 5. In the spectrum presented here, the symmetric stretching vibration is identified in the region around 3340 cm^{-1} and corresponds to a range of amide bands, hydrogen bonded N-H group (urethane nitrogen peak), indicating that most of the amide groups in TPU-CFF based polyurethanes are involved in hydrogen-bonding [8, 50, 56]. This small contribution of N-H groups bonded with ether oxygen in polyurethane (polyether soft segment in TPU – Figure 6.1) represents the urethane linkage [6]. The peaks at 2923 cm^{-1} and 2854 cm^{-1} are assigned to the asymmetric vibration of the CH of the methyl group [8, 56]. The carbonyl group stretching vibrations appear at 1707 cm^{-1} , are from C=O in free urethane [8, 50, 57]. This peak is affected by the H-bonding of urea, between the NH in the urethane and carbonyl groups from CFFs, and by the presence of keratin structure with the same C=O vibration [6]. The peak at 1537 cm^{-1} is attributed to in-plane bending of NH group, deformation vibration of N-H and the amide II absorption [8, 51, 57]. The 1220 cm^{-1} signal is associated with COC- groups in the urethane moieties whilst the lower frequency band is from -C-O-C- groups in the ether linkages. The band at 1114 cm^{-1} is assigned to the stretching of the -C-O-C- group, i.e. it is the urethane ether peak [50, 56, 58]. Aromatic groups are observed in a pair of peaks at 867 and 819 cm^{-1} from the polyurethanes [6]. Shoulders on peaks from C-N , C-O-N and C-O vibrations around 1262 cm^{-1} , 1052 cm^{-1} and 808 cm^{-1} , respectively, were not significantly changed for 20 %·w/w CFF bio-composite after moulding. The bands from C=O , N-H and C-O-C groups are classical for TPU-polyether [6], suggesting that hard and soft segments of the TPU were linked via ether bonds in both the TPU-polyether and TPU-CFF 20 %·w/w bio-composite since these signals appeared in all spectra.

To compare the properties of the new bio-composites with existing similar materials a range of measurements were made in the laboratory and sourced from Polymer Database – PoLyInfo [59]. The results are shown in Table 6.5 and Figure 6.11.

Table 6.5: Comparison of the physical properties of the TPU-CFF bio-composites with related materials

Composites	Relative recovery strain (%)	Strain at maximum force (%)	Density (g cm ⁻³)	Elastic Modulus (MPa)	Storage Modulus (GPa) at 25 °C	Loss modulus MPa 25 °C	Tg (°C)	Temp. at 5 % mass loss (°C)
TPU-polysiloxane - C	81	8.8	1.09	0.3	0.2	31	123	312
TPU-polysiloxanes - P	85	10.4	1.04	0.3	0.3	87	123	313
TPU-polyester	-	-	1.14	-	0.1	13	-47	311
TPU-graphite (1 %)	-	-	-	-	0.07	4	-44	293
TPU-Voranol 3010	-	-	1.01	-	0.05	5	-45	292
TPU-polyether	75	11.6	1.14	0.3	0.1	20	-52	313
TPU-CFF 20 %-w/w	69	1.3	1.11	2.0	1.6	80	-54	290

Key to table

C = created via casting, P = created via precipitation, - = no data available

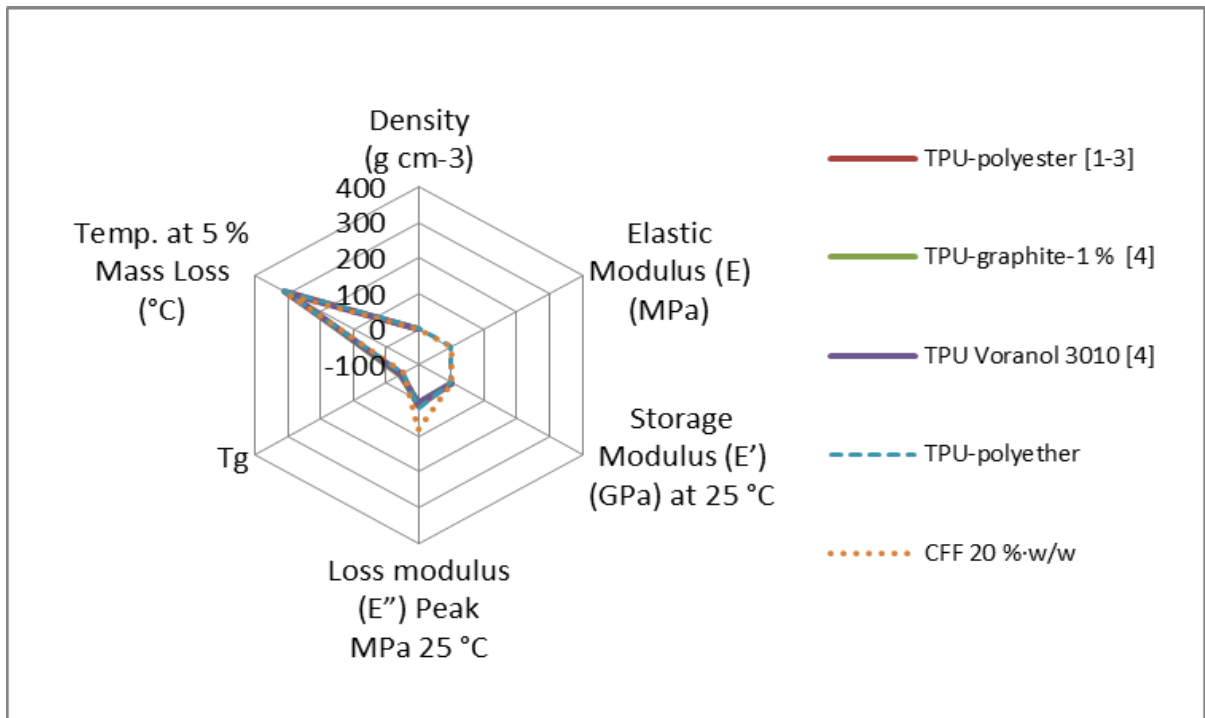


Figure 6.11: Comparison of the physical properties of the TPU-CFF bio-composites with related materials

Compared with the raw TPU-polyether the optimum bio-composite (incorporating 20 %·w/w CFF) showed the following property changes. The elastic modulus E increased by 567 % and the storage modulus E' increased by 45 %, the deformation (elongation) at maximum force decreased by 10.3 %, the storage modulus was 16 times higher and the loss modulus was enhanced by a factor of four (and by 16 compared with TPU-polyether Voranol 3010). The T_g did not change significantly but is still low compared with the other polymers tested. The CFF bio-composite had the lowest temperature at 5 % mass loss (290 °C) compared with all the other polymers tested.

It is worth noting that the source of feather fibre is different to other commercial fibres on the market. Feathers are effectively a self-sustainable, continuously renewable resource. Poultry is raised for food continuously thus a predictable supply always occurs. In comparison, trees can be harvested roughly every twenty years and wool, cotton and kenaf (hemp) around twice a year. Feather fibres are thus cost effective as well as bringing new desirable properties to polymer bio-composites made from them.

6.4 Conclusions

'Greener', polyurethane ether-keratin fibre bio-composites with improved thermo-mechanical properties were prepared by blending CFFs with TPU-polyether through a solvent, casting evaporation method. Macro-photographic and SEM imaging of the reinforced TPU-CFF bio-composites demonstrated effective adhesion, no agglomeration, and an even distribution of fibres that reflected the compatibility between the CFF reinforcement and the TPU matrix.

Molecular modelling, together with FTIR spectroscopy characterisation, indicated that there was not just a physical but a chemical interaction between the feather keratin and the

TPU-polyether. The addition of CFFs to the TPU-polyether was found to increase the mass loss but decrease the remaining char ratio, although the opposite occurred at higher temperatures; in addition, it enhanced heat resistance of the bio-composite but decreased the glass transition temperatures of the composites. Reinforcing of the polymer with CFFs not only made the TPU-polyether stiffer but reduced the deformation of the bio-composites. As the volume fraction of feather fibres increased the bio-composites showed a concomitant increase in elastic modulus, compared with the TPU-polyether, but the loss tangent and recovery strain decreased. The optimum volume fraction of feather fibres in the composite was found to be 20 % as the resulting bio-composite showed the highest elasticity at all studied temperatures.

The bio-composites created here are made from renewable ingredients e.g. feathers that would otherwise go to landfill or be incinerated. The processing method used is not as energy intensive as others and does not produce as much waste. The feather component of the product is biodegradable and it is possible to make polyurethane from vegetable oils [60, 61]. Additionally, it would be possible to add biodegradable additives in carrier resins to help biodegradation and this could be done with the TPU polymer backbone of the composite. Using the waste from one industry (e.g. feathers from the poultry industry) as the source for another (plastics) is the definition of industrial ecology. The bio-composites produced can, therefore, be classified as green [1-3]. Ultimately, feather fibre is a multipurpose, cost effective reinforcement for polymer composites which may enable valuable new, valuable products to be created.

Although the primary structures (chemical composition and sequence) of proteins are relevant in structure and molecular interactions, the secondary (regular local sub-structures on a polypeptide backbone, dependent on hydrogen bonding - primarily α -helix and β -pleated

sheet) and tertiary (overall three-dimensional shape of an entire protein molecule) structures are more important for function [12]. Indeed, while the basic structural elements found in natural systems are relatively weak they can surpass the mechanical properties of synthetic materials because of their secondary and tertiary structure. For example, keratin strength comes from its structure rather than its composition [12].

The properties and performance of thermoplastic polyurethane are determined by several factors such as chemical structures and micro-phase morphologies [14], the latter include the extent of competitive hydrogen bonding between the hard-hard and the hard-soft segments [15]. Therefore, knowing if there is any hydrogen bonding between the keratin and the TPU-polyether is important.

Common methods to study and predict protein structure are X-ray crystallography, NMR spectroscopy and computational modelling. Computational modelling is convenient as virtually no equipment is required and there are open source on-line servers available to facilitate such experiments [16]. The Iterative Threading ASSEmbly Refinement (I-TASSER) server is one of the most widely used because it gives five different predicted structures and a comprehensive set of scores or parameters that are useful to evaluate its reliability. These parameters include characterisation-score (C-Score), an estimation of prediction accuracy, and template-modelling-score (TM-score) with which the root-mean-square deviation (RMSD) of atomic position values measure the structural similarity between the model and structures in database libraries [17].

The utilisation of eco-friendly "green", bio-based composites has been reported in many areas including, but not limited to, the packaging, insulation, automotive, building and roofing industries, as well as for separation membranes for water

treatment [6, 8, 18, 19]. The application of the produced bio-composites are steps towards more environmentally-friendly, greener and more cost effective products. The outcomes from this research can be used as a model system and/or the basis for research on similar composites based on alternative polymers and biological materials.

6.9 References

1. Zini, E. and M. Scandola, *Green composites: an overview*. Polymer composites, 2011. **32**(12): p. 1905-1915.
2. Zia, K.M., M. Barikani, I.A. Bhatti, M. Zuber, and H.N. Bhatti, *Synthesis and characterization of novel, biodegradable, thermally stable chitin-based polyurethane elastomers*. Journal of applied polymer science, 2008. **110**(2): p. 769-776.
3. Quirino, R.L., T.F. Garrison, and M.R. Kessler, *Matrices from vegetable oils, cashew nut shell liquid, and other relevant systems for biocomposite applications*. Green Chemistry, 2014. **16**(4): p. 1700-1715.
4. Shen, L., J. Haufe, and M.K. Patel, *Product overview and market projection of emerging bio-based plastics PRO-BIP 2009*. Report for European Polysaccharide Network of Excellence (EPNOE) and European Bioplastics, 2009. **243**.
5. Miller, R. *Ester & Ether – The Polyurethane Sisters*. Plastic Tubing 2010; Available from: <https://plasticubes.wordpress.com/2010/09/29/ester-ether-the-polyurethane-sisters/>.
6. Saucedo-Rivalcoba, V., A. Martínez-Hernández, G. Martínez-Barrera, C. Velasco-Santos, and V. Castaño, *(Chicken feathers keratin)/polyurethane membranes*. Applied Physics A, 2011. **104**(1): p. 219-228.
7. Liu, J., D. Ma, and Z. Li, *FTIR studies on the compatibility of hard–soft segments for polyurethane–imide copolymers with different soft segments*. European polymer journal, 2002. **38**(4): p. 661-665.
8. Flores-Hernández, C.G., A. Colín-Cruz, C. Velasco-Santos, V.M. Castaño, J.L. Rivera-Armenta, A. Almendarez-Camarillo, P.E. García-Casillas, and A.L. Martínez-Hernández, *All green composites from fully renewable biopolymers: Chitosan-starch reinforced with keratin from feathers*. Polymers, 2014. **6**(3): p. 686-705.
9. Martínez-Hernández, A.L., C. Velasco-Santos, M. de-Icaza, and V.M. Castaño, *Dynamical–mechanical and thermal analysis of polymeric composites reinforced with keratin biofibers from chicken feathers*. Composites Part B: Engineering, 2007. **38**(3): p. 405-410.
10. Wielage, B., T. Lampke, H. Utschick, and F. Soergel, *Processing of natural-fibre reinforced polymers and the resulting dynamic–mechanical properties*. Journal of Materials Processing Technology, 2003. **139**(1–3): p. 140-146.
11. Barone, J.R. and W.F. Schmidt, *Effect of formic acid exposure on keratin fiber derived from poultry feather biomass*. Bioresource technology, 2006. **97**(2): p. 233-242.
12. Meyers, M.A., P.-Y. Chen, A.Y.-M. Lin, and Y. Seki, *Biological materials: structure and mechanical properties*. Progress in Materials Science, 2008. **53**(1): p. 1-206.

13. Spoljaric, S. and R.A. Shanks, *Novel polyhedral oligomeric silsesquioxane-substituted dendritic polyester tougheners for linear thermoplastic polyurethane*. Journal of Applied Polymer Science, 2012. **126**(S2): p. E440-E454.
14. Yilgör, E., I. Yilgör, and E. Yurtsever, *Hydrogen bonding and polyurethane morphology. I. Quantum mechanical calculations of hydrogen bond energies and vibrational spectroscopy of model compounds*. Polymer, 2002. **43**(24): p. 6551-6559.
15. Zhang, C., J. Hu, S. Chen, and F. Ji, *Theoretical study of hydrogen bonding interactions on MDI-based polyurethane*. Journal of molecular modeling, 2010. **16**(8): p. 1391-1399.
16. Rangwala, H. and G. Karypis, *Introduction to Protein Structure Prediction: Methods and Algorithms*. Vol. 18. 2011: John Wiley & Sons.
17. Roy, A., A. Kucukural, and Y. Zhang, *I-TASSER: a unified platform for automated protein structure and function prediction*. Nature protocols, 2010. **5**(4): p. 725-738.
18. Wrześniewska-Tosik, K., S. Zajchowski, A. Bryskiewicz, and J. Ryszkowska, *Feathers as a flame-retardant in elastic polyurethane foam*. Fibres & Textiles in Eastern Europe, 2014(1 (103)): p. 119--128.
19. Manrique-Juárez, M.D., A.L. Martínez-Hernández, O.F. Olea-Mejía, J. Flores-Estrada, J.L. Rivera-Armenta, and C. Velasco-Santos, *Polyurethane-Keratin Membranes: Structural Changes by Isocyanate and pH, and the Repercussion on Cr (VI) Removal*. International Journal of Polymer Science, 2013. **2013**.
20. PoultryHub. *Chicken meat (broiler) industry*. 17 February 2017]; Available from: <http://www.poultryhub.org/production/industry-structure-and-organisations/chicken-meat/>.
21. Sudalaiyandi, G., *Characterizing the cleaning process of chicken feathers*. Master of Engineering thesis, University of Waikato, Hamilton, New Zealand (2012).
22. Spoljaric, S., *Functionalised polymer nanocomposites and blends*. 2011.
23. Gregg, K., S. Wilton, D. Parry, and G. Rogers, *A comparison of genomic coding sequences for feather and scale keratins: structural and evolutionary implications*. The EMBO journal, 1984. **3**(1): p. 175.
24. Yang, J. and Y. Zhang, *I-TASSER server: new development for protein structure and function predictions*. Nucleic acids research, 2015. **43**(W1): p. W174-W181.
25. Ponnamma, D., K.K. Sadasivuni, M. Strankowski, P. Moldenaers, S. Thomas, and Y. Grohens, *Interrelated shape memory and Payne effect in polyurethane/graphene oxide nanocomposites*. RSC Advances, 2013. **3**(36): p. 16068-16079.
26. Nair, K.M., S. Thomas, and G. Groeninckx, *Thermal and dynamic mechanical analysis of polystyrene composites reinforced with short sisal fibres*. Composites Science and Technology, 2001. **61**(16): p. 2519-2529.
27. Tai, Y., J. Qian, Y. Zhang, and J. Huang, *Study of surface modification of nano-SiO₂ with macromolecular coupling agent (LMPB-g-MAH)*. Chemical Engineering Journal, 2008. **141**(1): p. 354-361.
28. Tao, Y., Y. Tao, B. Wang, and Y. Tai, *Preparation and investigation of nano-AlN lubricant with high performance*. Materials Chemistry and Physics, 2014. **147**(1): p. 28-34.
29. Dutta, S. and N. Karak, *Synthesis, characterization of poly(urethane amide) resins from Nahar seed oil for surface coating applications*. Progress in Organic Coatings, 2005. **53**(2): p. 147-152.
30. Barone, J. and W. Schmidt, *Polymer composites containing keratin*. 2005, U.S. Patent 20050148703 A1.


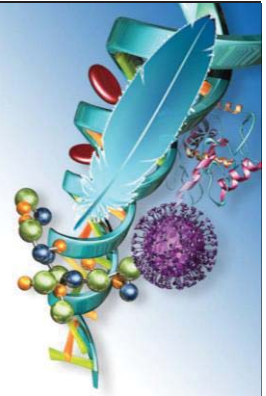
31. Cheng, S., K.-t. Lau, T. Liu, Y. Zhao, P.-M. Lam, and Y. Yin, *Mechanical and thermal properties of chicken feather fiber/PLA green composites*. Composites Part B: Engineering, 2009. **40**(7): p. 650-654.
32. Frick, A. and A. Rochman, *Characterization of TPU-elastomers by thermal analysis (DSC)*. Polymer testing, 2004. **23**(4): p. 413-417.
33. Martinez-Hernandez, A.L., C. Velasco-Santos, M. De Icaza, and V.M. Castano, *Microstructural characterisation of keratin fibres from chicken feathers*. International journal of environment and pollution, 2005. **23**(2): p. 162-178.
34. Popescu, C. and P. Augustin, *Effect of chlorination treatment on the thermogravimetric behaviour of wool fibres*. Journal of thermal analysis and calorimetry, 1999. **57**(2): p. 509-515.
35. Herrera, M., G. Matuschek, and A. Kettrup, *Thermal degradation of thermoplastic polyurethane elastomers (TPU) based on MDI*. Polymer degradation and stability, 2002. **78**(2): p. 323-331.
36. Mathew, S., M. Brahmakumar, and T.E. Abraham, *Microstructural imaging and characterization of the mechanical, chemical, thermal, and swelling properties of starch-chitosan blend films*. Biopolymers, 2006. **82**(2): p. 176-187.
37. Espíndola-González, A., A.L. Martínez-Hernández, F. Fernández-Escobar, V.M. Castaño, W. Brostow, T. Datashvili, and C. Velasco-Santos, *Natural-synthetic hybrid polymers developed via electrospinning: the effect of PET in chitosan/starch system*. International journal of molecular sciences, 2011. **12**(3): p. 1908-1920.
38. Wan, Y., X. Lu, S. Dalai, and J. Zhang, *Thermophysical properties of polycaprolactone/chitosan blend membranes*. Thermochimica Acta, 2009. **487**(1): p. 33-38.
39. Gupta, T. and B. Adhikari, *Thermal degradation and stability of HTPB-based polyurethane and polyurethaneureas*. Thermochimica acta, 2003. **402**(1): p. 169-181.
40. Brostow, W., H.E. Hagg Lobland, and M. Narkis, *Sliding wear, viscoelasticity, and brittleness of polymers*. Journal of materials research, 2006. **21**(09): p. 2422-2428.
41. Berta, M., C. Lindsay, G. Pans, and G. Camino, *Effect of chemical structure on combustion and thermal behaviour of polyurethane elastomer layered silicate nanocomposites*. Polymer Degradation and Stability, 2006. **91**(5): p. 1179-1191.
42. Drobny, J.G., *Handbook of Thermoplastic Elastomers*. 2007: William Andrew Publishing/Plastics Design Library.
43. Chattopadhyay, D. and D.C. Webster, *Thermal stability and flame retardancy of polyurethanes*. Progress in Polymer Science, 2009. **34**(10): p. 1068-1133.
44. *ASTM E 111 - 97*. Standard Test Method for Young's Modulus, Tangent Modulus, and Chord Modulus.
45. Vincent, J., *Structural biomaterials*. 2012: Princeton University Press.
46. Czajka, M., R.A. Shanks, and D. Oldfield, *Carbon Monoxide Reduced Low-Defect Graphene Nanocomposites with Poly(styrene-b-butadiene-b-styrene) Composites*, in *Society of Plastic Engineers Annual Technical Conference (SPE-ANTEC)*. 2015: Orlando, Florida, USA. p. 419-423.
47. Maji, P.K. and A.K. Bhowmick, *Influence of number of functional groups of hyperbranched polyol on cure kinetics and physical properties of polyurethanes*. Journal of Polymer Science Part A: Polymer Chemistry, 2009. **47**(3): p. 731-745.
48. Andreopoulos, A. and P. Tarantili, *Study of the off-axis properties of composites reinforced with ultra high modulus polyethylene fibres*. European polymer journal, 1999. **35**(6): p. 1123-1131.

49. Chen, L. and M. Wang, *Production and evaluation of biodegradable composites based on PHB-PHV copolymer*. Biomaterials, 2002. **23**(13): p. 2631-2639.
50. Saito, T., J.H. Perkins, D.C. Jackson, N.E. Trammel, M.A. Hunt, and A.K. Naskar, *Development of lignin-based polyurethane thermoplastics*. RSC Advances, 2013. **3**(44): p. 21832-21840.
51. Zhao, P. and J. Zhang, *Room temperature and low temperature toughness improvement in PBA-g-SAN/ α -MSAN by melt blending with TPU*. RSC Advances, 2016. **6**(19): p. 15701-15708.
52. Zhang, Y., Y. Liu, L. Xie, and X. Xu, *RSC Advances*.
53. Yang, L., S.L. Phua, C.L. Toh, L. Zhang, H. Ling, M. Chang, D. Zhou, Y. Dong, and X. Lu, *Polydopamine-coated graphene as multifunctional nanofillers in polyurethane*. RSC Advances, 2013. **3**(18): p. 6377-6385.
54. Yang, J., Y. Gao, J. Li, M. Ding, F. Chen, H. Tan, and Q. Fu, *Synthesis and microphase separated structures of polydimethylsiloxane/polycarbonate-based polyurethanes*. RSC Advances, 2013. **3**(22): p. 8291-8297.
55. Chen, R., C. Zhang, and M.R. Kessler, *Anionic waterborne polyurethane dispersion from a bio-based ionic segment*. RSC Advances, 2014. **4**(67): p. 35476-35483.
56. Saucedo-Rivalcoba, V., A. Martínez-Hernández, G. Martínez-Barrera, C. Velasco-Santos, J. Rivera-Armenta, and V. Castaño, *Removal of hexavalent chromium from water by polyurethane-keratin hybrid membranes*. Water, Air, & Soil Pollution, 2011. **218**(1-4): p. 557-571.
57. Martinez-Hernandez, A.L., C. Velasco-Santos, M.d. Icaza, and V.M. Castaño, *Grafting of methyl methacrylate onto natural keratin*. e-Polymers, 2003. **3**(1): p. 209-219.
58. Pereira, I.M., V. Gomide, R.L. Oréfice, M.d.F. Leite, A.A. Zonari, and A.d.M. Goes, *Proliferation of human mesenchymal stem cells derived from adipose tissue on polyurethanes with tunable biodegradability*. Polímeros, 2010. **20**(4): p. 280-286.
59. PolyInfo, Anon. http://polymer.nims.go.jp/index_en.html accessed 15/02/2017.
60. Petrović, Z.S., *Polyurethanes from vegetable oils*. Polymer Reviews, 2008. **48**(1): p. 109-155.
61. Guo, A., D. Demydov, W. Zhang, and Z.S. Petrovic, *Polyols and polyurethanes from hydroformylation of soybean oil*. Journal of Polymers and the Environment, 2002. **10**(1-2): p. 49-52.

6.10 Publication from this Chapter

- Pourjavaheri, F., Jones, O.A.H., Martinez Pardo, I., & Shanks, R. A. “Characterisation of green keratin–fibre polyurethane–polyether bio-composites” *Green Chemistry*. To be submitted in 2017.
 - With a supplementary video
- Pourjavaheri, F., Jones, O.A.H., Mohaddes, F., Sherkat, F., Kong, I., Gupta, A., & Shanks, R.A. (2017) "Avian Keratin Fiber Based Bio-composites" *World Journal of Engineering* **14**(3) · Doi: 10.1108/WJE-08-2016-0061.
- Pourjavaheri, F., Jones, O.A.H., & Shanks, R.A. (2016) “CF keratin in TPU-polyether”, *Plastics & Waste Conference (SPE-ANTEC)*, 17 November, Melbourne, Australia. (Poster Presentation)
- Pourjavaheri, F., Jones, O.A.H., Mohaddes, F., Sherkat, F., Kong, I., Gupta, A., & Shanks, R.A. (2016) "Analysis and Characterization of Novel Avian Keratin Fibre Based Bio-composites", *International Conference on Composites/Nano-Engineering (ICCE)*, 17-23 July, Hainan Island, China.
- Pourjavaheri, F., Jones, O.A.H., Mohaddes, F., Sherkat, F., Gupta, A., & Shanks, R.A. (2016) "Green Plastics: Utilizing Chicken Feather Keratin in Thermoplastic Polyurethane Composites to Enhance Thermo-Mechanical Properties", *Society of Plastic Engineers Annual Technical Conference (SPE-ANTEC)*, 23-25 May, Indianapolis, Indiana, USA.
- Pourjavaheri, F., Jones, O.A.H., Mohaddes, F., A., & Shanks, R.A. (2016) "Chicken Feather Keratin and Thermoplastic Polyurethane Composites", *Society of Plastic Engineers Annual Technical Conference (SPE-ANTEC)*, 23-25 May, Indianapolis, Indiana, USA. (Poster Presentation)
- Pourjavaheri, F., Jones, O.A.H., Mohaddes, F., Sherkat, F., Kong, I., Gupta, A., & Shanks, R.A. (2016) “Development of Keratin Biofiber-TPU Green Plastics with Improved Thermo-Mechanical Properties”, *AGILENT Young Scientist Forum*, 4 March, Melbourne, Australia. (Oral Presentation)
- Pourjavaheri, F., Jones, O.A.H., & Shanks, R.A. (2016) “Green plastics: utilising chicken feather keratin as a sustainable resource to enhance the thermo-mechanical properties of polyurethane composites”, *Environmental Science Research Forum (EnSuRe)*, 18 February, Melbourne, Australia. (Oral Presentation)

CHAPTER 7



DESIGN AND CHARACTERISATION
OF SUSTAINABLE BIO-COMPOSITES
FROM CHICKEN FEATHER KERATIN
AND THERMOPLASTIC
POLYSILOXANE-POLYURETHANE

7.1 Introduction

The thermoplastic polyurethanes (TPU) are a versatile group of multi-phase segmented polymers with diverse physical and chemical properties, including, relative hardness, high abrasion [1] and chemical resistance [2, 3]. The applications of polyurethanes, particularly in medical devices, are numerous due to their outstanding mechanical properties and ability to be readily thermally processed. Applications have however, been limited in some cases by the low biological stability [4] and poor fire resistance of soft grade TPU [1]. Conversely, while silicone rubbers are widely used throughout the medical device industry due to their excellent biological performance their potential applications are limited by low mechanical performance and lack of processing options. Co-polymers of silicone macrodiols and polyurethanes with high levels of silicone, exhibit physical and mechanical performance equivalent to conventional polyurethanes with increased biological stability (that surpasses rigid, bio-stable polyurethanes) and are readily thermally processed using conventional technologies [4]. Organosiloxane polymers, in particular, are known for their excellent thermal and thermo-oxidative stabilities, good electrical properties, high moisture resistance, and low glass transition temperature (T_g , -123°C), and mechanical stress [5, 6].

The development of TPU polymers with enhanced thermo-mechanical properties can be accomplished via the incorporation of reinforcing materials and would be beneficial to a range of industries. Many biological materials, including CFs, have the potential to fulfill this role. Incorporating different parts of the feather into a polymer matrix can result in different thermo-mechanical properties in the final composite [7]. As said earlier, given the unique thermo-mechanical properties of feathers, the development of new plastic composites incorporating feather keratin has become an attractive research topic in recent years [7-9].

However, there have to date, been limited development and characterisation studies of TPU composites made with these materials [9].

Due to the miscibility and flexibility of TPU, arising from its intrinsic thermoplastic nature, it is expected that incorporation of CFFs into a soft segment polysiloxane - hard segment TPU matrix at an optimum level could result in a thermo-mechanically superior substrate. TPU-polyether has a chemical structure compatible with CFF keratin. They both contain NH-C=O moieties and the urethane groups of the polymer are compatible with amide groups of the feathers via hydrogen bonding, as shown in Figure 7.1.

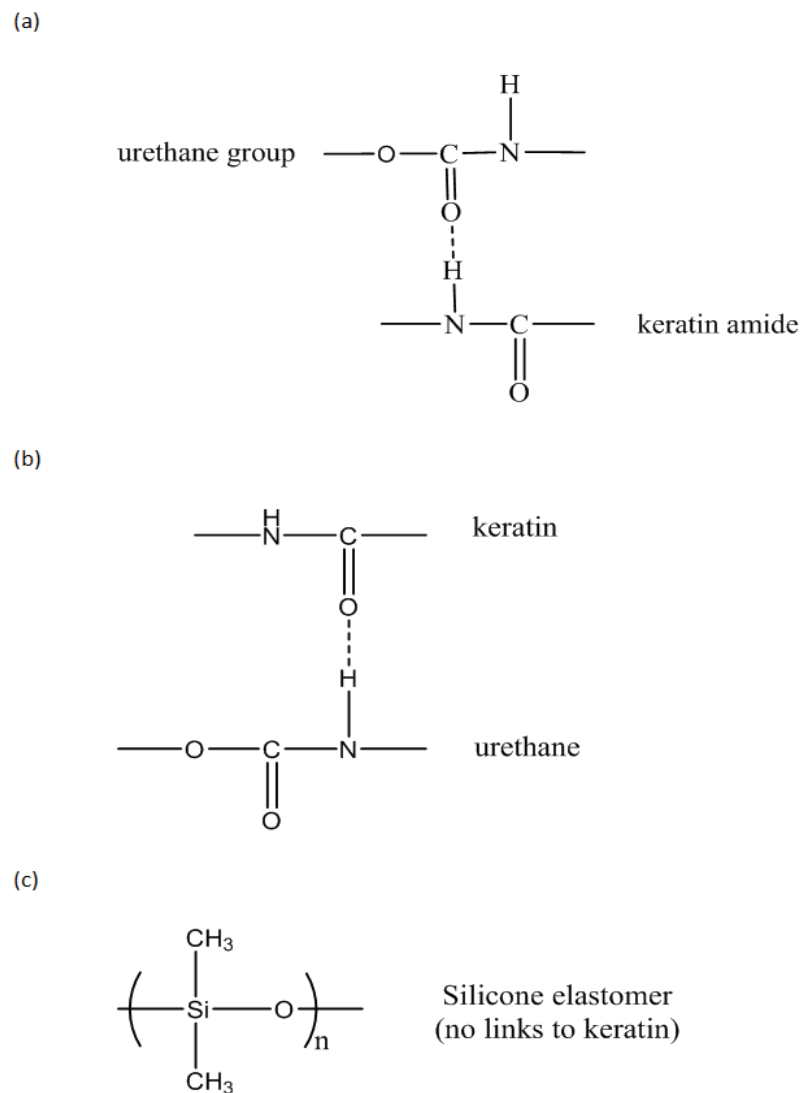


Figure 7.1: Proposed links between the CFF and polysiloxane-TPU

Linkages between urethane and amide groups are well known in organic chemistry and have been illustrated in polymers previously [10]. In contrast, polysiloxane TPU is hydrophobic and does not form hydrogen bonds. Hydrophilic groups on the peptide backbone (e.g. serine, threonine, aspartate) of organic fibres however, offer chemically distinct sites for covalently bonding the polymer to the fibre [11]. In this study, computational modelling was used to study and predict the structure and changes in thermo-mechanical properties associated with such modification of the TPU-polysiloxane matrix, before and after incorporation of CFFs.

7.2 Experimental

7.2.1 Materials

The CFFs used are detailed in section 6.2.1 and Table 3.2.

7.2.2 Composite fabrication

Solvent dispersion was performed as detailed in Section 6.2.2. Briefly, this was achieved by dissolving 80 %·w/w of polysiloxane TPU polymers in 100 mL of THF separately, ground CFFs were then added to the polymer slurry in the ratios listed in Table 7.1. All composites were prepared in triplicate by solvent–casting–evaporation–compression moulding (as detailed in section 6.2.2) or thermal press and solvent–precipitation–evaporation–compression moulding under normal laboratory conditions (20 °C ± 2 °C and 60 % ± 2 % relative humidity). For the former method the mixtures were stirred for 24 h at 400 rpm using a magnetic stirrer and then cast into a glass petri dish and the solvent allowed to evaporate overnight. In the latter method, the mixtures were poured into a container containing 30 mL of methanol while undergoing continuous stirring via a magnetic stirrer.

This caused polymer precipitation; the precipitate was then transferred to a glass petri dish and the solvent allowed evaporating overnight. The air-dried dishes were then placed in an oven at 70 °C for 24 h and then under a vacuum of 25 mm·Hg for a further 24 h. The films were then allowed to cool to room temperature gradually and removed from the petri dishes. The resulting sheets were cut into quarters, stacked and placed inside a square metal mould (70 mm x 70 mm x 1 mm) then heated to 175 °C as detailed in section 3.3.9, to enable flow of the composite without degradation. All composites were allowed to sit at ambient conditions for one week prior to testing.

Table 7.1: Concentrations used in the preparation and characterisation of TPU-CFF bio-composites and their respective densities

Composites material ratios	Weight Fraction (%·w/w)		Volume Fraction (%·v/v)		Density (g cm ⁻³)
	Filler CFF	Matrix TPU	Filler CFF	Matrix TPU	
solvent–casting–evaporation–compression moulding					
CFF: TPU-polysiloxane 0	0	100	0	100	1.09
CFF: TPU-polysiloxane 20	20	80	24	76	0.98
solvent–precipitation–evaporation–compression moulding					
CFF: TPU-polysiloxane 0	0	100	0	100	1.04
CFF: TPU-polysiloxane 20	20	80	24	76	0.94

7.2.3 Physical appearance

A digital camera was used to record images of all the TPU-polysiloxane polymers. Images of the CFF reinforced bio-composites were taken in order to show the distribution of fibres in the polymer matrix.

7.2.4 Molecular modelling visualisation

The linear amino acid sequence of CFK [12] was used to construct a molecule using the

server for protein structure prediction - I-TASSER [13, 14]. The TPU-polysiloxanes polymeric chains were simulated following the example in patent US8674035 B2 [15] and had a molecular weight of *ca.* 1645 g/mol. A unit cell with amorphous configuration and periodic boundary conditions was created using one chain of the TPU-polysiloxane and one molecule of keratin using Material Studio (Dassault Systèmes, San Diego, USA). The unit cell had a cubic lattice of 43.5 nm x 43.5 nm x 43.5 nm with a density of 1.00 g/cm³ at 25 °C. This cell represented the TPU-polysiloxanes -CFF bio-composite with 20.2 %·w/w CFF. The amorphous cell was visualized and analysed using BIOVIA Discovery Studio Visualizer V16 software (Dassault Systèmes, San Diego, USA) and all non-intramolecular hydrogen bonds were shown using the standard setup (a distance parameter of 0.340 nm and an angle criterion between 90° and 180°).

7.2.5 Thermal analysis

A PerkinElmer TGA 7 thermogravimetric analyser was employed, as detailed in section 3.3.7.2 to evaluate thermal degradation, mass loss, remaining char ratio, and the changes in degradation behaviour associated with CFFs, TPU-polysiloxane and TPU-polysiloxane-CFF bio-composites. Details are as section 6.2.4.2.

7.2.6 Thermo-mechanical analysis

Stress–strain tensile mechanical analysis of the pure TPU-polysiloxane polymer and TPU-CFF bio-composites was performed by using a DMA Q800 system (section 3.3.10.2 and 6.2.4.3). Hysteresis analysis performed as detailed in section 3.3.10.3.

Dynamic mechanical analysis (DMA) was carried out on a Perkin Elmer Pyris Diamond DMA 2003 with test specimens displaying average dimensions of 25 mm x 7 mm x 1 mm

(cut with an xacto knife). Test conditions included a specimen gauge length of 11 mm, operated in tension mode at 2 Hz frequency, and a temperature range of -90 °C to 120 °C. Modulated force thermomechanometry (mf-TM) was used to measure the viscoelastic properties with frequency and temperature. Time-temperature superposition was used to determine the extremes of response time of the composites. The storage modulus (E'), loss modulus (E''), loss tangent ($\tan\delta$), and associated T_g were measured as a function of temperature at a heating rate of 2 K·min⁻¹.

7.3 Results and discussion

7.3.1 Fibre dispersion

The macro photographic images of the pure TPU-polysiloxane polymer and TPU-CFF reinforced bio-composites are shown in Figure 7.2.

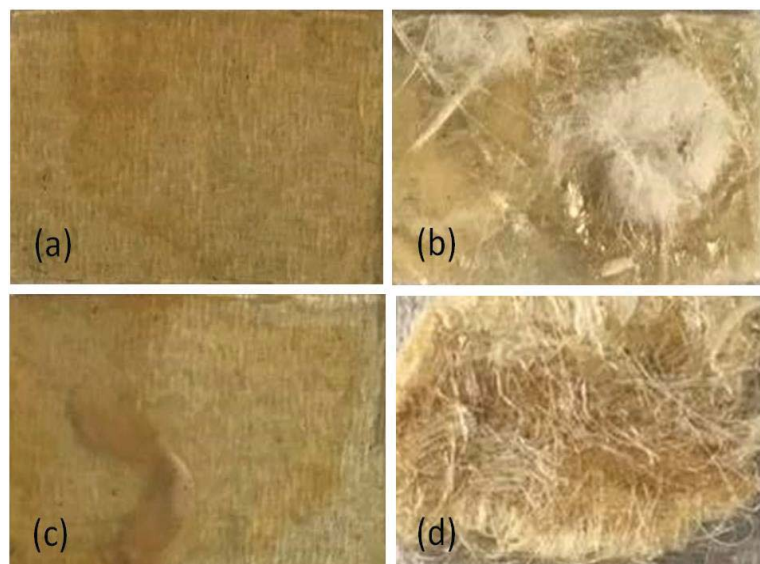


Figure 7.2: Macro photographic images of a) pure TPU-polysiloxane and b) TPU-polysiloxane with 20 %·w/w CFF made via the casting technique; c) pure TPU-polysiloxane and d) 20 %·w/w CFF - TPU-polysiloxane made via the precipitation method

The high transparency of TPU-polysiloxane allowed for the easy observation of the spatial distribution of CFFs in the composites. The CFFs were found to be uniformly distributed throughout the entire polymer matrix, without clumping, in the 20 %·w/w CFF bio-composites prepared via precipitation. Although agglomeration was observed in the 20 %·w/w CFF bio-composites prepared via casting, overall an even distribution was observed in both bio-composites. This result showed the compatibility of the TPU-polysiloxane matrix with the CFFs. Both the size and hydrophobic behaviour associated with CFFs played important roles in resulting this even dispersion and during thermal pressing [8, 16].

Figure 7.3 shows a schematic representation of the chemical structure of TPU-polysiloxane, which is a block copolymer of hydroxy terminated polysiloxane (poly(butane-1,4-diol)) and polyurethane (from methane diphenyl diisocyanate), where the polysiloxanes blocks are an elastic matrix and polyurethane are separated hard physical crosslinking blocks.

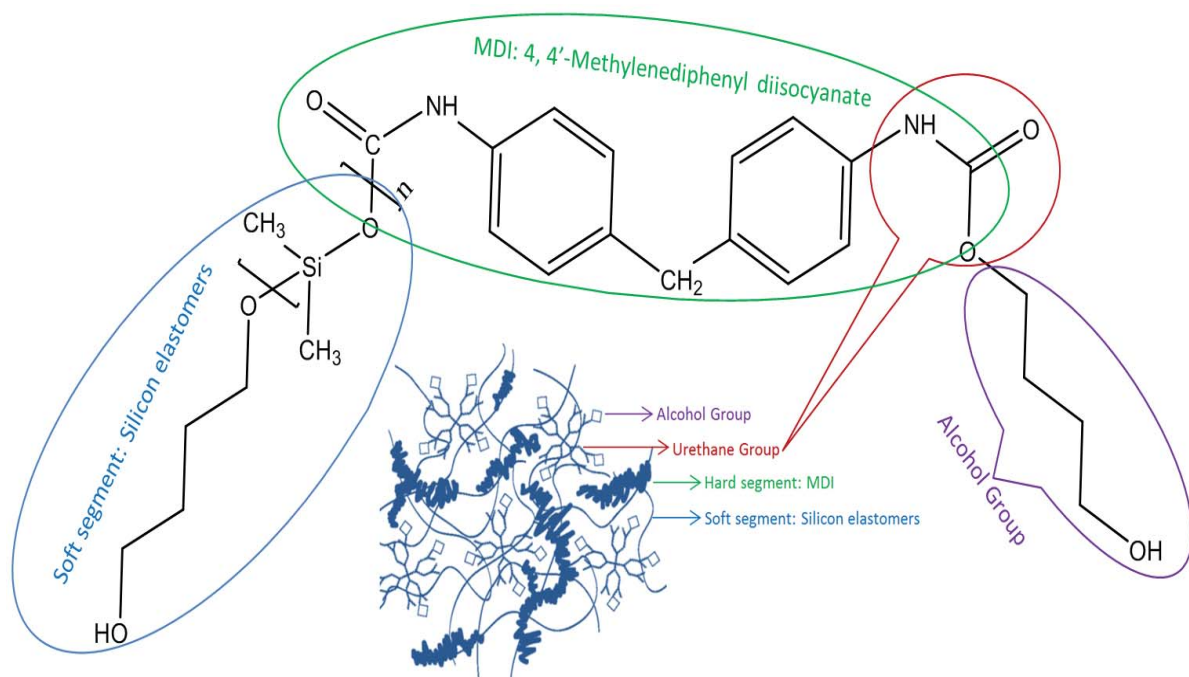


Figure 7.3: Schematic representation of the chemical structure of TPU-polysiloxane (adopted from [17])

7.3.2 Molecular visualisation

The generated amorphous cell for the keratin protein surrounded by the TPU-polysiloxanes and the interactions between them are shown in Figure 7.4.

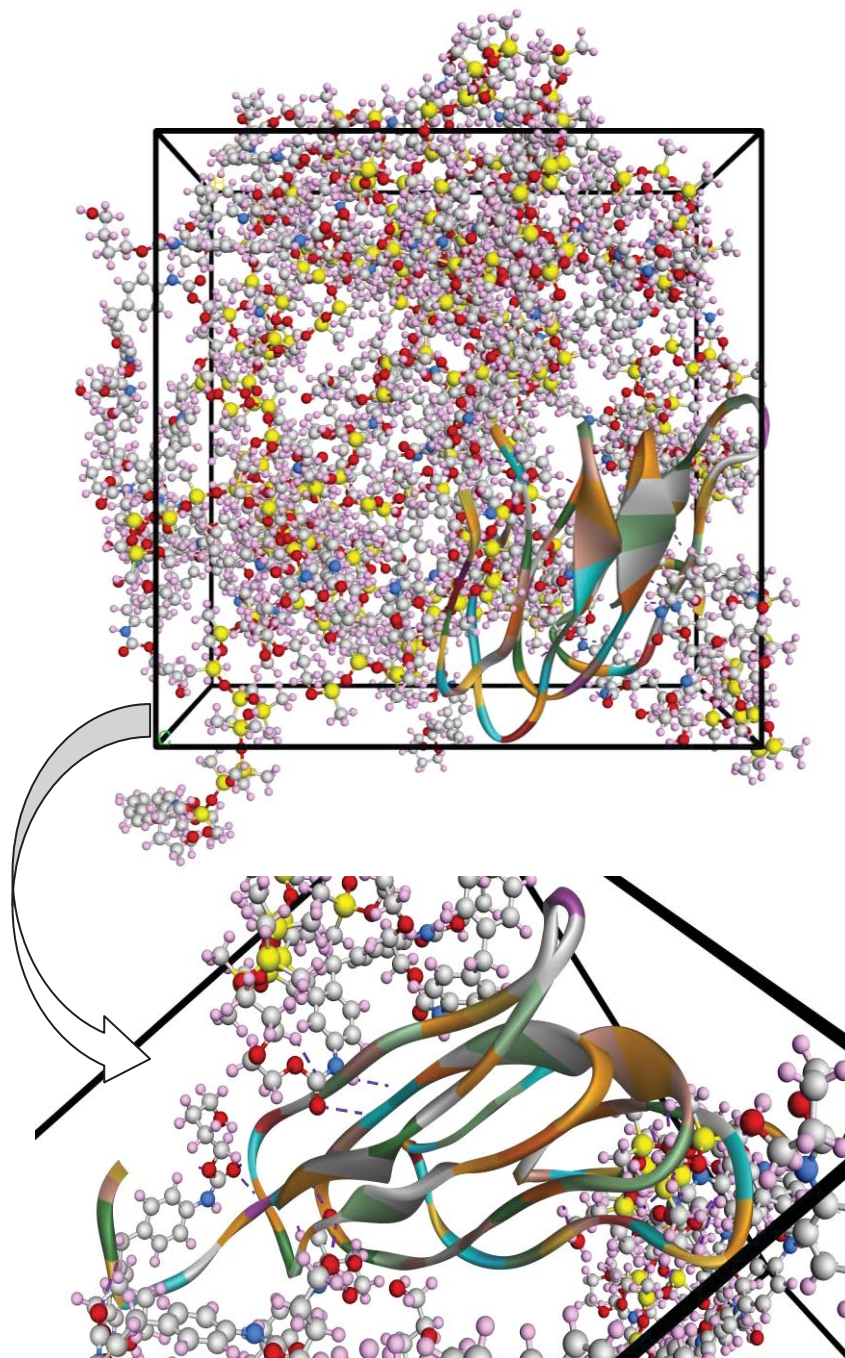


Figure 7.4: Molecular modeling visualization of one molecule of CFF keratin surrounded by one molecule of TPU-polysiloxane. Key: O: red, Si: yellow, C: grey, H: pink, N: blue, purple dashed lines: hydrogen bonds

The colours of the keratin molecule represent different amino acid residues in the primary structure. The various intermolecular hydrogen bond interactions between the keratin and the TPU-polysiloxanes indicate that not only physical but chemical interactions may exist between the feather keratin and the polymer. It appears that more intermolecular interactions between the keratin and the TPU-polysiloxanes could potentially exist but these are limited due to the large number of existing intramolecular interactions within the keratin molecule that create its complex secondary and tertiary structure.

7.3.3 Thermal degradation and remaining char ratio

The thermogravimetric analysis of the TPU-polysiloxane and TPU-CFF bio-composites are presented in Figure 7.5 and Table 7.2. The thermal behaviour observed for these composites can be described in three main steps (Figure 7.5, panel A). The first is a minor mass loss of approximately 4 % over the range of ~30 °C to ~300 °C. This loss is likely due to the loss of water bound up in the matrix released after denaturation of the helix structure of the keratin, as well as losses from thermal pyrolysis of the protein chain linkages and peptide bridges [18, 19]. This behaviour could likewise be explained by the presence of a high oxygen content and dehydration reactions [20]. Although the TPU-CFF bio-composites started their mass loss at lower temperatures than the TPU-polysiloxane polymer, they were found to need higher temperatures to fully decompose.

The second mass loss step was much larger, around 90 %, and occurs from ~300 °C to ~480 °C. It is likely related to decomposition of the hard segments of the TPU-polysiloxane [17]. In the TPU-CFF bio-composites this large mass loss was likely to be the result of several complex processes that include dehydration of the protein structure together with depolymerisation and decomposition of urethane and polysiloxane [8, 21-23]. This stage is

associated with the destruction of disulfide bonds and the elimination of H_2S originating from the amino acid cysteine, which is a major component of keratin [18, 19].

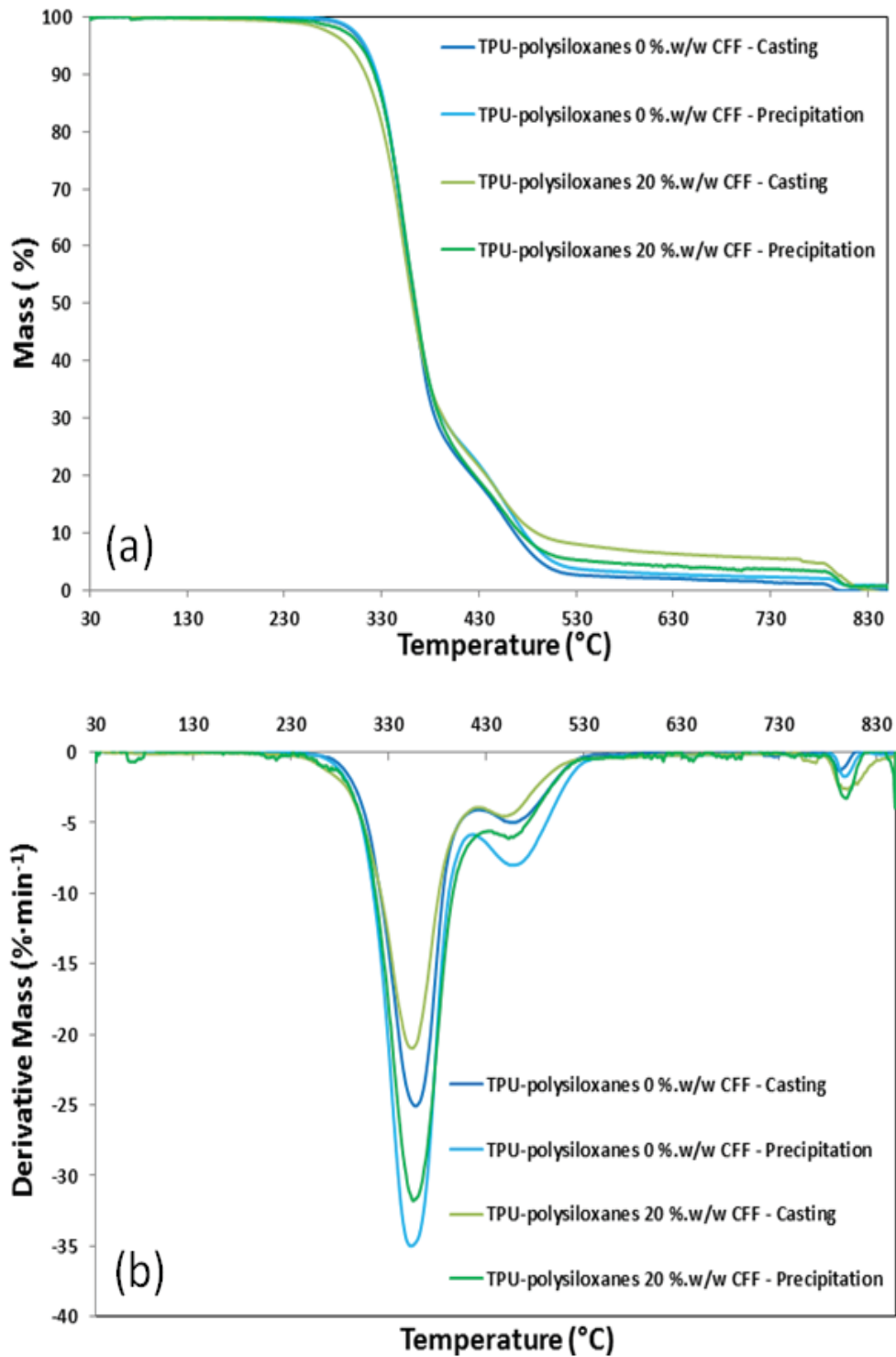


Figure 7.5: TGA thermograms of TPU-polysiloxane polymer and TPU-CFF bio-composites at 0 to 20 %·w/w CFF concentrations via casting and precipitation techniques a) mass loss, b) first derivative

The third step occurred from *ca.* 480 °C to 850 °C with the greatest mass loss corresponding to decomposition of the soft segments of the TPU-polysiloxane (Figure 7.5) [17] and complete degradation of the polymer [8, 21-23]. Both the reinforced bio-composites benefited from the presence of keratin bio-fibres here, since, at 600 °C, the highest mass loss was for the TPU-polysiloxane polymer matrix (i.e. 97.0 % to 97.8 % at 600 °C). At temperatures more than *ca.* 490 °C, the bio-composites showed better fire resistance by demonstrating more char than the TPU-polysiloxane. The TPU-polysiloxane via casting technique had the highest mass loss at 600 °C (97.8 %), and 20 %·w/w CFF bio-composites made via the precipitation technique had the lowest relative mass loss, of 93.3 %, at this temperature.

Table 7.2: Thermal data of TPU-polysiloxane and TPU-CFF bio-composites at 20 %·w/w concentrations via casting and precipitation techniques obtained by TGA

TPU-CFF Composites	Temperature at 5 % Mass Loss (°C)	Mass Loss (%) at 300 °C	Char Levels (%) at 600 °C
solvent–casting–evaporation–compression moulding			
CFF: TPU-polysiloxane 0	312	2.5	2.2
CFF: TPU-polysiloxane 20	295	6.0	4.5
solvent–precipitation–evaporation–compression moulding			
CFF: TPU-polysiloxane 0	313	2.3	3.0
CFF: TPU-polysiloxane 20	308	3.5	6.7

Addition of CFFs to the matrix increased the thermal stability and remaining char level of the bio-composites at temperatures above 490 °C. This effect is related to the inherent variations of natural materials and follows the progression of fibre fractions shown [8]. The TPU-polysiloxane exhibited a peak at *ca.* 350 °C, and a shoulder about *ca.* 450 °C in the

derivative mass curve as shown in Figure 7.5(b). Similar trends were observed for both bio-composites, which showed same peak and shoulder.

7.3.4 Stress–strain tensile mechanical analysis

As per the ASTM E 111-97 standard, the elastic modulus (E) was taken from the initial slope of the stress–strain curve (0.25 % strain). The value of E was lowest for the pure TPU-polysiloxane (0.3 MPa) and highest for the 20 %·w/w CFF composite via precipitation technique (2.2 MPa), presumably because the flexibility of the bio-fibres allowed for transfer of stress [9]. This means that the pure TPU-polysiloxane was the most flexible substance and the 20 %·w/w CFF was a stiffer, but still elastic, composite (Table 7.3).

Table 7.3: DMA data of TPU-polysiloxane and 20 %·w/w CFF composites via casting and precipitation techniques

DMA Data	Composites		Precipitation TPU-polysiloxane	
	Casting TPU-polysiloxane		CFF	CFF
	CFF 0 %·w/w	CFF 20 %·w/w	0 %·w/w	20 %·w/w
Elastic Modulus (E) (MPa)	0.3	1.8	0.3	2.2
Strain at maximum force (%)	8.8	1.7	10.4	1.3
Minimum strain (%)	1.7	0.6	1.6	0.6
Recovery strain (%)	7.1	1.1	8.8	0.7
Relative recovery strain (%)	81	65	85	54
Storage Modulus (E') (GPa) at 25 °C	0.2	1.3	0.3	1.6
Loss modulus (E'') Peak (MPa) at 25 °C	31	154	87	212
Loss Tangent ($\tan\delta$) at 25 °C	0.2	0.2	0.3	0.2

Stress–strain tensile mechanical analysis was used to characterise and compare the mechanical performance of the pure TPU-polysiloxane and 20 %·w/w CFF bio-composites as presented in Figure 7.6.

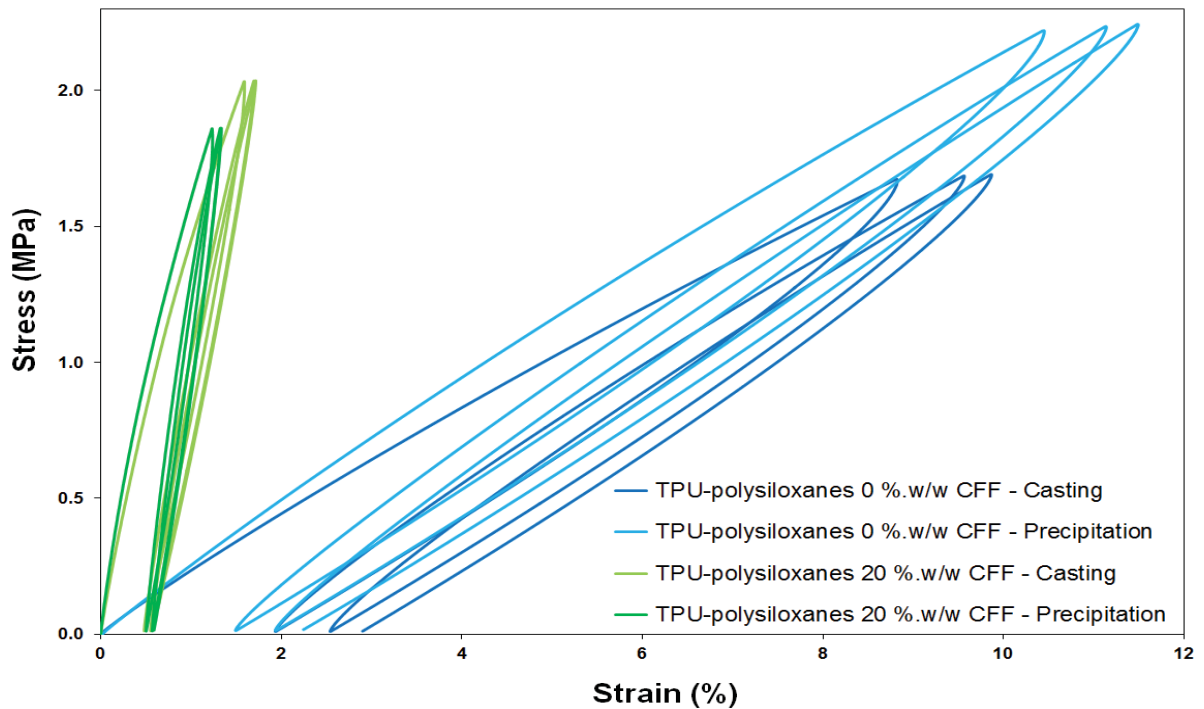


Figure 7.6: Stress–strain hysteresis tensile mechanical analysis of pure TPU-polysiloxane and 20 %·w/w CFF bio-composites via casting and precipitation techniques

Hysteresis loops, which present the reversible performance of the materials, are formed as stress to the composite is progressively increased and then decreased. The maximal strain value for the pure TPU-polysiloxane made via precipitation was 10.4 %. The incorporation of CFF diminished its elongation, with strain values decreasing to 1.3 % for 20 %·w/w CFF (Table 7.3). The change in the strain on recovery (max strain – final strain) was compared via the hysteresis loops [24]. There was a decrease in the recovery strain, or deformation once CFFs were added, this value made the composite more consistent and uniform with the least amount of deformation on recovery after stress compared with pure TPU-polysiloxane - which had the higher deformation rate. Addition of CFF to the matrix decreased the relative recovery strain (%) (Recovery strain (%) / Strain at maximum force (%)) of the composites. The difference between the second and third stress hysteresis loops were more noticeable for pure TPU-polysiloxane than 20 %·w/w CFF bio-composites. Slight deformation upon

straining showed equal properties upon dynamic cycling.

7.3.5 Modulated force – thermomechanometry

The mechanical properties of the TPU-polysiloxane reinforced bio-composites were studied using DMA. From these measurements the storage modulus (E') loss modulus (E'') and loss tangent ($\tan\delta$) were obtained at 25 °C. A material with high E' will not be elastic and hard, therefore, CFF reinforcement is likely to decrease the deformation of the TPU composites, since their E' was higher than that of the pure TPU-polysiloxane matrix. The E' value of the reinforced composites decreased, possibly due to the presence of the keratin that promoted intermolecular interactions that strongly reinforced the matrix and hence yielded good thermo-mechanical characteristics [8]. The E' of the TPU-polysiloxane bio-composites was most relevant at ambient temperature (*ca.* 25 °C), that E' of pure TPU-polysiloxane were 0.2 and 0.3 GPa, and 20 %·w/w CFF were 1.3 and 1.6 GPa for casting and precipitation methods, respectively. The E'' was again highest for 20 %·w/w CFF (212 MPa) via precipitation technique and lowest for the pure TPU-polysiloxane matrix (31 MPa) via casting method. Damping ($\tan\delta$) represents the ratio between the loss modulus and storage modulus (E''/E'), and depends on the fibre and matrix adhesion. Thus a weak fibre–matrix bonding will result in high $\tan\delta$ values [25, 26]. All the composites showed low $\tan\delta$ values of 0.2 to 0.3 at *ca.* 25 °C.

7.4 Conclusions

The ability to combine the advantageous properties of both CFF keratin and TPU polymer materials in a single material was evaluated in this study. Macro photographic images of the reinforced TPU-polysiloxane CFF bio-composites demonstrated effective

adhesion, minimal agglomeration (especially in the 20 %·w/w CFF bio-composites prepared via precipitation) and an even distribution of fibres that reflected the compatibility between the CFF reinforcement and the TPU matrix.

Addition of CFFs to TPU-polysiloxane enhanced char formation and heat resistance elastic modulus, storage modulus and loss modulus of the bio-composite, as the mass loss, loss tangent, and recovery strain of the composites decreased, compared with the pure TPU-polysiloxane. More enhancements in the thermo-mechanical properties of raw TPU-polysiloxane and TPU-polysiloxane CFF bio-composites were observed with the precipitation technique demonstrated better thermo-mechanical properties than the casting method. This study illustrates the potential for creating novel bio-composites, by incorporating agricultural waste such as CFs into a polymer matrix to form useful materials.

7.5 References

1. Wang, L., Q. Ji, T. Glass, T. Ward, J. McGrath, M. Muggli, G. Burns, and U. Sorathia, *Synthesis and characterization of organosiloxane modified segmented polyether polyurethanes*. *Polymer*, 2000. **41**(13): p. 5083-5093.
2. McGrath, J.E. and J.E. McGrath, *Block Copolymers: Overview and Critical Survey*. 1977: Academic Press.
3. Woods, G., *The ICI polyurethane book 2nd ed.* 1990, John Wiley & Sons, New York. p. p. 24.
4. AorTech International plc. *Best in Class Biostable Co-Polymer*. 23 January 2017]; Available from: <https://www.aortech.net/our-polymer-technology/elast-eon/>.
5. Ho, T.-H. and C.-S. Wang, *Modification of epoxy resins with polysiloxane thermoplastic polyurethane for electronic encapsulation: I*. *Polymer*, 1996. **37**(13): p. 2733-2742.
6. Tyagi, D., I. Yilgör, J. McGrath, and G. Wilkes, *Segmented organosiloxane copolymers: 2 Thermal and mechanical properties of siloxane—urea copolymers*. *Polymer*, 1984. **25**(12): p. 1807-1816.
7. Barone, J.R. and W.F. Schmidt, *Effect of formic acid exposure on keratin fiber derived from poultry feather biomass*. *Bioresource technology*, 2006. **97**(2): p. 233-242.
8. Flores-Hernández, C.G., A. Colín-Cruz, C. Velasco-Santos, V.M. Castaño, J.L. Rivera-Armenta, A. Almendarez-Camarillo, P.E. García-Casillas, and A.L. Martínez-Hernández, *All green composites from fully renewable biopolymers: Chitosan-starch reinforced with keratin from feathers*. *Polymers*, 2014. **6**(3): p. 686-705.

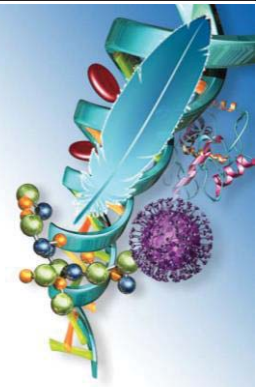
9. Martínez-Hernández, A.L., C. Velasco-Santos, M. de-Icaza, and V.M. Castaño, *Dynamical–mechanical and thermal analysis of polymeric composites reinforced with keratin biofibers from chicken feathers*. Composites Part B: Engineering, 2007. **38**(3): p. 405-410.
10. Dutta, S. and N. Karak, *Synthesis, characterization of poly(urethane amide) resins from Nahar seed oil for surface coating applications*. Progress in Organic Coatings, 2005. **53**(2): p. 147-152.
11. Barone, J. and W. Schmidt, *Polymer composites containing keratin*. 2005, U.S. Patent 20050148703 A1.
12. Gregg, K., S. Wilton, D. Parry, and G. Rogers, *A comparison of genomic coding sequences for feather and scale keratins: structural and evolutionary implications*. The EMBO journal, 1984. **3**(1): p. 175.
13. Roy, A., A. Kucukural, and Y. Zhang, *I-TASSER: a unified platform for automated protein structure and function prediction*. Nature protocols, 2010. **5**(4): p. 725-738.
14. Yang, J. and Y. Zhang, *I-TASSER server: new development for protein structure and function predictions*. Nucleic acids research, 2015. **43**(W1): p. W174-W181.
15. Padsalgikar, A., *Biostable polyurethanes*. 2014: United States.
16. Nair, K.M., S. Thomas, and G. Groeninckx, *Thermal and dynamic mechanical analysis of polystyrene composites reinforced with short sisal fibres*. Composites Science and Technology, 2001. **61**(16): p. 2519-2529.
17. Spoljaric, S. and R.A. Shanks, *Novel polyhedral oligomeric silsesquioxane-substituted dendritic polyester tougheners for linear thermoplastic polyurethane*. Journal of Applied Polymer Science, 2012. **126**(S2): p. E440-E454.
18. Martínez-Hernández, A.L., C. Velasco-Santos, M. De Icaza, and V.M. Castano, *Microstructural characterisation of keratin fibres from chicken feathers*. International journal of environment and pollution, 2005. **23**(2): p. 162-178.
19. Popescu, C. and P. Augustin, *Effect of chlorination treatment on the thermogravimetric behaviour of wool fibres*. Journal of thermal analysis and calorimetry, 1999. **57**(2): p. 509-515.
20. Saucedo-Rivalcoba, V., A. Martínez-Hernández, G. Martínez-Barrera, C. Velasco-Santos, and V. Castaño, *(Chicken feathers keratin)/polyurethane membranes*. Applied Physics A, 2011. **104**(1): p. 219-228.
21. Mathew, S., M. Brahmakumar, and T.E. Abraham, *Microstructural imaging and characterization of the mechanical, chemical, thermal, and swelling properties of starch–chitosan blend films*. Biopolymers, 2006. **82**(2): p. 176-187.
22. Espíndola-González, A., A.L. Martínez-Hernández, F. Fernández-Escobar, V.M. Castaño, W. Brostow, T. Datashvili, and C. Velasco-Santos, *Natural-synthetic hybrid polymers developed via electrospinning: the effect of PET in chitosan/starch system*. International journal of molecular sciences, 2011. **12**(3): p. 1908-1920.
23. Wan, Y., X. Lu, S. Dalai, and J. Zhang, *Thermophysical properties of polycaprolactone/chitosan blend membranes*. Thermochimica Acta, 2009. **487**(1): p. 33-38.
24. Czajka, M., R.A. Shanks, and D. Oldfield, *Carbon Monoxide Reduced Low-Defect Graphene Nanocomposites with Poly(styrene-*b*-butadiene-*b*-styrene) Composites*, in *Society of Plastic Engineers Annual Technical Conference (SPE-ANTEC)*. 2015: Orlando, Florida, USA. p. 419-423.

25. Andreopoulos, A. and P. Tarantili, *Study of the off-axis properties of composites reinforced with ultra high modulus polyethylene fibres*. European polymer journal, 1999. **35**(6): p. 1123-1131.
26. Chen, L. and M. Wang, *Production and evaluation of biodegradable composites based on PHB-PHV copolymer*. Biomaterials, 2002. **23**(13): p. 2631-2639.

7.6 Publication from this Chapter

- Pourjavaheri, F., Jones, O.A.H., Martinez Pardo, I., & Shanks, R. A. "Keratin-fibre polysiloxane-polyurethane bio-composites" *Green Chemistry*. To be submitted in 2017.
- Pourjavaheri, F., Jones, O.A.H., Martinez Pardo, I., Sherkat, F., Gupta, A., & Shanks, R.A. (2017) "Keratin bio-composites with polysiloxane thermoplastic polyurethane", *Society of Plastic Engineers Annual Technical Conference (SPE-ANTEC)*, 8-10 May, Anaheim, California, USA.
- Pourjavaheri, F., Jones, O.A.H., Martinez Pardo, I., Sherkat, F., Gupta, A., & Shanks, R.A. (2017) "Design and characterisation of keratin composites", *Society of Plastic Engineers Annual Technical Conference (SPE-ANTEC)*, 8-10 May, Anaheim, California, USA. (Poster Presentation)

CHAPTER 8



EXTRACTION OF KERATIN FROM CHICKEN FEATHER FIBRES

8.1 Introduction

A priority for sustainable chemical processes is design of chemical products that reduce or eliminate hazardous substances [1]. Green chemistry will direct the development of next generation materials, products and processes [2]. Bio-polymers based on renewable agricultural bio-mass form the basis for a portfolio of sustainable, eco-efficient products that can compete and capture markets currently dominated by products based exclusively on ecologically destructive processes [2].

Feather keratins are small proteins, uniform in size, with a molar mass reported to be 10-36 kg/mol [3-9]. The peculiar structure of keratin confers insolubility, mechanical stability and resistance of feathers to common proteolytic enzymes and chemicals [10]. However, keratins are stabilised by many of intra- and inter-molecular disulfide cross-links plus other protein structural features, such as hydrogen-bonding and crystallinity. Their high strength and stiffness is because of many cysteine residues in the polypeptide backbone, which form multiple disulfide bonds [3]; leading to insolubility in polar liquids such as water, weak acids and bases, as well as in dipolar aprotic liquids [11]. Keratin can be made soluble and reactive if the cysteine units are reduced, oxidised or hydrolysed [3, 12, 13]; Keratin displays non-covalent interactions (electrostatic forces, hydrogen bonds, hydrophobic forces) and covalent interactions (disulfide bonds), which must be disrupted to facilitate dissolution of feathers [12]. Keratin molecular chains provide tight packing of alpha (α) helix and beta (β) sheet structures, which makes keratin difficult to extract and dissolve in water or most organic solvents [4]. The reduction method is commonly used for extraction, due to its efficiency in breaking disulfide cross-links [4]. The function of reducing agents is to cleave the disulphide links and decrease the stability of keratin fibres in

the solid form found in feathers, then an alkaline solution can overcome hydrogen bonds and salt linkages of the keratin fibres. This will allow proteases to have access to the polypeptide backbone and degrade the amide linkages resulting in short water-soluble peptides [14, 15]. However, a large amount of reductive or oxidative agents, such as thiols and peroxides, must be used for breaking the disulfide bonds, and these reagents cannot be recycled, are harmful, often toxic and difficult to handle [12, 16]. Physical and chemical keratin extraction methods require considerable energy investments [17]. Thus, researchers have focused on finding simple and eco-friendly processing methods to dissolve feather keratin [12]. From an environmental view, enzymatic hydrolysis is the most attractive method, due to relatively mild treatment conditions and preservation of functional properties of the hydrolysates [15].

This study found that chicken feathers consist of 50 %·w/w fibre (barbs and barbules) and 50 %·w/w quill (calamus and rachis), in agreement with the literature [18-21]. The quill fraction is composed of more β -sheet than α -helix whereas the feather fibre has a higher proportion of α -helix compared with β -sheet [22]. Recently, various attempts have been made to develop methods for the extraction of keratin from CFF, including hydrothermal [15, 23], physicochemical (oxidative and reductive chemistry) [11, 14], chemical (ionic liquids) [12, 24, 25], and biochemical (enzymatic hydrolysis) [4, 26] methods. The focus of prior investigations has been fairly narrow as there is relatively little-published data on the general characterisation and behaviour of CFF α -helix, β -sheet and whole CFF keratin. An objective was to produce chicken feather keratin (CFK), compare it with α -helix and β -sheet enriched keratin, then characterise several aspects of their behaviour that may have implications for its general use as a biomaterial. An objective was to develop an appropriate procedure to

extract keratin from CFF with low environmental impact [15]. Therefore, dissolution of keratin in L-cysteine solution was explored, which is a newly developed, environmentally sustainable methodology compared with the sodium sulphide method [14]. Then the structures and properties of both regenerated keratins were characterised using sodium dodecyl sulfate-polyacrylamide gel electrophoresis (SDS-PAGE), liquid chromatography-mass spectrometry (LC-MS/MS), vibrational spectroscopic analysis (including FTIR and Raman), solid-state nuclear magnetic resonance (NMR), and thermogravimetry (TGA).

8.2 Experimental

8.2.1 Materials

All materials used are detailed in Chapter 3 (Table 3.2).

8.2.2 Chicken feather preparation

The CFFs were purified from stains, oil, dirt and pathogens according to the ethanol-extraction purification method detailed in Chapter 4. This step has influence on the molar mass of the final extracted keratin [8]. Barbs and barbules (α -helix structure) of CFFs were stripped off the calamus and rachis (β -sheet structure) fibres.

8.2.3 Extraction of keratin

Ground CFF a) whole feather, b) calamus and rachis, c) barbs and barbules, were added separately at ratios of 1:20 (for complete immersion) to 100 mL of aqueous solutions containing A) 0.5 mol/L sodium sulfide (Na_2S) solution or B) 8 mol/L urea (NH_2CONH_2) and L-cysteine (0.165 mol/L), adjusted to pH 10.5 using NaOH

(2 mol/L) (dissolving step). The formulation of the aqueous Solutions-A and -B were based on previous studies by Gupta et al. [27] and Xu and Yang [28], respectively. To avoid severe peptide bond scission and, therefore, to obtain high-quality keratin with suitable molar mass, the process conditions reported here have been optimised. The solutions containing the feather parts were conditioned at 40 ± 1 °C and $60 \pm 2\%$ RH with continuous stirring using a magnetic stirrer at 300 rpm for 6 h (Figure 8.1).



Figure 8.1: The extraction process of keratin from waste chicken feathers using sodium sulfide and L-cysteine

The solution was then centrifuged at 10,000 rcf for 20 min at 10 °C. The supernatant liquid was collected and the solid part containing particles was discarded.

Hydrochloric acid (7 mol/L) was added to the solution until a pH of 4 [29, 30] (isoelectric-point (pI) of keratin) was obtained (precipitation step). The solution was then left without heating or stirring for 2 h, to precipitate the proteins [31]. Precipitated keratin was washed three times with deionised water, filtered and the surface water was removed using a filter paper. The solid precipitated keratin particles were dried in a 40 °C oven to obtain keratin powders using a Rocklabs Ringmill Grinder (equipped with a zirconia mill head) for up to 3 min, then stored in sealed light-sensitive glass containers, at 4 °C before being analysed and characterised. Each experiment was carried out in triplicate.

8.2.4 Yield calculation

The keratin yield and weight loss were determined according to the following formulas:

$$\begin{aligned}\text{Keratin yield} &= (W_{fk} / W_{ik}) \times 100 (\%) \\ \text{Keratin loss} &= ((W_{ik} - W_{fk}) / W_{ik}) \times 100 (\%) \\ \text{Total weight loss} &= ((W_i - W_f) / W_i) \times 100 (\%)\end{aligned}$$

where W_{ik} and W_{fk} refer to keratin weight initially and after extraction, respectively, and W_i and W_f stand for the initial CFF weight and final weight of the extracted keratin, respectively [32].

8.2.5 Characterisation of keratin

8.2.5.1 Biuret test

The keratin solutions collected from the final precipitated keratin solution were mixed with 1 %·w/v potassium hydroxide solution at a 1:1 ratio, followed by dropwise addition of 1 % copper sulphate solution for detecting the presence of peptide bonds, which are identifiable by forming a violet-colored solution. Changes in the solution were observed and

images taken.

8.2.5.2 Keratin concentration

The concentration of the keratin solutions was determined spectrophotometrically prior to estimating their molar mass with uv-vis absorbance, using a BioPhotometer plus (Eppendorf, AG, Hamburg, Germany) spectrophotometer, at 280 nm. In addition, the keratin content was measured as per the Bradford assay procedure [33].

8.2.5.3 Sodium dodecyl sulfate-polyacrylamide gel electrophoresis

The molar masses of the extracted keratins were estimated using sodium dodecyl sulfate-polyacrylamide gel electrophoresis (SDS-PAGE) technique. Approximately 1 mg of the experimental keratins were dissolved separately in 1 mL of solution containing 8 mol/L urea, 50 mM tris, and 0.1 mol/L β -mercaptoethanol at pH 8.4. Keratin solutions concentrations were measured as described. Then *ca.* 1 μ g was mixed with a 5x loading buffer (containing 10 %·v/v SDS, 250 mM tris-HCl buffer (pH 6.8), 50 %·v/v glycerol, 0.5 mol/L dithiothreitol (DTT), and 0.02 %·w/v bromophenol blue) at a ratio of 4:1. The solutions in Eppendorf tubes were heated in a dry bath-heating block at 95 °C for 5 min. The stacking and the separating gels were 4 % and 15 % polyacrylamide, respectively. Electrophoresis voltage used was 60 V for 30 min, followed by 180 V for 50 min. After electrophoresis, the gel was washed with distilled water and stained with a staining solution containing 40 %·v/v methanol, 10 %·v/v acetic acid, and 0.05 %·w/v Coomassie brilliant blue R-250). The specimens were de-stained with a destaining solution (10 %·v/v ethanol and 10 %·v/v glacial acetic acid). A protein standard (precision plus protein standards, unstained, BIO-RAD) was used for calibration.

8.2.5.4 Proteomic analysis

8.2.5.4.1 LC-MS/MS

Extracted keratin (1 μ g) from whole CFF under L-cysteine, was processed by SDS-PAGE using a 15 % gel and the tris-glycine buffer system. The 11 kg/mol protein band observed in the Coomassie stained gel was excised and processed for proteomic analysis.

The destained gel piece was reduced with 10 mM DTT in 55 mM triethylammonium bicarbonate (TEAB) (55 °C for 45 min) and alkylated with 55 mM iodoacetamide made up in 50 mM TEAB (incubated at room temperature (in the dark for 30 min). The keratin was then incubated with 200 μ g/ μ L sequencing grade trypsin (Sigma Aldrich) (incubated at 37 °C overnight). The digestion was stopped by the addition of formic acid (FA) to a final concentration of 1 % w/v and dried in a vacuum centrifuge.

The digested keratin was analysed by liquid chromatography–mass spectroscopy (LC-MS/MS, Thermo Scientific) using a Q-Exactive mass spectrometer (Thermo Scientific).

8.2.5.4.2 MS data analysis

The UniProt database was used to search the chicken protein data that were searched against the chicken (*Gallus gallus*) UniProt database using MASCOT (Matrix Science Ltd., London, UK). The search parameters were restricted to the following: assuming trypsin enzyme with two missed cleavages, fixed modifications of carbamidomethyl (c), variable modifications of oxidation (M), a fragment ion mass tolerance of 0.20 g/mol (Da), and peptide mass tolerance of 20 ppm. Only proteins with at least two peptides (filter by ion score \geq 20) uniquely assigned to the respective sequence were considered identified.

8.2.5.5 Fourier-transform infrared spectroscopy

The chemical structures of keratin powders were analysed by FTIR spectroscopy, as detailed in Chapter 3 (section 3.3.5).

8.2.5.6 Vibrational spectroscopic analysis

Raman spectroscopy of the keratin powders was conducted as detailed in Chapter 3 (section 3.3.6).

8.2.5.7 Nuclear magnetic resonance spectroscopy (solid-state)

The CFK were separated into three groups; α - and β -keratin (whole feathers), α -keratin enriched (barbs/barbules only), and β -keratin enriched (calamus/rachis only). The keratins were ground into a powder using a Rocklabs Ringmill Grinder (with a zirconia mill head) for 3 min. NMR spectra were externally referenced to adamantane (δ_C 29.2). The NMR spectra were acquired with an Agilent DD2 500 MHz NMR spectrometer equipped with a 4 mm MAS solid-state triple resonance probe. Spectra for the feather keratins were acquired at a spin rate of 10 kHz, 4 (proton) or 4000 (carbon) scans, and a delay time of 5 s (section 3.3.4).

8.2.5.8 Thermogravimetry

A PerkinElmer TGA (Pyris 1) Thermogravimetric Analyser (Melbourne, Australia) was employed to evaluate thermal degradation, mass loss and its derivative as a function of temperature, remaining char ratio, and the changes in degradation behaviour associated with CFF keratin. The mass loss curve was recorded between 30 °C and 750 °C under a nitrogen purge (20 mL/min) and between 750 °C and

850 °C under an air purge (20 mL/min) at a heating rate of 20 K·min⁻¹. To minimise the effect of thermal lag, a small sample mass of *ca.* 2 mg was chosen.

8.3 Results and discussion

8.3.1 Reduction of disulfide bonds

Limited efforts have been made on fundamental understanding of CFK that contains high amount of cysteine residues along the polypeptide backbone [3]. These cysteine residues form disulfide links between keratin molecules limiting conformation (α -helix and β -sheet) and rendering the keratin insoluble. Keratin with disulphide cross-links is insoluble in water but it becomes soluble in the presence of reducing agents that can release the disulphide cross-links. Both disulfide cross-link reduction and solubility in water increase with temperature. Keratin solubility in sodium sulphide solution is further increased by a high pH (about 12) which is much higher than the keratin pI. Hence, as per Khosa and Ullah [3] pragmatic research is required to investigate how the cysteine–cysteine cross-links can be disrupted after experimental and theoretical identification of scientific gap in such cross-links.

Keratin with disulphide cross-links is insoluble in water, and its solubility in water increases at higher temperature in the presence of reducing agents [3]. On reduction, the disulfide (–S–S–) cross-links in hydrophilic Solution-A were split into free thiols (-SH), along with protonation of some –NH₂ (this can only occur in acid solution; in alkali the –COOH groups react to form –COO⁻ making the keratin surface negative) and other groups in keratin making its surface positive and, therefore, solubilisation took place [3], by a chemical reduction using sodium sulfide solution as a reducing agent.

To break disulfide bonds of keratins in Solution-B, a swelling agent, urea, was used to denature the compact crystal structure of keratin, crystals became amorphous and the disulfide bonds were exposed to the L-cysteine, therefore allowing them to be reduced.

Reduced keratin from both the A- and B-Solutions were dissolved in water or urea-water solution, respectively. After addition of HCl, the NH₂ groups will be protonated, though at pI the positive and negative groups should be neutralised or equal, hence keratins were precipitated from solution. The salt produced using Solution-A and the urea in Solution-B were washed out in the last stage of extraction (i.e. washing stage). These reactions are shown in Figure 8.2.

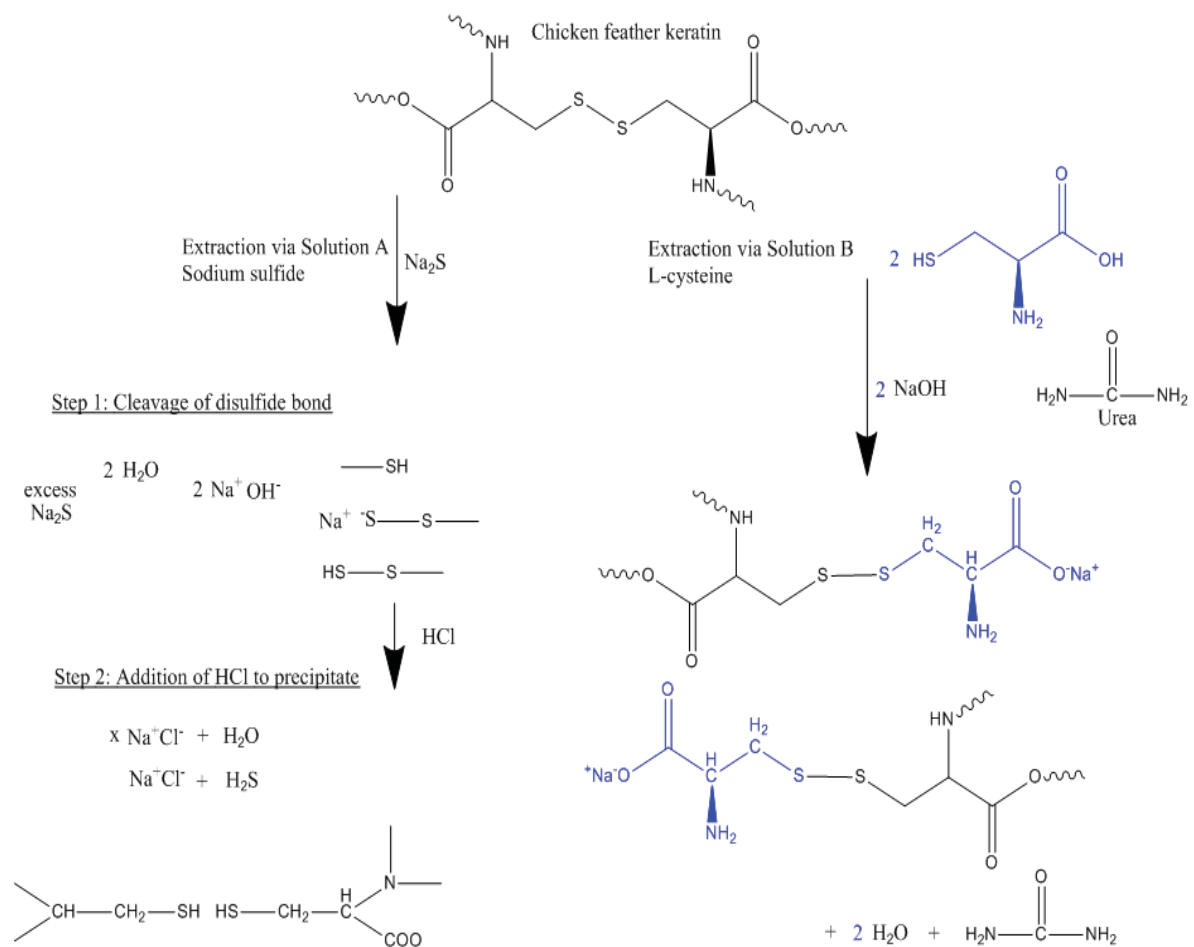


Figure 8.2: Reducing disulfide bonds of chicken feather keratin via Solutions-A and -B

8.3.2 Yield analysis

The yield was calculated based on total available keratin in chicken feathers, which is known to be *ca.* 91 % [11, 34, 35] of total feather mass. The keratin yields were *ca.* 88 ± 3 % and 66 ± 4 % and the weight loss were determined as shown in Table 8.1.

Table 8.1: The keratin yield analysis

Yield and loss	Extracted with sodium sulfide (%)	Extracted with L-cysteine (%)
Keratin yield	88 ± 3	66 ± 4
Keratin loss	12 ± 0.4	44 ± 3
Total weight loss	20 ± 3	40 ± 4

The weight loss in keratin extraction was 20 % under sodium sulfide and 40 % under L-cysteine, attributable to feathers containing 1 % lipid and 7 % water [11, 34, 35] additional to the 91 % keratin mentioned above. Therefore, only 12 ± 0.4 % and 44 ± 3 % keratin, respectively, has been lost during the extraction process, which can be due to incomplete precipitation, loss of keratin during changing containers, or in the washing process. However, an 88 ± 3 % yield via sodium sulfide is considered high, and is 22 % more than was achieved by the L-cysteine method, which is because less keratin was precipitated by HCl due to the presence of urea.

8.3.3 Characterisation of the extracted chicken feather keratin

8.3.3.1 Biuret test

The biuret test was employed to detect the existence of peptide bonds, since in the presence of peptides, a copper (II) ion forms a violet-colored complex in an alkaline solution and it is readily quantitative [36]. Figure 8.3, demonstrated the keratin solutions produced from whole, β -sheet and α -helix CFFs, using sodium sulfide and L-cysteine solutions.

The more peptide bonds that were present, the more intense was the purple colour produced. The diversity between the purple colours of the different solutions was visible, in accordance with the absorbance of biuret solution and amount of protein obtained, the higher the amount of chicken feather dissolved the more protein obtained.

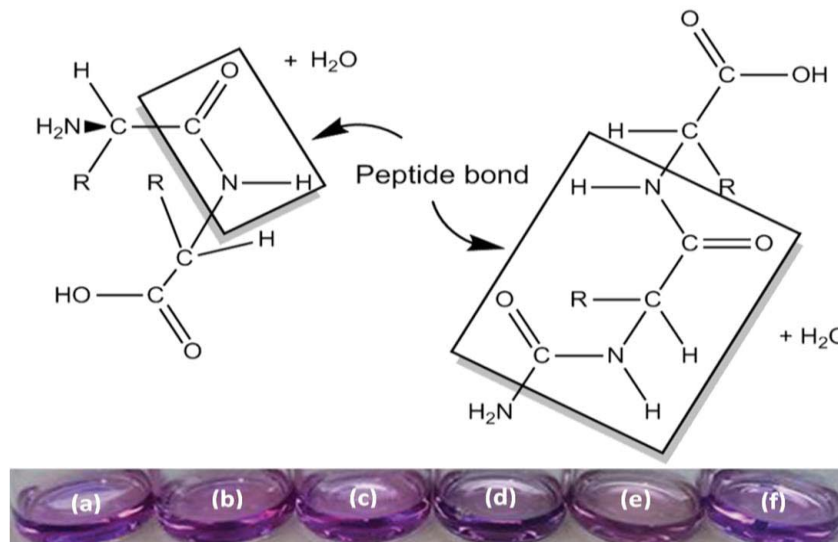


Figure 8.3: The peptide bond in the biuret solution caused a violet colour in different keratin solutions containing CFF in Na₂S (a) whole, (b) β-sheet, (c) α-helix, and in L-cysteine (d) whole, (e) β-sheet, (f) α-helix

8.3.3.2 Keratin concentration

The concentration of keratin was measured as shown in Table 8.2. The results of both protein concentration methods were comparable. However, the amount of keratin was estimated higher within the methods extracted using sodium sulfide than L-cysteine, due to the existence of urea in the latter system.

Table 8.2: Estimated concentrations of extracted keratins (via BioPhotometer plus Eppendorf spectrophotometer and Bradford assay)

Extraction method	Spectrophotometer (mg/mL)	Bradford assay (mg/ mL)
whole CFFs in Na ₂ S	1.08	1.48
β-sheet CFFs in Na ₂ S	3.78	4.81
α-helix CFFs in Na ₂ S	1.98	1.87
whole CFFs in L-cysteine	0.13	0.32
β-sheet CFFs in L-cysteine	0.15	0.45
α-helix CFFs in L-cysteine	0.02	0.16

8.3.3.3 Keratin molar mass

SDS-PAGE gel electrophoresis was used to estimate the average molar mass values of the isolated protein homologs, the patterns, and the purity of the keratin extracted via sodium sulfide and L-cysteine are shown in Figure 8.4. The molar mass of keratin was calculated by reference to standard markers [37].

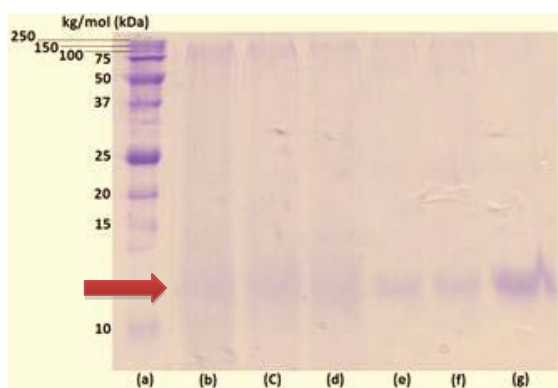


Figure 8.4: The SDS-PAGE patterns of (a) protein standard, and the various extracted CFK using Na₂S (b), α -helix (c) β -sheet, d) whole, and in L-cysteine (e) α -helix, (f) β -sheet, (g) whole. The red arrow indicates the main keratin bands at 11 kg/mol (11 kDa)

The SDS-PAGE data revealed that the extracted keratins form a major, diffuse cluster of bands *ca.* 11 kg/mol, which represented the molar mass of keratin obtained and suggests that there was no significant difference between the α -helix and β -sheet molar mass of CFF keratin. In addition, the molar mass did not change during the different keratin extraction processes (i.e. via sodium sulfide and L-cysteine) as they were all *ca.* 11 kg/mol. This was in agreement with LC-MS/MS outcomes of 11 kg/mol. According to Gregg et al [38], using the ExpASY Compute pI/Mw tool, the predicted molecular weight for chicken feather keratin was 10.032 kg/mol, which is close to our results. It is apparent from Figure 8.4 that the L-cysteine purification method produced a more distinct and discrete keratin banding pattern, which could be due to L-cysteine residues on the extracted keratins. The purity of the keratin from SDS-PAGE was estimated $\geq 95\%$ as clearly shown in Figure 8.4, lane (g). This

analysis demonstrated that keratin has been purified from chicken feathers to near homogeneity.

8.3.3.4 LC-MS/MS

In the *ca.* 11 kg/mol gel piece, there were three proteins namely type II keratin, which was the most abundant, histone and chicken hemoglobin subunit alpha A-protein. The molar mass of extracted keratin in LC-MS/MS technique confirmed that peptides matching the literature value were present and agreed with our SDS-PAGE results.

8.3.3.5 Infrared spectroscopy

The FTIR spectra of the keratins were compared with those from the purified CFF obtained from ethanol-extraction purification treatment, used in previous studies (Chapter 4). To examine the effects of different extraction processes on CFK, FTIR spectra were measured in the range of 4000–600 cm^{-1} for the extracted keratins via sodium sulfide and L-cysteine using whole, β -sheet and α -helix enriched keratins, and compared with six-month aged keratins as shown in Figure 8.5. Typical infrared spectra of purified CFF (Figure 8.5(a)) have been described in detail previously (Chapter 4 and 5). The characteristic peaks of the spectra of four keratins Figure 8.5(b to e) extracted via Solution-A (Figure 8.5(f)) were similar to the purified CFF that contained 91 % keratin [11, 34, 35] (Figure 8.5(a)). The processing methods have some effect on the chemical structure of proteins extracted via L-cysteine, as the spectra of four keratins (Figure 8.5(g) to (j)) extracted via Solution-B (Figure 8.5(k)), exhibited similar peaks that confirmed the existence of residual urea or L-cysteine in the extracts. The spectra of both L-cysteine and urea powders are given in Figure 8.5(l) and (m), respectively. The characteristic absorption bands are mainly assigned

to vibrations of the peptide bonds ($-\text{CONH}$) which are known as the amide A and I–III modes [12, 39, 40].

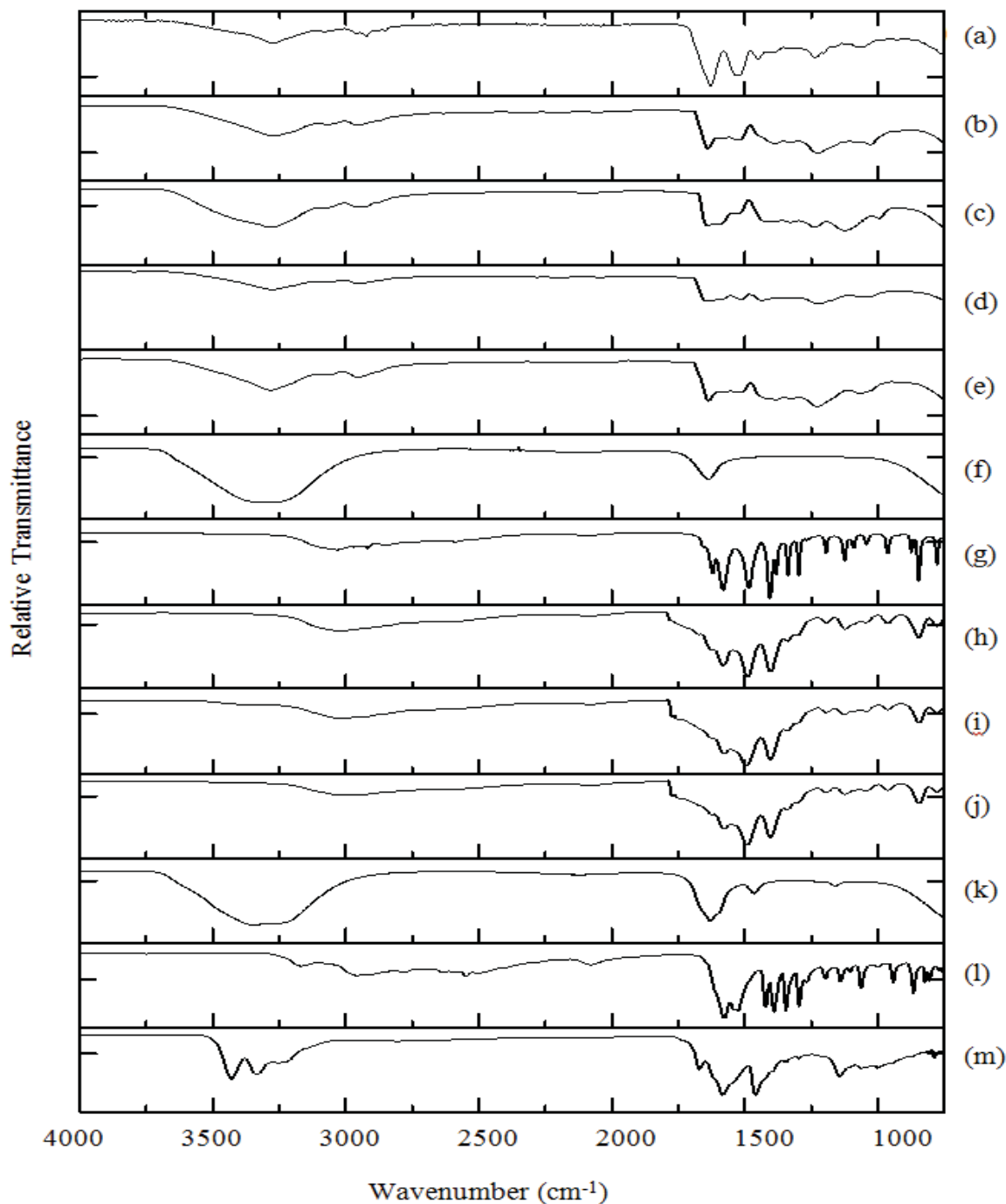


Figure 8.5: FTIR spectra of (a) purified CFFs, (b) keratin extracted from whole CFF via Na₂S aged after six-months, (c) keratin extracted from whole CFF via Na₂S, (d) keratin extracted from β -sheet parts of CFF via Na₂S, (e) keratin extracted from α -helix parts of CFF via Na₂S, (f) Solution-A, (g) keratin extracted from whole CFF via L-cysteine aged after six-months, (h) keratin extracted from whole CFF via L-cysteine, (i) keratin extracted from β -sheet parts of CFF via L-cysteine, (j) keratin extracted from α -helix parts of CFF via L-cysteine, (k) Solution-B, (l) L-cysteine powder, (m) urea powder

The broad absorption band region from 3500 cm^{-1} to 3200 cm^{-1} (amide A) indicates α -helix structure [4, 41-43], and the band at 3281 cm^{-1} is attributed to the stretching vibrations of O–H and N–H groups (amide A). Bands that fall in the range of $3000\text{--}2800\text{ cm}^{-1}$ originate from C–H stretching modes [15]. The band at 2923 cm^{-1} is attributed to the symmetrical CH_3 stretching vibration [44]. The FTIR spectra were analysed to evaluate any changes in the secondary structure of α -helix and β -sheet structure resulting from the urea treatment. The distinct absorption peaks in the wavenumber region of $1550\text{--}1750\text{ cm}^{-1}$ constitute the amide I region (Figure 8.5(h to j)), with characteristic peaks assigned to α -helical ($1650\text{--}1656\text{ cm}^{-1}$) and β -sheet ($1632\text{--}1641\text{ cm}^{-1}$, and 1695 cm^{-1}) structures, as corresponding to the model by Fraser et al. [45].

The peaks from $1700\text{--}1600\text{ cm}^{-1}$ [11, 46, 47] (amide I) originate mainly from C=O stretching vibrations and signify secondary structural elements such as α -helix and β -sheet [4, 41, 42], while the strong transmission band at 1630 cm^{-1} is assigned to C–O stretching [40]. The amide II region from $1580\text{--}1480\text{ cm}^{-1}$ [11, 15] is derived from N–H bending and C–H stretching [12, 40]. There is a weak band in the range of $1340\text{--}1220\text{ cm}^{-1}$, known as the amide III region and is due to the combination of C–N stretching, $\text{C}_\alpha\text{-H}$ deformations and N–H in-plane bending [48, 49] as well as some contribution from C–C stretching and C–O bending vibrations [50, 51]. It can be seen from Figure 8.5 that these bands exist in all extracted keratins. The amide I–III bands provide critical information on the protein conformation and backbone structure [4]. The N–H out-of-plane bending associated with the amide group occurs in a range between $750\text{--}600\text{ cm}^{-1}$ [43]. As the amide peaks cover the range from $1700\text{--}1220\text{ cm}^{-1}$, [46, 47] the C–O stretching vibration associated with the ester-linkage expected to occur around 1267 cm^{-1} [52] was undetectable. There was a significant change observed in the overlay of the FTIR spectra for the fresh (Figure 8.5(g)) and six-

months aged (Figure 8.5(h)) keratin extracted from whole CFF via L-cysteine, which is ascribed to L-cysteine residues. This was not the case for keratin extracted via sodium sulfide (Figure 8.5(b) and (c)) that was again confirmed by the Raman spectra.

8.3.3.6 Vibrational spectroscopic analysis

Raman spectra support the chemical disparity between keratin extracted via Na₂S and L-cysteine using whole, β -sheet and α -helix rich-segments of CFF, and when compared with six-month aged keratin (Figure 8.6). Raman spectra were recorded from rachis and calamus (β -sheet), barbs and barbules (α -helix) of chicken feathers as shown in Figure 8.6(a) and (b), respectively. It was found that the spectra obtained from the β -sheet enriched quill fraction showed several intense peaks at 1004, 1242, 1461 and 1667 cm⁻¹, which can similarly be observed for α -helix enriched quill fraction, however, the intensity of peaks varies as expected for a natural material. Typical spectra obtained from the β -sheet enriched quill fraction are in agreement with those obtained from quill by Akhtar and Edwards [53] and from rachis and calamus by Church et al. [54]. The strong peaks at 1241 and 1667 cm⁻¹ in the amide I and III bands indicate a dominant β -sheet structure [54, 55]. The α -helix part of CFF shows weak bands from 1610–1605 cm⁻¹ and at 1580 cm⁻¹ (Figure 8.6(b)), which may be indicative of stretching of the C=C bonds in the aromatic ring of tyrosine and phenylalanine, which comprise 1.4 and 3.1 %·w/w of feather keratin, respectively [53].

Raman spectroscopy has been used to monitor disulfide linkages in keratin [44, 53, 56]. The S-S bonds generate weak peaks in the 500–550 cm⁻¹ range of the spectrum. In this study, the disulfide stretching [53] vibrations of 510 cm⁻¹ and 526 cm⁻¹, were observed in Figure 8.6(a) and (b), respectively.

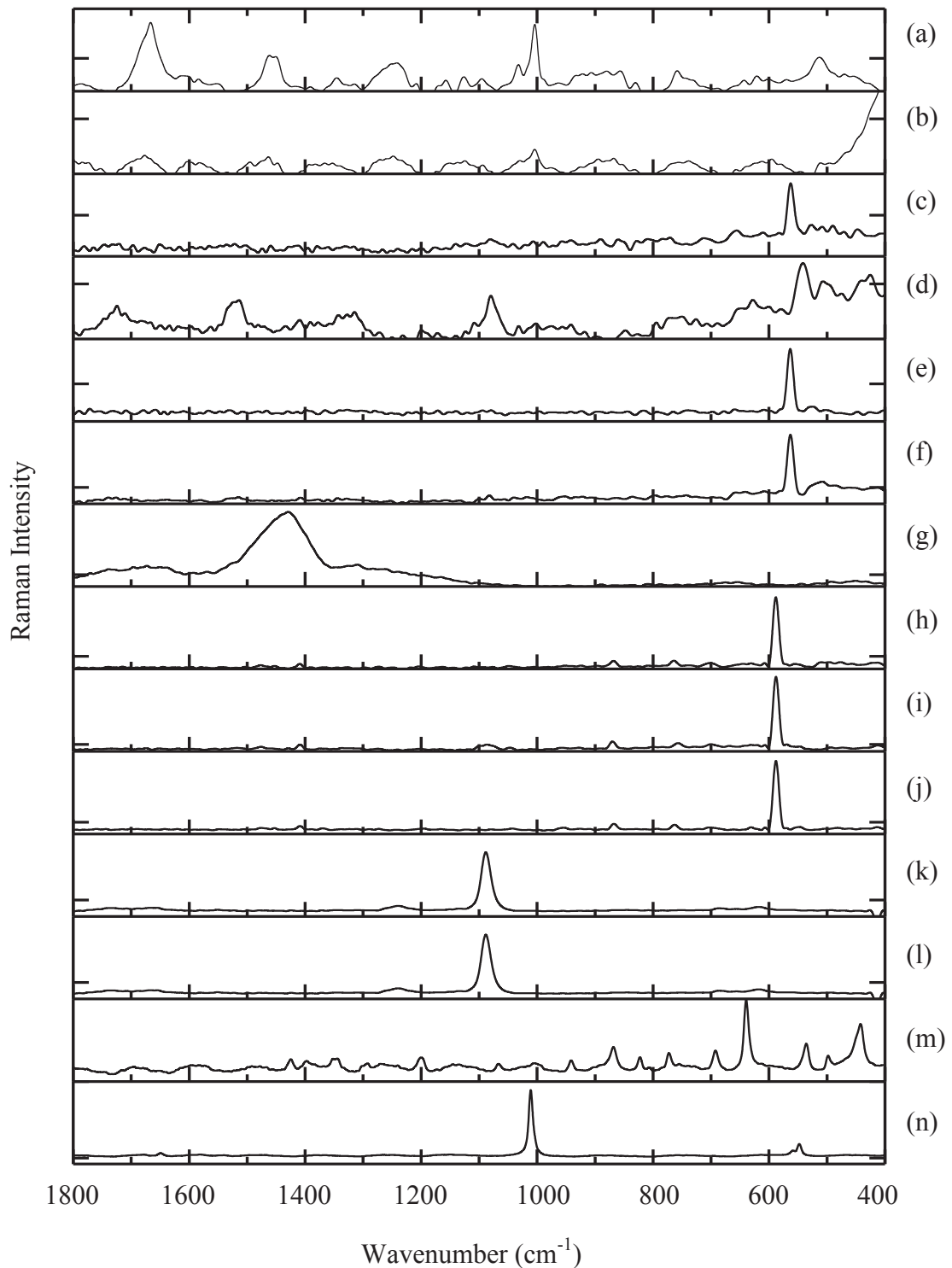


Figure 8.6: Raman spectra of (a) β -sheet parts of CFFs, (b) α -helix parts of CFFs, (c) keratin extracted from whole CFF via Na_2S aged after six-months, (d) fresh keratin extracted from whole CFF via Na_2S , (e) keratin extracted from β -sheet parts of CFF via Na_2S , (f) keratin extracted from α -helix parts of CFF via Na_2S , (g) Solution-A, (h) keratin extracted from whole CFF via L-cysteine aged after six-months, (i) keratin extracted from whole CFF via L-cysteine, (j) keratin extracted from β -sheet parts of CFF via L-cysteine, (k) keratin extracted from α -helix parts of CFF via L-cysteine, (l) Solution-B, (m) L-cysteine powder, (n) urea powder

Figure 8.6(c) and (d) represent fresh and six-month old keratins that have been extracted by Na_2S . The aging of keratin has resulted in Raman bands at 1080 cm^{-1} and 1514 cm^{-1} disappearing, with these Raman bands only appearing for fresh keratin. The band at 542 cm^{-1} has been shifted to 562 cm^{-1} indicating sulphur content changes over time. However, the extracted keratin from L-cysteine did not show any significance changes as result of aging, as is shown in Figure 8.6(h) and (i). The L-cysteine powder shows a strong peak at 588 cm^{-1} and similar peaks are observed in the spectra of extracted keratins though shifted to lower wavenumber for other keratins (Figure 8.6(h), (i) and (j)). However, the structure of keratin did not alter over six-months and was preserved by the L-cysteine method.

Raman spectra from both Na_2S extracted keratins (Figure 8.6(e) and (f)) showed strong peaks at 563 cm^{-1} and the rest of the spectra showed no significant differences. The mentioned peak diminishing in intensity for the keratin from α -helix segments of chicken feathers (Figure 8.6(k)) extracted via L-cysteine showed identical spectrum to mixture of urea and L-cysteine solution (Figure 8.6(l)) that was initially used to extract the keratin. The strong peak at 1088 cm^{-1} shows the existence of urea residues in the keratin. These Raman and infrared spectra both indicate that the effect of aging on keratin structure was not affected by the L-cysteine extraction method, which was not the case with the Na_2S method.

8.3.3.7 Solid-state NMR studies

The un-extracted chicken feathers were analysed via solid state NMR to characterize α -helix and β -sheet keratin, and to identify potential markers to distinguish between the two structures of keratin. These ^{13}C SSNMR results revealed characteristic NMR signals for amide carbonyl carbons of keratin protein ($\sim 170\text{ ppm}$), for aromatic groups from the amino acids tryptophan, tyrosine and phenylalanine in keratin ($\sim 129\text{ ppm}$), along with leucine

residues (~ 55 ppm, ~ 40 ppm and ~ 24 ppm) [14]. Comparison of the ^{13}C SSNMR spectra for the keratins showed no significant difference between the α - and β -keratin enriched keratins, which are attributed to the identical carbon-carbon connectivity in α - and β -keratin.

Figure 8.7 shows the ^1H SSNMR spectra for the un-extracted feathers. Whilst the ^{13}C SSNMR was unable to distinguish between the different feather segments, ^1H SSNMR was able to reveal small differences between the α -helix and β -sheet structures due to different hydrogen interactions. Figure 8.7(a) shows the ^1H SSNMR spectrum for α -helix enriched feather fibres. Two dominant broad signals are observed at ~ 0.6 and ~ 2.4 ppm, however the signal at ~ 2.4 ppm appears slightly sharper and with greater intensity. The β -sheet enriched quill fraction (Figure 8.7(b)) displays these two signals, however the signal at ~ 0.6 ppm appears with greater intensity than the signal at ~ 2.4 ppm. The whole feather containing both α - and β -keratin (Figure 8.7(c)) shows the presence of both signals in approximately equal proportion to one another, as would be expected for the whole chicken feather. This slight difference in the ^1H SSNMR spectra suggests that ^1H SSNMR could potentially be used as an analytical tool to distinguish between α -helix and β -sheet structures of keratin in different feather components. Seeing as the quill and feather fibre fractions are not pure α -helix or β -sheet keratin, but rather mixtures of both containing enriched fractions of one or the other, it is difficult to characterise the α -helix or β -sheet keratin independently. However, the ^1H SSNMR results suggest that pure α -helix keratin would result in one signal observed at ~ 2.4 ppm whilst pure β -sheet keratin would result in one signal observed at ~ 0.6 ppm.

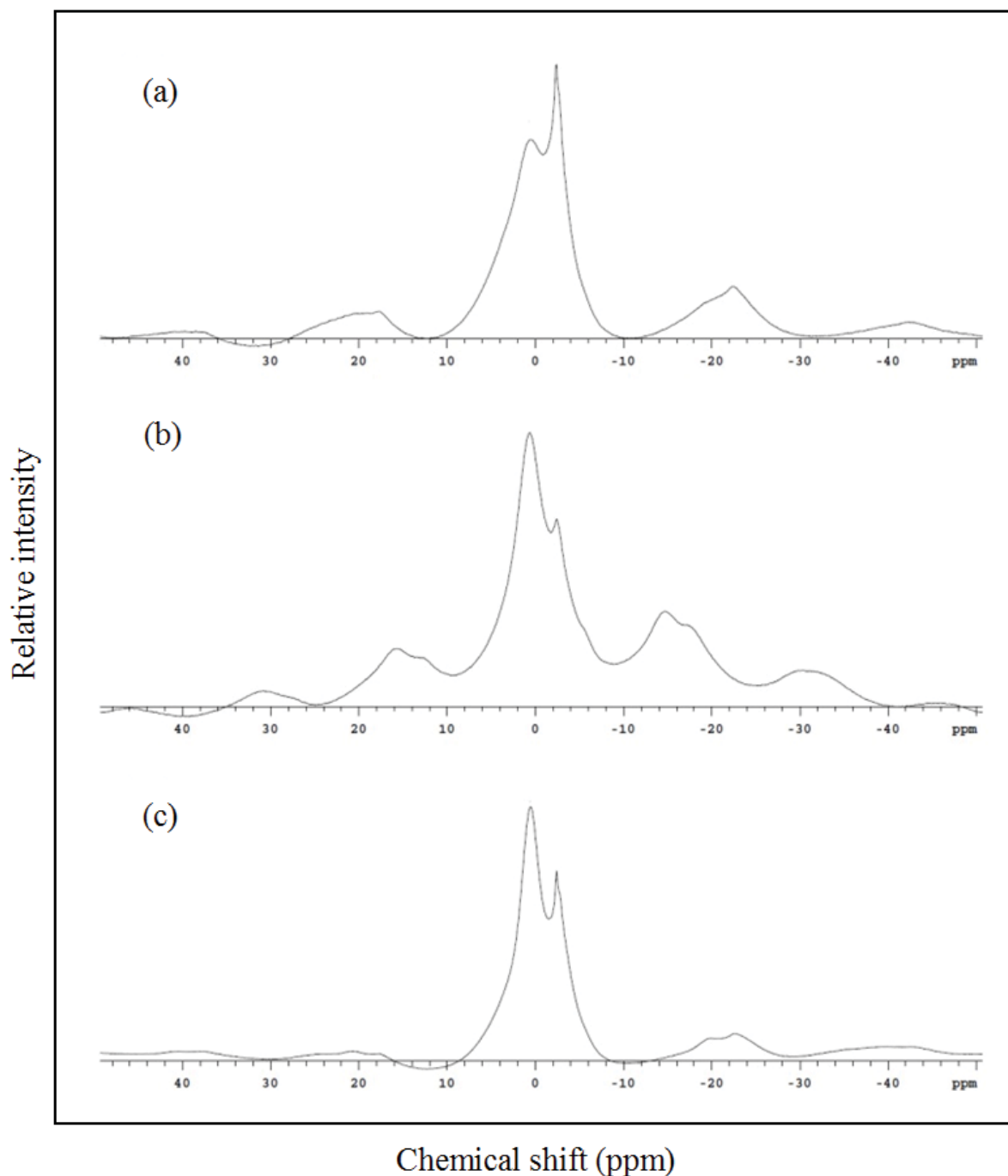


Figure 8.7: ^1H SSNMR spectra of chicken feathers (a) barbs and barbules (composed mainly of α -helix), (b) calamus and rachis (composed mainly of β -sheet structures), (c) whole feather

Figure 8.8 shows the ^1H SSNMR spectra for the feathers extracted using L-cysteine. A similar profile was observed when comparing the α -helix enriched and β -sheet enriched keratins. The α -helix enriched feather fibre displayed two signals at ~ 1.0 and ~ -2.4 ppm,

with the signal at ~ -2.4 ppm being more intense. The β -sheet enriched quill fraction displayed two signals at ~ 1.0 and ~ -2.4 ppm, with the signal at ~ 1.0 ppm being more intense.

The SSNMR spectra of extracted keratins agree with the spectrum of feathers prior to extraction. L-cysteine was detected in the extracted keratin. Conversely, residual urea was not detected.

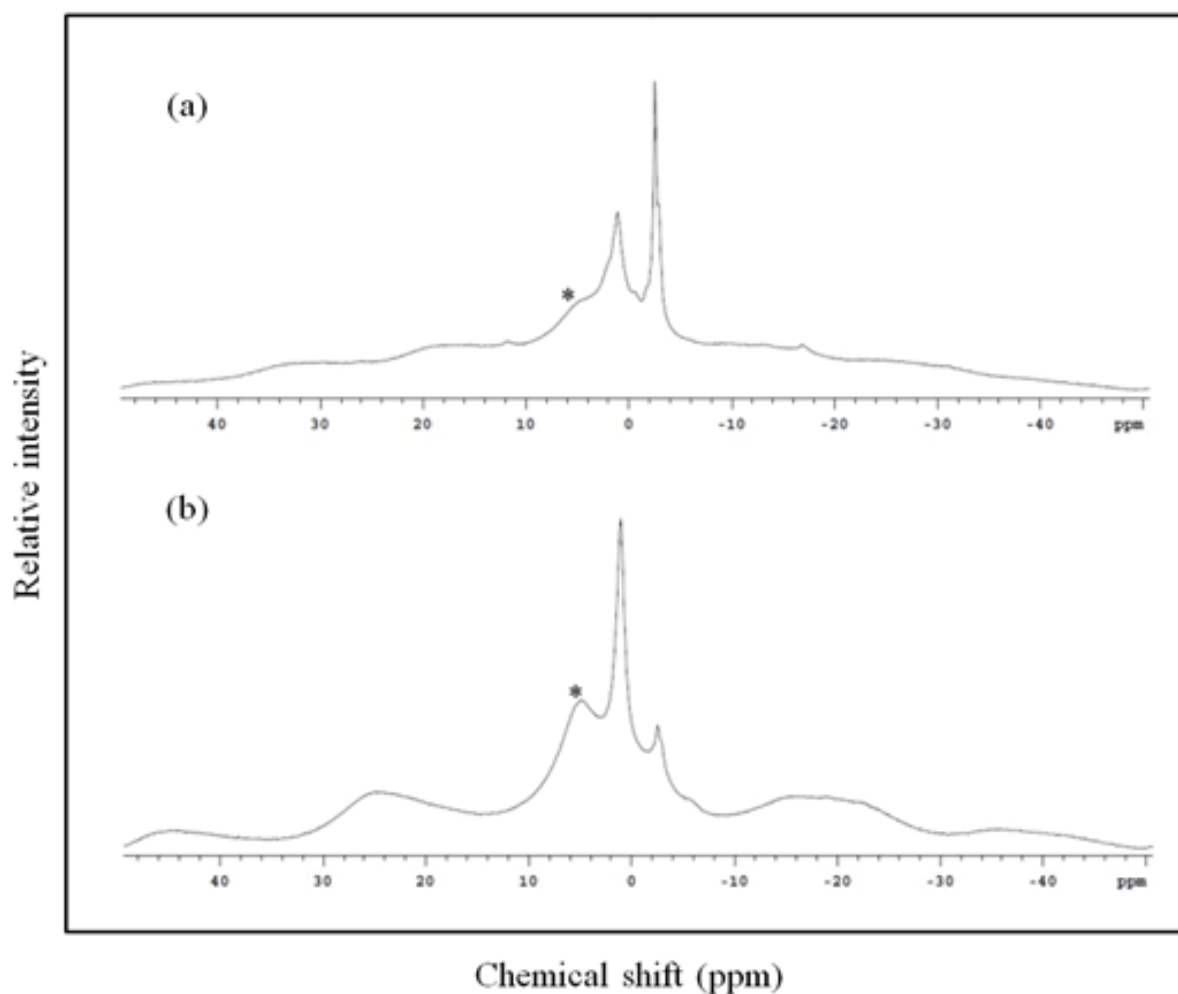


Figure 8.8: ^1H SSNMR spectra of extracted chicken feathers (a) barbs and barbules (composed mainly of α -helix), (b) calamus and rachis (composed mainly of β -sheet structures), and (asterisk indicates residual cysteine)

8.3.3.8 Thermal behaviour

Thermogravimetry of the purified CFF segments and extracted keratins are presented in Figure 8.9 and Table 8.3. The first decomposition process step was a minor mass loss over

the range of ~30 °C to ~230 °C. The weight loss of purified chicken feather fibres and keratin extracted via both sodium sulfide and L-cysteine were approximately 1-5 %, which can be attributed to the evaporation of incorporated water near 100 °C. The presence of ~5 % moisture substantiates our hypothesis that the purity of keratin could be as high as 95 % based on the composition of nitrogen and water [57], which is in agreement with the SDS-PAGE results.

The second mass loss step was much larger, around 80 %, and occurs from ~230 °C to ~280 °C, for keratin extracted via L-cysteine. This partly overlaps with decomposition of L-cysteine (Figure 8.9(a)), which indicates that L-cysteine residues were left in the resultant keratin. The similarity of the TGA curves for L-cysteine and L-cysteine reduced keratin indicates presence of L-cysteine in the keratin as detected by SSNMR. The TGA curves for keratin extracted via sodium sulfide and original purified chicken feather showed virtually identical behaviour of decomposition in contrast to the L-cysteine reduced keratin curves, in the temperature range of ~230 °C - ~750 °C, which was caused by the degradation of the protein structure: destruction of chain linkages, peptide bonds and amino acid skeletal degradation [4, 6, 42, 50]. A third mass loss stage was from ~280 °C to 750 °C, which was 12.5 % for keratin extracted via L-cysteine reduction.

Derivative thermogravimetry (DTG) curves were calculated, and showed the temperature corresponding to the maximum mass loss rate [6]. The temperature difference between keratin extracted via L-cysteine versus sodium sulfide was ~85 °C. Figure 8.9(b) shows that the maximum mass loss rate of thermal decomposition of keratins extracted under sodium sulfide were slightly lower compared with the original purified chicken feathers, due to prior cleavage of the disulfide bonds during the extraction process of keratin [14, 16].

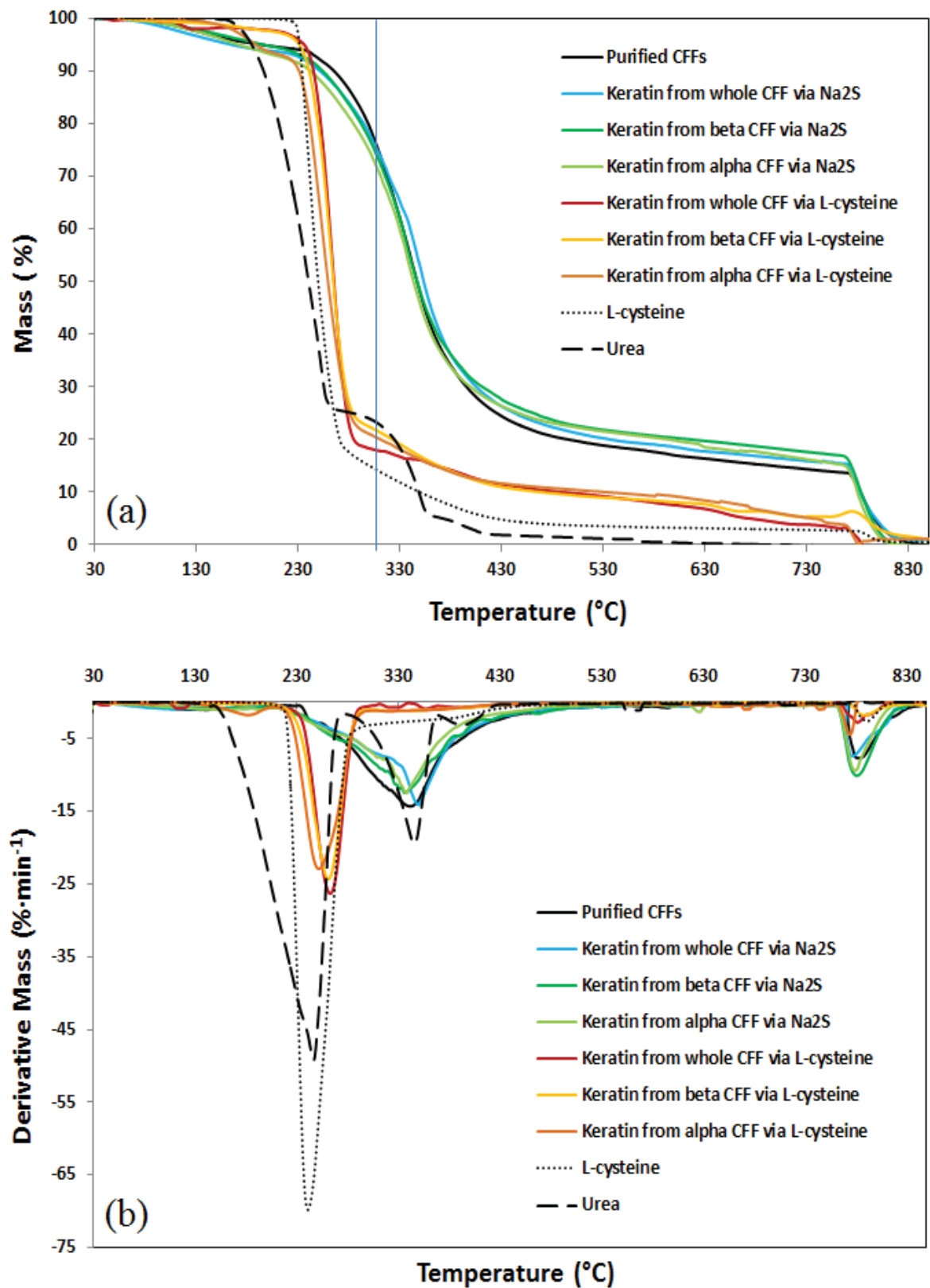


Figure 8.9: (a) TGA, and (b) DTG thermograms (mass loss) of L-cysteine, urea and purified CFF compared with keratin extracted from whole CFF, β -sheet and α -helix parts via Na₂S and L-cysteine

Table 8.3: Thermal data of L-cysteine, urea, purified CFF and keratin extracted from whole CFF, β -sheet and α -helix parts via Na_2S and L-cysteine

Materials	Temp. at 5 % Mass Loss (°C)	Mass Loss (%) at 300 °C	Char Levels (%) at 500 °C
L-cysteine	231	85	4
Urea	184	76	1
Purified CFFs	194	21	20
CFK, whole, Na_2S	165	22	21
CFK, β -sheet, Na_2S	195	23	23
CFK, α -helix, Na_2S	171	25	22
CFK, whole, L-cysteine	236	82	10
CFK, β -sheet, L-cysteine	231	78	9
CFK, α -helix, L-cysteine	188	79	10

8.4 Conclusions

Both L-cysteine and sodium sulfide were used for the rupture of disulfide cross-links, dissolution and purification of chicken feather keratin. Both extracted keratins exhibited similar protein quality as they shared the same molar mass of *ca.* 11 kg/mol and purity of $\geq 95\%$, based on SDS-PAGE, LC-MS/MS and TGA outcomes. The TGA, NMR, FTIR and Raman analyses confirmed the existence of L-cysteine residues in keratin extracted via Solution-B, which was not the case for urea, since it is highly water-soluble. Solid state NMR confirmed that the structure of keratin was retained following extraction via both methods, and that ^1H SSNMR could potentially be used as an analytical tool to differentiate between α - and β -keratin. The TGA and DTG curves for pure chicken feathers and keratin extracted via sodium sulfide showed virtually identical behaviour of decomposition, which proves the purity of the extracted keratin.

Keratin protein can be extracted from chicken feathers using both sodium sulfide and L-cysteine. Although extraction with sodium sulfide poses environmental issues, the yield obtained (88 %) was higher in comparison to the more eco-friendly L-cysteine method (66 % total yield including residues). The results from this investigation show that what is

currently a waste product of the poultry industry can potentially be a new, cheaper and sustainable source of keratin, a substance currently in demand, with applications in a variety of products including (but not limited to) beauty treatments, polymer science, tissue engineering, health and biomedical industries.

8.5 References

1. Matlack, A., *Introduction to green chemistry*. 2nd ed. 2010, FL, U.S.: CRC Press.
2. Clark, J.H., *Green chemistry: challenges and opportunities*. Green Chemistry, 1999. **1**(1): p. 1-8.
3. Khosa, M. and A. Ullah, *A sustainable role of keratin biopolymer in green chemistry: a review*. J. Food Process. Beverage, 2013. **1**: p. 1-8.
4. Ma, B., X. Qiao, X. Hou, and Y. Yang, *Pure keratin membrane and fibers from chicken feather*. International Journal of Biological Macromolecules, 2016. **89**: p. 614-621.
5. Arai, K.M., R. Takahashi, Y. Yokote, and K. Akahane, *Amino-Acid Sequence of Feather Keratin from Fowl*. European Journal of Biochemistry, 1983. **132**(3): p. 501-507.
6. Ullah, A., T. Vasanthan, D. Bressler, A.L. Elias, and J. Wu, *Bioplastics from feather quill*. Biomacromolecules, 2011. **12**(10): p. 3826-3832.
7. Fraser, R., T. MacRae, and G.E. Rogers, *Keratins: their composition, structure, and biosynthesis*. 1972: Charles C. Thomas.
8. Yin, X.-C., F.-Y. Li, Y.-F. He, Y. Wang, and R.-M. Wang, *Study on effective extraction of chicken feather keratins and their films for controlling drug release*. Biomaterials Science, 2013. **1**(5): p. 528-536.
9. Ayuthaya, S.I.N., S. Tanpichai, and J. Wootthikanokkhan, *Keratin Extracted from Chicken Feather Waste: Extraction, Preparation, and Structural Characterization of the Keratin and Keratin/Biopolymer Films and Electrospuns*. Journal of Polymers and the Environment, 2015. **23**(4): p. 506-516.
10. Parry, D.A. and A. North, *Hard α -keratin intermediate filament chains: substructure of the N-and C-terminal domains and the predicted structure and function of the C-terminal domains of type I and type II chains*. Journal of structural biology, 1998. **122**(1): p. 67-75.
11. Zhao, W., R. Yang, Y. Zhang, and L. Wu, *Sustainable and practical utilization of feather keratin by an innovative physicochemical pretreatment: high density steam flash-explosion*. Green Chemistry, 2012. **14**(12): p. 3352-3360.
12. Wang, Y.-X. and X.-J. Cao, *Extracting keratin from chicken feathers by using a hydrophobic ionic liquid*. Process biochemistry, 2012. **47**(5): p. 896-899.
13. Thannhauser, T.W., Y. Konishi, and H.A. Scheraga, *Sensitive quantitative analysis of disulfide bonds in polypeptides and proteins*. Analytical biochemistry, 1984. **138**(1): p. 181-188.
14. Wang, K., R. Li, J. Ma, Y. Jian, and J. Che, *Extracting keratin from wool by using L-cysteine*. Green Chemistry, 2016. **18**(2): p. 476-481.

15. Eslahi, N., F. Dadashian, and N.H. Nejad, *An investigation on keratin extraction from wool and feather waste by enzymatic hydrolysis*. Preparative Biochemistry and Biotechnology, 2013. **43**(7): p. 624-648.
16. Tonin, C., M. Zoccola, A. Aluigi, A. Varesano, A. Montarsolo, C. Vineis, and F. Zimbardi, *Study on the conversion of wool keratin by steam explosion*. Biomacromolecules, 2006. **7**(12): p. 3499-3504.
17. Kornilłowicz-Kowalska, T. and J. Bohacz, *Biodegradation of keratin waste: theory and practical aspects*. Waste Management, 2011. **31**(8): p. 1689-1701.
18. Schmidt, W., *Microcrystalline keratin: from feathers to composite products*. MRS Symp. Proceed., Boston, MA, 702: 25, DOI: 10.1557/PROC-702-U1.5.1, 2002. **29**.
19. Reddy, N. and Y. Yang, *Structure and properties of chicken feather barbs as natural protein fibers*. Journal of Polymers and the Environment, 2007. **15**(2): p. 81-87.
20. Ullah, A. and J. Wu, *Feather Fiber-Based Thermoplastics: Effects of Different Plasticizers on Material Properties*. Macromolecular Materials and Engineering, 2013. **298**(2): p. 153-162.
21. Winandy, J.E., J.H. Muehl, J.A. Micales, A. Raina, and W. Schmidt, *Potential of chicken feather fiber in wood MDF composites*. Proceedings EcoComp 2003, 2003. **20**: p. 1-6.
22. Wallenberger, F.T. and N. Weston, *Natural fibers, plastics and composites*. Materials Source Book, Editors: Wallenberger, Frederick T., Weston, Norman (Eds.) 2004.
23. Lamoolphak, W., W. De-Eknamkul, and A. Shotipruk, *Hydrothermal production and characterization of protein and amino acids from silk waste*. Bioresource technology, 2008. **99**(16): p. 7678-7685.
24. Ji, Y., J. Chen, J. Lv, Z. Li, L. Xing, and S. Ding, *Extraction of keratin with ionic liquids from poultry feather*. Separation and Purification Technology, 2014. **132**: p. 577-583.
25. Schrooyen, P.M., P.J. Dijkstra, R.C. Oberthür, A. Bantjes, and J. Feijen, *Stabilization of solutions of feather keratins by sodium dodecyl sulfate*. Journal of colloid and interface science, 2001. **240**(1): p. 30-39.
26. Mokrejs, P., P. Svoboda, J. Hrnčirik, D. Janacova, and V. Vasek, *Processing poultry feathers into keratin hydrolysate through alkaline-enzymatic hydrolysis*. Waste management & research, 2011. **29**(3): p. 260-267.
27. Gupta, A. and R. Perumal, *Process for Extracting Keratin*. Patents US8575313 B2, 2013.
28. Xu, H. and Y. Yang, *Controlled De-Cross-Linking and Disentanglement of Feather Keratin for Fiber Preparation via a Novel Process*. ACS Sustainable Chemistry & Engineering, 2014. **2**(6): p. 1404-1410.
29. Manrique-Juárez, M.D., A.L. Martínez-Hernández, O.F. Olea-Mejía, J. Flores-Estrada, J.L. Rivera-Armenta, and C. Velasco-Santos, *Polyurethane-Keratin Membranes: Structural Changes by Isocyanate and pH, and the Repercussion on Cr (VI) Removal*. International Journal of Polymer Science, 2013. **2013**.
30. Özdemir, G. and Ö. Sezgin, *Keratin-rhamnolipids and keratin-sodium dodecyl sulfate interactions at the air/water interface*. Colloids and surfaces B: Biointerfaces, 2006. **52**(1): p. 1-7.
31. Gupta, A., N.B. Kamarudin, C.Y.G. Kee, and R.B.M. Yunus, *Extraction of keratin protein from chicken feather*. Journal of Chemistry and Chemical Engineering, 2012. **6**(8): p. 732.

32. Bertsch, A. and N. Coello, *A biotechnological process for treatment and recycling poultry feathers as a feed ingredient*. Bioresource technology, 2005. **96**(15): p. 1703-1708.
33. Bradford, M.M., *A rapid and sensitive method for the quantitation of microgram quantities of protein utilizing the principle of protein-dye binding*. Analytical Biochemistry, 1976. **72**(1): p. 248-254.
34. Schmidt, W. and M. Line, *Physical and chemical structures of poultry feather fiber fractions in fiber process development*. Nonwovens. Conference, Atlanta, GA, USA, 1996: p. 135-140.
35. Acda, M.N., *Waste chicken feather as reinforcement in cement-bonded composites*. Philippine Journal of Science, 2010. **139**(2): p. 161-166.
36. Rose, F., *Über die Verbindungen des Eiweiss mit Metalloxyden*. Annalen der Physik, 1833. **104**(5): p. 132-142.
37. Wang, Y., P. Li, P. Xiang, J. Lu, J. Yuan, and J. Shen, *Electrospun polyurethane/keratin/AgNP biocomposite mats for biocompatible and antibacterial wound dressings*. Journal of Materials Chemistry B, 2016. **4**(4): p. 635-648.
38. Gregg, K., S. Wilton, D. Parry, and G. Rogers, *A comparison of genomic coding sequences for feather and scale keratins: structural and evolutionary implications*. The EMBO journal, 1984. **3**(1): p. 175.
39. Sun, P., Z.-T. Liu, and Z.-W. Liu, *Particles from bird feather: A novel application of an ionic liquid and waste resource*. Journal of hazardous materials, 2009. **170**(2): p. 786-790.
40. Idris, A., R. Vijayaraghavan, U.A. Rana, A. Patti, and D. MacFarlane, *Dissolution and regeneration of wool keratin in ionic liquids*. Green Chemistry, 2014. **16**(5): p. 2857-2864.
41. Senoz, E. and R.P. Wool, *Microporous carbon–nitrogen fibers from keratin fibers by pyrolysis*. Journal of applied polymer science, 2010. **118**(3): p. 1752-1765.
42. Martinez-Hernandez, A.L., C. Velasco-Santos, M. De Icaza, and V.M. Castano, *Microstructural characterisation of keratin fibres from chicken feathers*. International journal of environment and pollution, 2005. **23**(2): p. 162-178.
43. Pavia, D., G. Lampman, G. Kriz, and J. Vyvyan, *Introduction to Spectroscopy*. 2008: Cengage Learning.
44. Edwards, H., D. Hunt, and M. Sibley, *FT-Raman spectroscopic study of keratotic materials: horn, hoof and tortoiseshell*. Spectrochimica Acta Part A: Molecular and Biomolecular Spectroscopy, 1998. **54**(5): p. 745-757.
45. Takahashi, K., H. Yamamoto, Y. Yokote, and M. Hattori, *Thermal behavior of fowl feather keratin*. Bioscience, biotechnology, and biochemistry, 2004. **68**(9): p. 1875-1881.
46. Aluigi, A., M. Zoccola, C. Vineis, C. Tonin, F. Ferrero, and M. Canetti, *Study on the structure and properties of wool keratin regenerated from formic acid*. International journal of biological macromolecules, 2007. **41**(3): p. 266-273.
47. Mohanty, A.K., M. Misra, and L.T. Drzal, *Natural Fibers, Biopolymers, and Biocomposites*. 2005: CRC Press.
48. Vasconcelos, A., G. Freddi, and A. Cavaco-Paulo, *Biodegradable materials based on silk fibroin and keratin*. Biomacromolecules, 2008. **9**(4): p. 1299-1305.
49. Wojciechowska, E., A. Włochowicz, and A. Wesełucha-Birczyńska, *Application of Fourier-transform infrared and Raman spectroscopy to study degradation of the wool fiber keratin*. Journal of Molecular Structure, 1999. **511**: p. 307-318.

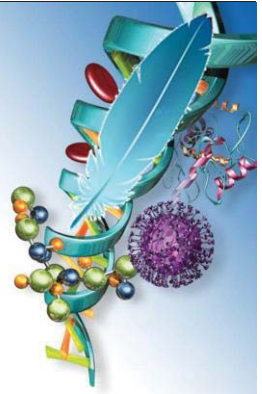
50. Idris, A., R. Vijayaraghavan, U.A. Rana, D. Fredericks, A. Patti, and D. MacFarlane, *Dissolution of feather keratin in ionic liquids*. *Green chemistry*, 2013. **15**(2): p. 525-534.
51. Zhang, J., Y. Li, J. Li, Z. Zhao, X. Liu, Z. Li, Y. Han, J. Hu, and A. Chen, *Isolation and characterization of biofunctional keratin particles extracted from wool wastes*. *Powder technology*, 2013. **246**: p. 356-362.
52. Al-Itry, R., K. Lamnawar, and A. Maazouz, *Improvement of thermal stability, rheological and mechanical properties of PLA, PBAT and their blends by reactive extrusion with functionalized epoxy*. *Polymer Degradation and Stability*, 2012. **97**(10): p. 1898-1914.
53. Akhtar, W. and H. Edwards, *Fourier-transform Raman spectroscopy of mammalian and avian keratotic biopolymers*. *Spectrochimica Acta Part A: Molecular and Biomolecular Spectroscopy*, 1997. **53**(1): p. 81-90.
54. Church, J., A. Poole, and A. Woodhead, *The Raman analysis of films cast from dissolved feather keratin*. *Vibrational Spectroscopy*, 2010. **53**(1): p. 107-111.
55. Fabian, H. and P. Anzenbacher, *New developments in Raman spectroscopy of biological systems*. *Vibrational Spectroscopy*, 1993. **4**(2): p. 125-148.
56. Barone, J.R., W.F. Schmidt, and N. Gregoire, *Extrusion of feather keratin*. *Journal of applied polymer science*, 2006. **100**(2): p. 1432-1442.
57. Kakkar, P., B. Madhan, and G. Shanmugam, *Extraction and characterization of keratin from bovine hoof: A potential material for biomedical applications*. SpringerPlus, 2014. **3**(1): p. 596.

8.6 Publication from this Chapter

- Pourjavaheri, F., Gupta, A. & Shanks, R. A. "Keratin from chicken feather fibers" *Green Chemistry*. To be submitted in 2017.
- Pourjavaheri, F., Jones, O.A.H., Close, C. Sherkat, F. & Shanks, R.A. (2017) "Eco-friendly keratin extraction from waste chicken feathers", *Society for Environmental Toxicology and Chemistry (SETAC)*, 4-6 September, Gold Coast, Queensland, Australia. (Oral Presentation)
- Pourjavaheri, F., Jones, O.A.H., Smooker, P.M., Brkljača, R., Ostovar pour, S., Sherkat, F., Gupta, A., & Shanks, R.A. (2017) "Ecofriendly keratin extraction and characterisation from waste chicken feathers", *RACI National Centenary Conference*, 23-28 July, Melbourne, Australia. (Oral Presentation)
- Pourjavaheri, F., Jones, O.A.H., & Shanks, R.A. (2017) "Chicken feather keratin extraction", *ACS on Campus*, 21 July, Melbourne, Australia. (Poster Presentation)
- Pourjavaheri, F., Jones, O.A.H., Sherkat, F. & Shanks, R.A. (2017) "Applications of chicken feather keratin", *8th Annual ASMR VIC Student Research Symposium*, 1 June, Melbourne, Australia. (Abstract only)
- Pourjavaheri, F., Jones, O.A.H., & Shanks, R.A. (2017) "Chicken feather keratin", *Beyond Research*, 21-23 February, Melbourne, Australia. (Poster Presentation)

[Type text]

CHAPTER 9



APPLICATIONS OF KERATIN EXTRACTED FROM CHICKEN FEATHER FIBRES

9.1 Introduction

There is no compendious literature on the prospects for industrial applications of CFK [1]. Both *E. coli* (Gram-negative) and *S. aureus* (Gram-positive) organisms are known to be opportunistic pathogens in the majority of the infections such as urinary tract, burn and wound infections [2]. A review conducted by Qiu et al. [3] found that biopolymers could promote antimicrobial activity in three ways: the creation of an anti-adhesive surface, the disruption of cell-cell communication through antibacterial agents, or lysing the cell membrane to kill the bacteria. This study presents the antimicrobial effect of protein keratin derived from chicken feathers via different extraction methods including sodium sulfide and L-cysteine. Antimicrobial effects of the keratins were tested using disc diffusion and well diffusion assays.

Based on the findings by Neely and Maley [4, 5], keratin can be used as an ideal wound dressing since it exhibits bactericidal properties. Paul *et al.* [2] investigated antimicrobial peptides and protein keratin to verify their antibacterial activity. Gram-positive bacteria such as *S. aureus* are able to survive at least one day when inoculated onto the surface of materials commonly used in healthcare applications, with some microorganisms being able to survive for more than three months. Consequently, materials that could provide antimicrobial properties, are being examined for biomedical applications, as they would help in containing or reducing hospital-acquired infections. Contamination with waste CF has been blamed for fowl cholera, chlorosis, bacterial contamination of animal food and human food borne illnesses [4, 6, 7]. Alternatively, contamination through conventional plastics is a major risk, where the material can be toxic or harmful and may leach into consumables [8]. Hence, an antimicrobial study was conducted on the bio-composites prepared in previous studies, using thermoplastic polyurethanes (polyether and polysiloxane) and ground CFF. This approach

could provide a way to mitigate both effects.

There is relatively narrow published data on the general behaviour of keratin biomaterials. Hence, in this study, the superior CFK extracted using sodium sulfide as reducing agent, has been tested in a hair conditioner and leather cream to demonstrate feasibility for hair treatment and leather repair applications.

Hair fibers are elongated cross-linked hard keratin structures that are composed of 90 % keratin and 1 to 9 % of lipid [9]. The diameter of hair fibres varies between 40 and 150 μm and its major structure consists of a cuticle, cortex and medulla [10]. Most hair fibre mass is in the cortex, which is responsible for the great tensile strength of hair fibre [11]. It is made of long filaments packed together, named microfibrils that contain organised α -helical rods of keratin, embedded in an amorphous matrix [12, 13]. The cortex is covered by an external cuticle, consisting of overlapping layers of scales composed of β -keratin [14]. The medulla consists of specialised cells that contain air spaces and is frequently broken or missing from the hair shaft in fine hair [15]. The major function of keratin cuticle is to protect the cortex of the hair from damage caused by several factors including heat, chemicals and daily maintenance [9]. The chemical structure of hair can be modified by ageing and by environmental factors such as pollution and sunlight [13]. Permanent waving, straightening or relaxing, bleaching during hair colouring processes, and brushing can cause damage to hair [15, 16]. Protein hydrolysates, in particular, those with low molecular weight subunits, have been known to protect hair against chemical and environmental damage [10]. Oligopeptides with a molecular mass $<1,000$ g/mol are able to penetrate the cortex [9] and are efficient restorers of hair health. Hair-care products with active peptides are reparative and conditioning agents that strengthen the hair fibres and

reduce breakages [9]. In permanent waving and bleaching, proteins have a substantial protecting effect on the hair structure [9]. The addition of protein hydrolysates to hair colouring sprays and toners enables hair to absorb dyes more uniformly [9]. In the leave-on products, a natural conditioning effect of protein hydrolysates is reported [17, 18]. Many types of protein hydrolysates from plants and animal sources such as wheat protein [19] and keratin from nails, horns and wool [20] have been used in hair repair products and in skin cosmetics.

Conversely, applications of acid, alkali or enzyme-hydrolysed keratin and hydrolysates have been reported [21-27] for cosmetics. Keratin preparations include treatment of human hair and skin [28-30] and in leather processing during chrome tanning to enhance the absorption of chromium salt by leather [21]. There are different approaches to converting the keratin into keratin hydrolysates such as microbial, enzymatic hydrothermal and chemical treatments with acid or alkali, [9, 31-33] that break disulfide linkages of keratin and yield soluble polypeptides, oligopeptides or even amino acids [34-36]. Uncontrolled processes may result in partial to complete hydrolysis of amino acid links, which contain peptides with varying molecular weight therefore leading to losses of essential amino acids such as lysine, methionine and tryptophan, and cause the formation of non-nutritive amino acids such as lysinoalanine and lanthionine [37, 38]. Thus in this study, the keratin has not been hydrolysed, to keep the essential amino acids and to examine if the disulfides linkages are open or closed.

The research reported in this study has a beneficial effect on the environment as it provides a facile and recyclable method to readily convert an otherwise polluting material such as CF into biocompatible and useful materials that could be used in

tissue engineering, drug delivery, wound and burn infections treatments [39].

9.2 Experimental

9.2.1 Materials

Keratins were extracted using extraction methods reported in Chapter 7. Dodecyl sulfate sodium (SDS) ≥ 95.0 % ($C_{12}H_{25}Na_4S$, CAS NO. 151-21-3) was obtained from Merck-Millipore, Darmstadt, Germany. Hydrochloric acid 32 %•w/w (AR, HCl, CAS NO. 7647-01-0) and 2-mercaptoethanol ≥ 99.0 % ($HSCH_2CH_2OH$, CAS NO. 60-24-2); were obtained from Sigma-Aldrich (MO, USA). Tris ($C_4H_{11}NO_3$, CAS NO. 77-86-1) was obtained from Astral Scientific, NSW, Australia. Urea 99.0 % (LR, NH_2CONH_2 , CAS NO. 57-13-6) were obtained from Ajax Finchem Pty Ltd (Auckland, New Zealand). Dimethyl Sulfoxide-D6 (DMSO) (D, 99.9 %) (CD_3SOCD_3 , CAS NO. 67-68-5) was obtained from Cambridge Isotope Laboratories, Inc. Massachusetts, USA. Mueller Hinton Agar (MHA) CM0337, and sterile 8 mm filter discs were purchased from Sigma-Aldrich, Sydney, Australia. The bacterial cultures used in this study were obtained from the American Type Culture Collection (ATCC, Rockville, MD), which were Gram-negative *Escherichia coli* (*E. coli* - ATCC 25922), rod-shaped with thin layer of peptidoglycan, and Gram-positive *Staphylococcus aureus* (*S. aureus* - ATCC 25923), cocci shaped in clusters, with a thick layer of peptidoglycan cell wall reference were standardised to ca. 5×10^5 cfu/mL. Disks containing 10 μ g gentamicin were obtained from Oxoid, SpA, Italy.

A commercial conditioner containing no keratin (control) and a commercial conditioner containing keratin for the purpose of keratin therapy were obtained from Melbourne outlets. Two types of human scalp hairs were collected, which were untreated natural hair as control together with dyed relaxed hair as damaged hair.

The experimental cream was made using paraffin oil (white oil) and paraffin wax (polawax GP200) supplied by Ajax Finchem Pty Ltd (Auckland, New Zealand), sorbitan monostearate (polysorbate 60) or Tween 60 supplied by Acros Organics (Geel, Belgium), sorbitol 70 % solution from BDH Experimental Supplies (Poole, England), sorbitan monooleate (span 80), stearic acid and benzyl alcohol from Sigma-Aldrich (MO, USA). All the chemicals utilised in the experiments were of analytical grade, used as received without further purification.

9.2.2 Nuclear magnetic resonance spectroscopy (NMR) (liquid-state)

The CFKs and a human epidermis keratin (supplied by Sigma-Aldrich as a standard to identify and compare diagnostic keratin NMR signals) were dissolved in dimethyl sulfoxide- d_6 (d_6 -DMSO) and in an 8 mol/L urea, 50 mM Tris and 0.1 M β -mercaptoethanol (pH 8) solution at a concentration of 100 mg·keratin/700 μ L solvent. The NMR spectra were referenced to solvent signals using d_6 -DMSO (δ_H 2.50) or using a D_2O capillary placed within the NMR tube (δ_H 4.64). The NMR spectra were acquired on a 500 MHz Agilent DD2 console (Santa Clara, CA, USA). Spectra for the feather keratins dissolved in d_6 -DMSO acquired include proton (256 scans) and gCOSY (16 scans, 512 increments) experiments. Proton spectra (256 scans) for the human epidermis keratin and two original purified CFs were dissolved in an 8 mol/L urea, 50 mM Tris and 0.1 M β -mercaptoethanol (pH 8) solution and were acquired using the PRESET sequence (4-step purge) with suppression of both the water and urea signals. gCOSY (4 scans, 400 increments) and HSQCAD (16 scans, 512 increments) NMR spectra were additionally acquired for these samples with suppression using the PRESET sequence (section 3.3.4).

9.2.3 Antimicrobial assays on chicken feathers and chicken feather keratins

The CFs and keratins extracted from CF components via sodium sulfide or L-cysteine were tested for their antibacterial activity on model bacterial strains *E. coli* (ATCC 25922), and *S. aureus* (ATCC 25923), according to Australian Standard AS ISO 20776. 1:2017 under a sterile class II cabinet using aseptic technique. The diameter of the inhibition zone in the agar plate was measured in millimetres (mm).

9.2.3.1 Standardising of *Escherichia coli* and *Staphylococcus aureus* to 0.5 McFarland (*ca.* 1×10^8 cfu/mL)

Using a sterile swab *ca.* 1-2 and *ca.* 2-3 colonies of *E. coli* and *S. aureus* were separately inoculated into sterile saline inside Wasserman tubes. Tubes were vortexed and their turbidity was compared with 0.5 McFarland Standard tube aiming for 0.5 standard. Disks containing gentamicin (10 µg) were used as positive controls to assess the sensitivity of the bacterial strains. All experiments were performed in triplicate and the average reported. Contamination was minimised as steps were done under the curtain of Bunsen burner hot air.

9.2.3.2 Disk diffusion plating method

The standardised *E. coli* or *S. aureus* in 0.5 McFarland concentration of 50 µL was mixed with a 9.95 mL sterile saline bottle. A sterile plastic spreader was used to spread 100 µL of this solution onto the MHA agar plate. Controls and test plates were set up and allowed to dry under a sterile class II cabinet using aseptic technique. Keratins (0.5 mg) were dissolved in 1 mL of *d*₆-DMSO or UTM-Solution (i.e. 0.33 mol/L urea, 0.05 mol/L sodium dodecyl sulfate (SDS), 0.095 mol/L 2 mercaptoethanol and 0.016 mol/L tris adjusted to pH 8.0 using HCl) in screw cap Eppendorf tubes separately and left overnight at 70 °C in a hybridization oven. The β-mercaptoethanol in the UTM-Solution would break the S-S bonds

of the keratin, which keeps the protein insoluble in polar solvents; urea stops re-annealing of the keratin and breaks apart hydrogen bonds, and SDS stops the continuous breaking of the protein via formation of a complex bond with keratin [40]. The concentration of the keratin solutions was analysed using a BioPhotometer plus (Eppendorf, AG, Hamburg, Germany) spectrophotometer, at 280 nm. Then 8 μ L of the keratin solution was pipetted onto the sterile 8 mm filter discs that were then incorporated at the centre of the MHA agar plate. The MHA plates were incubated at 37 °C and observed after 24 h. The antibacterial activity was measured by evaluating the diameter of the zone of inhibition around each disc.

9.2.3.3 Well diffusion plating method

Standardised *E. coli* or *S. aureus* at 0.5 McFarland concentration of 150 μ L was mixed with 3 mL sterile saline in a bottle. The full content of the bottle was poured onto the MHA agar plate and swirled for exactly 30 s to ensure bacterial confluency is achieved on all plates and then discarded. Wells with the size of 5 mm in diameter were carved out of the agar using a sterile metal well maker and set aside. Keratin powders (*ca.* 0.1 mg) were seeded to the centre of each well using a small sterile spatula, then the removed MHA agar piece was replaced on the agar well to keep the keratin powders intact and the plates were incubated as mentioned above.

9.2.3.4 Feather diffusion plating method

The CFs (*ca.* 2 cm) purified with the ethanol-extraction method (Chapter 4) were spread onto the MHA agar plates using sterile spreaders, and *ca.* 100 μ L of the standardised *E. coli* or *S. aureus* in 0.5 McFarland concentration were transferred onto MHA agars together with controls., followed by incubation as mentioned above.

9.2.4 Keratin hair conditioning preparation

Keratin powder was added to commercial conditioner at 2.5 and 5.0 %, thoroughly mixed manually and left overnight before applying onto natural untreated hair and dyed relaxed hair samples, for 5 min, followed by rinsing the hairs with tap water. Commercial hair conditioner containing no added keratin was used as control.

9.2.5 Keratin-enriched cream preparation

The cream was prepared by measuring distilled water into a metal beaker heated to 50-55 °C under a digital overhead stirrer (IKA®-Werke EuroStar, Staufen, Germany) with an IKA R 1342 Propeller stirrer 4 blade at 500 rpm. Then paraffin wax, paraffin oil, sorbitan, sorbitol and stearic acid were added. While continuously stirring, the mixture was allowed to cool to 40 °C, then benzyl alcohol and keratin powder (at ratios of 2.5 and 5 %·w/w) were added. The cream thus produced was further cooled to 30-35 °C prior to being transferred into storage containers.

9.2.6 Characterisation of keratin-based materials

9.2.6.1 Morphological analysis via scanning electron microscopy

The impact of the experimental and commercial keratin-enriched conditioners on the structure of natural untreated hair and dyed relaxed hair was investigated by using an FEI Quanta 200 scanning electron microscope (FEI, Oregon, USA) with a 20 kV acceleration voltage under high vacuum. Hair specimens were mounted onto aluminium stubs using carbon tape and coated with a thin layer (*ca.* 20 nm) of gold using an SPI Sputter Coater Z11430 (Structure & Probe Inc., West Chester, Pennsylvania, USA).

The surface morphology of bovine treated leather was compared with leathers treated with experimental keratin-enriched creams containing 2.5-5 % keratin. The uncoated leathers were mounted on the aluminium stubs using carbon adhesive tape and were analysed at 30 kV acceleration voltage in low vacuum.

9.2.6.2 Mechanical properties

Tensile properties of treated and untreated, healthy and damaged human hair were evaluated via tensile mechanical analysis (stress–strain analysis). Prior to testing, the diameters of the hair were measured using a Dino-Lite digital microscope (Dino-Lite AM4013T-M40 from AnMon Electronics Co., using DinoCapture 2.0 operating software). Specimen preparation for a single fibre tensile testing was carried out according to ASTM D3822 47, using a paper template to mount the fibre and grip it to the tensile clamps. Tensile testing was performed using a TA Instruments DMA Q800 (at 30 °C; ramped force from 0.2 to 18 N at 0.01 N min⁻¹) equipment to measure stress–strain properties of the hairs.

Modulated force thermomechanometry (MF-TM) or dynamic mechanical analysis (DMA) was carried out using a PerkinElmer Diamond DMA to determine storage modulus (E'), loss modulus (E''), and loss tangent ($\tan\delta$) associated with untreated and treated bovine leathers. Test conditions included specimen gauge length of 11 mm, deformation of 20 μm , frequency of 0.5 Hz at 18 °C.

9.3 Results and discussion

9.3.1 Liquid-state NMR studies

The study in Chapter 7 utilised solid-state NMR to differentiate between α -helix and β -sheet enriched keratins. Solid-state NMR requires specialised hardware, therefore in this

study, the ability of NMR to differentiate and characterise α -helix and β -sheet rich keratins in solution-state was evaluated. The authentic human epidermis keratin was used as a standard to identify diagnostic keratin NMR signals. The proton spectra of the CFK and the authentic human epidermis keratin (Figure 9.1) showed a series of broad resonances in the downfield region (6-8 ppm), whilst these represent different types of keratin, similar chemical shifts and coupling would be observed between the different keratin types. The similarity in the chemical shifts confirms that keratin has been successfully extracted from CF and that the extraction method retained the molecular structure of the keratin. No difference or characteristic signals could be observed between α -helix and β -sheet-rich keratins. The NMR tubes contained precipitate at the bottom indicating that the solutions were saturated with keratin. The keratin extracted from the feathers was not highly soluble and could not be dissolved at high concentrations, which limited the signal-to-noise of the spectra.

The gCOSY and HSQCAD NMR spectra of the authentic human epidermis keratin (Figure 9.2) revealed that the downfield proton signals of keratin correlate with neighbouring hydrogens, and were bonded to distinct carbon signals. The gCOSY spectra (Figure 9.2) showed no difference or characteristic signals between α -helix and β -sheet for the extracted CFK. Due to poor signal-to-noise, HSQCAD spectra could not be acquired for the extracted keratins.

These results show that while keratin can be observed in the extract from CF, it is not possible to use solution state NMR to distinguish between α - and β -keratin. The proton environments do not differ substantially making it difficult to find a potential marker. It may be possible that differences in the carbon chemical shifts occur between α -helix and β -sheet keratin, however, it was not possible to dissolve enough of the extracted keratin to obtain HSQCAD NMR data.

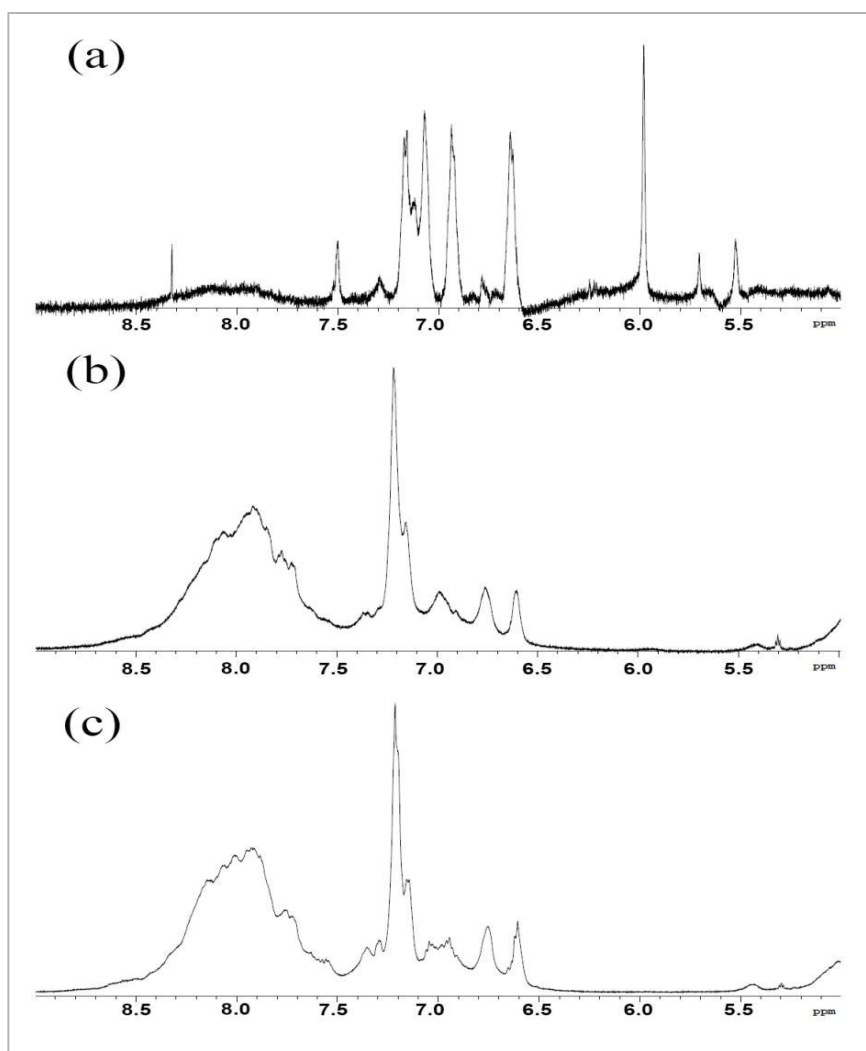


Figure 9.1: ^1H NMR spectra of (a) authentic human epidermis keratin, and keratin extracted with sodium sulfide from chicken feathers components: (b) barbs and barbules (composed mainly of α -helix) (c) calamus and rachis (composed mainly of β -sheet structures)

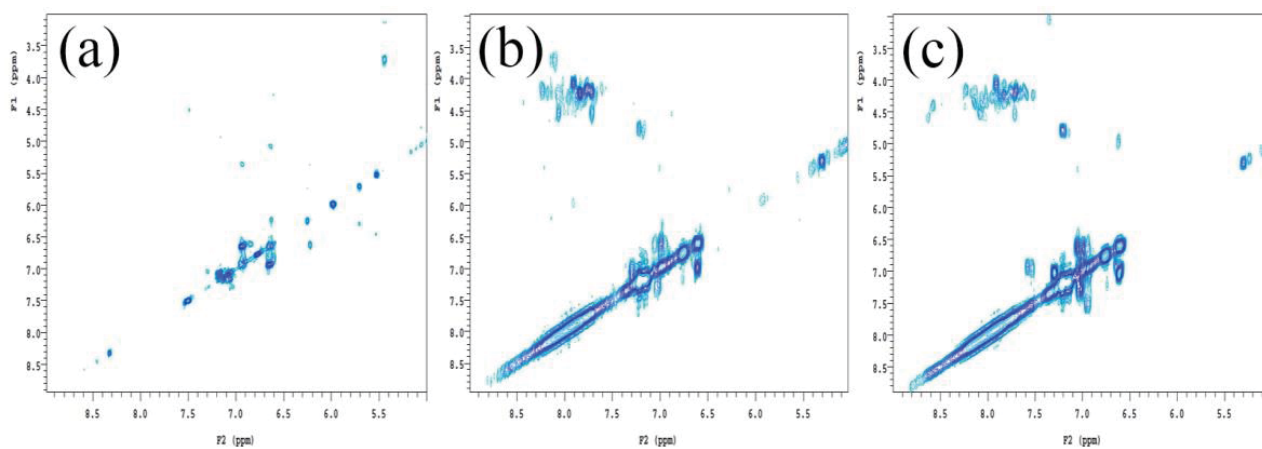


Figure 9.2: The gCOSY NMR spectra of (a) authentic human epidermis keratin, and extracted chicken feather keratins using sodium sulfide; (b) barbs and barbules (composed mainly of α -helix) (c) calamus and rachis (composed mainly of β -sheet structures)

9.3.2 Antibacterial analysis

The aim of this study was to determine if the CFK extracted with sodium sulphide or L-cysteine, possessed any antibacterial activity. In the well diffusion method, the keratin powders were tested in their solid-state, whereas in disk diffusion test, the keratins were dissolved in d_6 -DMSO solution or a UTM-Solution as described in section 8.2.3.2. The concentrations of the keratin solutions as measured by BioPhotometer plus spectrophotometer are shown in Table 9.1.

Table 9.1: Concentrations of extracted chicken feather keratins (CFKs) with sodium sulfide or L-cysteine from different segments of chicken feather fibres (CFFs) dissolved in d_6 -DMSO and UTM-Solution

Material and Extraction Method	Concentration (mg/mL)	
	d_6 -DMSO	UTM-Solutions
whole CFFs in Na_2S	0.121	0.481
β -sheet CFFs in Na_2S	0.551	0.083
α -helix CFFs in Na_2S	0.568	0.087
whole CFFs in L-cysteine	0.032	0.035
β -sheet CFFs in L-cysteine	0.034	0.045
α -helix CFFs in L-cysteine	0.039	0.027

As expected, no inhibition zones were found around the disks of *S. aureus* or *E. coli* with the control d_6 -DMSO solution, but none with those containing keratin, indicating that there was no antibacterial activity at the concentrations tested (Table 9.2). However, the keratin dissolved in the UTM-Solution showed zones for of inhibition for the Gram-positive *S. aureus*, but not Gram-negative *E. coli*. The UTM-Solution control displayed a larger zone of inhibition (20.0 mm) in comparison with the one containing keratin (12.0-15.0 mm). This suggests that keratins in the UTM-Solution promote the growth of bacteria, therefore are less inhibitory, or, the zones of inhibition became smaller because keratin reduced toxicity. This is in agreement with the literature [1, 39] that said the bactericidal effect of feathers is strong against *S. aureus* due to their low α -helix content. UTM-Solution containing keratin extracted with L-cysteine showed a larger inhibition zone (15.0 mm) on *S. aureus* than the solution

containing keratin extracted with sodium sulfide (12.0 mm). This was mainly due to the SDS (17.0 mm) compound of the UTM-Solution, followed by its urea (9.0 mm) and β -mercaptoethanol (8.5 mm) compounds, as depicted in the individual compounds of the UTM-Solution that were tested by measuring each inhibition size to distinguish the component caused the inhibitory action. When compared with gentamicin, which was used as the standard control, keratins had significantly lower activity in *S. aureus* bacterial strains, in both disc and well diffusion methods (Tables 9.2 and 9.3).

Table 9.2: Zone of inhibition diameter of keratin powders in d_6 -DMSO or UTM-Solution, on selected strains, using disk diffusion method

d_6-DMSO, UTM-Solution and chicken feather keratin (CFK) solutions	Zone of inhibition (mm)	
	<i>S. aureus</i>	<i>E. coli</i>
Control d_6 -DMSO solution	0	0
Whole CFK via Na_2S in d_6 -DMSO	0	0
β -sheet CFK via Na_2S in d_6 -DMSO	0	0
α -helix CFK via Na_2S in d_6 -DMSO	0	0
Whole CFK via L-cysteine in d_6 -DMSO	0	0
β -helix CFK via L-cysteine in d_6 -DMSO	0	0
α -sheet CFK via L-cysteine in d_6 -DMSO	0	0
Whole CFK via Na_2S in UTM-Solution	12.0 \pm 0.5	0
β -sheet CFK via Na_2S in UTM-Solution	12.0 \pm 0.5	0
α -helix CFK via Na_2S in UTM-Solution	12.0 \pm 0.4	0
Whole CFK via L-cysteine in UTM-Solution	15.0 \pm 0.2	0
β -helix CFK via L-cysteine in UTM-Solution	15.0 \pm 0.3	0
α -sheet CFK via L-cysteine in UTM-Solution	15.0 \pm 0.2	0
Control UTM-Solution	20.0 \pm 0.2	0
0.330 mol/L urea (99.0 %)	9.0 \pm 0.2	0
0.050 mol/L SDS (\geq 95.0 %)	17.0 \pm 0.5	0
0.095 mol/L 2-mercaptoethanol (\geq 99.0 %)	8.5 \pm 0.2	0
Gentamicin (control)	35.0 \pm 0.1	35.0 \pm 0.1

Keratins were additionally tested in their solid-state using well diffusion method as shown in Table 9.3. There was no inhibition zone around the disks for *E. coli*, however, zone of inhibition was observed around the disks of *S. aureus*. This difference may be explained by the presence of compact cell wall with two phospholipid bilayers around Gram-negative bacteria, whereas in Gram-positive bacteria, the cell wall is almost exclusively composed of

peptidoglycan and teichoic acid, which are not effective at excluding antimicrobial agents from the cell [41]. The well diffusion results confirmed the disk diffusion antibacterial outcomes. As shown in Table 9.3, the L-cysteine extracted keratin was active but not the sodium sulphide. According to Tran et al. [39], the antimicrobial activity is dependent not only on the type of the protein but on its relative concentration. Therefore, further investigation is required in order to determine the optimum keratin concentration on its antimicrobial activities.

Table 9.3: Zone of inhibition diameter of keratin powders on selected strains using well diffusion method

(Well diffusion method) Chicken feather keratin (CFK) powders	Zone of inhibition diameter (mm)	
	<i>S. aureus</i>	<i>E. coli</i>
Whole CFK via Na ₂ S	0	0
β-sheet CFK via Na ₂ S	0	0
α-helix CFK via Na ₂ S	0	0
Whole CFK via L-cysteine	10.0 ± 0.3	0
β-helix CFK via L-cysteine	10.0 ± 0.3	0
α-sheet CFK via L-cysteine	10.0 ± 0.2	0
Gentamicin (control)	35.0 ± 0.1	35.0 ± 0.1

The use of well diffusion method provided an alternative method to test the keratin in its precipitate form thus eliminating the solutions that caused false positives. The keratin powders extracted with L-cysteine exhibited a zone of inhibition against Gram-positive *S. aureus* which is responsible for human skin infections [42]. This could be one of the reasons why keratin improves the healing process of skin wounds and burns. Since CFs contain a majority of keratin (i.e. 91 % keratin 1 % lipid and 7 % water [43]) their direct antibacterial effect was investigated on MHA plates but there was no observable antimicrobial activity against *E. coli* and *S. aureus*. In addition to eco-toxicity [44], the conventional petroleum-based plastics used in many applications poses the risk of contamination, potentially causing non-bacterial toxicity when used in medical applications, and contamination when used in food packaging [4]. Non-traditional materials such as

keratin are being examined for their potential use in the production of bio-plastics such as thermoplastic polyurethanes (polyether) as discussed in Chapter 6. In terms of antibacterial activity, the keratin is a suitable filler for bio-plastics, as no bacterial attachment was observed on these materials after 24 h of inoculation when *S. aureus* and *E. coli* on their surface [4]. This feather diffusion plating method is the preliminary antibacterial study on keratin bio-plastics without plasticisers, in previous bio-composite studies (Chapters 6 and 7).

9.3.3 Scanning electron microscopy

The SEM images demonstrating the morphology of the natural untreated hair and dyed relaxed hair, treated with experimental keratin-enriched (0.5 %) and commercial keratin conditioners are shown in Figure 9.3. The keratin-treated hair images showed some keratin residues. Figure 9.3(a) presents the natural untreated human hair whereas 3(b) presents dyed relaxed human hair without further treatment. Figure 9.3(c) natural hair and 9.3(d) dyed relaxed hair, were treated with our experimental control conditioner containing no keratin.

Compared with untreated hair, the scales of the dyed relaxed hair treated with conditioner looked smoother. Figure 9.3(e) natural hair and 9.3(f) dyed relaxed hair were treated with experimental conditioner containing 2.5 % keratin. Keratin particles were observed on both hairs and no obvious differences were noticeable compared with the hair treated with the control conditioner. In Figure 9.3(g) natural hair and in 9.3(h) dyed relaxed hair both showed scales with improved sealing when experimental conditioner containing 5.0 % keratin was applied. Figure 9.3(i) natural hair and 9.3(j) dyed relaxed hair, treated with commercial keratin conditioner (with an unknown amount of keratin) showed sealed scales similar to hair treated with experimental conditioner with 2.5 % keratin (e) and (f). The higher resolution images show the sealing of the scales more clearly.

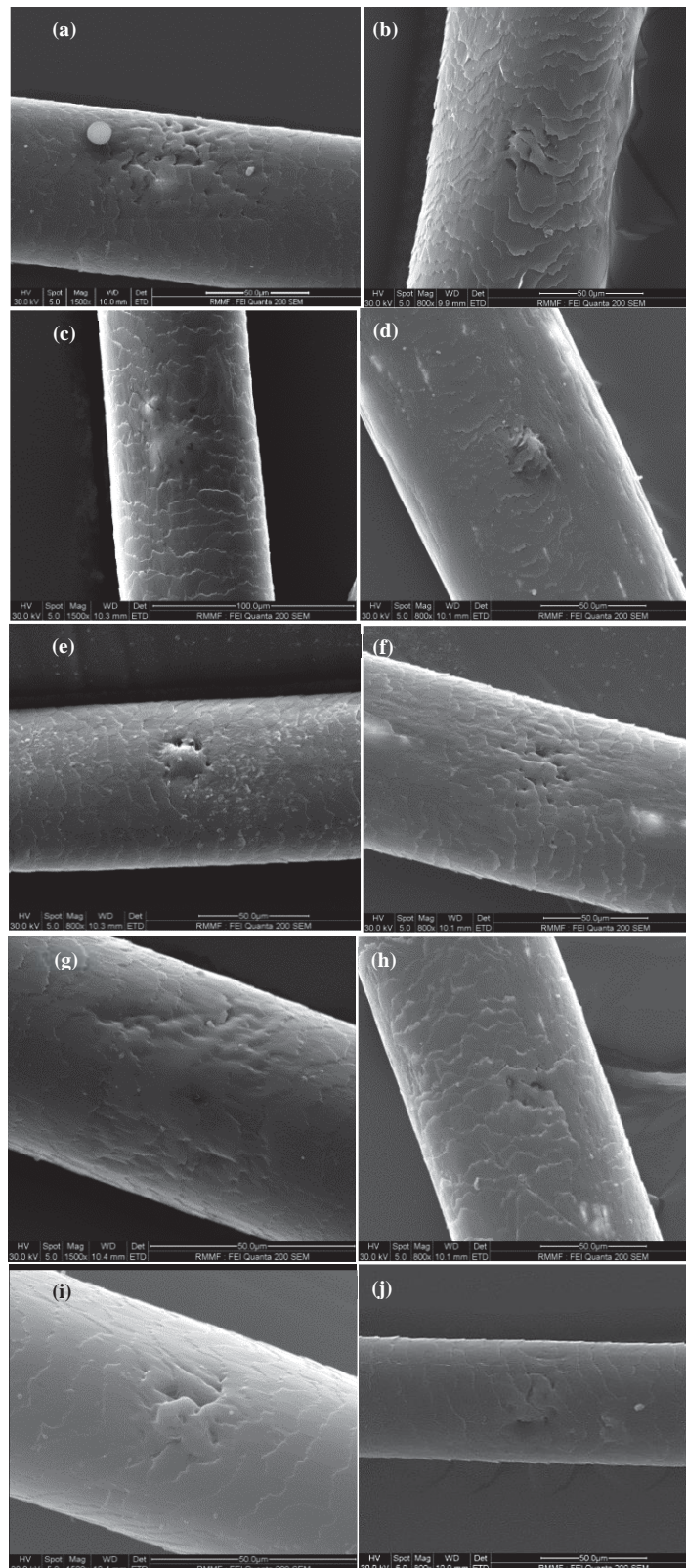


Figure 9.3: Human hair at 800X to 1500X magnifications: (a) Untreated natural, (b) dyed relaxed; Treated with experimental keratin-free conditioner (c) natural and (d) dyed relaxed hair; Treated with experimental conditioner with 2.5 % keratin, (e) natural and (f) dyed relaxed hairs; Treated with experimental conditioner with 5.0 % keratin, (g) natural and (h) dyed relaxed hair; Treated with commercial keratin conditioner, (i) natural and (j) dyed relaxed hairs

The SEM images of the natural untreated bovine leather and the leather treated with the experimental creams containing 2.5 and 5.0 % keratin are shown in Figure 9.4. No significant differences were found in the texture of the untreated leathers and those treated with the experimental creams containing 2.5 and 5 % keratin.

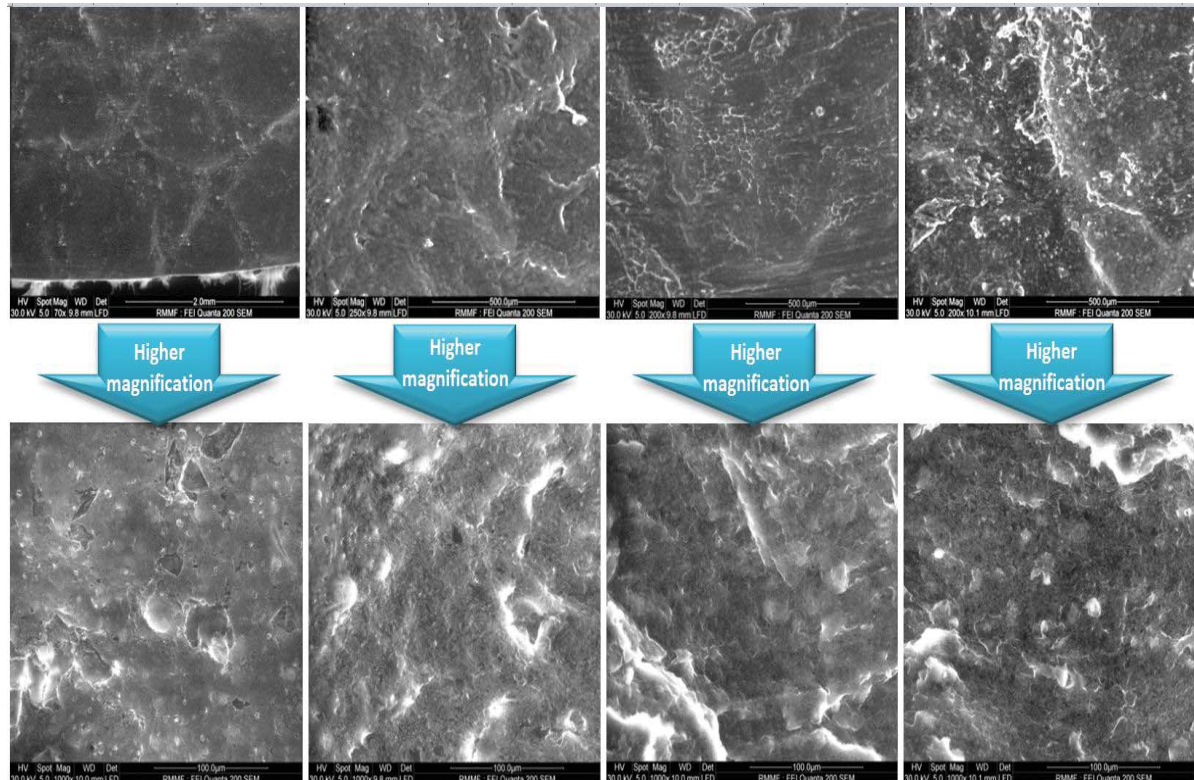


Figure 9.4: Original bovine leather at (upper = 70-250X, lower = 1000X) magnifications: (a) Untreated, (b) Treated with experimental 0 % keratin cream, (c) Treated with experimental 2.5 % keratin cream, (d) Treated with experimental 5.0 % keratin cream

9.3.4 Mechanical properties

The effect of keratin in the experimental (control, 2.5 and 5.0 %) and commercial keratin conditioners, on the stress-strain properties of natural and dyed relaxed hair was evaluated with a DMA Q800 system as shown in Figure 9.5.

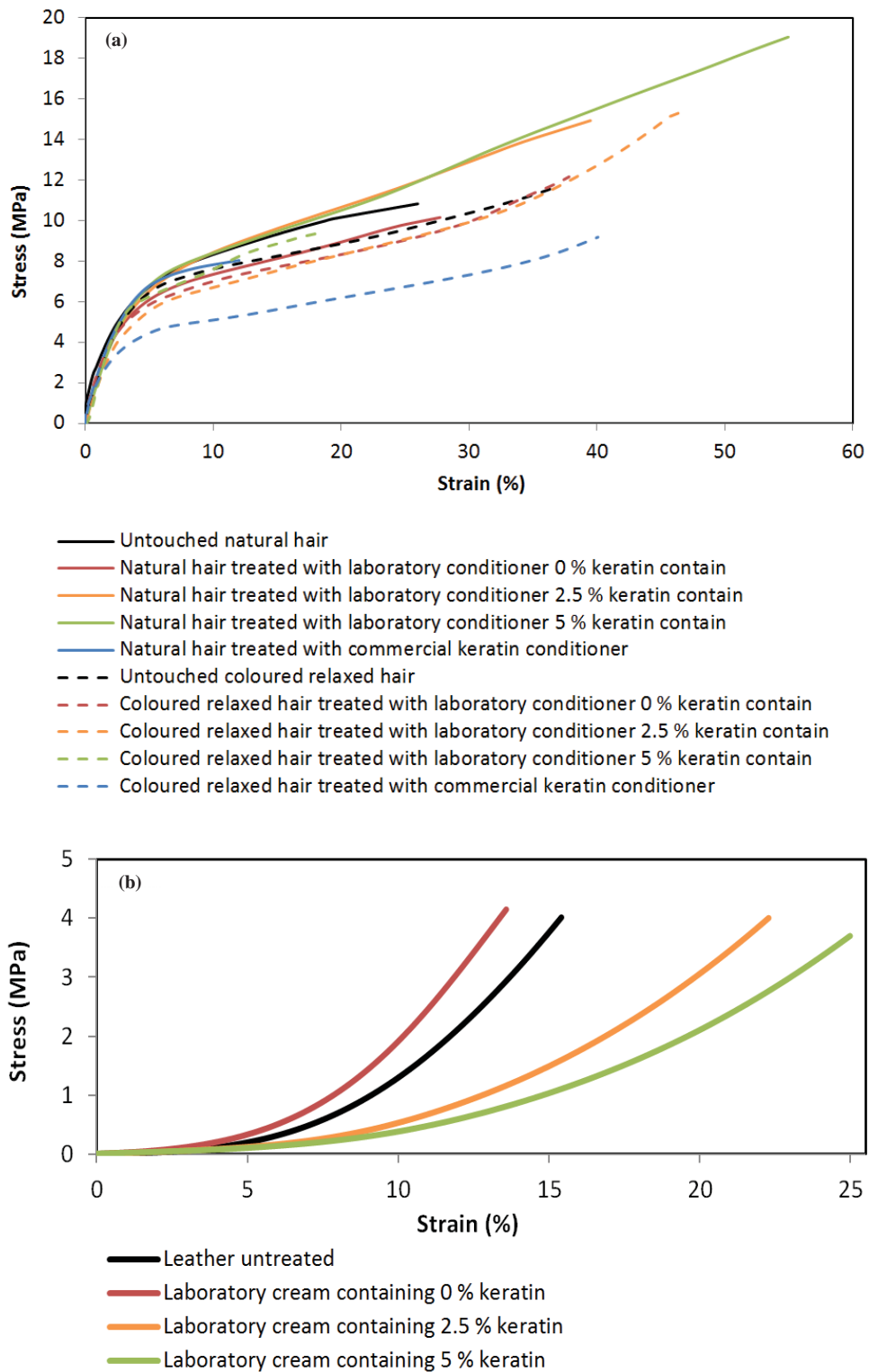


Figure 9.5: Tensile stress–strain curve of (a) human hair, and (b) bovine leather

Table 9.4 shows the average values of the elastic modulus (E), yield stress, breaking stress, strain at break, diameter, standard deviation (SD), and percentage standards error

values associated with 20 similar natural and dyed relaxed hair, untreated and treated with experimental conditioners containing 2.5-5.0 % keratin, determined within 90 % of confidence. The toughest hair belonged to the specimens treated with 5 % keratin concentration as their E , which was the initial slope of the stress–strain curve at 0.25 % strain (as per the ASTM E 111-97 standard 56), were 0.5 GPa and 0.8 GPa for natural and dyed relaxed hair, respectively. The softest hair was the untreated natural hair with E of 0.36 GPa. Even though it was the strongest of all with 6.7 MPa yield stress and dyed relaxed hairs treated by any hair conditioner were the weakest with *ca.* 3 MPa yield stress.

As the area below the stress–strain curve associated with the natural hair treated with experimental conditioner containing 5 % keratin (stress of 19 MPa and the corresponding strain value of 55 %), was considerably larger than other samples, it was concluded that this hair specimen was significantly tougher than all, which confirms the visual difference in hair structure in Figure 9.3(d). Conversely, the natural hair treated with commercial keratin conditioner was the most brittle specimen (stress of 8 MPa and the corresponding strain value of 12 %).

Table 9.5 shows the average values of E' as an indication of elasticity, E'' , representing the amount of energy absorbed, and $\tan\delta$, showing damping associated with untreated bovine leather and leathers treated with experimental creams containing 2.5-5.0 % keratin, determined within 90 % of confidence, performed at a constant temperature of 18 °C. Untreated leathers demonstrated lower E' but higher values of E'' than leather treated with the control cream and higher $\tan\delta$ of the leather treated with the experimental cream with 5 % keratin. Treatment with keratin-enriched cream increased the E' (making the leathers stiffer) and E'' but decreased the $\tan\delta$ values.

Table 9.4: Mechanical properties of keratin-treated and untreated human hair

Hair treatments	Elastic modulus (E) (GPa)		Yield stress (MPa)		Breaking stress (MPa)		Strain at break (%)		Diameter* (mm)	
	Natural	Dyed relaxed	Natural	Dyed relaxed	Natural	Dyed relaxed	Natural	Dyed relaxed	Natural	Dyed relaxed
Untreated	0.36	0.44	6.7	4.7	11	11	26	36	0.096	0.108
SD	0.031	0.011	0.265	0.058	0.108	0.200	0.010	0.854	0.007	0.008
Standard error (%)	4.945	1.398	2.280	0.714	0.573	1.022	0.022	1.374	3.944	0.438
Experimental 0 % keratin conditioner	0.37	0.41	6.1	3.4	10	12	28	37	0.102	0.086
SD	0.002	0.004	0.146	0.306	0.396	0.306	0.480	0.458	0.011	0.005
Standard error (%)	3.62	0.565	1.378	5.239	2.202	1.419	1.006	0.707	6.123	3.357
Experimental 2.5 % keratin conditioner	0.40	0.49	4.6	3.4	15	15	40	47	0.115	0.090
SD	0.006	0.002	0.100	0.200	0.038	0.458	0.021	0.252	0.004	0.002
Standard error (%)	0.840	0.180	1.255	3.396	0.146	1.718	0.030	0.311	2.008	1.487
Experimental 5.0 % keratin conditioner	0.50	0.80	4.4	2.6	19	9	55	18	0.089	0.109
SD	0.046	0.351	0.252	0.058	0.104	0.252	0.030	0.058	0.003	0.006
Standard error (%)	5.292	0.203	3.327	1.299	0.310	1.568	0.031	0.183	1.866	3.021
Commercial keratin conditioner	0.39	0.57	3.7	3.3	8	9	12	40	0.100	0.085
SD	0.003	0.010	0.058	3.3	0.153	0.300	0.025	0.346	0.009	0.003
Standard error (%)	0.395	1.013	0.909	1.269	1.058	1.862	0.121	0.505	4.927	1.953

* The mean diameter value of five-point measurements of 20 hairs.

Table 9.5: Mechanical properties of untreated and treated bovine leather

Leather treatments	Average* storage modulus (E') (MPa)	Average* loss modulus (E'') (MPa)	Average* loss tangent ($\tan\delta$)
Untreated	19.3	6.5	0.34
SD	2	0.2	0.02
Standard error (%)	5.560	2.072	3.724
Experimental 0 % keratin conditioner (control)	19.5	5.9	0.37
SD	0.4	0.3	0.02
Standard error (%)	1.264	2.862	3.653
Experimental 2.5 % keratin conditioner	24.5	8.5	0.35
SD	1	0.3	0.01
Standard error (%)	3.134	2.226	1.018
Experimental 5.0 % keratin conditioner	34.3	11.1	0.32
SD	0.3	0.1	0.001
Standard error (%)	0.487	0.333	0.222

* The mean values are an average of 3 measurements.

9.4 Conclusions

The liquid-state NMR results showed that while keratin can be observed in the extracts from CF, it is not possible to use solution-state NMR to distinguish between the whole, α - and β - keratin segments. The CF and CFK extracted via sodium sulfide and L-cysteine were evaluated for their possible antibacterial properties against two pathogenic bacteria. Disc diffusion, well diffusion and feather diffusion methods were used to assess the antimicrobial activity of the keratin against the test pathogens. The highest antibacterial activity was observed with keratin extracted with L-cysteine against *S. aureus*, where a mean inhibition zone of 15.0 mm was recorded, followed by keratin extracted via Na₂S with a mean inhibition zone of 12.0 mm recorded both in UTM-Solution tested under disk diffusion method. Conversely, in well diffusion method this keratin demonstrated the lowest antibacterial activity with a mean inhibition zone of 10.0 mm. The intact purified CFs did not inhibit any of the tested strains. There was no difference in the antimicrobial effect of the keratins extracted from whole feather or the α - and β -keratin components. The scales of the dyed relaxed hair treated with conditioner looked smoother compared with untreated hair. The hardest hair belonged to the specimens treated with 5 % keratin concentration as their elastic modulus (E) at 0.25 % strain were 0.5 GPa and 0.8 GPa for natural and dyed relaxed hair, respectively. There was no significant difference observed in the obtained SEM images of keratin treated bovine leathers, nor in the texture of the leathers treated with the experimental creams containing 0, 2.5 and 5 % keratin, compared with the original untreated leather. This study explored the feasibility of producing keratin-based materials using CFK in an attempt towards the establishment of more environmentally friendly value-added products. The non-toxic CFK with antimicrobial effects can be a novel solution to mitigate the joint dilemmas of toxicity and contamination when used in many applications.

9.5 References

1. Sundaram, M., R. Legadevi, N. Afrin Banu, V. Gayathri, and A. Palanisammy, *A study on antibacterial activity of keratin nanoparticles from chicken feathers waste against Staphylococcus aureus (Bovine mastitis bacteria) and its antioxidant activity*. European Journal of Biotechnology and Bioscience, 2015. **3**(6, 01-05): p. 1-5.
2. Paul, T., A. Mandal, S.M. Mandal, K. Ghosh, A.K. Mandal, S.K. Halder, A. Das, S.K. Maji, A. Kati, and P.K.D. Mohapatra, *Enzymatic hydrolyzed feather peptide, a welcoming drug for multiple-antibiotic-resistant Staphylococcus aureus: structural analysis and characterization*. Applied biochemistry and biotechnology, 2015. **175**(7): p. 3371-3386.
3. Qiu, Y., N. Zhang, Y. An, and X. Wen, *Biomaterial strategies to reduce implant-associated infections*. The International journal of artificial organs, 2007. **30**(9): p. 828-841.
4. Jones, A., A. Mandal, and S. Sharma, *Protein-based bioplastics and their antibacterial potential*. Journal of Applied Polymer Science, 2015. **132**(18).
5. Espert, A., F. Vilaplana, and S. Karlsson, *Comparison of water absorption in natural cellulosic fibres from wood and one-year crops in polypropylene composites and its influence on their mechanical properties*. Composites Part A: Applied science and manufacturing, 2004. **35**(11): p. 1267-1276.
6. Peleg, A.Y. and D.C. Hooper *Hospital-Acquired Infections Due to Gram-Negative Bacteria*. New England Journal of Medicine, 2010. **362**(19): p. 1804-1813.
7. Gould, I.M., *Costs of hospital-acquired methicillin-resistant Staphylococcus aureus (MRSA) and its control*. International Journal of Antimicrobial Agents. **28**(5): p. 379-384.
8. Lau, O.-W. and S.-K. Wong, *Contamination in food from packaging material*. Journal of Chromatography A, 2000. **882**(1): p. 255-270.
9. Villa, A.L.V., M.R.S. Aragão, E.P. dos Santos, A.M. Mazotto, R.B. Zingali, E.P. de Souza, and A.B. Vermelho, *Feather keratin hydrolysates obtained from microbial keratinases: effect on hair fiber*. BMC biotechnology, 2013. **13**(1): p. 15.
10. Kajiura, Y., S. Watanabe, T. Itou, K. Nakamura, A. Iida, K. Inoue, N. Yagi, Y. Shinohara, and Y. Amemiya, *Structural analysis of human hair single fibres by scanning microbeam SAXS*. Journal of structural biology, 2006. **155**(3): p. 438-444.
11. Roddick-Lanzilotta, A., R. Kelly, S. Scott, G. Mitchell, and S. Chahal, *Protecting the hair with natural keratin biopolymers*. Cosmetics and toiletries, 2006. **121**(5).
12. Harrison, S. and R. Sinclair, *Hair colouring, permanent styling and hair structure*. Journal of Cosmetic Dermatology, 2003. **2**(3-4): p. 180-185.
13. Horev, L., *Environmental and cosmetic factors in hair loss and destruction*, in *Environmental Factors in Skin Diseases*. 2007, Karger Publishers. p. 103-117.
14. Araújo, R., M. Fernandes, A. Cavaco-Paulo, and A. Gomes, *Biology of human hair: know your hair to control it*, in *Biofunctionalization of Polymers and their Applications*. 2010, Springer. p. 121-143.
15. Bolduc, C. and J. Shapiro, *Hair care products: waving, straightening, conditioning, and coloring*. Clinics in dermatology, 2001. **19**(4): p. 431-436.
16. Yuen, C., C. Kan, and S. Cheng, *Evaluation of keratin fibre damages*. Fibers and Polymers, 2007. **8**(4): p. 414-420.

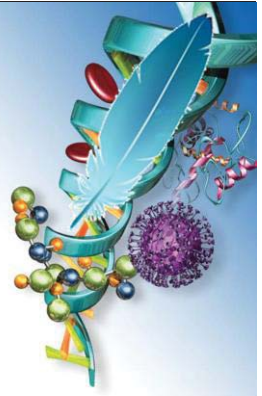
17. Sionkowska, A., J. Skopinska-Wiśniewska, J. Kozłowska, A. Płancka, and M. Kurzawa, *Photochemical behaviour of hydrolysed keratin*. International journal of cosmetic science, 2011. **33**(6): p. 503-508.
18. Freis, O., D. Gauche, U. Griesbach, and H.-M. Haake, *Fluorescence laser scanning confocal microscopy to assess the penetration of low molecular protein hydrolyzates into hair*. Cosmetics and toiletries, 2010. **125**(11).
19. Hütter, I., *Hair care with depth effect by low molecular proteins*. SÖFW-journal, 2003. **129**(1-2): p. 12-16.
20. Barba, C., S. Méndez, A. Roddick-Lanzilotta, R. Kelly, J. Parra, and L. Coderch, *Cosmetic effectiveness of topically applied hydrolysed keratin peptides and lipids derived from wool*. Skin Research and Technology, 2008. **14**(2): p. 243-248.
21. Karthikeyan, R., S. Balaji, and P. Sehgal, *Industrial applications of keratins—a review*. 2007.
22. Fleischner, A.M., *Keratin hydrolysate formulations and methods of preparation thereof*. U.S. Patent 4,818,520, 1989.
23. Naito, S. and T. Nemoto, *Odor-removing and deodorizing composition employing a hydrolysate of keratin material*. U.S. Patent 4,591,497, 1986.
24. Blortz, D., H. Bohrmann, D. Maier, and R. Muller, *Process for preparing a protein hydrolysate from protein containing animal products*. U.S. Patent 5,985,337, 1999.
25. Edens, L., P.J. Dekker, and A.R. De, *Protein hydrolysate rich in tripeptides*. U.S. Patent US 20050256057 A1, 2003.
26. Gousterova, A., D. Braikova, I. Goshev, P. Christov, K. Tishinov, E. Vasileva-Tonkova, T. Haertle, and P. Nedkov, *Degradation of keratin and collagen containing wastes by newly isolated thermoactinomycetes or by alkaline hydrolysis*. Letters in applied microbiology, 2005. **40**(5): p. 335-340.
27. Grazziotin, A., F. Pimentel, E. De Jong, and A. Brandelli, *Nutritional improvement of feather protein by treatment with microbial keratinase*. Animal Feed Science and Technology, 2006. **126**(1): p. 135-144.
28. Wiegmann, H., Y. Kamath, S. Ruestsch, P. Busch, and H. Tesmann, *Characterization of surface deposits on human hair fibres*. J Soc Cosmet Chem, 1990. **44**: p. 387-390.
29. Innoe, T., *Hair cosmetic for protection of skins*. Eur Pat Appl, EP, 1992. **469**: p. 232.
30. Kim, W.W. and S.L. Kendall, *Additive for hair treatment compositions*. U.S. Patent 4,906,460, 1990.
31. Eggum, B.r.O., *Evaluation of protein quality of feather meal under different treatments*. Acta Agriculturae Scandinavica, 1970. **20**(4): p. 230-234.
32. Papadopoulos, M., A. El Boushy, and E. Ketelaars, *Effect of different processing conditions on amino acid digestibility of feather meal determined by chicken assay*. Poultry Science, 1985. **64**(9): p. 1729-1741.
33. Gousterova, A., M. Nustorova, I. Goshev, P. Christov, D. Braikova, K. Tishinov, T. Haertle, and P. Nedkov, *Alkaline hydrolysate of waste sheep wool aimed as fertilizer*. Biotechnology & Biotechnological Equipment, 2003. **17**(2): p. 140-145.
34. Penaud, V., J. Delgenes, and R. Moletta, *Thermo-chemical pretreatment of a microbial biomass: influence of sodium hydroxide addition on solubilization and anaerobic biodegradability*. Enzyme and microbial technology, 1999. **25**(3): p. 258-263.
35. Barrett, G., *Chemistry and biochemistry of the amino acids*. 2012: Springer Science & Business Media.

36. Wang, X. and C. Parsons, *Effect of processing systems on protein quality of feather meals and hog hair meals*. Poultry Science, 1997. **76**(3): p. 491-496.
37. Papadopoulos, M.C., *Effect of processing on high-protein feedstuffs: a review*. Biological Wastes, 1989. **29**(2): p. 123-138.
38. Latshaw, J.D., N. Musharaf, and R. Retrum, *Processing of feather meal to maximize its nutritional value for poultry*. Animal Feed Science and Technology, 1994. **47**(3-4): p. 179-188.
39. Tran, C.D., F. Prosenc, M. Franko, and G. Benzi, *Synthesis, structure and antimicrobial property of green composites from cellulose, wool, hair and chicken feather*. Carbohydrate Polymers, 2016. **151**: p. 1269-1276.
40. Yin, X.-C., F.-Y. Li, Y.-F. He, Y. Wang, and R.-M. Wang, *Study on effective extraction of chicken feather keratins and their films for controlling drug release*. Biomaterials Science, 2013. **1**(5): p. 528-536.
41. Iarikov, D.D., M. Kargar, A. Sahari, L. Russel, K.T. Gause, B. Behkam, and W.A. Ducker, *Antimicrobial surfaces using covalently bound polyallylamine*. Biomacromolecules, 2013. **15**(1): p. 169-176.
42. Tong, S.Y., J.S. Davis, E. Eichenberger, T.L. Holland, and V.G. Fowler, *Staphylococcus aureus infections: epidemiology, pathophysiology, clinical manifestations, and management*. Clinical microbiology reviews, 2015. **28**(3): p. 603-661.
43. Zhao, W., R. Yang, Y. Zhang, and L. Wu, *Sustainable and practical utilization of feather keratin by an innovative physicochemical pretreatment: high density steam flash-explosion*. Green Chemistry, 2012. **14**(12): p. 3352-3360.
44. Song, J., R. Murphy, R. Narayan, and G. Davies, *Biodegradable and compostable alternatives to conventional plastics*. Philosophical Transactions of the Royal Society B: Biological Sciences, 2009. **364**(1526): p. 2127-2139.

9.6 Publication from this Chapter

- Pourjavaheri, F., Jones, O.A.H., & Shanks, R.A. (2016) "Chicken feather keratin in bio-composites", *All Hands Australia Conference*, 5 October, Melbourne, Australia. (Poster Presentation)
- Pourjavaheri, F., Jones, O.A.H., & Shanks, R.A. (2017) "Chicken feather keratin", *ACS on Campus*, 21 July, Melbourne, Australia. (Poster Presentation)
- Pourjavaheri, F., Mohaddes, F., Shanks, R. A., & Sherkat, F. "7. Applications of chicken feather keratin" *Green Chemistry*. To be submitted in 2017.

CHAPTER 10



OVERALL PROJECT ANALYSIS AND EVALUATION

10.1 Overall discussion

Bactericidal performance of surfactants (anionic, non-ionic, and cationic), bleach (ozone and chlorine dioxide), ethanol extraction, and a combined method comprising surfactant-bleach-ethanol extraction on CFs was investigated via a) standard plate count and enumeration of *Escherichia coli*, *Pseudomonas* species, coagulase positive *Staphylococcus*, aerobic and anaerobic spore-formers and b) *Salmonella* and *Campylobacter* detection tests.

The CFs purified by ‘ethanol-extraction purification’ were confirmed to have fatty esters and *Salmonella* removed and exhibited minimal bacterial counts compared with the other methods. The ‘combined surfactant-oxidant-ethanol purification’ method was found to be the second best in reducing bacterial counts and destroying *Salmonella*. Elimination of fatty esters from the CFFs purified via both of these techniques was confirmed by Fourier-transform infrared spectroscopy. The ‘combined surfactant-oxidant-ethanol purification’ method resulted in superior morphological and mechanical properties compared with ethanol-extraction purification.

Optical evaluation of the treated CFFs suggested a similar morphology for the CFFs purified via ozonation and chlorine to the CFFs purified by anionic, non-ionic and cationic surfactants. SEM-EDS results confirmed the presence of sodium lauryl sulphate remnants in CFFs treated via combined purification method; therefore, ethanol-extraction purification method was chosen as the safest single purification for future studies. However, as far as benefiting from superior mechanical properties in bio-composites production, the combined purification method was found to be more promising due to offering fibres of superior tensile strength than ethanol-extraction purification method.

Purification with ‘ionic and non-ionic surfactants’ was found to have cleaned the feathers without changing their texture. The ‘ethanol-extraction purification’ removed fatty and waxy substances leaving the keratin fibre to aggregate along the rachis. Both ‘purifications with

ozonation' and chlorine dioxide whitened feathers, leaving them with a similar texture to those treated with surfactants. No fibre damage was observed in any SEM images. No significant changes in the X-ray diffraction pattern of CFFs were observed, however, the wide-angle X-ray scattering analysis showed that the crystallite size of calamus and rachis was larger than that of barbs and barbules. Infrared spectra and Raman spectroscopy of the feathers were both unchanged, consistent with the small amount of ethanol extract of fatty-waxy material. Thermogravimetry showed rapid decomposition occurring between 225 °C and 500 °C for all feather specimens. A close examination of the derivative showed that the peak temperature for feathers purified via ozonation, chlorine dioxide and anionic surfactant had lower temperatures of decomposition, whereas 'ethanol-extraction purification' and 'purification via non-ionic' resulted in higher decomposition temperatures in comparison with the untreated CFs.

After identification of a reliable technique of feather purification, the purified CF fibres were incorporated in thermoplastic polyether-polyurethane, to form bio-composites. The aim of the work was to enhance the thermo-mechanical properties of polyurethane, to determine whether it was compatible with the feather fibres in an attempt to find a sustainable use for waste feathers. Eco-friendly bio-composites with improved thermo-mechanical properties were prepared by blending CFFs with thermoplastic polyether-polyurethane through a solvent-casting-evaporation-compression moulding method at a feather to polymer ratio of 10, 20, 30, 40, 50, 60 and 70 %·w/w; and thermoplastic polysiloxane-polyurethane through a solvent-casting-evaporation-compression moulding together with solvent-precipitation-evaporation-compression moulding method at a feather to polymer ratio of 10 and 20 %·w/w. TPU-polysiloxane Macro-photographic and SEM imaging of the resulting bio-composites demonstrated effective adhesion, no agglomeration, and an even distribution of

fibres that reflected the compatibility between the CFF and the thermoplastic polyurethane matrix. Molecular modelling, together with Fourier-transform infrared spectroscopy characterisation, indicated that there were both physical and chemical interactions between the feather keratin and the thermoplastic polyether-polyurethane. The addition of CFFs to the thermoplastic polyurethane-polyether was found to increase the mass loss (more flame retardant) but decrease the remaining char ratio, although the opposite occurred at higher temperatures; in addition, it enhanced heat resistance or thermal stability of the biocomposite but decreased the glass transition temperatures of the composites. Reinforcing the polymer with CFFs made the biocomposite stiffer and reduced its deformation. As the volume fraction of feather fibres increased the bio-composites showed a concomitant increase in elastic modulus, compared with the pure thermoplastic polyether-polyurethane, but the loss tangent and recovery strain decreased. The optimum volume fraction of FFs in the composite was found to be 20 % as the resulting bio-composite showed the highest elastic modulus at all studied temperatures. The thermomechanical properties of this bio-composite were enhanced compared with the control polymer.

The addition of CFFs to TPU-polysiloxane enhanced char formation and heat resistance (or thermal stability) elastic modulus, storage modulus and loss modulus of the biocomposite, as the mass loss, loss tangent, and recovery strain of the composites decreased, compared with the pure TPU-polysiloxane. More enhancements in the thermo-mechanical properties of raw TPU-polysiloxane and TPU-polysiloxane CFF bio-composites were observed with the precipitation technique demonstrated better thermo-mechanical properties than the casting method. This part of the study illustrated the potential for creating novel biocomposites, by incorporating agricultural waste CFs into a polymer matrix to form useful materials.

These bio-composites were made from a renewable and biodegradable ingredient, i.e. CFs and since their fabrication is not energy intensive and did not produce much waste they lend themselves to be classed as green material. However, unless the polymer matrix could be made from renewable materials such as vegetable oils [1, 2] this classification may not be applicable. Additionally, it would be possible to add biodegradable additives in carrier polymers to boost their biodegradability, when the above conditions are met then the bio-composites produced could be classified as green [3-5].

Although extraction with sodium sulfide poses environmental issues as a large quantity of the reductive or oxidative agents used for breaking the disulfide bonds, such as thiols and peroxides, cannot be recycled, are harmful, often toxic and difficult to handle [6, 7], the obtained yield was 22 % higher in comparison to the more eco-friendly L-cysteine method. The presence of protein obtained from different extraction methods was confirmed using the biuret test, and the Bradford assay enabled the concentration of keratin to be determined. The extracted keratin was characterised using gel electrophoresis, which confirmed soluble protein with molar mass of 11 kg/mol and estimated purity of over 95 %, for both extraction methods. Liquid chromatography-mass spectrometry verified that the molar mass of the extracted material matched that of chicken keratin. Vibrational and nuclear magnetic resonance spectroscopies confirmed that the structure of keratin was retained following extraction. The TGA of purified CF and keratin extracted via sodium sulfide showed virtually identical decomposition behaviour, proving the purity of the keratin.

The TGA, Raman and NMR spectroscopy confirmed the presence of L-cysteine residues in keratin extracted via L-cysteine method. The SSNMR confirmed that the structure of keratin was retained following extraction via both methods and that ^1H SSNMR could potentially be used as an analytical technique to differentiate between α - and β -keratin.

Thermogravimetry and derivative thermogravimetry curves for purified CFs and keratin extracted via sodium sulfide showed the virtually identical behaviour of decomposition, which proved the purity of the extracted keratin.

This study confirmed the feasibility of transforming disposable CFs into useful keratin powders using both sodium sulfide and L-cysteine. The results obtained showed that what is currently a waste product of the poultry industry can potentially be a new, low-cost and sustainable source of keratin, a substance currently in demand, with applications in a variety of products including but not limited to beauty treatments, polymer industry, tissue engineering, and health and biomedical industries. Solution-state nuclear magnetic resonance results showed that while keratin can be observed in the extracts from CF, it could not distinguish between the whole, *alpha*- and *beta*-keratin segments.

The CF and CFK extracted via sodium sulfide and L-cysteine were evaluated for their possible antibacterial perspective against two pathogenic bacteria i.e. *S. aureus* and *E. coli* as Gram-positive and Gram-negative species, respectively. Disc diffusion, well diffusion and feather diffusion methods were used to assess their antimicrobial activity against the test pathogens. The highest antibacterial activity of the keratin extracted via L-cysteine was observed against *S. aureus*, tested with disk diffusion method, whereas, the well diffusion method gave the lowest activity. The direct feathers diffusion did not result in any antibacterial effect against *E. coli* or *S. aureus*. The antimicrobial assays showed no observable differences between whole, *alpha*- and *beta*-keratin components.

The CFK extracted with sodium sulfide, was incorporated at 2.5 and 5.0 % into hair conditioner and cream, and placed onto untreated and dyed, relaxed hair, and leathers to determine their interactions with the tissues. The keratin-based products such as keratin conditioner, and keratin cream at three levels were produced and the effect of CFK on

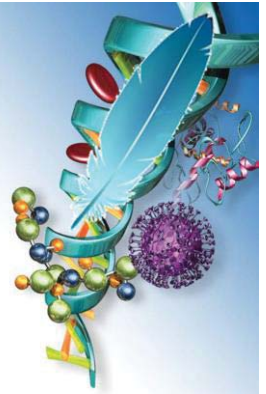
untreated and coloured, relaxed hair was investigated. The scales of the coloured relaxed hair treated with all conditioners looked smoother compared with untreated hair. The toughest hair belonged to the specimens treated with 5 % keratin conditioner according to the DMA results. No significant difference was observed in the SEM images of keratin-treated bovine leathers nor in the texture of the leathers treated with the experimental creams containing 2.5 and 5 % keratin, compared with the original untreated leather.

The greatest climate-related challenges are man-made damages to the environment which are compounded by the generation of waste products that pollute the environment. As mentioned earlier, millions of tons of feathers are generated annually as a by-product of the worldwide poultry industry. These feathers, pose a significant and costly waste disposal problem for said industry and are an environmental pollution hazard since, at present, they are mostly either incinerated or sent to landfill. To curb this problem we need to find more advance, non-traditional uses for the waste feathers. This project has attempted to design safe and reliable techniques for purifying the waste feathers from dirt, dust, oil, and most importantly, the hazardous pathogens, and to incorporate the purified feathers into prototype bio-composite materials for potential industrial applications. This has the double advantage of both reducing the amount of waste that needs to be disposed of and creating a new, high-value material that is environmentally sustainable. Furthermore, this project used the CFs in order to produce keratin powders while employing an eco-friendly technique that is currently highly needed among the researchers.

10.2 References

1. Petrović, Z.S., *Polyurethanes from vegetable oils*. Polymer Reviews, 2008. **48**(1): p. 109-155.
2. Guo, A., D. Demydov, W. Zhang, and Z.S. Petrovic, *Polyols and polyurethanes from hydroformylation of soybean oil*. Journal of Polymers and the Environment, 2002. **10**(1-2): p. 49-52.
3. Zini, E. and M. Scandola, *Green composites: an overview*. Polymer composites, 2011. **32**(12): p. 1905-1915.
4. Zia, K.M., M. Barikani, I.A. Bhatti, M. Zuber, and H.N. Bhatti, *Synthesis and characterization of novel, biodegradable, thermally stable chitin-based polyurethane elastomers*. Journal of applied polymer science, 2008. **110**(2): p. 769-776.
5. Quirino, R.L., T.F. Garrison, and M.R. Kessler, *Matrices from vegetable oils, cashew nut shell liquid, and other relevant systems for biocomposite applications*. Green Chemistry, 2014. **16**(4): p. 1700-1715.
6. Wang, Y.-X. and X.-J. Cao, *Extracting keratin from chicken feathers by using a hydrophobic ionic liquid*. Process Biochemistry, 2012. **47**(5): p. 896-899.
7. Tonin, C., M. Zoccola, A. Aluigi, A. Varesano, A. Montarsolo, C. Vineis, and F. Zimbardi, *Study on the conversion of wool keratin by steam explosion*. Biomacromolecules, 2006. **7**(12): p. 3499-3504.

CHAPTER 11



CONCLUSIONS AND RECOMMENDATIONS

11.1 Conclusions

The structure and properties of the different components of CF were characterised and compared with pigeon feather and sheep wool as another keratin source, in order to determine their suitability for various applications. The physical and morphological properties and the suitability and safety of whole CF and its components including calamus and rachis together with barbs and barbules, as sources of keratin for biomedical materials formulation were studied. The raw CFFs taken from a poultry processing plant were treated by anionic, non-ionic and cationic surfactants followed by purification, bleaching with ozone and chlorine dioxide, fat removal with ethanol using a Soxhlet extraction method and - including the analysis of any extractable components before and after treatments to observe the effects of each treatment on the CFFs.

Keratin derived from waste CFs was purified, characterised, compared and evaluated as a material for inclusion in biomaterials with potential structural and biomedical applications, which was the aim of this project.

The scope of this project included developing methods for the purification of raw poultry feathers, extraction of keratin protein from them, designing of keratin-based materials and their characterisation and comparison of the chemical, physical and morphological structure of keratin using FTIR spectroscopy, wide angle X-ray scattering, optical microscopy, macro photography and scanning electron microscopy.

While some properties of the feather fibres have previously been reported, this project comprehensively quantifies these material properties as its main objectives: 1) To purify CFs by ionic, non-ionic and cationic surfactant treatments, bleaching with ozone and chlorine dioxide, Soxhlet extraction with ethanol and a combination of these techniques. 2) To characterise and compare the chemical, physical and morphological structure of CFK (using

FTIR spectroscopy, wide angle X-ray scattering, optical microscopy, macro photography and SEM) with keratin from other feather sources such as pigeon, or with other keratins such as wool. 3) To separate CFs into wool (α -helix) and rachis (pleated sheet) components for separate evaluation and application. 4) To prepare compositions (using CFFs) in polymers, waxes or oils (using keratin) and evaluation of the thermal and mechanical properties of the bio-composites incorporating CFs. 5) To extract keratin from CFs using reducing agents, then optimise keratin extraction and keratin purification methods. 6) To evaluate the antibacterial effects of the CF and extracted keratins for medical applications.

To manufacture a sustainable bio-material, the purified CFFs were mixed with a polymer, thermoplastic polyurethane-polyether at different ratios. The uniformity of the feather fibre dispersion in the polymer matrix was investigated via light-photography, whereas the compatibility of the polymer with the CFFs was determined with SEM of the fracture surfaces of bio-composites. The bio-composites were then characterised using TGA, DMA and stress-strain measurements to investigate their thermo-mechanical properties. The molecular modelling visualisation was used together with FTIR analysis in order to determine whether the polyurethane was compatible with the CFFs. Ultimately, FF is a multipurpose, cost effective reinforcement for polymer composites which may enable valuable new products to be developed. The keratin was then extracted from the purified CFFs and compared with human epidermis keratin as a commercial keratin. This part of the study provides ideas of keratin-based materials towards the establishment of more environmentally friendly value-added products.

The prepared bio-materials provide examples on possible pathways for make a use to thousands of tonnes of waste feathers produced annually, thus reducing its environmental impact. Creating lower density composites reduces their transport costs and associated CO₂

emissions, whilst eliminating a source of corrosive substances which are a threat to the environment, when carried out in a sustainable way. The findings of this project in relation to the purification, design and characterisation of keratin-based materials and compositions from CFs, may lead to new derivatives and applications that can lead to novel ideas for value-adding to a waste material.

This project proposes to reduce waste and thus turns a material that currently increases global warming into one that reduces consumption of energy by combining CFs and polymers to reduce the use of them while reducing burning or composting of feathers. Both these actions diminish the production of greenhouse gases. The study conclusively demonstrates that the resulting bio-composite materials have enhanced thermo-mechanical properties compared with pure polymer and illustrates that keratin derived from feathers can be used, simply and cheaply to create new composite materials, with potentially large environmental benefits.

11.2 Applications

Waste keratin has potential to be converted into usable materials, fibrous, films or membranes that can lead to many potential applications, particularly in the biomedical, tissue engineering and cosmetic fields. There are many potential applications for keratin-based materials mainly in pharmaceuticals, drug therapies, coatings for drugs, wound and burn healing creams, tissue engineering, artificial bone, bone scaffold, composites, building materials, textile applications, cosmetics, personal care products such as conditioning shampoo, sulfite hair straightener, facial cleanser, etc.

The current project not only offers the possibility of novel products from troublesome waste CFs, but will reduce various environmental problems such as chlorosis, fowl cholera

and various human ailments [1] (i.e. abdominal pain, diarrhea, fever, nausea and vomiting), when disposed of in landfills, hence, solves an environmentally sensitive issue of waste disposal, by reducing solid wastes being sent to landfills.

11.3 Future directions and novel applications of keratin

To date some efforts have been made to develop green materials using extracted keratin from different sources, yet there is still much work needed to replace chemically synthesised polymers with degradable and eco-friendly biomaterial. As far as the biological and chemical behaviour of functional groups is concerned, limited efforts have been made to understand the fundamental properties of the CFK. Thus, more in-depth research is required to investigate how the cysteine–cysteine crosslinks can be fully reduced without hydrolyzing the protein to its constituent peptides and amino acids. Development of hybrid nano-biomaterials by in-situ nano-modifications of keratin, through effective exploitation of nanotechnology, along with the development and application of biopolymers can potentially lead to the development of green products with enhanced properties for applications in textiles, composites, nano-biomaterials, and other bioproducts.

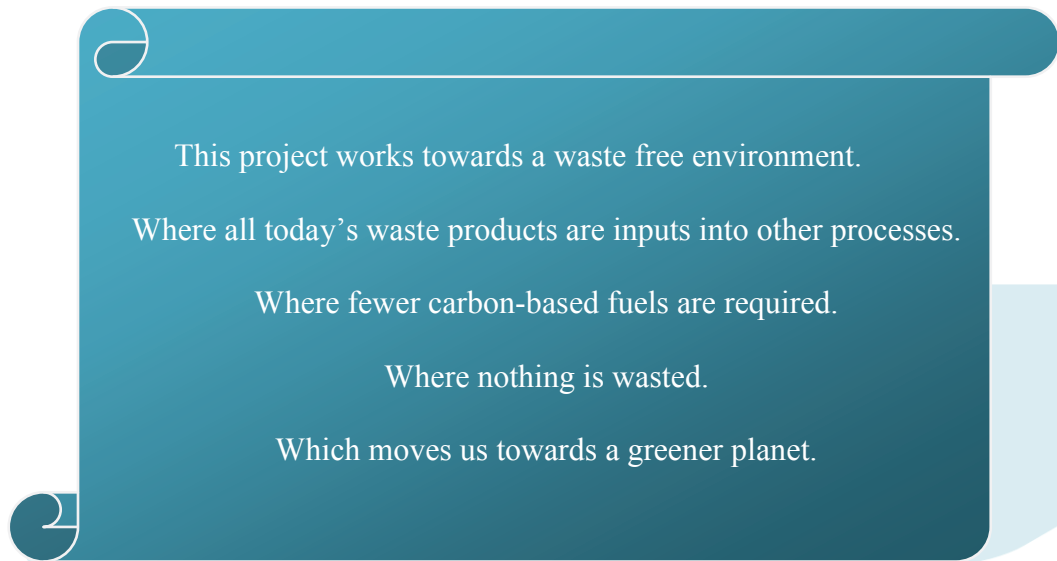
The advanced method used in this study for the extraction, purification and characterisation of keratin from CFs may lead to new applications that can open novel directions for value-adding to waste materials, such as the potential growth in keratin-based green material development and applications in the biomedical field.

11.4 Recommendations

With the knowledge gained in this study, there are different areas of interest that could be further investigated:

- Establish the relationship between the degree of fluorescence and the quality of CFF-extracted keratin.
- Investigate the structure of protein crystals in various parts of the feathers in greater detail using the synchrotron.
- Measure feather whiteness, after bleaching with various treatments using a colourimeter and determine if there is a relation between colour change and the crystalline structure of feather protein, and so the quality of the final material i.e. the extracted keratin
- Scale up the production of the bio-composites for use in food packaging as well as in bio-medical applications. The large-scale process could produce fibre quality that is more consistent in terms of CFFs purification, and composite preparation. Further development should consider the scale-up and the equipment available within the relevant industry.
- Comparison of the knowledge obtained from this study such as the single fibre tensile test, with other types of fibres.
- Find more advanced industrial applications for the bio-composite material such as industrial insulation blocks.
- Prepare the bio-composites that are compatible with the human body for use in tissue engineering such as artificial ears and nose production.

- Determine the effect of CFFs on the properties of other polymers such as PVC where limited study has been carried out.
- Determine the toxicity, amino acid composition and chemical composition of the extracted keratin for better understanding of the properties of the protein obtained.
- Determine the optimum keratin concentration for antimicrobial activities.
- Develop a water-proof wound dressing, using suitable polymer, keratin alone and in combination with other additives.
- Further addition of different keratin ratio to the bio-composite blends, as well as the examination of other types of polymers would serve to determine what blends and materials should be used to produce bio-composites with the best combination of properties based on the application.
- Determine if keratin bio-composites could be utilised in medical settings, using testing based on the intended end use in areas such as packaging medical products, as well as infection testing for medical.
- Undertake antimicrobial studies on each bio-composite variation for medical applications.
- For food packaging applications, the determination of water vapour and oxygen permeability properties of the bio-composites would be crucial to determine, as they help establish their suitability for the intended use.
- Prepare organic keratin by using organic chicken feather fibres and compare their compositions.



11.5 References

1. Kumar, D.M., P. Priya, S.N. Balasundari, G. Devi, A.I.N. Rebecca, and P. Kalaichelvan, *Production and optimization of feather protein hydrolysate from Bacillus sp. MPTK6 and its antioxidant potential*. Middle-East journal of scientific research, 2012. **11**(7): p. 900-907.



APPENDIX **1**

JOURNAL PUBLICATIONS

Avian keratin fibre-based bio-composites

Firoozeh Pourjavaheri, Farzad Mohades, Oliver Jones and Frank Sherkat
School of Science, RMIT University, Melbourne, Victoria, Australia

Ing Kong

Department of Mechanical, Materials and Manufacturing Engineering,
The University of Nottingham Malaysia Campus, Jalan Broga, Selangor Darul Ehsan, Malaysia
and School of Science, RMIT University, Melbourne, Victoria, Australia

Arun Gupta

Faculty of Chemical and Natural Resources Engineering, Universiti Malaysia Pahang, Kuantan, Malaysia, and

Robert A. Shanks

School of Science, RMIT University, Melbourne, Victoria, Australia

Abstract

Purpose – This paper aims to use the solvent-casting-evaporation method to prepare new bio-composites with thermoplastic poly(ether urethane) (TPU-polyether) as the polymer matrix and reinforced with natural chicken feather fibre (CFF).

Design/methodology/approach – To produce the bio-composites, 0 to 60 per cent-w/w of fibres in steps of 30 per cent-w/w were added to the polymer matrix. The uniformity of distribution of the keratin fibres in the polymer matrix was investigated via scanning electron microscopy, and the results suggested compatibility of the TPU-polyether matrix with the CFFs, thereby implying effective fibre-polymer interactions.

Findings – Addition of natural fibres to the polymer was found to decrease the mass loss of the composites at higher temperatures and decrease the glass transition temperature, as well as the storage and loss modulus, at lower temperatures, while increasing the remaining char ratio, storage modulus and loss modulus at higher temperatures.

Originality/value – The investigation confirmed that waste keratin CFF can improve the thermo-mechanical properties of composites, simply and cheaply, with potentially large environmental and economic benefits.

Keywords Bio-composites, Keratin chicken feather fibre, Thermoplastic poly(ether urethane)

Paper type Research paper

Introduction

Industrial ecology is the study and design of sustainable industrial systems. Ideally, such systems should be connected, with the waste products of one industry becoming the raw materials for another, thereby creating a closed-loop system mimicking, and drawing inspiration from, natural ecosystems (Wielage *et al.*, 2003).

Millions of tons of feathers are generated as a by-product of the poultry industry worldwide annually (Williams *et al.*, 1990). Feathers, particularly from chickens, pose a significant waste disposal problem for the industry and are an environmental pollution hazard, as, at present, they are mostly either incinerated or sent to landfill. Recently, there has been increasing interest in trying to overcome this issue by finding uses for the waste feathers. One potential application is in composite materials; this has the double advantage of both reducing the amount of waste that needs to be disposed of and helping make the resulting plastics more degradable and environmentally sustainable (Jin *et al.*, 2011).

A possible polymer matrix for chicken feather fibres (CFFs) is linear thermoplastic poly(ether urethane), or TPU-polyether. One form of TPU is marketed as Pellethane[®], and this consists of poly(tetramethylene glycol) and methylene diphenyl diisocyanate (MDI) 2103-85AE elastomer, which mostly has an amorphous structure, apart from a small amount of crystallinity in the polyether groups. A bio-based TPU polymer (Pearlthane ECO) also exists and is made up of block copolymers consisting of a sequence of polyol soft segments and hard polyurethane segments. Together, CFFs and TPU-polyether have great potential to make a strong, useful and sustainable material. There are, however, few studies detailing composites made from protein fibres obtained from agricultural sources. This work was undertaken as a proof-of-concept study and investigated keratin obtained from waste feathers from the poultry industry as a fibre resource for bio-composite creation. The overall aim of the work was to optimize the thermo-mechanical properties of polyurethane-based bio-composites made with CFF-derived material.

The solvent-casting-evaporation technique was used to create new bio-composites with TPU-polyether as the polymer matrix and reinforced with natural CFFs. TPU-polyether has a chemical structure compatible with CFF

The current issue and full text archive of this journal is available on Emerald Insight at: www.emeraldinsight.com/1708-5284.htm



World Journal of Engineering
14/3 (2017) 183-187
© Emerald Publishing Limited [ISSN 1708-5284]
[DOI 10.1108/WJE-08-2016-0061]

Received 10 August 2016
Revised 23 September 2016
Accepted 10 October 2016



Cite this: RSC Adv., 2015, 5, 69899

Purification of avian biological material to refined keratin fibres

Firoozeh Pourjavaheri, Farzad Mohaddes, Prue Bramwell, Frank Sherkat and Robert A. Shanks*

Keratin derived from chicken feather fibres (CFFs) has many potential applications that are constrained by the quality and pathogen content after purification treatment. The pathogen activity after purification has not been evaluated elsewhere. Plucked chicken feathers are prone to impose biological hazards due to accommodating blood-borne pathogens; therefore, establishing an efficient purification process is crucial. Bactericidal performance of surfactants (anionic, non-ionic, and cationic), bleach (ozone and chlorine dioxide), ethanol extraction, and a combination method comprising surfactant-bleach-ethanol extraction on chicken feathers was investigated via (A) standard plate count and enumeration of *Escherichia coli*, *Pseudomonas* species, coagulase positive *Staphylococcus*, aerobic and anaerobic spore-formers and (B) *Salmonella* and *Campylobacter* detection tests. Among the purification methods, only ethanol extraction and combination methods eliminated *Salmonella* from the untreated feathers. Although ethanol extraction exhibited superior bactericidal impact compared to the combination method, the feathers treated through the latter method demonstrated superior morphological and mechanical properties. Scanning electron microscopy-energy dispersive spectroscopy was employed to determine the remaining content of selected purifiers on treated CFFs. Fourier-transform infrared spectroscopy confirmed the successful removal of fatty esters from CFFs using nominated purifiers. Ethanol extraction was found to be the most efficacious single treatment, while combination of surfactant and oxidative sterilizer with ethanol was superior.

Received 13th May 2015
Accepted 20th July 2015

DOI: 10.1039/c5ra08947f

www.rsc.org/advances

1. Introduction

The poultry industry generates millions of tonnes of feathers as a by-product per year worldwide.¹ Utilization of chicken feather fibres (CFFs) will not only be beneficial for the poultry industry, but will also reduce health hazards, and benefit the environment, by reducing solid wastes being sent to landfills.² Although CFFs are an abundant, inconvenient and troublesome waste product, they contain over 90% of keratin protein.^{3,4} According to Rouse and Van Dyke,⁵ keratins extracted from bio-fibres such as CFFs and wool are capable of forming self-assembled structures that regulate cellular recognition and behaviour; these qualities have led to the development of keratin biomaterials with applications in wound healing, drug delivery, tissue engineering, trauma and medical devices. Given the fibrous structure of CFFs, their application in bio-degradable and green composites has been studied.⁶

Due to contamination with intestinal contents, blood, fatty acids, offal fat, preen oil, and debris, fresh plucked feathers can be a suitable habitat for many microorganisms such as *Campylobacter*, *Salmonella* and *Escherichia* species (spp.), which

are known to cause gastroenteritis.⁷ The presence of pathogens in plucked feathers can impose potentially fatal biological hazards for humans; however, many microorganisms existing in feathers can be killed *via* either physical or chemical means.^{8–10} Efficient and non-degradative methods are required for purification and separation of CFF keratin to render it safe, clarified and an accessible abundant resource for a variety of uses.

Disinfectants are nonsporidicidal agents that destroy pathogenic microorganisms.¹¹ Rutala *et al.*¹² reported the disinfecting capacity of ethanol at various concentrations against a variety of microorganisms; *Pseudomonas aeruginosa* was killed in 10 s by ethanol at concentrations between 30% v/v and 100% v/v. *Escherichia coli* (*E. coli*) and *Salmonella typhosa* were killed in 10 s by any ethanol concentrations between 40% v/v and 100% v/v. *Staphylococcus aureus* (*S. aureus*) was slightly more resistant, requiring higher concentrations of ethanol, between 60% v/v and 95% v/v for the same period.

Sanitizers are defined as chemical agents capable of killing 99.999% of specific bacterial populations within 30 s, yet they may or may not destroy pathogenic or harmful bacteria.^{12,13} Ozone (O₃) is a well-known sanitizer capable of killing various pathogens and bacteria including spores.^{14,15} The bactericidal effect of O₃ is associated with its high oxidation potential and its ability to diffuse through biological cell membranes.¹⁴ Naidu¹⁶

School of Applied Sciences, RMIT University, VIC 3001, Australia. E-mail: robert.shanks@rmit.edu.au; Fax: +61 3 9925 3747; Tel: +61 3 9925 2122

Advanced Materials Research Vols. 941-944 (2014) pp 1184-1187
© (2014) Trans Tech Publications, Switzerland
doi:10.4028/www.scientific.net/AMR.941-944.1184

Effects of Different Purification Methods on Chicken Feather Keratin

Firoozeh Pourjavaheri^{1, a}, Farzad Mohaddes^{2, b}, Robert A. Shanks^{1, c},
Michael Czajka^{1, d} and Arun Gupta^{3, e}

¹School of Applied Sciences, RMIT University, VIC 3000 Australia

²Centre for Advanced Materials and Performance Textiles, RMIT University, Australia

³Faculty of Chemical and Natural Resources Engineering, Universiti Malaysia Pahang, Gambang Campus, 25100, Kuantan, Pahang, Malaysia

^afiroozeh.jad@student.rmit.edu.au, ^bfarzad.mohaddes@rmit.edu.au, ^crobert.shanks@rmit.edu.au,
^dMC1@pobox.com, ^earun@ump.edu.my

Keywords: keratin; purification; protein; poultry; chicken feathers

Abstract. Every year billion kilograms of unused feathers result from the poultry industry worldwide, which in effect impose a difficult disposal process to the environment. Chicken feathers are considered as a valuable and renewable keratin protein source, which could be used advantageously in a number of applications as alternatives to feather meal and feather disposal. Although the potential applications of keratin derived from chicken feathers have been investigated, the initial purification phase has not been fully described in the literature. Original chicken feathers contain many biological organisms along with other contaminants after plucking. Unprocessed chicken feathers are considered as potentially hazardous biological materials due to the presence of blood borne pathogens; therefore, the decontamination process is very important. The purpose of this work is to compare the effects of different purification techniques on chicken feathers prior to keratin isolation. These processes include surfactant washing, soxhlet extraction with ethanol, ozone, and sodium chlorite solutions. Thermogravimetric analysis, vibrational spectroscopy, and wide angle X-ray scattering were used to characterise the purified feathers prior to keratin extraction.

Introduction

Chicken feathers are a good source of natural fiber keratin, which is potentially valuable biopolymer. The amount of this waste is continuously increasing, in conjunction with the increase in fowl meat production. Many publications proposing applications for keratin preparations in the medical industries are described in literature and opportunities to use this interesting protein in other fields have arisen. Utilization of chicken feathers will be beneficial for the poultry industry by reducing health hazards and will benefit the environment by reducing solid wastes being sent to landfills [1]. The current project solves the environmentally sensitive problem of waste disposal. As unprocessed chicken feathers are a potential biological hazard, it is imperative that they are decontaminated before application. Although several investigations have been conducted to explore the possible applications of keratin extracted from chicken feathers, the initial decontamination phase has not been fully described. The aim of this study is to perform a comparative study of different purification approaches that can be used for chicken feathers prior to keratin isolation. The methods include surfactant washing using an ionic and a non-ionic surfactant. Soxhlet extraction with ethanol was performed to efficiently extract fatty and waxy materials. Ozone and sodium chlorite bleaching were used to sterilize and whiten the keratin. Thermogravimetric analysis, Raman, and wide angle X-ray scattering were used to characterise the feathers and residues after purification and prior to keratin extraction.



APPENDIX 2

JOURNALS TO BE PUBLISHED



Green Chemistry

ARTICLE

Keratin-fibre polyurethane-polyether green bio-composites preparation and characterisationFiroozeh Pourjavaheri^a, Oliver A.H. Jones^{a*}, Michael Czajka^a, Isaac Martinez Pardo^a, Ewan W. Blanch^a and Robert A. Shanks^{a*}

Received 00th January 20xx,

Accepted 00th January 20xx

DOI: 10.1039/x0xx00000x

www.rsc.org/

A polyurethane-polyether bio-based polymer and a sustainable, natural resource in the form of chicken feather (keratin) fibres, were combined to form a bio-composite via solvent-casting-evaporation at 0, 10, 20, 30, 40, 50, 60 and 70 % w/w. The aim was to enhance the thermo-mechanical properties of polyurethane and to determine whether the polyurethane was compatible with the feather fibres. The thermo-mechanical properties of the resulting composites were assessed using thermogravimetry, dynamic mechanical analysis and stress-strain measurements with hysteresis loops. The uniformity of the dispersion of the feather fibre in the polyurethane matrix was investigated via macro-photography. Scanning electron microscopy of fracture surfaces was used to verify that the adhesion between fibre and polymer was effective. A molecular modelling visualisation showed the existence of hydrogen bonding between fibres and polyurethane molecules and this result was supported by Fourier-transform infrared analysis of the composite. Addition of chicken feather fibres to the polyurethane matrix was found to decrease the glass transition temperature, recovery strain and mass loss of the composites, but increase the elastic modulus, storage modulus and char level. The results demonstrate that keratin derived from what is currently a waste product from the poultry industry (with significant disposal costs) is compatible with the matrix and can effectively and cheaply improve the thermo-mechanical properties of composites, with potentially large environmental benefits.

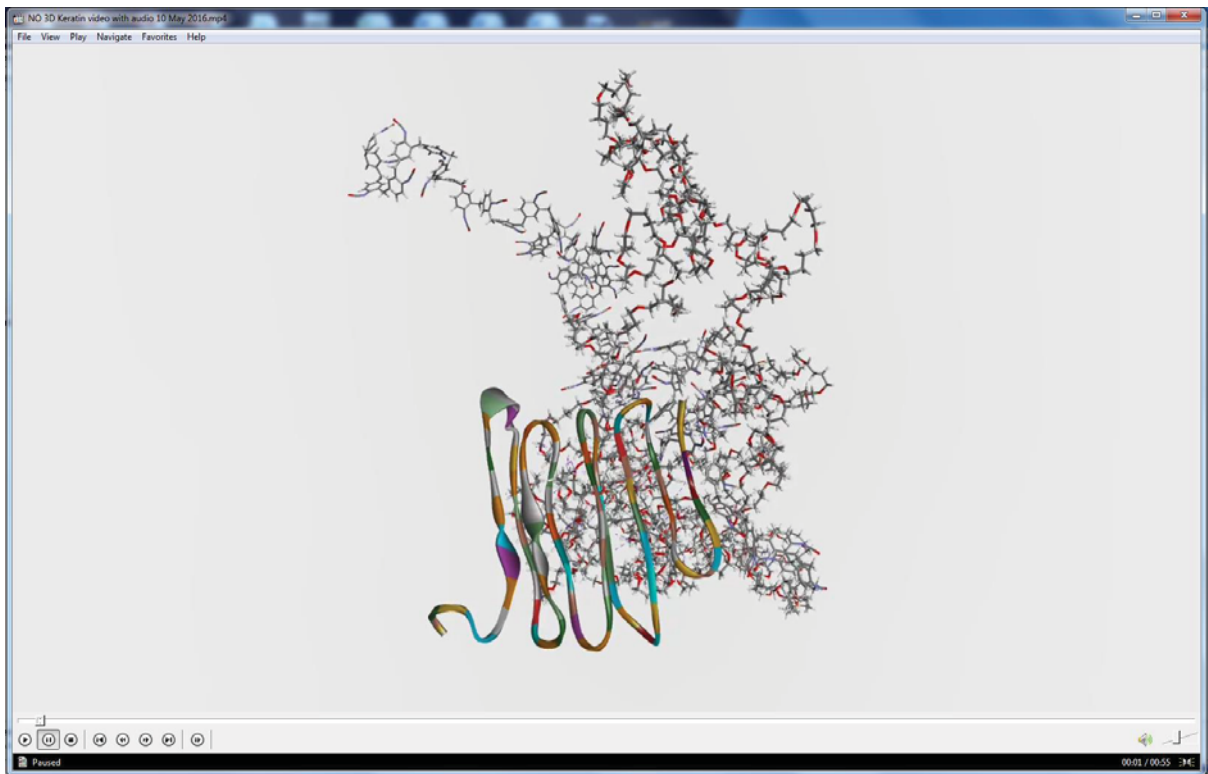
1. Introduction

Green composites are a specific class of bio-composites where a bio-based polymer matrix such as a biodegradable polyurethane is reinforced by natural fibres such as keratin feather fibres; both matrix and reinforcement derive from renewable resources¹⁻³. Additionally, bio-based polymers have been defined to include synthetic or machine-processed organic macromolecules derived from biological resources for plastic and fibre applications^{1, 4}. All bio-based materials contain a certain amount of bio-based carbon that can be calculated, as a weight fraction of the total C-content, from the relative amount of carbon-14 in the material, according to ASTM D6866 standard¹. The term bio-polymer polyurethane or thermoplastic polyether-polyurethane (TPU-polyether) covers a large class of polymers with diverse physical and chemical properties, expected to be suitable for any biomedical or industrial application². While ether-based polyurethane is an excellent choice for water applications⁵, the use of TPU-polyether in many other areas is often not practical due to its poor heat resistance and mechanical properties^{6, 7}. Development of TPU-polyether with enhanced

thermo-mechanical properties can be accomplished via the incorporation of reinforcing materials, the main aim of this study, and would be beneficial to a range of plastic-using industries. Biological material, in the form of feathers, has the potential to fulfil this reinforcing fibre role and has the added benefit of utilising a resource that would otherwise go to landfill.

Keratin in the form of ground chicken feathers is an interesting candidate for the development of new plastic composites, which has recently become an attractive area of research due to the unique properties of feathers such as low density (0.89 g·cm⁻³), toxicity, abrasiveness and associated machine wear, and with high thermal insulation, flame resistance, sustainability, biodegradability and bio-compatibility, good insulation properties and sheer physical abundance, thus low cost^{1, 8-10}. There has however, been limited development and characterisation of TPU-polyether bio-composites made with these materials⁹. Feathers have a remarkably complex structure. Interestingly, it is known that incorporating different parts of the feather (e.g. calamus, rachis, barbs and barbules¹¹) into a polymer matrix can result in different thermo-mechanical properties of the final composite¹². However, the segregation of each feather segment is time consuming and therefore expensive. Hence, a mixture consisting of fibres from whole feathers is generally more easily prepared and incorporated into a polymer matrix. Different polymer-feather ratios can be used if needed.

^a School of Science, RMIT University, Vic 3001 Australia. Fax: +61 3 9925 3747; Tel: +61 3 9925 2122; E-mail: robert.shanks@rmit.edu.au and oliver.jones@rmit.edu.au



Supplementary video to be published with the bio-composite manuscript

Green Chemistry



ARTICLE

Keratin extraction from waste chicken feather components

Firoozeh Pourjavaheri^a, Oliver A.H. Jones^{a*}, Peter M. Smooker^a, Robert Brkljača^a, Saeideh Ostovar pour^a, Ewan W. Blanch^a, Frank Sherkat^a, Arun Gupta^b and Robert A. Shanks^{a*}Received 00th January 20xx,
Accepted 00th January 20xx

DOI: 10.1039/x0xx00000x

www.rsc.org/

Keratin was extracted from different segments of disposable chicken feathers from the poultry industry including whole feathers, calamus and rachis (composed mainly of beta-pleated sheet structures), barbs and barbules (composed mainly of alpha-helix), using sodium sulfide or L-cysteine. The extraction process involved dissolving the chicken feathers after reduction of disulfide links, then separating the protein from the medium using a centrifuge. Once the feathers were dissolved, hydrochloric acid was added to bring the mixture to the isoelectric point for precipitation of protein. The mass ratio of feathers to reducing agents was 1:20, continuously stirred at 40 °C for 6 h and the yield of extracted keratin under sodium sulfide and L-cysteine was 88 ± 3 % and 66 ± 4 %, respectively. The precipitated keratin was washed three times with distilled water. Presence of protein obtained from different methods was confirmed using the biuret test, and the Bradford assay enabled the concentration of keratin to be determined. The extracted keratin was characterised using gel electrophoresis, which confirmed soluble protein of molar mass 11 kg/mol and estimated its purity to be over 95 %. Liquid chromatography-mass spectrometry verified the molar mass of the extracted material matched that of chicken keratin. Vibrational and nuclear magnetic resonance spectroscopy confirmed the structure of keratin was retained following extraction. Thermogravimetry of original purified chicken feather and keratin extracted via sodium sulfide showed virtually identical decomposition behaviour, proving the purity of the keratin. In contrast, thermogravimetry of the keratin extracted with L-cysteine indicated it may contain residual L-cysteine.

1. Introduction

One of the main priorities of sustainable chemical processes is the design of chemical products that reduce or eliminate hazardous substances¹. Green chemistry will direct the development of the next generation of materials, products and processes². Bio-polymers that are based on renewable agricultural bio-mass form the basis for a portfolio of sustainable, eco-efficient products that can compete and capture markets currently dominated by products based exclusively on ecologically destructive processes².

Worldwide, millions of tons of feathers are generated annually worldwide as waste by poultry industries annually. The amount of this waste is continuously increasing, in connection with the increase in fowl meat production, which is inconvenient and troublesome. This causes an environmentally difficult disposal problem, leading to pollution as feather waste is not easily biodegraded and can cause various environmental problems such as chlorosis, fowl cholera and various human ailments when disposed of in landfills.^{3,4} Therefore, from both the economic and environmental viewpoints, it is desirable and important to develop effective and profitable processes to use these resources and transform the waste feathers into new materials to increase their added value. Keratins are a family of structural proteins that can be isolated from a variety of tissues such as hair, feathers, nails, wool, hooves and horns of mammals, reptiles and birds⁵. With

unique properties of biodegradability, biocompatibility and non-toxic nature, keratin protein is a versatile biopolymer that can be modified and developed in various forms such as gels, films, beads and nano/micro-particles⁶. After modification, keratin finds numerous applications in green chemistry, food sciences, pharmaceutical, biomedical, cosmetic industries, tissue engineering, water purification, membrane technology, functional textile industry and composite materials^{6,7}. Feather keratins are small proteins, uniform in size, with a molar mass reported about 10-36 kg/mol⁶⁻¹². The peculiar structure of keratin confers indissolubility, mechanical stability and resistance of feathers to common proteolytic enzymes and chemicals¹³. However, keratins are stabilised by a large number of intra- and intermolecular disulfide cross-links plus other protein structural features, like crystallinity and hydrogen-bonding. Its high strength and stiffness is on account of a large amount of cysteine residues in the polypeptide backbone, which form multiple disulfide bonds⁶, which leads to insolubility in polar solvents like water, weak acids and bases, as well as in apolar solvents¹⁴. Keratin remains reactive, however, because the cysteine units can be reduced, oxidised and hydrolysed^{6,15,16}. Keratin displays a range of non-covalent interactions (electrostatic forces, hydrogen bonds, hydrophobic forces) and covalent interactions (disulfide bonds), which must be destroyed to facilitate the dissolution of feathers¹⁵. Its molecular chains present tight packing of alpha (α) helix and beta (β) sheet structures, which makes keratin difficult to extract and dissolve in water or normal most organic solvents⁷.

^a School of Science, RMIT University, VIC 3001 Australia. Fax: +61 3 9925 3747; Tel: +61 3 9925 2153; E-mail: firoozeh.pourjavaheri@rmit.edu.au

^b Faculty of Chemical & Natural Resources Engineering, Universiti Malaysia Pahang, 25100, Kuantan, Pahang, Malaysia



ARTICLE

Applications of chicken feather keratin

Firoozeh Pourjavahen^a, Oliver A.H. Jones^{a*}, Prue Bramwell^a, Robert Brkljača^a, Frank Sherkat^a, and Robert A. Shanks^{a*}Received 00th January 20xx,
Accepted 00th January 20xx

DOI: 10.1039/c0xx00000x

www.rsc.org/

The structure of keratins extracted from different segments of waste chicken feathers via sodium sulfide and L-cysteine, have been subjected to further nuclear magnetic resonance spectroscopy (NMR) and analysed for their antibacterial properties using *Staphylococcus aureus* and *Escherichia coli* as Gram-positive and Gram-negative species, respectively. The goal of this study was to produce an extracted form of keratin biomaterial, using a typical well-published technique, and to characterise several aspects of its behaviour that may have implications for its general use as a biomaterial. Hence, the superior chicken feather keratin extracted using sodium sulfide as a reducing agent, fabricated into hair conditioner and cream, was used in hair and leather treatments to determine their interactions with the cells tissues. These experiments confirmed and expanded earlier findings that keratin demonstrates excellent compatibility in biological systems.

1. Introduction

Waste feathers, the most abundant keratinous biomass worldwide, are a valuable and renewable protein source¹, which cannot be easily and economically converted to environmentally benign products². Structurally, keratin is a tough protein that is not easily dissolved in polar solvents like water. Although keratin has a high degree of molecular bonding with the adjacent molecules, reduction of the cysteine bonds and manipulation of disulphide bonds (S-S) to hydrogen bonds can lead to break down of the protein molecule and hence becomes soluble³. If the protein molecule is not broken down the feathers can be used whole as fibre reinforcement to improve thermo-mechanical properties of the resultant bio-composites.

Antibacterial activity can be defined as preventing the growth and propagation of bacteria³. Bacteria may be inhibited in a number of ways: a) by break down or prevention of peptidoglycan cell wall formation allowing excess water to enter the bacterial cell leading to cell apoptosis via osmotic pressure³. This mode of action is quite common in polypeptide and penicillin antibiotics³. b) Bacterial protein interference, which stops the organism from producing essential proteins necessary for survival. It targets the ribosome of the microbe that makes the essential protein^{4,5} or targets nucleic acid breakdown via the enzyme that coils and uncoils deoxyribonucleic acid (DNA) during the synthesis process³. These mechanisms are more pronounced when using synthetically made antimicrobials⁵. Both Wang *et al.*⁶ and Tran *et al.*² used keratin in different ways but came to a similar conclusion that suggests keratin is an ideal antimicrobial for wound dressing as it exhibits

bactericidal properties. Paul *et al.*⁷ studied antimicrobial peptides and concluded that the keratin showed antibacterial effect.

Escherichia coli (*E. coli*) and *Staphylococcus aureus* (*S. aureus*) can be found in a mammalian body. *E. coli* resides in the intestines of the gut and *S. aureus* can be found carried on the skin⁷. Structurally *E. coli* (Gram-negative) and *S. aureus* (Gram-positive) can be distinguished by their Gram-morphology i.e. the structure of their cell wall⁸. Both organisms are known to be opportunistic pathogens in the majority of the infections such as urinary tract, burn and wound infections⁷. A review conducted by Qin *et al.*⁹ found that biopolymers could promote antimicrobial activity in three ways: the creation of an anti-adhesive surface, the disruption of cell-cell communication through antibacterial agents, or lysing the cell membrane to kill the bacteria. This study presents the antimicrobial effect of protein keratin derived from chicken feathers via different extraction methods including sodium sulfide and L-cysteine. Antimicrobial effects of keratins were tested using disc diffusion and well diffusion assays by finding the right condition for solubilising the keratin. Keratin needs to be dissolved in a solvent for the disc diffusion method, preferably a solvent that will not inhibit the model organisms. However, keratin was not easily dissolvable in water without the assistance of a chemical compound to cut molecular bonds of the protein. Furthermore, the keratin had already undergone pre-cutting of the molecular bonds in the reduction stage and hence precipitated keratin was used in this experiment.

Based on the findings by Neely and Maley, Gram-positive bacteria such as *S. aureus* were able to survive at least 1 day when inoculated onto the surface of materials commonly used in healthcare applications, with some microorganisms being able to survive for more than 3 months^{10,11}. It is because of these issues that materials, which could provide antimicrobial properties, are being examined for biomedical applications, as they would help in

^a School of Science, RMIT University, VIC 3001 Australia. Fax: +61 3 9925 3747; Tel: +61 3 9925 2153; E-mail: firoozeh.pourjavahen@rmit.edu.au

^b Faculty of Chemical & Natural Resources Engineering, Universiti Malaysia Pahang, 25100, Kuantan, Pahang, Malaysia



APPENDIX 3

CONFERENCE PUBLICATIONS

SPE-ANTEC Society of Plastic Engineers International Conference, 8-10 May 2017, California, USA

KERATIN BIO-COMPOSITES WITH POLYSILOXANE THERMOPLASTIC POLYURETHANE

Firoozeh Pourjavaheri¹, Oliver A.H. Jones², Isaac Martinez Pardo¹, Frank Sherkat¹, Arun Gupta³ and Robert A. Shanks¹

¹ School of Science, RMIT University, GPO Box 2476, VIC 3001, Australia

² Australian Center for Research on Separation Science, School of Science, RMIT University, GPO Box 2476, VIC 3001, Australia

³ Faculty of Chemical & Natural Resources Engineering, Universiti Malaysia Pahang, 25100, Kuantan, Pahang, Malaysia

Abstract

A sustainable resource in the form of chicken feather derived keratin was used to enhance the thermo-mechanical properties of polysiloxane-polyurethane bio-composites. Two methods, solvent-casting-evaporation-compression molding, and solvent-precipitation-evaporation-compression molding were used to create new bio-composites incorporating 20 % w/w of chicken feather fibers into a polysiloxane-polyurethane matrix and the results were compared. A molecular modeling visualization indicated the possible existence of hydrogen bonding between fibers and polyurethane molecules. The thermo-mechanical properties of both the polysiloxane polymer and feather reinforced bio-composites were assessed using thermogravimetry, dynamic mechanical analysis and stress-strain measurements with hysteresis loops. The dispersion uniformity of the keratin fibers in the plastic matrix was investigated via macro photography. Addition of chicken feather fibers to the polysiloxane matrix was found to decrease the recovery strain and mass loss of the composites (at lower temperatures) but increase the elastic modulus, storage modulus, and char level (at higher temperatures). The results demonstrate that keratin derived from what is currently a waste product from the poultry industry (with significant economic and environmental disposal costs) can improve the thermo-mechanical properties of the tested bio-composites simply and cheaply, with potentially large cost savings and environmental benefits.

Introduction

The thermoplastic polyurethanes (TPU) are a versatile group of multi-phase segmented polymers with diverse physical and chemical properties, including, relative hardness, high abrasion [1] and chemical resistance [2, 3]. The applications of polyurethanes, particularly in medical devices, are numerous due to their outstanding mechanical properties and ability to be readily thermally processed. Applications have however, been limited in some cases by the low biological stability [4] and poor fire resistance of soft grade TPU [1].

Conversely, while silicone rubbers are widely used throughout the medical device industry due to their excellent biological performance their potential applications are limited by low mechanical performance and lack of processing options. Co-polymers of silicone macrodiols and polyurethanes with high levels of silicone, exhibit physical and mechanical performance equivalent to conventional polyurethanes with increased biological stability (that surpasses rigid, bio-stable polyurethanes) and are readily thermally processed using conventional technologies [4]. Organosiloxane polymers in particular are known for their excellent thermal and thermo-oxidative stabilities, good electrical properties, high moisture resistance, and low glass transition temperature (T_g -123°C), and mechanical stress [5, 6].

The development of TPU polymers with enhanced thermo-mechanical properties can be accomplished via the incorporation of reinforcing materials and would be beneficial to a range of industries. Many biological materials, including chicken feathers, have the potential to fulfill this role. Incorporating different parts of the feather into a polymer matrix can result in different thermo-mechanical properties in the final composite [7]. Given the unique thermo-mechanical properties of feathers i.e. high insulation and flame resistance, low density (0.89 g cm^{-3}), and sheer physical abundance (and thus low cost), the development of new plastic composites incorporating feather keratin has become an attractive research topic in recent years [7-9]. However, there have to date, been limited development and characterization studies of TPU composites made with these materials [9].

Due to the miscibility and flexibility of TPU, arising from its intrinsic thermoplastic nature, it is expected that incorporation of chicken feather fibers (CFFs) into a soft segment polysiloxane - hard segment TPU matrix at an optimum level could result in a thermo-mechanically superior substrate. TPU-polyether has a chemical structure compatible with CFF keratin. They both contain NH-C=O moieties and the urethane groups of the polymer are compatible with amide groups of the feathers via hydrogen bonding, as shown in Figure 1. Linkages between urethane and amide groups are well known in organic chemistry and have been illustrated in polymers

International Conference on Composites/Nano-Engineering (ICCE), 17-23 July 2016, Hainan Island, China

Analysis and Characterization of Novel Avian Keratin Fibre Based Bio-composites

Firoozeh Pourjavaheri^{a*}, Farzad Mohaddes^a, Oliver A.H. Jones^b, Frank Sherkat^a, Ing Kong^c, Arun Gupta^d and Robert A. Shanks^a

^a School of Science, RMIT University, GPO Box 2476, Melbourne, VIC 3001, Australia

^b Australian Centre for Research on Separation Science, School of Science, RMIT University, GPO Box 2476, Melbourne, VIC 3001, Australia

^c Faculty of Engineering, University of Nottingham, Jalan Broga, 43500 Semenyih, Selangor, Malaysia

^d Faculty of Chemical & Natural Resources Engineering, Universiti Malaysia Pahang, 25100, Kuantan, Pahang, Malaysia

*Email: firoozeh.pourjavaheri@rmit.edu.au

Introduction

Industrial ecology is the study and design of sustainable industrial systems. Ideally, such systems should be connected, with the waste products of one industry becoming the raw materials for another, thereby creating a close loop system mimicking, and drawing inspiration from, natural ecosystems [1].

Millions of tons of feathers are generated as a by-product of the poultry industry worldwide annually [2]. Feathers, particularly from chickens, pose a significant waste disposal problem for industry and are an environmental pollution hazard since, at present, they are mostly either incinerated or sent to landfill. Recently there has been increasing interest in trying to overcome this issue by finding uses for the waste feathers. One potential application is in composite materials; this has the double advantage of both reducing the amount of waste that needs to be disposed of and helping make the resulting plastics more degradable and environmentally sustainable [3].

A possible polymer matrix for chicken feather fibre (CFF) is thermoplastic poly(ether urethane), or TPU-polyether. Together, CFF and TPU-polyether have great potential to make a strong, useful, and green, material. There are however, few studies detailing composites made from protein fibers obtained from agricultural resources. This study therefore investigated keratin obtained from waste feathers from the poultry industry as a fiber resource for bio-composite creation. The overall aim of the work was to optimize the thermo-mechanical properties of polyurethane based bio-composites made with CFF derived material.

Solvent-casting-evaporation is a common method used to prepare new composite materials and therefore this was the method used to create new bio-composites with thermoplastic TPU-polyether as the polymer matrix and reinforced with natural CFF fibres. TPU-polyether has a chemical structure compatible with CFF keratin. They both contain NH-C=O moieties and the urethane groups of the polymer are compatible with amide groups of the feathers via hydrogen bonding.

To produce the bio-composites varying amounts of CFFs (from 0 to 60 % w/w) in steps of 30 % w/w were added to a TPU-polyether matrix. Factors including the size of CFFs used, the manufacturing process and processing parameters employed and the % amount of added fibre were all found to be important factors influencing the mechanical properties of the reinforced bio-composite materials. The final materials could however, be varied by post-treatment procedures [1].

Additionally selected, application-specific properties of the CFF reinforced composites were determined to help characterize the materials. The uniformity of distribution of the keratin fibres in the polymer matrix was investigated via scanning electron microscopy (SEM) and the thermo-mechanical properties of the bio-composites were assessed using thermogravimetry analysis (TGA) and dynamic mechanical analysis (DMA).

The results of the work indicate that feather derived bio-materials may find multiple applications including (but not limited to) packaging, insulation, roofing materials, flexible (but high strength) road posts, building materials, and separation membranes for water treatment.

Experimental

Materials

White CFFs with an average length of 3 - 20 cm were obtained from Baiada Poultry Pty Ltd (Melbourne, Australia). Linear thermoplastic poly(ether urethane) was provided by Lubrizol Corporation (Wickliffe, United States). Tetrahydrofuran (THF) was obtained from BDH Laboratory Supplies (Poole, England).

Preparation of bio-composites

All CFFs were purified according to the 'combined purification method' detailed in Pourjavaheri et al. [4-7] and then ground into small (<2 cm) particles. Solvent-casting-evaporation was performed according to the method outlined in Pourjavaheri et al. [8]. Briefly, the polymer was dissolved in THF and the CFFs were suspended in the matrix in the ratios listed in Table 1.

SPE-ANTEC Society of Plastic Engineers International Conference, 23-25 May 2016, Indianapolis, USA

GREEN PLASTICS: UTILIZING CHICKEN FEATHER KERATIN IN THERMOPLASTIC POLYURETHANE COMPOSITES TO ENHANCE THERMO-MECHANICAL PROPERTIES

Firoozeh Pourjavaheri¹, Oliver A.H. Jones¹, Farzad Mohaddes¹, Frank Sherkat¹, Arun Gupta² and Robert A. Shanks¹

¹ School of Science, RMIT University, VIC 3001, Australia

² Faculty of Chemical & Natural Resources Engineering, Universiti Malaysia Pahang, 25100, Kuantan, Pahang, Malaysia

Abstract

A 'green', sustainable resource, in the form of chicken feather derived keratin, was used to enhance the thermo-mechanical properties of polyurethane bio-composites. Solvent-casting-evaporation method was used to incorporate three levels of chicken feather fibers (0, 10 and 20 % w/w) into a polyurethane matrix. The thermo-mechanical properties of the resulting composites were then assessed using differential scanning calorimetry, thermogravimetry, dynamic mechanical analysis and stress-strain measurements with hysteresis loops. The uniformity of the dispersion of the keratin fiber in the plastic matrix was investigated via macro photography and optical microscopy. Scanning electron microscopy of fracture surfaces was used to verify that the adhesion between fiber and polymer was effective. Addition of chicken feather fibers to the polyurethane matrix was found to decrease the glass transition temperature, recovery strain and mass loss of the composites but increase the elastic modulus, storage modulus, and char level. The results demonstrate that keratin derived from what is currently a waste product from the poultry industry (with significant disposal costs) can improve the thermo-mechanical properties of composites, simply and cheaply, with potentially large environmental benefits.

Introduction

The utilization of eco-friendly, 'green', bio-based composites have been reported in many areas including, but not limited to, the packaging, insulation automotive, building materials and roofing industries, as well as for separation membranes for water treatment [1, 2]. The matrix used for such composites is polyurethane or thermoplastic poly(ether urethane) (TPU or TPU-polyether). This term covers a large class of polymers with diverse physical and chemical properties. While ether-based polyurethane is an excellent choice for water applications [3], the use of TPU in many other areas is often not practical due to its poor heat resistance and mechanical properties [2, 4]. Development of TPU with enhanced thermo-mechanical properties can be accomplished via the incorporation of reinforcing

materials; and would be beneficial to a range of plastic using industries. Biological material, in the form of feathers, has the potential to fulfill this role.

Millions of tons of feathers are produced worldwide annually as a by-product of poultry-processing plants [5]. Given their unique thermo-mechanical properties such as high insulation, flame resistance, low density (0.89 g·cm⁻³ [6]), and sheer physical abundance (and thus low cost), the development of new plastic composites incorporating feather keratin has become an attractive area of research in recent years [1, 7]. There has been very limited development and characterization of TPU composites made with these materials however [7].

Feathers have a surprisingly complex structure (Figure 1). Interestingly, it is known that incorporating different parts of the feather (e.g. calamus, rachis, barbs and barbules) into a polymer matrix can result in different thermo-mechanical properties of the final composite [6]. However, the segregation of each feather segment(s) is expensive and time consuming. Hence, a mixture consisting of staple fibers from whole feathers is generally more easily prepared and incorporated into the polymer matrix, at different polymer-feather ratios if needed.

Due to the miscibility and flexibility of TPU, arising from its intrinsic thermoplastic nature, it is assumed that incorporation of chicken feather fibers (CFFs) into a TPU-polyether matrix at a suitable level could result in a thermo-mechanically modified substrate, which could be successfully used in aqueous systems, such as foaming industry, since ether has two carbons bonded to an oxygen atom. In this study, the alterations in thermo-mechanical properties associated with such a modified system were evaluated both before and after incorporation of CFFs. Furthermore, the outcomes from this research can be used as a model system, the basis for research on similar composites based on alternative polymers.

The 5th International Conference on Manufacturing Science and Engineering, 19-20 Apr 2014 Shanghai, China

Effects of Different Purification Methods on Chicken Feather Keratin

Firoozeh Pourjavaheri^{1, a}, Farzad Mohaddes^{2, b}, Robert A. Shanks^{1, c},
Michael Czajka^{1, d} and Arun Gupta^{3, e}

¹School of Applied Sciences, RMIT University, VIC 3000 Australia

²Centre for Advanced Materials and Performance Textiles, RMIT University, Australia

³Faculty of Chemical and Natural Resources Engineering, Universiti Malaysia Pahang, Gambang Campus, 25100, Kuantan, Pahang, Malaysia

^afiroozeh.jad@student.rmit.edu.au, ^bfarzad.mohaddes@rmit.edu.au, ^crobert.shanks@rmit.edu.au, ^dMC1@pobox.com, ^earun@ump.edu.my

Keywords: keratin; purification; protein; poultry; chicken feathers

Abstract. Every year billion kilograms of unused feathers result from the poultry industry worldwide, which in effect impose a difficult disposal process to the environment. Chicken feathers are considered as a valuable and renewable keratin protein source, which could be used advantageously in a number of applications as alternatives to feather meal and feather disposal. Although the potential applications of keratin derived from chicken feathers have been investigated, the initial purification phase has not been fully described in the literature. Original chicken feathers contain many biological organisms along with other contaminants after plucking. Unprocessed chicken feathers are considered as potentially hazardous biological materials due to the presence of blood borne pathogens; therefore, the decontamination process is very important. The purpose of this work is to compare the effects of different purification techniques on chicken feathers prior to keratin isolation. These processes include surfactant washing, soxhlet extraction with ethanol, ozone, and sodium chlorite solutions. Thermogravimetric analysis, vibrational spectroscopy, and wide angle X-ray scattering were used to characterise the purified feathers prior to keratin extraction.

Introduction

Chicken feathers are a good source of natural fiber keratin, which is potentially valuable biopolymer. The amount of this waste is continuously increasing, in conjunction with the increase in fowl meat production. Many publications proposing applications for keratin preparations in the medical industries are described in literature and opportunities to use this interesting protein in other fields have arisen. Utilization of chicken feathers will be beneficial for the poultry industry by reducing health hazards and will benefit the environment by reducing solid wastes being sent to landfills [1]. The current project solves the environmentally sensitive problem of waste disposal. As unprocessed chicken feathers are a potential biological hazard, it is imperative that they are decontaminated before application. Although several investigations have been conducted to explore the possible applications of keratin extracted from chicken feathers, the initial decontamination phase has not been fully described. The aim of this study is to perform a comparative study of different purification approaches that can be used for chicken feathers prior to keratin isolation. The methods include surfactant washing using an ionic and a non-ionic surfactant. Soxhlet extraction with ethanol was performed to efficiently extract fatty and waxy materials. Ozone and sodium chlorite bleaching were used to sterilize and whiten the keratin. Thermogravimetric analysis, Raman, and wide angle X-ray scattering were used to characterise the feathers and residues after purification and prior to keratin extraction.

Experimental

Materials

Chicken feathers were supplied by Baiada Poultry Pty Ltd. Sodium lauryl sulphate (SLS) was

The 8th International Chemical Engineering Congress & Exhibition (ICChEC 2014)
Kish, Iran, 24-27 February 2014



Purification and Characterisation of Feathers prior to Keratin Extraction

Firoozeh Pourjavaheri-Jad^{1*}, Robert Shanks¹, Michael Czajka¹ and Arun Gupta²

¹ School of Applied Sciences, RMIT University, VIC 3000 Australia

² Faculty of Chemical and Natural Resources Engineering, Universiti Malaysia Pahang, Gambang Campus,
25100, Kuantan, Pahang, Malaysia

*Corresponding author: firoozeh.jad@student.rmit.edu.au

Abstract

Keratin derived from chicken feathers is an inconvenient waste product of the poultry-farming industry, and therefore it is presently the subject of much investigation. Feathers contain some fatty and waxy substances, other than keratin that exists in an α -helix conformation in feather barbs and barbules, and as β -sheet in calamus and rachis. Although investigations have been conducted exploring potential use of keratin derived from chicken feathers, the initial purification phase is important for isolating the keratin from other materials. An original chicken feather contains many biological organisms together with other extraneous material from the time it was plucked from a chicken. Unprocessed chicken feathers are potentially biologically hazardous, caused by the presence of blood borne pathogens, thus it is important that they are decontaminated upon receipt. The aim of this study is to conduct a comparative analysis of different purification techniques to decontaminate chicken feathers prior to keratin isolation. These processes include surfactant washing using an ionic and a non-ionic surfactant, soxhlet extraction with ethanol, ozone and sodium chlorite solution bleaching. Fourier transform infrared spectroscopy, optical microscopy, pH and scanning electron microscopy were used to characterise the feathers and residues after purification and extraction. FTIR analysis confirmed that there are no significant changes in the chemical structure of fibers after each wash treatment. However the residue from ethanol extraction was characteristic of a long hydrocarbon chain ester, typical of a fat.

Keywords: keratin, protein fiber, protein sheet, poultry, chicken feathers

Introduction

Keratin is a by-product from poultry available in large quantity that is only used to a small extent. It is the main structural fibrous protein in feathers. Chicken feathers are comprised of about 90 % of the structural protein, keratin, which is not a single substance, but it is composed of a complex mixture of proteins. The amount of this waste is continuously increasing, in connection with an increase in poultry meat production. The keratin included in chicken feathers is an inconvenient and troublesome waste product of the poultry-farming industry, hence it is presently the subject of investigations in many research developments. Utilization of chicken feathers will not only be beneficial for the poultry industry, but it will reduce health hazards, and benefit the environment, by reducing solid wastes being sent to landfills. The current project not only offers the possibility of novel products from chicken feathers, but solves an environmentally sensitive problem of waste disposal. As unprocessed chicken feathers are a potential biological hazard, it is imperative that they are decontaminated before application. Whilst several investigations have been conducted exploring the possible

International Conference on Advance Polymeric Materials, 11-13 Oct 2013, Kerala, India

Purification Methods for Chicken Feather Keratin

Firoozeh Pourjavaheri-Jad^{1*}, Robert Shanks¹, Michael Czajka¹ and Arun Gupta²

¹ School of Applied Sciences, RMIT University, VIC 3000 Australia

² Faculty of Chemical and Natural Resources Engineering, Universiti Malaysia Pahang, Gambang Campus, 25100, Kuantan, Pahang, Malaysia

*Corresponding author: firoozeh.jad@student.rmit.edu.au

Chicken feathers are an abundant, inconvenient and troublesome waste product from the poultry industry that can be utilised as a source of keratin. The keratin exists in α -helix conformation in feather wool, and as pleated sheet in barbs and rachis. In addition to keratin, feathers contain other fatty and waxy substances. Whilst investigations have been conducted exploring potential use of keratin derived from chicken feathers, the initial cleaning phase is important for isolating the keratin from other materials. An original chicken feather contains many biological organisms and blood together with other dirt from the time they plucked from the chickens. Unprocessed chicken feathers are potentially biologically hazardous, due to the presence of blood borne pathogens, it is imperative that they are decontaminated upon receipt. The aim of this work is to report the findings from a comparative study of different cleaning methods used to decontaminate chicken feathers prior to keratin isolation. These methods are: washing the original chicken feathers using an ionic surfactant, sodium lauryl sulphate (SLS) and comparing with a non-ionic surfactant, which was poly(ethylene glycol) (PEG). Soxhlett extraction with ethanol was performed, together with using ozone (O_3) and chlorine dioxide (ClO_2) solutions for the initial washing processes. Infrared spectroscopy, optical microscopy and scanning electron microscopy were used to characterise the feathers and residues after extraction. The results confirmed that SLS wash had the optimum outcome. Macro photographic images of the feathers are illustrated in Figure 1.



Figure 1: a) Unwashed chicken feather after oven drying at $34 \text{ }^\circ\text{C} \pm 1 \text{ }^\circ\text{C}$, b) ethanol extracted, c) sodium lauryl sulfate solution washed, d) poly(ethylene glycol) solution washed, e) ozone solution washed, f) chlorine dioxide solution washed



APPENDIX 4

POSTER PUBLICATIONS



CHICKEN FEATHER KERATIN AND THERMOPLASTIC POLYURETHANE COMPOSITES

CF-KERATIN + TPU-POLYETHER = GREEN COMPOSITE

WHY CHICKEN FEATHERS?
Human beings do not eat chicken feathers
(...at least purposely...)



7,200,000 tons in 2010

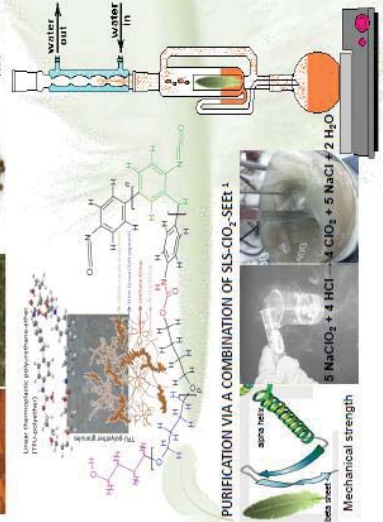
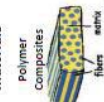
ABPs = animal by-products not intended for human consumption
Regulation (EC) No 1831/2003 Commission Regulation (EU) No 142/2011

CURRENTLY CHICKEN FEATHERS USED FOR:

Energy recovery by incineration



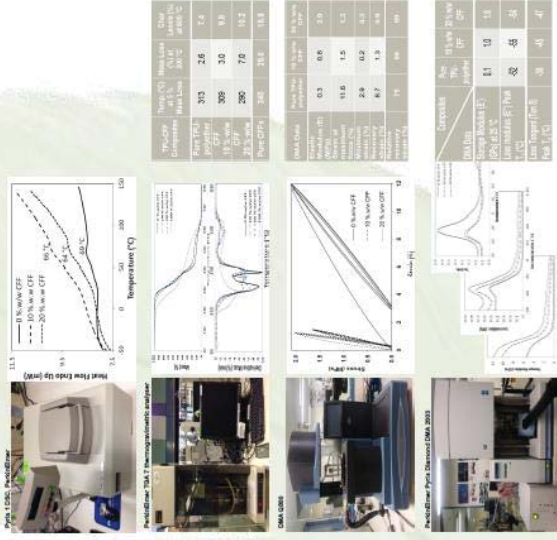
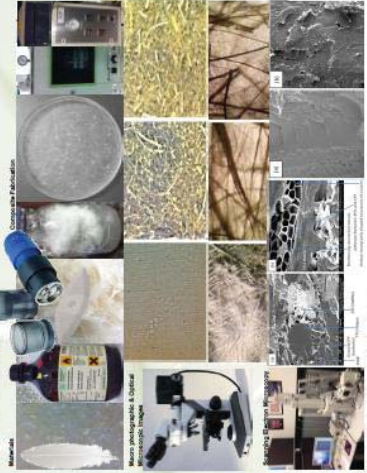
Technical materials



Firoozeh Pourjavaheri, Oliver Jones, Farzad Mohaddes & Robert Shanks
School of Science, RMIT University, VIC 3001, Australia

ABSTRACT
A green, sustainable resource, in the form of chicken feather derived keratin (CF-keratin), was used to enhance the thermo-mechanical properties of polyurethane-ether (TPU-polyether) bio-composites. Solvent-casting-evaporation method was used to incorporate three levels of chicken feather fibers (0, 10 & 20 % w/w) into a TPU-polyether matrix. The thermo-mechanical properties of the resulting composites were then assessed using differential scanning calorimetry, thermogravimetry, dynamic mechanical analysis & stress-strain measurements via hysteresis loops. The uniformity of the dispersion of the keratin fiber in the plastic matrix was investigated via macro photography & optical microscopy. Scanning electron microscopy of fracture surfaces was used to verify that the adhesion between fiber & polymer was effective. Addition of CF-keratin to the TPU-polyether matrix was found to decrease the glass transition temperature, recovery strain & mass loss of the composites but increase the elastic modulus, storage modulus, & char level. The results demonstrate that keratin derived from what is currently a waste product from the poultry industry (with significant disposal costs) can improve the thermo-mechanical properties of composites, simply & cheaply, with potentially large environmental benefits.

EXPERIMENTAL



CONCLUSIONS

Macro photographic, microscopic & SEM imaging of the reinforced bio-composites demonstrated effective adhesion, no agglomeration, & an even distribution of fibers that released the compatibility between the CF reinforcement & the TPU matrix. Addition of CFs to TPU ... enhanced char formation & heat resistance or thermal stability, elastic modulus, storage modulus & loss modulus of the bio-composite, decreased the mass loss, the glass transition temperatures, the loss tangent, & recovery strain compared to the TPU-polyether.

This study will assist the development of bio-composites from polymers, by incorporating agricultural waste – chicken feathers – into useful green composites.

REFERENCES

1. Pourjavaheri, F., Mohaddes, F., Bramwell, P., Sherkat, F. & Shanks, R. A. (2015) Purification of avian biological material to refined keratin fibres. RSC Advances, 5, 66906-69069.
2. Zini, E. & Scazzola, M. (2011) Green composites: an overview. Polymer composites, 32, 1905-1915.



DESIGN AND CHARACTERIZATION OF KERATIN COMPOSITES



ANTEC[®] 2017
ANAHEIM, CA

WHY CHICKEN FEATHERS?
Human beings do not eat chicken feathers
(...at least purposely...)

75 **SPF**
our past, our present, Your Future.

70-80 % meat

5-9 % feathers and down

20-25% Other wastes
(blood, head, feet, viscerae, bones)

2,000 tons / week in 2016

ABPs

ABPs = animal by-products not intended for human consumption
Regulation (EC) No 1831/2003 Commission Regulation (EU) No 142/2013

CURRENTLY CHICKEN FEATHERS ARE USED FOR:

Energy recovery by incineration

Composting or fertilizers

Feather meal for pet animals

Technical materials

Polymer composites

fibers

adhes

PURIFICATION VIA A COMBINATION OF SLS-ClO₂-SEET²

alpha helix

beta sheet

Mechanical strength

5 NaClO₂ + 4 HCl → 4 ClO₂ + 5 NaCl + 2 H₂O

Water In

Water Out

Water In

Water Out

Firoozeh Pourjavaheri & Nabeen Duial

School of Science, RMIT University,
VIC 3007, Australia

Faculty advisors: Robert A. Shanks,
Frank Sherkat & Oliver A.H. Jones

AIM
The ability to combine the advantageous properties of both CFF keratin & TPU-polyloxane polymer in a single material was evaluated in this study.

ABSTRACT
A sustainable resource in the form of CF derived keratin was used to enhance the thermo-mechanical properties of polyloxane-TPU bio-composites.

METHODS
1. Solvent-casting-*evaporation*-compression molding
2. Solvent-precipitation-*evaporation*-compression molding
were used to create new bio-composites incorporating 20 % w/w of CFFs into a polyloxane-polyurethane matrix.

RESULTS
Addition of CFFs to the TPU-polyloxane matrix was found to:
• decrease the recovery strain, mass loss & loss tangent of the composites (at lower temperatures)
• increase the elastic modulus, storage modulus, char level & heat resistance or thermal stability (at higher temperatures).

EXPERIMENTAL

Micro photographs & Molecular modelling visualization

(a) (b) (c) (d)

Prepared film between the CFF & polyloxane/TPU



CONCLUSIONS

The thermo-mechanical properties of raw TPU-polyloxane & TPU-polyloxane CFF bio-composites exhibited greater enhancements with the precipitation technique than the casting method.
Keratin derived from what is currently a waste product from the poultry industry (with significant economic & environmental disposal costs) can improve the thermo-mechanical properties of the tested bio-composites simply & cheaply, with potentially large cost savings & environmental benefits.

REFERENCES

1. Hickey S. The innovators: greener home insulation to leather your nest 2016 [Available from: <https://www.theguardian.com/business/2016/jan/10/the-innovators-schickens-feathers-as-students-greener-home-insulation>]
2. Pourjavaheri, F., Mohaddes, F., Branwell, P., Sherkat, F. & Shanks, R.A. (2015) Purification of avian biological material to refined keratin fibres. *RSC Advances*, 5, 9899-9900.
3. Pourjavaheri, F., Jones, O.A.H., Mohaddes, F., Sherkat, F., Gupta, A., & Shanks, R.A. (2016) 'Green Plastics: Utilizing Chicken Feather Keratin in Thermoplastic Polyurethane Composites to Enhance Thermo-Mechanical Properties'. Society of Plastic Engineers Annual Technical Conference (SPE-ANTEC), 23-25 May, Indianapolis, Indiana, USA.

SPE Poster Number: 2017-G23

2017 Society of Plastics Engineers Annual Technical Conference



RMIT UNIVERSITY

BEYOND RESEARCH 2017



Firoozeh Pourjavaheri
9709695R – E79601

Chicken feather KERATIN

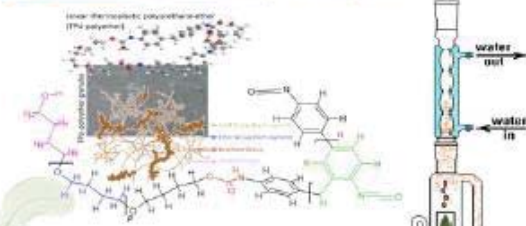
WHY CHICKEN FEATHERS?

Human beings do not eat chicken feathers
(...at least purposely...)

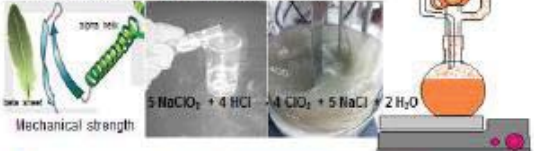


ABPs = animal by-products not intended for human consumption
Regulation (EC) No 1069/2009 Commission Regulation (EU) No 142/2011

CURRENTLY CHICKEN FEATHERS USED FOR:



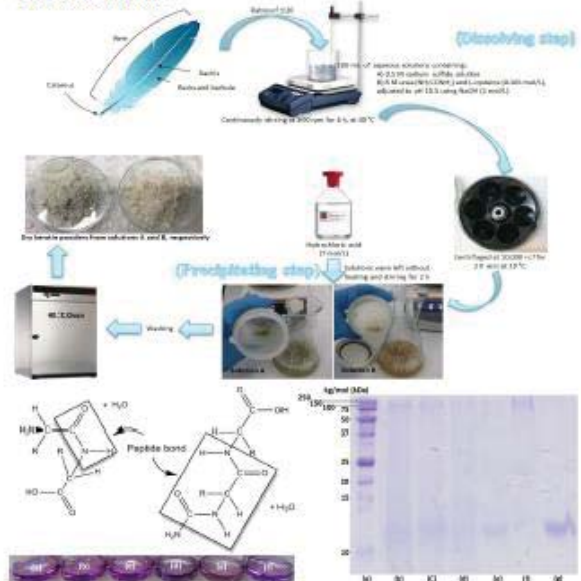
PURIFICATION VIA A COMBINATION OF SLS-ClO₂-SEEL¹



ABSTRACT

Keratin was extracted from different segments of disposable waste chicken feathers including whole feather, calamus/rachis (beta sheet) and barbs/barbules (alpha helix), separately using sodium sulfide, and L-cysteine. The yield of extracted keratin under sodium sulfide and L-cysteine were about 88 % and 66 % respectively, with mass ratio of feathers to reducing agent and enzyme were 1:20 at 40 °C for 6 h. The main processes involved were first dissolving chicken feathers, then separating the protein from the reducing agent and L-cysteine. Once the feathers were dissolved, hydrochloric acid was added to bring the mixture to the isoelectric point (pI) for precipitation of keratin. The precipitated protein was washed three times with water. Presence of protein was confirmed using the biuret test. Keratins were then characterised using sodium dodecyl sulfate-polyacrylamide gel electrophoresis (SDS-PAGE).

EXPERIMENTAL



CONCLUSIONS

Keratin has been successfully extracted from chicken feathers using sodium sulfide and L-cysteine. The molecular weight of both keratins obtained were ca. 11 kg/mol with purity of ≥ 98 % from SDS-PAGE.

REFERENCES

1. Pourjavaheri, F., Mohaddes, F., Bramwell, P., Sherkat, F. & Shanks, R. A. (2015) Purification of avian biological material to refined keratin fibres. *RSC Advances*, 5, 69899-69906.



Avian-Keratin Refinement & Application in Biomaterials



Firoozeh Pourjavaheri




ACKNOWLEDGMENT
 Prof. Afsar Ghaderi
 Assoc. Prof. Frank Shakeri
 Assoc. Prof. Shiva Ghaderi

ABSTRACT

Annually, landfills worldwide receive millions of tons of poultry feathers that take decades to biodegrade and cause a variety of environmental issues. They can carry diseases that endanger human health as well as that of flora and fauna. A portion of these waste feathers is incinerated, producing CO₂ and harmful SO₂ emissions. However, these feathers contain over 90 % keratin protein, which can be used for many applications such as cosmetics, healing products, and tissue engineering. The aim is to reduce the disposal of and better utilise feather waste, which the poultry industry currently pays for. Using chicken feathers as a sustainable source of keratin instead of materials like wool would reduce emissions (since poultry farming is less carbon-intensive than sheep farming) and utilise a major waste stream of the poultry industry (rather than wool, which has many other applications). The extraction process we have developed is greener than current technologies and will reduce the production time and cost, while increasing the yield.

WHY CHICKEN FEATHERS?


Human beings do not eat chicken feathers
 (...at least purposely...)



70-80 % meat



5-9 % feathers and down



2,000 tons / week
in 2016

ABPs
20-25% Other wastes
(blood, head, feet, viscerae, bones)

ABPs = animal by-products not intended for human consumption
 Regulation (EC) N° 1069/2009 Commission Regulation (EU) No 142/2011

CURRENTLY CHICKEN FEATHERS ARE USED FOR:

Energy recovery by incineration



Composting or fertilizers

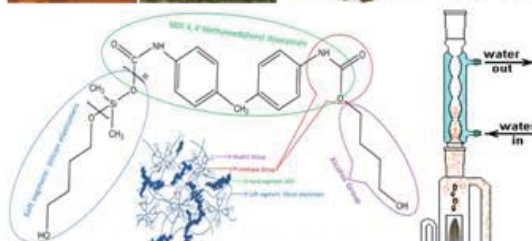


Feather meal for pet animals



Technical materials





EXPERIMENTAL



Column
Backward buffer



(Dissolving step)



Dry keratin powders from sodium sulfide and L-cysteine, respectively



Hydrochloric acid (1 mol/L)



Centrifuged at 33,000 rpf for 2 h with 50 °C

(Precipitating step)



Solutions were left without heating and stirring for 2 h

APPLICATIONS



CONCLUSIONS

Keratin has been successfully extracted from chicken feathers using sodium sulfide & L-cysteine. The molar mass of both keratins obtained were ca. 11 kg/mol with purity of 295 %.

REFERENCES

- Hickey S. The innovators: greener home insulation to feather your nest 2016 [Available from: <https://www.wtheguardian.com/business/2016/apr/10/the-innovators-chicken-feathers-students-greener-home-insulation>].
- Pourjavaheri, F., Mohaddes, F., Bramwell, P., Sherkat, F. & Shanks, R. A. (2015) Purification of avian biological material to refined keratin fibres. *RSC Advances*, 5, 69899-69906.